

**WETTABILITY ALTERATION USING SURFACTANTS TO IMPROVE OIL
RECOVERY FROM UNCONVENTIONAL LIQUID RESERVOIRS**

A Dissertation

by

JOHANNES ORLANDO ALVAREZ ORTIZ

Submitted to the Office of Graduate and Professional Studies of
Texas A&M University
in partial fulfillment of the requirements for the degree of

DOCTOR OF PHILOSOPHY

Chair of Committee, David S. Schechter
Committee Members, Maria A. Barrufet
 Ibrahim Y. Akkutlu
 James D. Batteas
Head of Department, A. Daniel Hill

August 2017

Major Subject: Petroleum Engineering

Copyright 2017 Johannes O. Alvarez

ABSTRACT

Improving oil recovery from unconventional liquid reservoirs (ULR) is a major challenge and knowledge of recovery mechanisms and interaction of completion fluid additives with the rock is fundamental in tackling the problem. Fracture treatment performance and consequently oil recovery could be improved by adding surfactants to stimulation fluids to promote imbibition by wettability alteration and interfacial tension (IFT) reduction. The Young-Laplace equation relates the capillary pressure to IFT and contact angle. Thus, it follows that capillarity is significant in nanopores associated with ULR and complex as the contact angle (CA) and IFT varies simultaneously. This study analyzes the potential of improving oil recovery by imbibition using different groups of surfactants as additives to completion fluids by characterizing their interaction with oil and heterogeneous siliceous and carbonate ULR samples from the Wolfcamp, Eagle Ford, Bakken and Barnett formations as well as the effect of wettability modification and IFT reduction in maximizing well performance after stimulation.

A correlated set of experiments were proposed beginning by characterizing ULR rocks and fluids and evaluating original wettability by measuring CA and zeta-potential. Then, different types of surfactants were evaluated to gauge their effectiveness in altering wettability and IFT. In addition, adsorption measurements were performed to calculate the amount of surfactant adsorbed into the rock. Moreover, spontaneous imbibition experiments were carried out in conjunction with CT scan technology to measure oil

recovery, fluid penetration (imbibition) and change of fluid saturation in the rock samples with time. Then, a core-flooding system was designed to be combined with the CT scanner to experimentally simulate the fracture-treatment and to represent surfactant imbibition in an ULR core fracture during a soaking and flowback production scheme. The results showed that surfactant solutions are capable of altering ULR wettability to water-wet with moderate reduction of IFT. However, the extent of wettability alteration strongly depends on rock lithology, surfactant and oil type. Surfactant adsorption measurements also showed the dependence of rock lithology on surfactant performance. Moreover, spontaneous imbibition and core-flooding experiments suggested that wettability alteration and IFT reduction are beneficial to oil recovery as evidenced by the improved oil recovery when surfactants were used. These findings were consistent with CA, zeta potential, surfactant adsorption and IFT measurements.

Next, to scale our laboratory results, imbibition rates and dimensionless time scaling curves were generated corroborating that fracture density and rock-fluid interactions are key parameters for oil recovery. From the results obtained, it can be concluded that moderate IFT reduction in addition to significant wettability alteration has optimum effect on improving oil recovery from these ULR. These findings provide insight in designing completion fluids and flowback schedules for these unconventional liquid resources.

DEDICATION

To my parents, Orlando and Mildred, for showing me the path that brought me here. For molding me by example. For always giving. Thank you for your unconditional love and support.

To my children, Daniela and Diego, for forgiving me the many hours I spent away pursuing this objective. During these years, I have seen you grow to beautiful and caring children, and I could not be prouder of you.

To my wife, Ingrid, for encouraging me to begin this journey and always giving me the strength to go forward. For all your support and sacrifices, even when you were pursuing your master's degree. For being Mom, student and wife altogether. But more importantly for all your love and devotion. This achievement belongs to both of us.

ACKNOWLEDGEMENTS

I would like to give my dearest gratitude to my committee chair and advisor Dr. David Schechter. For his constant guidance and teachings. For always pushing the envelope. For giving me this fantastic line of research and engaging with me every time I needed it. For that and many more, I sincerely appreciate all his support and friendship all these years.

I would also like to thank my committee members Dr. Maria A. Barrufet, Dr. Ibrahim Y. Akkutlu and Dr. James D. Batteas, for their teachings, guidance, interest and support throughout the course of this research.

I would like to thank Francisco Tovar for his friendship all his help during these years. Also to my fellow researchers I. Wayan Rakananda Saputra, Manoj Valluri, Zuhair Al Yousef, Fan Zhang, Rodolfo Marquez, Jared Clark, Thomas Connor, John Maldonado, Celine Liron and the whole Dr. Schechter's group for being that extremely needed extra-hand in the lab and the office, and most importantly for your friendship.

I would like to thank the Harold Vance Department of Petroleum Engineering, Texas Engineering Experimental Station, and the Crisman Institute Petroleum Research at Texas A&M University for funding the research.

Finally, thank you Texas A&M University and Aggieland for your values, your diversity, your community and for giving my family and me the best place to live and learn.

CONTRIBUTORS AND FUNDING SOURCES

Contributors

This work was supervised by a dissertation committee consisting of Professor David S. Schechter and Professors Maria A. Barrufet and Ibrahim Y. Akkutlu of the Department of Petroleum Engineering and Professor James D. Batteas of the Department of Chemistry.

Experimental work was completed by the student, in collaboration with I. Wayan Rakananda Saputra, Francisco Tovar, Manoj Valluri, Rodolfo Marquez, Jared Clark, Thomas Connor and John Maldonado of the Department of Petroleum Engineering. The data analyzed for Chapter IX was completed by the student, in collaboration with Fan Zhang of the Department of Petroleum Engineering.

All other work conducted for the dissertation was completed by the student independently.

Funding Sources

This research was supported by the Harold Vance Department of Petroleum Engineering, Texas Engineering Experimental Station (TEES), and the Crisman Institute Petroleum Research at Texas A&M University.

NOMENCLATURE

cp	Centipoise
cm	Centimeter
cm ³	Cubic centimeter
CT	Computer tomography
CT _{initial}	Average CT number of the core before spontaneous imbibition experiments
CT _{final}	Average CT number of the at the end of spontaneous imbibition experiments
ft	Feet
HU	Hounsfield unit
in	Inches
g/cc	Grams per cubic centimeters
gpt	Gallons per thousand gallons
gr	Grams
mg/g	Milligrams per grams
mg/L	Milligrams per liter
mV	Millivolts
mm	Millimeters
mN/m	Millinewton per meter

Nm	Nanometers
μ D	Micro Darcie
μ m	Microns
μ m	Micro meters
psi	Pounds per square inch
ULR	Unconventional liquid reservoir
wt	Weight
$^{\circ}$	degrees

TABLE OF CONTENTS

	Page
ABSTRACT	ii
DEDICATION	iv
ACKNOWLEDGEMENTS	v
CONTRIBUTORS AND FUNDING SOURCES.....	vi
NOMENCLATURE.....	vii
TABLE OF CONTENTS	ix
LIST OF FIGURES.....	xiii
LIST OF TABLES	xxii
CHAPTER I INTRODUCTION	1
CHAPTER II LITERATURE REVIEW	11
Wettability Fundamentals	11
Contact angle method.....	14
Amott-Harvey index method.....	16
USBM method.....	17
NMR method.....	18
Zeta potential measurements	19
Wettability Alteration Mechanisms	20
Ion-pair formation mechanism	21
Surfactant adsorption mechanism	22
Micellar solubilization mechanism	25
Surfactant Adsorption in Unconventional Liquid Reservoirs	26
Wettability and Imbibition in Conventional Reservoirs	28

Wettability and Imbibition in Unconventional Liquid Reservoirs	30
Scaling Models for Imbibition	41
CHAPTER III METHODOLOGY	52
Rock Petrophysical Characterization	53
X-ray diffraction analysis.....	53
Total organic carbon analysis.....	54
Scanning electron microscopy.....	54
Mercury injection capillary pressure.....	54
Fluid Characterization	55
Total acid number and total base number	55
Oil and brine density determination	56
IFT experiments	56
Chemical additives stability tests	58
Wettability Measurement Experiments	59
Contact angle experiments	59
Zeta potential experiments	62
Surfactant Adsorption Experiments	63
Spontaneous Imbibition Experiments	66
Core Flooding Experiments	70
Scaling Imbibition Results	74
CHAPTER IV ROCK, OIL AND WETTABILITY CHARACTERIZATION	78
Rock Petrophysical Characterization	79
X-ray diffraction and total organic carbon analysis	80
Scanning electron microscopy imaging	82
Mercury injection capillary pressure results	84
Fluid Characterization	87
Oil total acid number, total base number and densities.....	87
IFT measurements	88
Wettability Measurement Experiments	89
Contact angle results	89
Zeta potential results	94
Original Wettability Determination by Spontaneous Imbibition Experiments	
Monitored by CT Scan Methods	96
Spontaneous imbibition of oil into ULR cores.....	97

Spontaneous imbibition of water into ULR cores	101
Spontaneous Imbibition Experiments in Aged ULR Cores	104
CHAPTER V WETTABILITY AND IFT ALTERATION BY SURFACTANTS	111
Surfactant Stability and Emulsion Tendency Test	112
Wettability Alteration Results in Unconventional Liquid Reservoirs.....	115
Wettability alteration results in the Wolfcamp formation.....	115
Wolfcamp contact angle measurements results.....	116
Wolfcamp zeta potential measurements results	121
Wettability alteration results in the Eagle Ford formation	125
Eagle Ford contact angle measurements results.....	126
Eagle Ford zeta potential measurements results.....	129
Wettability alteration results in the Bakken formation	132
Bakken contact angle measurements results	134
Bakken zeta potential measurements results	138
Wettability alteration results in the Barnett formation.....	140
Barnett contact angle measurements results.....	142
IFT Alteration Results in Unconventional Liquid Reservoirs	144
IFT alteration results in the Wolfcamp formation.....	145
IFT alteration results in the Eagle Ford formation	147
IFT alteration results in the Bakken formation	149
IFT alteration results in the Barnett formation.....	151
CHAPTER VI SURFACTANT ADSORPTION	155
Surfactant Adsorption Results in Unconventional Liquid Reservoirs	155
Surfactant adsorption results in the Wolfcamp formation	159
Surfactant adsorption results in the Bakken formation	161
Surfactant adsorption results in the Eagle Ford formation.....	164
CHAPTER VII SPONTANEOUS IMBIBITION EXPERIMENTS MONITORED BY CT SCAN TECHNOLOGY	166
Spontaneous Imbibition Experiments in the Barnett Formation	167
Spontaneous Imbibition Experiments in the Wolfcamp Formation.....	169
Spontaneous Imbibition Experiments in the Eagle Ford Formation	184
Spontaneous Imbibition Experiments in the Bakken Formation	195

CHAPTER VIII CORE FLOODING IMBIBITION EXPERIMENTS MONITORED BY CT SCAN TECHNOLOGY	211
Core Flooding Imbibition Experiments Results in ULR.....	212
CHAPTER IX SCALING LABORATORY DATA TO THE FIELD	228
Scaling Laboratory Data to the Field in the Eagle Ford Formation	229
Scaling Laboratory Data to the Field in the Wolfcamp Formation	240
CHAPTER X FINAL CONSIDERATIONS, CONCLUSIONS AND RECOMMENDATIONS	250
REFERENCES.....	260

LIST OF FIGURES

	Page
Figure 1. Droplets of water in a water-oil-rock system.....	13
Figure 2. Contact angle of water in a water-oil-rock system.	15
Figure 3. Mechanism schematic showing the wettability alteration by ion-pair formation.	22
Figure 4. Mechanism schematic showing the wettability alteration by anionic surfactants.....	23
Figure 5. Experimental setup for measuring IFT. Reprinted with permission from Alvarez et al. (2014).....	57
Figure 6. Experimental setup for measuring contact angle. Reprinted with permission from Alvarez et al. (2014).	60
Figure 7. Modified Amott cell for spontaneous imbibition experiments. Reprinted with permission from Alvarez and Schechter (2017).....	68
Figure 8. Schematic of the experimental core-flooding system. Reprinted with permission from Alvarez et al. (2014)	71
Figure 9. Schematic of the artificially fractured shale cores.....	72
Figure 10. Experimental setup for core-flooding experiments in ULR.	72
Figure 11. SEM images for sample Bk-1/1 (top) and sample EF-2/1 (bottom). Reprinted with permission from Alvarez and Schechter (2016c).	83

Figure 12. SEM images for sample W-1/2 (top) and sample Br-2/ 2 (bottom). Reprinted with permission from Alvarez and Schechter (2016c).....	84
Figure 13. Normalized pore size distributions for Bakken, Eagle Ford, Wolfcamp and Barnett. Reprinted with permission from Alvarez and Schechter (2016c).....	85
Figure 14. Cross plot for permeability and porosity for Bakken, Eagle Ford, Wolfcamp and Barnett. Reprinted with permission from Alvarez and Schechter (2016c).....	87
Figure 15. Oil-water IFT for Bakken, Eagle Ford, Wolfcamp and Barnett. Reprinted with permission from Alvarez and Schechter (2016c).....	89
Figure 16. Original wettability for Bakken and Eagle Ford. Reprinted with permission from Alvarez and Schechter (2016c).....	91
Figure 17. Original wettability for Wolfcamp and Barnett. Reprinted with permission from Alvarez and Schechter (2016c).....	92
Figure 18. Original wettability for Bakken, Eagle Ford, Wolfcamp and Barnett samples vs. TOC. Reprinted with permission from Alvarez and Schechter (2016c).....	93
Figure 19. Original wettability for Bakken, Eagle Ford, Wolfcamp and Barnett samples grouped by lithology. Reprinted with permission from Alvarez and Schechter (2016c)	93
Figure 20. Zeta potential results for water-rock system in wells from Bakken, Eagle Ford, Wolfcamp and Barnett. Reprinted with permission from Alvarez and Schechter (2016c)	95
Figure 21. Oil imbibition of Eagle Ford core at t=0 h (left) and at t=1 h (right). Reprinted with permission from Alvarez and Schechter (2016c).....	99

Figure 22. CT images for core slices from Bakken, Eagle Ford, Wolfcamp and Barnett under oil imbibition. Reprinted with permission from Alvarez and Schechter (2016c).	100
Figure 23. CT images for core slices from Bakken, Eagle Ford, Wolfcamp and Barnett under water imbibition. Reprinted with permission from Alvarez and Schechter (2016c).	103
Figure 24. Oil recovered by spontaneous imbibition as percentage of OOIP vs. time for Bakken, Eagle Ford and Wolfcamp cores.	105
Figure 25. CT images for core slices from Bakken, Eagle Ford and Wolfcamp. Reprinted with permission from Alvarez and Schechter (2016c).	107
Figure 26. Cores Bk-2/1 (left), EF-1/2 (center) and W-1/4 (right) under spontaneous imbibition experiment. Reprinted with permission from Alvarez and Schechter (2016c).	109
Figure 27. Stability test at 2 gpt (top) for surfactant solutions and emulsion tendency test for surfactant solutions and crude oil (bottom).	114
Figure 28. Contact angle results for well W-1 at depth 1.	117
Figure 29. Contact angle results for well W-1 at depth 2.	118
Figure 30. Contact angle results for well W-1 at depth 3.	120
Figure 31. Contact angle results for well W-2 at depth 1.	121
Figure 32. Zeta potential results for well W-1 depth 1 water-rock system.	122
Figure 33. Zeta potential results for well W-1 depth 3 water-rock system.	123

Figure 34. Zeta potential results for well W-1 water-oil system.....	124
Figure 35. Contact angle results for well EF-1 at depth 1.....	127
Figure 36. Contact angle results for well EF-1 at depth 2.....	127
Figure 37. Contact angle results for well EF-2 at depth 1.....	128
Figure 38. Contact angle results for well EF-2 at depth 2.....	129
Figure 39. Zeta potential results for well EF-2 depth 1 water-rock system.	130
Figure 40. Zeta potential results for well EF-2 depth 2 water-rock system.	131
Figure 41. Zeta potential results for well EF-2 water-oil system.....	132
Figure 42. Contact angle results for well Bk-1 at depth 1.....	134
Figure 43. Contact angle results for well Bk-1 at depth 2.....	135
Figure 44. Contact angle results for well Bk-2 at depth 1.....	137
Figure 45. Zeta potential results for well Bk-1 depth 1 water-rock system.	138
Figure 46. Zeta potential results for well Bk-2 depth 1 water-rock system.	139
Figure 47. Zeta potential results for well Bk-1 water-oil system.....	140
Figure 48. Contact angle results for well Br-1 at depth 1.....	142

Figure 49. Contact angle results for well Br-1 at depth 2	143
Figure 50. Contact angle results for well Br-2 at depth 1	144
Figure 51. IFT results for Well W-1.	146
Figure 52. IFT results for Well EF-2.....	148
Figure 53. IFT results for Well Bk-1.....	150
Figure 54. IFT results for Well Br-1.	152
Figure 55 . IFT results for Well Br-2.	153
Figure 56. Light adsorption for surfactant Anionic A.....	156
Figure 57. Light adsorption for surfactant CNF.....	157
Figure 58. Calibration curves for surfactants Anionic A and CNF.....	158
Figure 59. Surfactant adsorption measurement with time of well W-1/1.	160
Figure 60. Surfactant adsorption measurement with time of well W-1/3.	161
Figure 61. Surfactant adsorption measurement with time of well Bk-1.	162
Figure 62. Surfactant adsorption measurement with time of well Bk-2.	163
Figure 63. Surfactant adsorption measurement with time of well EF-2-1.....	164

Figure 64. Core Br-2/3 before (left) submerging in anionic surfactant and after 24 hours (right). Reprinted with permission from Alvarez et al. (2014)	168
Figure 65. Core Br-2/3 before (left) submerging in nonionic surfactant and after 24 hours (right). Reprinted with permission from Alvarez et al. (2014).....	168
Figure 66. Cores at the beginning of the spontaneous imbibition experiments (up) and when oil begins to be expelled from the cores (bottom). Reprinted with permission from Alvarez and Schechter (2017).....	172
Figure 67. Oil recovered for well WC-1, depth 1 (siliceous) by spontaneous imbibition	174
Figure 68. Oil recovered for well WC-1, depth 2 (carbonate) by spontaneous imbibition	176
Figure 69. CT images for well WC-1, depth 1 (siliceous).	178
Figure 70. CT images for well WC-1, depth 2 (carbonate).....	179
Figure 71. Oil recovered for well EF-2 by spontaneous imbibition.....	187
Figure 72. CT images for well EF-2.	191
Figure 73. Oil recovered for well Bk-1 (siliceous) by spontaneous imbibition.	197
Figure 74. Oil recovered for well Bk-2 (carbonate) by spontaneous imbibition.	199
Figure 75. CT images for well Bk-1. Reprinted with permission from Alvarez and Schechter (2016a)	202

Figure 76. CT images for well Bk-2. Reprinted with permission from Alvarez and Schechter (2016a).....	203
Figure 77. Contact angles before and after spontaneous imbibition experiments for well Bk-1 cores.....	206
Figure 78. Contact angles before and after spontaneous imbibition experiments for well Bk-2 cores.....	207
Figure 79. Penetration magnitude for core flooding imbibition experiments.	215
Figure 80. CT images for core flooding imbibition experiments.....	217
Figure 81. Oil recovered at the end of the core flooding imbibition experiments.	219
Figure 82. Oil recovered in core flooding imbibition experiments.....	220
Figure 83. Contact angles before and after core flooding imbibition experiments.....	223
Figure 84. Oil recovery vs. dimensionless time for Eagle Ford using scaling group by Ma, Morrow, and Zhang (1995).....	230
Figure 85. Normalized oil recovery vs. dimensionless time for Eagle Ford using scaling group by Ma, Morrow, and Zhang (1995).	231
Figure 86. Oil recovery vs. dimensionless for Eagle Ford using scaling group by Gupta and Civan (1994) and Guo, Schechter, and Baker (1998).....	232
Figure 87. Normalized oil recovery vs. dimensionless time for Eagle Ford using scaling group by Gupta and Civan (1994) and Guo, Schechter, and Baker (1998).....	233

Figure 88. Production rates for the Eagle Ford spontaneous imbibition experiments	234
Figure 89. Distribution of induced fractures and hydraulic fractures along the horizontal well.....	236
Figure 90. Predicted field production rates by imbibition from scaling laboratory data in the Eagle Ford.....	237
Figure 91. Predicted Eagle Ford field production using case 3.	240
Figure 92. Oil recovery vs. dimensionless time in spontaneous imbibition experiments for Wolfcamp using scaling group by Ma, Morrow, and Zhang (1995).	241
Figure 93. Normalized oil recovery vs. dimensionless time for Wolfcamp using scaling group by Ma, Morrow, and Zhang (1995).	242
Figure 94. Oil recovery vs. dimensionless time for Wolfcamp using scaling group by Gupta and Civan (1994) and Guo, Schechter, and Baker (1998).....	243
Figure 95. Normalized oil recovery vs. dimensionless time for Wolfcamp using scaling group by Gupta and Civan (1994) and Guo, Schechter, and Baker (1998).....	243
Figure 96. Production rate for the Wolfcamp spontaneous imbibition experiments.....	244
Figure 97. Predicted field production rate by imbibition from scaling laboratory data in the Wolfcamp.	246
Figure 98. Predicted Wolfcamp field production using case 3	248
Figure 99. Effect of contact angle and IFT in oil recovered.	252

Figure 100. Effect of capillary pressure and contact angle in oil recovered.253

Figure 101. Effect of penetration magnitude and capillary pressure in oil recovered. ..255

LIST OF TABLES

	Page
Table 1. Literature values for original ULR wettability.....	4
Table 2. Flow regimes and characteristic lengths for scaling imbibition data	44
Table 3. ULR rock sample sources and depths. Reprinted with permission from Alvarez and Schechter (2016c).....	80
Table 4. XRD and TOC results for Bakken and Eagle Ford. Reprinted with permission from Alvarez and Schechter (2016c)	81
Table 5. XRD and TOC results for Wolfcamp and Barnett. Reprinted with permission from Alvarez and Schechter (2016c)	82
Table 6. Petrophysical properties for Bakken, Eagle Ford, Wolfcamp and Barnett. Reprinted with permission from Alvarez and Schechter (2016c).....	86
Table 7. Oil properties for Bakken, Eagle Ford, Wolfcamp and Barnett. Reprinted with permission from Alvarez and Schechter (2016c).	88
Table 8. Oil spontaneous imbibition experiment results. Reprinted with permission from Alvarez and Schechter (2016c)	98
Table 9. Water spontaneous imbibition experiment results. Reprinted with permission from Alvarez and Schechter (2016c)	102
Table 10. Spontaneous imbibition experiment results. Reprinted with permission from Alvarez and Schechter (2016c)	108

Table 11. Surfactant properties	113
Table 12. Lithological composition of rock samples from Wolfcamp wells W-1 and W-2.....	116
Table 13. Lithological composition of rock samples from wells EF-1 and EF-2	125
Table 14. Lithological composition of rock samples from wells Bk-1 and Bk-2	133
Table 15. Lithological composition of rock samples from wells Br-1 and Br-2.....	141
Table 16. Initial core properties for Wolfcamp spontaneous imbibition experiments.....	170
Table 17. Lithological composition of rock samples from well W-1	171
Table 18. Wolfcamp spontaneous imbibition experiment results	181
Table 19. Wolfcamp capillary pressure and inverse Bond numbers	182
Table 20. Initial core properties for Eagle Ford spontaneous imbibition experiments.....	185
Table 21. Surfactant properties 2	186
Table 22. Eagle Ford spontaneous imbibition experiment results	193
Table 23. Eagle Ford capillary pressures and inverse Bond numbers.....	194
Table 24. Initial core properties for Bakken spontaneous imbibition experiments.....	196

Table 25. Bakken spontaneous imbibition experiment results.....	205
Table 26. Bakken capillary pressure and inverse Bond numbers.....	208
Table 27. Surfactant properties 3	212
Table 28. Lithological composition of rock samples from well WC-2.....	213
Table 29. Initial core properties for Wolfcamp core flooding imbibition experiments	214
Table 30. Core flooding imbibition experiment results	224
Table 31. Characteristic core lengths for the Eagle Ford	235
Table 32. Completion methods and fracture geometries.....	237
Table 33. Cumulative field oil production by imbibition for the Eagle Ford	239
Table 34. Characteristic core lengths for Wolfcamp.....	245
Table 35. Cumulative field oil production by imbibition for the Wolfcamp	247

CHAPTER I

INTRODUCTION

Unconventional liquid resources (ULR) have become an important source of energy in the United States. The increasing hydrocarbon exploitation of shale oil has positioned the country as one of the biggest oil producers on the planet (Doman 2015). However, ULR low porosity and ultralow permeability lead to current recovery factors that do not exceed more than 10% of the original oil in place (OOIP) with average values of 5 to 6% (Alharthy et al. 2015, Wang et al. 2016).

The nature of these ULR makes them very special to study. Their mineralogy, ultra-small pore size, organic content, and heterogeneity petrophysically characterize them as unconventional resources. Contrary to conventional reservoirs, ULR have the distinctiveness of being both rock source and reservoir with characteristic low porosity and ultralow permeability (Jarvie 2012). Due to their low porosity and ultralow permeability, ULR are currently produced by multiple fracture treatments in horizontal wells. This technique allows these liquid rich shales to produce at commercial flow rates by creating effective paths for hydrocarbons to flow towards the wellbore. The effectiveness of fracture treatments in increasing recovery and consequently current low oil recovery factors may possibly be improved if proper surfactants are added to completion fluids, thereby altering wettability, reducing interfacial tension (IFT) and consequently improving water imbibition.

Wettability is defined as the tendency of one fluid to spread onto a solid surface in the presence of other immiscible fluids (Anderson 1986a, Craig 1993). A solid surface can demonstrate water-wet, intermediate-wet or oil-wet behavior, which can be determined by measuring contact angle, Amott-Harvey index and USBM (U.S. Bureau of Mines) method as quantitative methods, and by nuclear magnetic resonance (NMR) and zeta potential measurement, among others, as qualitative methods.

Wettability alteration in reservoir rocks can improve oil recovery by changing capillary forces when shifting intermediate and oil-wet reservoirs to water-wet. Altering wettability in ULR as an improved oil recovery (IOR) method can be reached while fracking the formation by adding chemical additives such as surfactants to completion fluids.

However the wettability is quantified, in a water-oil-rock system, a water-wet rock prefers water to contact the rock surface. Also, water imbibes into the rock displacing the oil from the pores and rock surface. In the same manner, an oil-wet rock has tendency to be in contact to oil, and when imbibing, oil displaces the water from the rock surface (Anderson 1986a, Wang et al. 2012). Hence, wettability controls flow behavior and distribution of the fluids in the reservoir, so it is an important subject of study for IOR and enhanced oil recovery (EOR) methods in conventional reservoir and lately in unconventional reservoirs.

In unconventional liquid reservoirs, the presence of both inorganic pores (water-wet) and organic pores (oil-wet) makes them in many cases intermediate-wet depending on organic to inorganic matter proportions (Alvarez and Schechter 2016c). In order to shift

rock wettability to water-wet and enhance water imbibition by changing capillary forces and causing water to penetrate into the matrix displacing the oil in place, surfactants can be used.

Capillary forces mainly influence completion fluid penetration or imbibition in ULR. The Young-Laplace equation (Eq. 1) relates capillary pressure (P_c) to interfacial tension (IFT) denoted as (σ), wettability as contact angle (θ), and pore radius (r).

$$P_c = \frac{2\sigma \cos\theta}{r} \dots \quad (1)$$

Wettability in these unconventional rocks are originally oil and intermediate-wet due to the mixture of water-wet inorganic pores and oil-wet organic pores. Currently, there are few studies reporting original wettability in ULR, and **Table 1** (Alvarez and Schechter 2016c, b) compiles different wettability measurements for ULR available in the literature.

Table 1. Literature values for original ULR wettability

Reference	ULR	Method used	Original wettability
Odusina, Sondergeld, and Rai (2011)	Eagle Ford Bakken Barnett Floyd Woodford	NMR	Intermediate-wet
Wang et al. (2012)	Middle Bakken Upper Bakken	Amott-Harvey	Oil-wet to intermediate-wet
Shuler et al. (2011)	Middle Bakken	Not reported	Oil-wet to intermediate-wet
Kathel and Mohanty (2013)	Undisclosed	Contact angle	Oil-wet to intermediate-wet
Nguyen et al. (2014)	Eagle Ford	Contact angle	Intermediate-wet
Morsy and Sheng (2014)	Bakken	Contact angle	Intermediate-wet
Mirchi et al. (2014a)	Undisclosed	Contact angle	Water-wet
Mirchi et al. (2014b)	Undisclosed	Contact angle	Intermediate-wet
Alharthy et al. (2015)	Three Folks Bakken	Contact angle	Oil-wet
Habibi et al. (2016)	Montney	Contact angle	Oil-wet and intermediate-wet

From Table 1 most the wettability studies reported oil and intermediate-wet behaviors in ULR. However, some of these studies used different immiscible fluids such as oil and air instead of oil and water, outcrops rather than pay zone samples or performed other wettability measurement methods that may not be suitable for ultralow permeability ULR samples. Nevertheless, further wettability characterization for unconventional resources is needed to have a more comprehensive database. Consequently, this study aims to close that gap in the literature by characterizing the original wettability of Wolfcamp, Bakken, Eagle Ford and Barnett, four of the most important unconventional liquid reservoirs in the United States.

In addition to wettability, the Young-Laplace equation stays that pore radius inversely affects capillary pressure; hence, initial capillary pressures are negative with high values. In fact, in oil-wet systems, fluid imbibition does not take place because oil is captured by the matrix, driven by capillarity. In order to achieve water imbibition into the matrix to displace liquid hydrocarbons from the pores and fracture surface, wettability must be shifted to water-wet. Wettability alteration changes capillary pressure values from negative to positive, favoring spontaneous imbibition and mobilizing oil by the aid of gravitational forces (Anderson 1987, Hirasaki and Zhang 2004).

Wettability alteration in shale formations can be an important factor in improving the performance of hydraulic fracturing treatments. However, its effectiveness strongly depends on lithology, and oil and surfactant type. For that reason, ULR characterization is vital to properly recommend a specific surfactant type and understand wettability alteration mechanisms. Currently, there is no comprehensive study that relates lithology, organic content and oil and surfactant type with the wettability alteration mechanisms reported in the literature. This study addresses this issue for different unconventional plays with varying lithology and petrophysical properties.

The use of chemical additives also results in IFT alteration. As showed before, The Young-Laplace equation (Eq. 1) relates the capillary pressure to IFT and contact angle. Thus, it follows that capillarity is significant in nanopores associated with ULR and complex as the CA and IFT varies simultaneously; hence, a trade-off between mean pore throat size, contact angle and IFT is necessary to maximize well performance after stimulation.

There is very scant literature on the study of combined effect of wettability and IFT alteration on imbibition process in ULR. Also, there is no experimental methodology to evaluate and compare the impact of wettability alteration and the efficiency of surfactants in altering wettability and recovering hydrocarbons from shale cores. Hence, this research proposes a set of correlated experiments to evaluate this process in the laboratory and obtain the required data to history match experimental results and upscale them to a full well and reservoir basis. In addition, this study focuses on addressing the effectiveness of fracture treatments in ULR when surfactants are added to completion fluids and the role of wettability and IFT in improving water imbibition and the exploitation of liquid rich shales. In addition, it aims to identify the proper chemical additive that maximizes well performance after stimulation. The specific objectives are described as follows:

- Characterize original wettability for four of the most important ULR in the United States (Wolfcamp, Bakken, Eagle Ford and Barnett) and its impact on oil recovery.
- Analyze the relation of rock mineralogy, oil type and total organic content (TOC) to wetting affinity.
- Evaluate and compare the ability of different groups of surfactants in altering wettability and IFT in oil shale cores by conducting contact angle, zeta potential and IFT measurement experiments at reservoir conditions.
- Analyze the impact of wettability and IFT alteration on recovering hydrocarbons ULR cores on spontaneous and forced imbibition experiments.

- Determine surfactant adsorption during imbibition experiments to correlate with surfactant type, rock lithology and oil recovery.
- Use CT methods to quantify and relate magnitude of fracture fluid imbibition, penetration, and improvement in oil recovery in shale cores
- Address the implication of oil and surfactant type with rock lithology in wettability alteration mechanisms and their impact on completion fluids imbibition and oil recovery after stimulation.
- Study the relation and trade-off between pore size, contact angle and IFT to improve water imbibition and oil recovery in ULR using surfactants in completion fluids.
- Evaluate imbibition rates and scaling groups to correlate imbibition data and predict oil recovery at field scale.
- Recommend an experimental procedure to evaluate surfactants on wettability alteration and oil recovery in ULR.

To achieve these objectives, this research combines the effect of contact angle and zeta potential experiments, adsorption and IFT measurement, spontaneous and forced imbibition experiments and computed tomography scan technology to evaluate and compare the efficiency of different chemical additives in altering wettability and recovering hydrocarbons from shale cores at reservoir conditions.

This manuscript is structured as follows: Chapter 2 introduces a literature review on wettability fundamentals and measurement methods as well as wettability alteration

mechanisms. In addition, it summarizes wettability and imbibition in conventional reservoirs and describes the state-of-the-art on wettability alteration in ULR. Chapter 3 describes the methodology used to characterize, in the laboratory, ULR original wettability and oil and rock properties as well as to evaluate and compare the efficiency of different groups of chemical additives in altering wettability and recovering hydrocarbons during injection of completion fluids. Chapter 4 uses siliceous and carbonate preserved and aged cores from the Wolfcamp, Bakken, Eagle Ford and Barnett to determine their original wettability. Initial wettability is measured by contact angle, zeta potential and spontaneous imbibition. In addition, rock mineralogy, oil type and total organic content (TOC) is experimentally determined to evaluate the relation of wettability and these variables. ULR petrophysical properties such as permeability, porosity, pore size distribution, XRD analyses and scanning electron microscopy (SEM) images as well as oil properties like IFT, API gravity, oil total acid number (TAN) and oil total basic (TBN) are measured to further understand wettability states from these ULR. Then in Chapter 5, chemical additives capability of altering wettability and reducing IFT is studied using several surfactant types and concentrations as well as oil and core samples from the Wolfcamp, Bakken, Eagle Ford, and Barnett. Moreover, the relation of pore size, rock mineralogy, oil type and total organic content (TOC) to wetting affinity is carefully analyzed. Similarly, Chapter 6 studies surfactant adsorption onto ULR rocks using ultraviolet-visible spectroscopy. Calibration curves for surfactant solutions are determined by relating surfactant concentration to light absorbance and used to calculate the amount of surfactant adsorption and its implications in wettability alteration and oil recovery.

Next, Chapter 7 investigates chemical additives' potential for improving water imbibition and oil recovery on these ULR by spontaneous imbibition experiments at reservoir temperature. In addition, the relation and trade-off between mean pore throat size and, contact angle and IFT is studied. This chapter also evaluates and compares the efficiency of different types of surfactants in altering wettability and IFT and their impact on recovering hydrocarbons from carbonates and siliceous shale cores. By this, I aim to further understand the implication of oil and surfactant type with rock lithology in wettability alteration mechanisms and their impact on completion fluids imbibition and oil recovery after stimulation. Next, surfactant effectiveness at improving oil recovery after stimulation is also studied in Chapter 8 by using a core-flooding system at reservoir conditions to represent surfactant penetration in ULR fractures during a frac job. The experimental results from Chapters 7 and 8 are analyzed using CT scan technology and compared to validate the hypothesis that wettability and IFT alteration could increase oil recovery in ULR by changing capillarity when changing oil and intermediate-wetness to water-wetness, and reducing IFT without reaching ultralow values. Moreover, in Chapter 9, different scaling groups available in the literature are evaluated to match experimental results, asses their validity in ULR and, if possible, predict oil recovery at field scale. Finally, concluding remarks and future proposed research studies are in Chapter 10.

In summary, this novel line of investigation focuses on surfactant additives in unconventional liquid reservoirs to maximize oil recovery after stimulation. I evaluate and compare the efficiency of different groups and blends of surfactants on recovering liquid hydrocarbons from siliceous and carbonate shale cores by analyzing the effects of

lithology, oil and surfactant type on wettability and IFT alteration, adsorption and their impact on imbibition and oil recovery when added to completion fluids. To my knowledge, this has not been done in ultra-low permeability shale reservoirs. I perform this study using an innovative correlated set of experiments to evaluate surfactant potential of improving oil recovery in ultralow permeability and low porosity rocks. The results obtained by this methodology can be used for scaling up and simulating flowback after stimulation. The findings from this research provide an important understanding of designing completion fluid treatments that perform better with specific rock lithologies and surfactant types to reduce costs and maximize oil recovery after stimulation.

CHAPTER II

LITERATURE REVIEW *

This chapter is oriented to overview wettability and IFT alteration as well as surfactant adsorption effects on oil recovery and their application on unconventional liquid reservoirs. Fundamentals of wettability alteration methods are reviewed along with the proposed mechanism for conventional reservoirs. Next, the current state-of-the-art applications in ULR are summarized to highlight the potential importance of encouragement of further investigation in wettability alteration in ULR as a mean to improve oil recovery. Lastly, scaling models for imbibition to predict oil recovery at field basis and its limitations are described.

Wettability Fundamentals

Wettability is defined as the affinity of a fluid for a specific type of rock. In liquids-on-solid systems, which in our case would be the water-oil-rock system, wettability represents the tendency of either water or oil to spread onto rock surface. The wetting phase is related to the fluid with higher affinity to rock and non-wetting phase to the other

* Parts of the literature review presented in this chapter have been reprinted from “Application of Wettability Alteration in the Exploitation of Unconventional Liquid Resources” by J.O. Alvarez and D.S. Schechter. Petroleum Exploration and Development. Volume 43. Issue 5. Copyright 2016 by Elsevier. Reproduced with permission of Elsevier. Further reproduction prohibited without permission.

fluid (Salehi, Johnson, and Liang 2008). Hence, in a water-wet rock, water tends to contact rock surfaces and occupy small pores whereas in an oil-wet rock, oil is in contact to the majority of rock and fill the small pores (Basu and Sharma 1997). When the rock has no preference to adhere to either fluid, the system is called intermediate-wet (Anderson 1986a). In reservoir rocks, wettability can also be classified as homogeneous and heterogeneous. Homogenous wettability refers to relative uniform preference to either oil or aqueous phase; on the other hand, heterogeneous wettability describes a system with different affinities to oil and aqueous phases in the same rock (Wang et al. 2011). Conventional reservoirs exhibit mostly homogeneous wettability due to their rather uniform mineralogy and the absence of organic matter on their matrix. Conversely, unconventional reservoirs such as shale oil exhibit heterogeneous wettability due to their juxtaposed layers with different mineralogy and the presence of organic matter as well as chemical heterogeneity of their surface due to their nature and depositional environment. For this study, I focused on the wettability classification that relates the affinity of the fluid to the surface in contact.

In water-oil-rock systems, as in **Fig. 1**, in which water is the denser fluid, the rock is water-wet when the contact angle between water and solid goes from 0° - 75° , intermediate-wet from 75° - 105° , and oil-wet from 105° - 180° (Anderson 1986a). However, it is important to note that different publications consider different ranges of contact angle for wettability characterization; nevertheless, the variation seen in those publications has a maximum of $\pm 10^\circ$ from the ones presented in this study.

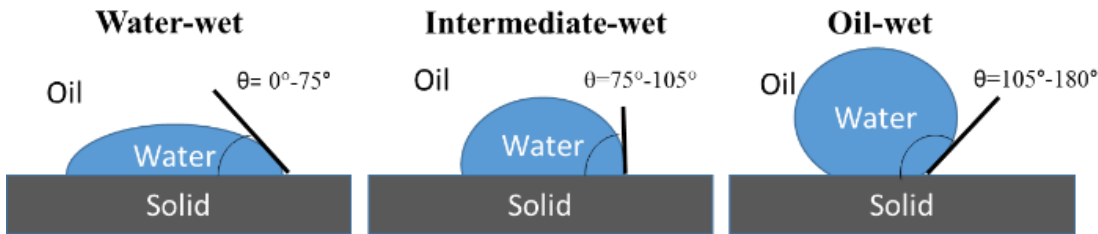


Figure 1. Droplets of water in a water-oil-rock system.

Original wettability can be affected by charged compounds present in crude oil by surface precipitation, acid/base interactions and ion binding interactions (Buckley, Liu, and Monsterleet 1998). Thus, siliceous rocks with negative surface charges tend to absorb basic oil compounds, whereas carbonate rocks favor acid compounds. At the end, these interactions are responsible for rock wettability. For that reason, it is imperative to characterize not only rock mineralogy but also oil type as defined by total acid number (TAN), total base number (TBN) and oil API gravity. In addition, in ULR the presence of organic matter influences wettability, so its determination is required.

Wettability can be measured by contact angle, Amott-Harvey index, USBM (U.S. Bureau of Mines) method, and magnetic resonance (NMR). When wettability of a specific surface is needed, contact angle method is used, whereas when an average wettability of a volume, such as a core, is needed, Amott-Harvey and USBM methods are used. In addition, wettability states can be evaluated qualitatively using NMR and zeta potential measurements (Alvarez and Schechter 2016b).

Contact angle method

Contact angle is defined by the tangent to the water-oil interface at the point of intersection with the rock sample (Kolasinski 2012). The rock sample should be flat and smooth to avoid significant errors in the measurements. Other limitations in these measurements are contact angle hysteresis due to surface heterogeneity, and failure to represent the wettability of whole system (Basu and Sharma 1997, Hansen, Hamouda, and Denoyel 2000, Hirasaki 1991). This is a simple widely used and accurate way to measure wettability in reservoir rocks (Basu and Sharma 1997, Wang and Gupta 1995). Sessile drop, captive bubble, tilting plate, and capillary rise, among others, are some of the methods used to measure contact angles; however, in the oil industry, contact angle is commonly measured by captive bubble (Anderson 1986b, Rajayi and Kantzias 2009).

At equilibrium, the forces are balanced and the liquid will not continue wetting the surface and it will stay as a drop with a specific contact angle over the surface. This is expressed by the Young equation (**Eq. 2**) (Young 1855), assuming the solid does not deform when contact liquid phases, and illustrated in **Fig. 2**. Tangential forces of oil-solid (σ_{os}) interface are equal and contrary to the sum of the forces of solid-water (σ_{sw}) and oil water (σ_{ow}).

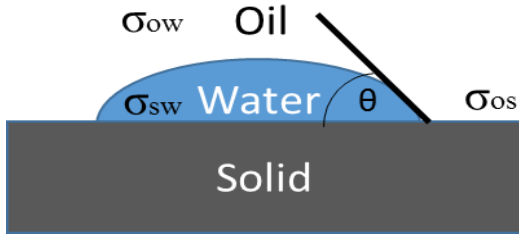


Figure 2. Contact angle of water in a water-oil-rock system.

Varying contact angles can help explain extreme situations; for example, when the angle is $\theta=0^\circ$, water will uniformly wet the surface. Then, when the angle increases, a droplet is formed and water will wet the surface at a specific angle. Finally, when the angle is $\theta=180^\circ$, water will not wet the surface (Kolasinski 2012, Somasundaran and Zhang 2006).

Although the relationship between the phases can be well explained by the Young equation, surface tension is a property that fails to describe the microscopic forces that involve wettability (Kolasinski 2012). Hirasaki (1991) describes these microscopic forces as electrostatic, Van der Waals and structural forces. Electrostatic forces depend on the type of minerals, and fluid properties such as pH, salinity and composition. Van der Waals, electrostatic and structural forces are related to the disjoining pressure which is the force that acts to separate the two interfaces and it is the results of ionic and molecular interactions.

Amott-Harvey index method

The Amott-Harvey Index method is based on the fact that a wetting fluid will spontaneously and later forcedly imbibe the rock displacing a non-wetting fluid. This will give an average core wettability and relative permeability. Viscosity and initial saturation can be adjusted using the ratio of spontaneous imbibition to force imbibition (Anderson 1986b). Initial water saturation is calculated by flooding or centrifuging the samples with water and then oil. Then, four steps are archived as follows (Salehi, Johnson, and Liang 2008):

1. The amount of spontaneously imbibed water is measured (S_{ws})
 2. Core is flooded with water to obtain residual oil saturation (S_{or})
 3. The amount of spontaneously imbibed oil is measured (S_{os})
 4. Core is flooded with oil to obtain initial water saturation (S_{iw})

In addition, S_{wf} is the water saturation after forced imbibition of aqueous phase and S_{of} is oil saturation after oil imbibition of oil phase. Once the saturations are measured, the Amott-Harvey index is calculated by **Eq. 3** to **Eq. 5**. For strongly water-wet systems, I_{A-H} is 1 and for strongly oil-wet systems I_{A-H} is -1. A water-wet system is between 0.3 and 1, and oil-wet between -1 and -0.3 (Cuiec 1984).

$$Iw = \frac{Sws - Siw}{Swf - Siw} \quad \dots \dots \dots \quad (3)$$

$$I_{A-H} = I_w I_o \quad \dots \dots \dots \quad (5)$$

The main disadvantage of this method is the inability of measuring intermediate-wet states. Also, the initial saturation of the rock is a main factor to measure wettability (Anderson 1986b).

USBM method

The USBM method is very similar to the Amott-Harvey method with the advantage that takes into account intermediate-wet states. As Amott-Harvey index method, this method will give an average core wettability and compares the work (W) necessary to displace the non-wetting fluid by centrifugation. Work is calculated by using Eq. 6 to the area under the capillary pressure curves (Anderson 1986b).

$$W = \log\left(\frac{A_1}{A_2}\right) \dots \quad (6)$$

Where A_1 and A_2 are the area under the capillary pressure curve. The core is water-wet when W is greater than zero, oil-wet when less than zero and intermediate-wet when close to zero. The difference on the area under capillary curves is due to the easiness of water, for example, to imbibe a water-wet surface, but the resistance to be displaced by oil in the same surface.

The explained wettability measurement methods have been commonly used in the industry for many years. However, these methods were developed for rock with high

permeability (mD to Darcy) and porosity (> 20%). In addition, contact angles are performed in polished surfaces, and USBM and Amott-Harvey methods are performed in porous media. ULR have completely different petrophysical characteristics, permeability is in the range of μ D to nD and porosities are less than 10%. Under these circumstances, USBM and Amott-Harvey methods are extremely hard to perform because fluids cannot flow through these rocks. Wang et al. (2012) used a modified Amott-Harvey index method to measure wettability Bakken samples; however, permeability and porosity values of these experiments average on 7 mD and 4.4%, respectively. Contact angle method was used by Nguyen et al. (2014) in Bakken and Eagle Ford, by Alvarez et al. (2014) in an undisclosed ULR, and later by Alvarez and Schechter (2017) in the Permian Basin and by Alvarez and Schechter (2016a) in the Bakken. Next, some qualitative methods to address wettability are described.

NMR method

The NMR method provides qualitative indication of fluid affinity. This technique identifies the fluids inside the matrix, and uses thermal relaxation of hydrogen atoms to characterize them. Surface relaxation dominates the wetting fluid relaxation, and the wetting fluid relaxes faster than the bulk whereas non-wetting fluids relax as late as bulk determining which is the wetting fluid (Odusina, Sondergeld, and Rai 2011). In addition, the intensity of the NMR can estimate the proportion of one fluid to the other as well as the hydrogen index. However, the method has an ambiguous relationship between the relaxation rate and fractional wettability, and sample preparation might alter wettability

of the sample (Anderson 1986a). Odusina, Sondergeld, and Rai (2011) have used this method as alternative to USBM and Amott-Harvey to estimate wettability in ultralow permeability and low porosity in several ULR.

Zeta potential measurements

Wettability changes in ULR can be addressed using zeta potential measurements. The idea is to measure the stability of the thin water film on the shale rock surface to determine rock affinity for water. Zeta potential is the electrical potential on the double layer, and its magnitude is related to surface charges at rock-fluid interface. Consequently, an increment of electrical potential on the double layer as exhibited as stable liquid films suggest a repulsion that alters rock wettability to water-wet by detaching the oil from the rock surface. On the other hand, unstable thin water films can be interpreted as intermediate and even oil-wet behavior (Alvarez and Schechter 2017, Xie et al. 2014). The thickness and stability of the water layer between the rock surface and oil depends on oil, water and rock surface charges (Hirasaki 1991). When addressing stability, it is a consensus that zeta potential values greater than +30 mV or lower than -30 mV are treated as stable whereas values between -30 to +30 mV are known as unstable. Moreover, zeta potential measurements give an indication of the strength of surface charges on a solute particle as well as the nature of the charge.

In summary, wettability can be quantitatively measured by contact angle, Amott-Harvey and USBM methods, and qualitatively measured by NMR and zeta potential. Some of these methods are well used in the industry to measure wettability in conventional

reservoirs; however, when used in ULR with low porosity and ultralow permeability many of these methods are not practical. In fact, wettability is extremely hard to measure using commonly applied methods such as USBM and Amott-Harvey because fluids cannot flow through these rocks. For that reason, contact angle method is better suited for ULR; their surface tightness reduces measurement errors due to roughness. Zeta potential measurements can give an indication of wetting affinity. Also, NMR does not require fluid flow through the rock, so it can be used in ULR; however, the relationship between the relaxation rate and fractional wettability as well as sample preparation are important factors that may alter wettability of the sample. Thereby, contact angle determination, NMR methods and zeta potential measurements seems to be the most appropriate means to estimate wettability in these unconventional resources, but it is important to have in mind that these methods have their limitations.

Wettability Alteration Mechanisms

In a reservoir that is originally intermediate to oil-wet, wettability can be altered by addition of surfactants to shift rock wettability to water-wet. Surfactants are amphiphilic compounds that have both a hydrophobic and a hydrophilic group. Based on their head group, surfactants are most commonly classified in cationic (positive charge), anionic (negative charge), nonionic (no charge) and zwitterionic or amphoteric (positive and negative charge). Surfactants have been successful in altering wettability in reservoir rocks by flowing and/or diffusing into the matrix and shifting wettability and reducing

IFT, which reduces capillary pressure. Then, water spontaneously imbibes the rock expelling the oil in the pores (Gupta and Mohanty 2011). Cationic, anionic and nonionic surfactants efficacy in changing wettability have been extensively studied in sandstones and carbonates, as conventional reservoirs, and three main mechanisms have been proposed as responsible of shifting wettability: ion-pair formation (Standnes and Austad 2000b), surfactant adsorption (Austad and Milter 1997a, Standnes and Austad 2000b) and micellar solubilization (Kumar, Dao, and Mohanty 2008).

Ion-pair formation mechanism

Ion-pair formation mechanism was proposed by Standnes and Austad (2000b) after observing cationic surfactants irreversibly imbibed oil-wet chalk cores recovering more than 70% of the oil in place within 30 days of exposure in comparison with anionic surfactants, which recovered only 5% of the oil in place. This mechanism is showed in **Fig. 3**, after Standnes (2001), and suggests an ion-pair formation between the positive heads of cationic surfactants, in blue, and the negatively charged material, mostly absorbed carboxylates, in the oil, in black, that are attached to the rock surface by electrostatic forces in the head groups and hydrophobic forces in the tail groups.

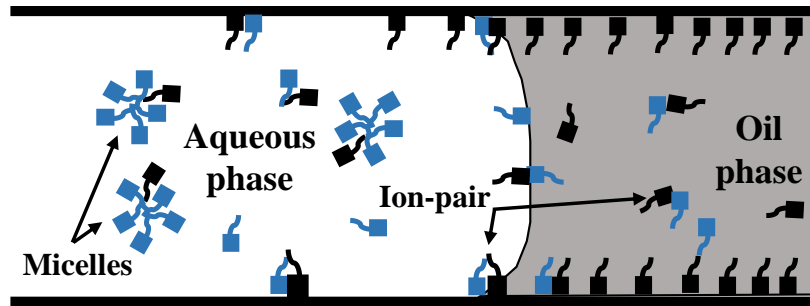


Figure 3. Mechanism schematic showing the wettability alteration by ion-pair formation.

The layer of oil in the surface is desorbed as ion-pairs forming micelles and transported due to their hydrophobicity to the oil phase. Then, with a water-wet surface after desorption of organic materials, water can imbibe the rock by capillary forces. Standnes and Austad (2000b) also suggested that critical micelle concentration (CMC) and hydrophobicity are important to achieve wettability alteration. Evaluated cationic surfactants decrease their efficiency in altering wettability at lower CMC due to the decrease of monomer concentration. Moreover, more hydrophobicity increases the contact of surfactant in the oil interface.

Surfactant adsorption mechanism

Proposed by Austad and Milter (1997a) and Standnes and Austad (2000b) after the poor performance of anionic surfactants imbibing oil-wet carbonate cores. The anionic surfactants create electrostatic repulsion between the surfactant heads and the negatively charged compounds of oil on the chalk surface; hence, ion-pair formation cannot take place. Instead, as showed in **Fig. 4**, after Standnes (2001), surfactant can create a double

layer due to hydrophobic interactions with the oil layer adsorbed to the chalk surface. The hydrophobic surfactant tails, in blue, are adsorbed by the hydrophobic oil-wet surface, and their hydrophilic heads are facing the solution altering its wettability to water-wet. This creates a weak water zone, which reduces capillary pressure to favor water imbibition. In addition, the authors affirmed that the efficiency of anionic surfactants, measured by imbibition rate, increased when raising the number of ethoxylated groups, which creates a more compact surfactant monolayer by the reduction of charge density of the head group. This was also validated by Gupta and Mohanty (2011). In addition, because the oil is not desorbed from the chalk surface as the case of ion-pair mechanism, this mechanism is reversible and takes place only when favorable electrostatic interactions are not present.

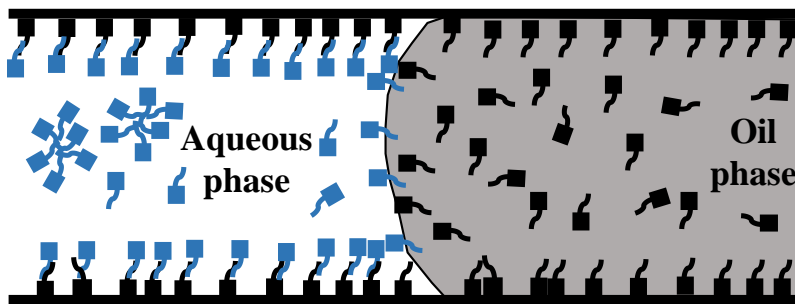


Figure 4. Mechanism schematic showing the wettability alteration by anionic surfactants.

Salehi, Johnson, and Liang (2008) verified experimentally ion-pair and surfactant adsorption mechanisms proposed by Standnes and Austad (2000b) and Austad and Milter (1997a). First, they tested the ion-pair formation by assuming that if cationic surfactants were better at recovering oil from carbonate surfaces due to the interaction of positively

charged surfactant heads to the negatively charged compounds of crude oil on chalk surface, anionic surfactants should perform better in sandstone surfaces by the interaction of negatively charged surfactants heads and the positively charged oil molecules adsorbed to the sandstone rock. Initially, sandstone rocks are considered negatively charged, the authors assumed that, based on Buckley, Liu, and Monsterleet (1998) findings, basic compounds of the particular oil used on these experiments changed the rock surface charge to positive and anionic surfactant head formed ion-pair with positively charged oil particles in the surface. On the other hand, cationic surfactants lack the electrostatic interaction to the basic oil compounds due to their positive charge avoiding ion-pair formation. Experimental results showed that indeed anionic surfactant performed significantly better than cationic surfactant in altering wettability and producing oil out sandstone cores by spontaneous imbibition. In addition, to rule out the possibility that spontaneous imbibition can be caused by lower IFT in anionic surfactants compared to cationic surfactants, Salehi, Johnson, and Liang (2008) used the inverse Bond number (**Eq. 7**) developed by Du Prey (1978) and Schechter, Zhou, and Orr Jr (1994) and is explained in the next sections. The authors found inverse Bond numbers bigger than 5 which represented that capillary forces are responsible of imbibition with a countercurrent flow. Moreover, Salehi, Johnson, and Liang (2008) proposed the same imbibition flow mechanism explained by Austad et al. (1998) and Chen et al. (2001) in which oil flow is initially dominated by capillary forces as countercurrent flow, and later gravity forces take places to displace the oil in the core.

In order to verify surfactant adsorption mechanism, Salehi, Johnson, and Liang (2008) prepared a polyethylene oil-wet surface without adsorbed charged oil compounds to force surfactants, both anionic and cationic, to change wettability by aligning their tails with the oil molecules. They found that surfactant adsorption behaved as Langmuir type adsorption isotherms, confirming bilayer formation between surfactants tails and the oil in the rock surface. Moreover, they measured wettability changes by the Amott-Harvey method. The results indicate that wettability was shifted from strongly oil-wet to intermediate-wet when surfactants were flooded throughout the cores and anionic surfactants performed better than cationic surfactants. Then, during the second imbibition cycle, the wettability was restored to oil-wet due to the surfactant layer removal when water was injected as forced imbibition. Hydrophilic surfactant heads are facing the solution, so they were removed by injected water. They also confirmed this observation by measuring recovered aqueous solution IFT and confirming that recovered water IFT is reducing as time passed due to surfactant removal from the surface. With these findings, the authors also corroborated the reversible character of surfactant adsorption mechanism.

Micellar solubilization mechanism

Kumar, Dao, and Mohanty (2008) postulated the Micellar solubilization mechanism by using atomic force microscopy (AFM) on mineral surface, mica and silicon, to represent carbonate and siliceous rocks. Both anionic and cationic surfactants were evaluated with better performance by anionic surfactants. Even though both surfactants could alter wettability on initially oil-wet surfaces and favor water imbibition,

anionic surfactants were better and faster than cationic surfactants. This conclusion was reached by measuring forces of adhesion and contact angle on parallel plates. The authors explained these results by the fact that anionic surfactants reduce in greater amount oil-water IFT, so the aqueous phase imbibes the parallel plates due to the reduction of capillary pressure leaving a thin oil layer attached to the surface. Then, micellar solubilization of the oil film by anionic surfactants into the adsorbed anionic oil material on the surface alter wettability to water-wet. Conversely, cationic surfactants do not reduce IFT as low as anionic surfactants, so cationic surfactant goes to the oil phase by dissolution and forms ion-pairs desorbing oil molecules from the surface. Cationic surfactant mechanism is slower than anionic surfactants due fact that surfactant solution is not entering the plates and interacting with the thin oil layer, but it interacts with the oil meniscus and slowly dissolves into the oil phase.

In summary, previous studies in conventional reservoirs suggested that wettability could be chemically altered using surfactants by three different mechanisms: ion-pair formation, surfactant adsorption and micellar solubilization, which mainly depend on surfactant nature and mineralogical composition of the rock.

Surfactant Adsorption in Unconventional Liquid Reservoirs

Surfactant adsorption in ULR has not been studied in detail, and the current available investigations on the subject suggest that a more comprehensive work is needed. A few years ago, Zelenev, Champagne, and Hamilton (2011) determined nonionic

surfactant and microemulsion static adsorption in siliceous Marcellus shale outcrops by measuring surface tension of diluted solutions before and after crushed shale equilibrium. Their results showed adsorption values ranged from 1 to 30 mg/g at the maximum surfactant concentration of 3000 mg/L with nonionic surfactant adsorbing close to 15 mg/g. Next, Mirchi et al. (2014b) performed static adsorption measurements using ultraviolet-visible (UV-Vis) spectroscopy in an undisclosed crushed calcite and clay rich ULR sample and an anionic surfactant, noticing very low adsorption values (0.508 mg/g at CMC of 0.03 wt.%) and Langmuir type adsorption behavior. This low adsorption was attributed to shale surface capacity for attracting predominately cations instead of anions. Lastly, Zhang, Wang, and Olatunji (2016) studied static surfactant adsorption in siltstone Middle Bakken samples with permeability from 0.004 to 0.008 md using anionic, nonionic and blended surfactants. The authors used the UV-Vis spectroscopy and their results showed adsorption capacities of 0.62 mg/g for the blended surfactant and 11.91 to 33.08 mg/g for nonionic and anionic surfactants. The authors attributed the latter elevated values to unreliable measurements caused by solution turbidity.

In summary, these studies did not perform dynamic surfactant adsorption experiments in ULR in which surfactant adsorption can be measured with time to address adsorption mechanisms. In addition, these studies did not evaluate different types of lithology and surfactant charge nature to successfully investigate the impact of electrostatic and rock-fluid interactions in surfactant adsorption on ULR surfaces. In this study, we attempt to fill these current gaps on the literature.

Wettability and Imbibition in Conventional Reservoirs

Originally, conventional reservoirs were considered water-wet because siliceous rocks have affinity for water and because before oil migration, pores were filled with water and this initial water remained in contact with the rock surface after oil migration and formation of the reservoir. However, experimental studies have demonstrated that there are significant amounts of oil-wet reservoirs. Treiber and Owens (1972) studied, using contact angle method, wettability of 55 reservoirs of which 66 percent were oil-wet, 27 percent water-wet and 7 percent intermediate-wet. When differentiating reservoirs by mineralogy, on 30 siliceous reservoirs, 13 are water-wet, 15 oil-wet and 2 are intermediate-wet. Also, out of 25 carbonate reservoirs, 22 are oil-wet, 2 water-wet and 1 intermediate-wet. All these reservoirs range in depths from 1,770 to 13,000 ft., temperatures from 80° to 240 °F and gravity from 14° to 50° API. However, it is important to point out that all these reservoirs were Amoco operated and under flooding methods, so original wettability might be altered by additives in water flooding. In addition, Chilingar and Yen (1983) studied 161 carbonate reservoirs from different parts of the world by contact angle, and 80 percent of them were oil-wet or strongly oil-wet. Downs and Hoover (1989) also corroborated these observations.

The change in wettability from originally water-wet to oil-wet in some conventional reservoirs is primarily due to the adsorption of migrated crude oil polar components, mainly asphaltenes, onto the rock surface (Anderson 1986b, Babadagli, Al-Bemani, and Boukadi 1999, Mohammed and Babadagli 2015, Anderson 1986a, Basu and Sharma 1997, Buckley, Liu, and Monsterleet 1998, Salehi, Johnson, and Liang 2008,

Standnes and Austad 2000b). Moreover, Buckley, Liu, and Monsterleet (1998) identified wettability alteration factors by crude oils such as surface precipitation, acid/base interactions to control surface charges and ion binding interactions among oil, brine and rock, so carbonate rocks with positive charges would attract acidic oil compounds and sandstones would have higher affinity to basic oil compounds.

Altering wettability in reservoir rocks has the specific purpose of changing internal forces that govern fluid flow on the matrix and subsequently to the wellbore to increase hydrocarbon production. Several studies have been performed to enhance oil recovery in conventional reservoirs, mainly fractured carbonates and sandstones, using wettability alteration by anionic, cationic and nonionic surfactants (A. and M. 2008, Austad et al. 1998, Austad and Milter 1997a, b, Chen et al. 2001, Hirasaki and Zhang 2004, Kumar, Dao, and Mohanty 2008, Standnes and Austad 2000b, a, Zhang and Austad 2005, Kao et al. 1988, Downs and Hoover 1989, Zhang et al. 2006, Gupta and Mohanty 2011). However, these studies have limited application in ULR due to their petrophysical properties such as low porosities, ultralow permeability, mixed lithology and TOC content, some of these methods and studies have limited application in ULR. For example, wettability measurement methods used, surfactant additive purposes and forces that contribute to imbibition may vary from conventional to unconventional reservoir analysis. The fact that liquids cannot flow through these rocks due to their low porosity and ultralow permeability creates a challenge for IOR in ULR in which water and chemical flooding is a limited option.

Wettability and Imbibition in Unconventional Liquid Reservoirs

Unconventional liquid resources, specifically shales, have distinct characteristics that make them apart from conventional reservoirs. Their heterogeneity in mineralogy from play to play (Barnett, Eagle Ford, Bakken, Wolf-camp, etc.) and even in the same reservoir with depth (from siliceous to carbonate rocks in the same well), make wettability characterization much more complicated. In addition, the presence of organic matter as kerogen material creates a mixed wettability due to water-wet inorganic pores and oil-wet organic pores (Handwerger, Keller, and Vaughn 2011, Odusina, Sondergeld, and Rai 2011). As an example from the information showed Table 1, Odusina, Sondergeld, and Rai (2011) analyzed 50 samples from Eagle Ford, Floyd, Barnett and Woodford using NMR. They found that rocks imbibe both brine and oil as an evidence of mixed wettability being organics the responsible of oil-wetness. In addition, Wang et al. (2012) studied the wettability from three wells at different depths in Bakken formation using modified Amott-Harvey method, the results indicated that shale cores generally were oil-wet to intermediate-wet. These findings were also corroborated by Shuler et al. (2011) among few others. Nevertheless, further wettability characterization for unconventional resources is needed in order to have more comprehensive data base (Alvarez and Schechter 2016b).

The recent use of ULR as a source of liquid hydrocarbons has caught the attention of the industry in regards to wettability alteration and imbibition in ultralow permeability reservoirs. Currently, there is scant literature on wettability alteration and imbibition in ULR, and the most relevant is described next.

Shuler et al. (2011) studied the performance of fifteen different types and mixtures of anionic and nonionic surfactants to be added to frac fluids in cores from the Middle Bakken Shale (permeability from 2 to 10 mD) at 185 °F (a few degrees lower than reservoir temperature, which is over the water boiling point). After compatibility tests with frac fluids, only seven surfactants remained and the authors evaluated wettability alteration and oil recovery by spontaneous imbibition using Amott cells. Amott cells is a device in which the core is submerged into the fluid of study in a closed cell. The cell has in the top a graduated cylinder in which oil recovered can be measured. A few hours after the cores were submerged in surfactant solutions at 0.1 wt.%, oil was recovered in a range from 15 to 60% of original oil in place (OOIP). Conversely, the cores evaluated with only frac water recovered only 3% of the OOIP. It was also reported that the surfactants with the best percentage of oil recovered lowered the most IFT whereas the ones that recover the least did not reduce IFT in great amount. The authors did not disclose which surfactant, anionic or nonionic, shows the best performance in recovering oil. In addition, it is assumed that wettability is altered due to the spontaneous imbibition of frac fluids into originally oil to intermediate-wet cores; however, wettability was not measured. For the results, the authors concluded that adding surfactants to frac fluids increased oil recovery from Bakken Shale when hydraulically fractured.

In order to study the impact of adding either non-emulsifying or weakly emulsifying surfactants into completion fluids to enhance oil production, Xu and Fu (2012) used crushed Eagle Ford samples to increase their surface area. The crushed material was saturated with oil from the same reservoir and packed in a pressure column.

Then, surfactant solutions were flooded through this porous medium to evaluate oil recovery. The results showed that weakly emulsifying surfactant recovered more oil than non-emulsifying surfactant by reducing capillary pressure. The authors determined that rock wettability was altered by surfactants using the Washburn method, but no direct wettability measurement was performed. In addition, a case study was presented for six wells in the Eagle Ford with similar geological characteristics in which three wells were hydraulically fractured using weakly emulsifying surfactant and the other three using non-emulsifying surfactant. Based on the production history of the wells up to 45 days after stimulation, the wells fracked with weakly emulsifying surfactant produced about 25% more oil and 50% more gas than the ones fracked with non-emulsifying surfactant. These results are explained by the fact that weak surfactant emulsions can solubilize oil droplets into their micelles and transport them out of pores by reducing interfacial tension. However, the authors pointed out that ultralow IFT might cause oil redeposition in the rock surface.

Next, Wang et al. (2012) experimented on wettability alteration in oil to intermediate-wet shale cores from the Middle and Upper Bakken by surfactants formulations. They tested four surfactants, one zwitterionic (0.1 wt.%), one nonionic (0.05 wt.%) and two anionic (0.1 wt.%), at reservoir conditions of 194 to 248 °F and high formation water salinity (300,000 mg/L) in cleaned and uncleaned cores with juxtaposed layer of siltstone, limestone and dolomite. Middle Bakken has an average permeability and porosity of 7 mD and 4.4%, respectively whereas Upper Bakken has similar porosity values, but two to three orders of magnitude less permeability values. Wettability

alteration and oil recovery was measured using a modified Amott-Harvey method to avoid precipitation due to high temperatures and high salinities. Results showed that surfactants increased from 6.8 to 10.2% of the OOIP over experiments performed with brine alone. Also, from the evaluated surfactants, anionic surfactants showed higher oil recovery than zwitterionic and nonionic surfactants. Regarding different parameters such as temperature, porosity, preservation and core location into the reservoir, the authors could not find an identifiable trend in their results. Moreover, the modified Amott-Harvey method might not be suitable for shale plays with ultralow permeability, so this methodology may not be translated to other shale resources such as Eagle Ford or Barnett. This method requires flowing oil and water through the porous media, which is extremely hard in rocks with permeability on the micro and nano Darcy range. Finally, the authors concluded that surfactant solutions effectively altered wettability and imbibed into the shale cores recovering more oil than only brine and showing potential as an IOR method.

One year later, Kathel and Mohanty (2013) published their results on evaluating wettability alteration and oil recovery using eight anionic and three nonionic surfactants, all at concentration of at 0.1 wt.%, in a tight sandstone reservoir at 138 °F and salinity of 132,000 mg/L. Reservoir permeability ranged from 0.01-0.1 mD and porosity from 8 to 14%. Even though rock permeability is less than the one used by Shuler et al. (2011) and Wang et al. (2012), they are still high to the shale standards where permeability can vary from 10 to 1000 nD. Wettability was measured in polished and aged cristobalite plates by measuring contact angle before and after submersion in surfactant solution. The results showed that anionic surfactants could alter wettability from oil-wet to water-wet whereas

nonionic surfactants failed in shifting wettability. However, the effectiveness of nonionic surfactants increased as the ethoxy group number increased. Using the surfactants that alter wettability in contact angle tests (anionic), oil recovery was evaluated by spontaneous imbibition experiments in tight sandstone rocks using Amott cells. The authors reported oil recoveries from 42 to 68% of the OOIP in imbibition experiments and proposed a countercurrent flow due to capillary forces. This flow mechanism was corroborated using the inverse Bond number and observation of oil droplets on the core. Inverse Bond numbers were extremely high due to the reduced permeability, suggesting a process governed by capillary forces. Also, oil droplets appeared all over the core while submerged in surfactant solution as an indication of countercurrent imbibition. Finally, the authors reported increase in oil recovery rate with rising IFT, which is somewhat contrary to the statement formulated by Shuler et al. (2011).

A few months later, Nguyen et al. (2014) experimented with outcrops from Eagle Ford (porosities from 8 to 14%) and reservoir cores from Bakken (porosities from 5 to 6.5% and permeability from 0.002 to 0.09 mD). Two cationic, three nonionic, two zwitterionic, three anionic and blends at concentration from 0.1 to 0.2 wt.% were tested in a 27 wt.% brine for Bakken and 2 wt.% brine for Eagle Ford at reservoir temperatures from 194 to 248 °F. Spontaneous imbibition experiments were performed in Amott cells at reservoir temperature. The results showed that in Bakken formation all surfactants improve oil recovery in spontaneous imbibition experiments with nonionic surfactant being the most effective with almost 56% of OOIP followed by anionic surfactants. Cationic surfactants recovered the least amount of oil from the reservoir cores with 24%

of OOIP. In Eagle Ford, anionic surfactants recovered 48% of the OOIP and cationic surfactants 38% and 23% of OOIP. However, for the second cationic surfactant, brine alone was better in recovering oil (30% of OOIP). The authors failed in properly measuring contact angles, and they were qualitatively measured just by dispensing a brine drop to the shale surface. This measurement is not reliable, so it is hard to relate recovered oil with wettability alteration. The authors also concluded that wettability alteration is the main mechanism for oil recovery because they did not find correlation with IFT and recovered oil. Finally, they proposed a flow mechanism influenced by capillary imbibition and gravity forces based on the appearance of oil droplet on the top and sides of the cores during spontaneous imbibition experiments.

In addition, Mirchi et al. (2014a) and Mirchi et al. (2014b) studied anionic and nonionic surfactants, respectively, at concentrations from 0.01 to 0.1 wt.% in an undisclosed ULR with porosities from 1.3 to 1.6% at 176 °F. They studied surfactant adsorption by ultra violet-visible (UV-Vis) spectroscopy for both surfactant types concluding that they follow Langmuir type isotherms with low values (0.5 mg/g for anionic and 3 mg/g for nonionic surfactant) with maximum adsorption near the CMC. Also, IFT decreases from 23 to 0.3 mN/m in anionic surfactants and from 27 to 15 mN/m in nonionic surfactants at reservoir conditions. However, the authors affirmed that anionic surfactants increase contact angle in an originally weak water-wet system, and nonionic surfactants do not change contact angle in an originally strongly water-wet system. The authors did not perform oil recovery experiments, so the implication of decreasing IFT

and changing contact angle by different surfactant types was not related to imbibition and oil recovery as in the previous studies.

Moreover, Feng and Xu (2015) tested anionic and cationic surfactants using crude oil from different shale plays in the US. They measured total acid number (TAN) and total base number (TBN) to better relate rock surface and oil electrostatic charges when in contact with amphiphilic compounds. For IFT measurements, the authors found that Eagle Ford oil with higher TAN tends to have lower IFT when contacted with cationic surfactant, whereas oil with higher TBN have lower IFT when contacted with anionic surfactant. This proved that electrostatic interactions between the fluids played a main role in IFT reduction. Then, surfactants, anionic and cationic, were flooded through oil-saturated crushed Berea sandstone and Indiana limestone to represent the siliceous and carbonate reservoir environments; the results showed better oil recovery in oil saturated carbonates with higher TAN by cationic surfactants and better oil recovery in oil saturated carbonates with higher TBN by anionic surfactants. However, the authors did not use actual ULR core samples, so factors inherent to shale rocks such as TOC, surface area and clay content were not considered. These results suggest that ion-pair formation mechanism is responsible for wettability alteration driven by electrostatic interactions.

Wang et al. (2016) performed spontaneous imbibition experiments with different surfactants on cores from the Middle Member of the Bakken formation (permeability from 0.009 to 0.096 mD and porosities from 4 to 8%), recovering close to 32% of the OOIP (20% over brine alone). In addition, they observed that the imbibition rates varied inversely with time with most of the oil recovered in the first hours of surfactant exposure.

The authors then scaled up their results, suggesting that surfactant imbibition can increase primary production rates when natural fractures are connected to the induced hydraulic fractures. However, the authors did not disclose the surfactant type used in their work.

Most recently, Xu et al. (2015) performed core-flooding in artificially fractured cores from a liquid-rich play in Texas using anionic and nonionic surfactants. The results showed that both surfactants penetrated further into the rock than water alone as calculated by CT scan technology. Also, the authors claimed that reducing IFT improved surfactant penetration into the matrix and oil recovery. However, the authors did not address wettability changes to correlate their results. Moreover, oil recovery values are not reported to support some of their conclusions.

In addition to the listed existing literature about wettability alteration and its impact in oil recovery in ULR, this investigation has already published three papers, Alvarez et al. (2014), Alvarez and Schechter (2017) and Alvarez and Schechter (2016a) addressing wettability and IFT alteration and completion fluid imbibition in Barnett, Wolfcamp, and Bakken, respectively. Some of the authors mentioned in this section in fact used some of the experimental procedures proposed in these published studies.

From the available studies in wettability alteration in unconventional liquid reservoirs reported in this section, it can be seen that the industry has developed a growing interest in this area but the literature on wettability alteration and its potential for IOR is still sparse. In addition, some of these studies either did not reveal surfactant types used or measured wettability and oil recovery by methods that do not represent the phases interacting in the reservoir and may not be suitable for ultralow permeability ULR. Hence,

there is a lack of a standardized experimental procedure to successfully evaluate the impact of wettability and IFT alteration in ULR as well as a detailed correlation of the factors involved in oil recovery by imbibition when surfactants are added to completion fluids.

IOR processes are designed to improve water imbibition by capillary and/or gravity forces. Imbibition is responsible for recovering oil in water-wet systems due to the release of oil from the matrix replaced by water. The forces that contribute to imbibition and drainage of oil by water are capillary, gravitational and viscous forces. Capillary and gravitational forces are related by the inverse Bond number (**Eq. 7**) (Du Prey 1978, Schechter, Zhou, and Orr Jr 1994). This number quantify the ratio of capillary to gravitational forces, and it is applied to determine if imbibition is driven by gravitational forces as cocurrent flow or capillary forces as countercurrent flow. The inverse of the Bond Number (N_B^{-1}) is shown as follows:

$$N_B^{-1} = C \frac{\sigma \sqrt{\frac{\phi}{k}}}{(\Delta\rho)gh} \quad \dots \quad (7)$$

where C is a constant related to pore geometry, σ is IFT, ϕ is porosity, k permeability, Δp density difference of the immiscible fluids, g the gravitational acceleration and h the length of the studied core. Schechter, Zhou, and Orr Jr (1994) concluded for low IFT imbibition that when N_B^{-1} is bigger than 5, capillary forces are responsible for imbibition with a countercurrent flow. Conversely, when N_B^{-1} is smaller than 1, gravitational forces govern with a cocurrent flow. Finally, N_B^{-1} numbers between

1 and 5 have contribution of both capillary and gravitational forces. It is important to have in mind that the values reported by (Schechter, Zhou, and Orr Jr 1994) were obtained for a controlled system and the range might change for different lithologies and fluids. Nevertheless, inverse bond number relation is widely used when studying imbibition mechanisms on experimental trials, and gives an interesting insight for unconventional resources. In ULR, permeability values are extremely low which gives high inverse bond numbers. This is a clear indication that capillary forces are greater than gravitational forces and are the ones that control imbibition in ULR.

The effect of wettability in capillary pressures is determined by the contact angle of two immiscible fluids and the rock surface. From Eq. 1, in a water-wet system, contact angles are less than 90 degrees, which leads to positive capillary pressure values. In contrast, in an oil-wet system, contact angles are greater than 90 degrees, resulting in negative capillary pressure values. To achieve water imbibition into the matrix, and consequently displace oil from the pores and rock surface, capillary pressure must be greater than zero indicating water-wet behavior. Hence, when wettability is altered, it changes capillary pressure from negative to positive favoring imbibition. In addition to wettability values, IFT plays an important role in imbibition because capillary pressure is proportional to the product of IFT and the cosine of contact angle.

In both conventional and unconventional reservoirs, wettability is altered to favor spontaneous imbibition in the matrix and to let the oil be displaced by water. This process can ultimately favor IOR; however, there is an important distinction in its application between conventional and unconventional reservoirs. In conventional reservoirs, EOR

processes are achieved by injecting fluids such as water with additives (surfactants, ions/salts, among others) that can alter wettability in the rocks and remove oil from bypassed pores in which water by itself could not overcome capillary forces, and by increasing temperatures in processes such as steam injection to thermally induce wettability reversal to favor steam or water imbibition into the matrix.

On the other hand, in unconventional reservoirs, IOR processes are under early research stages due to the complexity of the matrix in terms of petrophysical properties. Ultralow permeability limits fluid flow in the reservoir and horizontal wells combined with multiple hydraulic fracture techniques must be applied to produce these resources at commercial flow rates. Once matrix-fracture interaction is enhanced and effective paths for hydrocarbons to flow towards the wellbore are created, capillary imbibition becomes an important recovery mechanism for producing hydrocarbons due to the reduced reservoir pore size. Hence, wettability alteration in ULR is not meant to be used in water flooding nor as a thermal recovery method, but as an IOR method while fracking the formation by adding additives in the completion fluids. Having in mind capillary pressure equation (Eq. 1), ULR have nanoscale pore sizes, which increase capillary pressures binding oil to the matrix and limiting primary oil recovery. Pore size is a property of the rock that cannot be altered by physical or chemical means; on the other hand, wettability can be altered to change capillary pressures and favor water imbibition into the rock. This completion fluids imbibition can increase the current ULR recovery factor of 5 to 6% to higher values recovering more reserves and making the exploitation of unconventional liquid resources more profitable.

Scaling Models for Imbibition

Mattax and Kyte (1962) studied oil recovery by imbibition in fractured and water-wet reservoirs. Using imbibition theory and experimental work, they showed that the square of the distance between fractures is proportional to the time needed to recover oil from a matrix block. Hence, oil recovery can be scaled for a determined rock type and oil-to-water viscosity ratio by the following dimensionless time (t_D). This scaling group represents an inverse of the capillary number as the ratio capillary forces to viscous resistance (Morrow and Mason 2001). This is demonstrated by the Eq. 8.

$$t_D = t \sqrt{\frac{k}{\phi}} \frac{\sigma}{\mu_w L^2} \dots \dots \dots \quad (8)$$

where t is the actual time of imbibition, k and ϕ are permeability and porosity respectively, σ is IFT, μ_w is water viscosity and L is the block dimension. Experimentally, the authors verified the imbibition theory and oil recovery factors by addressing the impact of block size, permeability and viscosity, and concluded that laboratory results can be scaled to reservoir blocks to predict oil recovery by imbibition. However, this study is based on the assumptions that there is a negligible amount of oil as well as fluid flow resistance in the fractures compared to the matrix. Also, as evidenced in Eq. 8, gravitational forces are negligible compared to capillary forces.

Mattax and Kyte (1962) performed brine imbibition experiments using alundum (synthetic material) and sandstone cores with final recoveries of around 65 and 48% of the

OOIP respectively. Imbibition data for scaling was obtained by having very similar sample shapes, boundary conditions oil/water viscosity ratios, relative permeability and initial fluid distribution. These conditions can be difficult to satisfy in a more heterogeneous system with varying sample sizes. Consequently, more than 30 years later, Ma, Morrow, and Zhang (1995) redefined the dimensionless time to take into account different samples sizes, shape and boundary conditions with different oil-water viscosity ratios and by introducing a generalized characteristic length (L_c) as shown on **Eq. 9**. The main change of this group was the consideration that oil recovery is inversely proportional to the geometric mean of the water and oil viscosities.

$$t_D = t \sqrt{\frac{k}{\phi}} \frac{\sigma}{\sqrt{\mu_o \mu_w}} \frac{1}{L_c^2} \dots \dots \dots \quad (9)$$

where t is the actual time of imbibition, k and ϕ are permeability and porosity respectively, σ is IFT, μ_w and μ_o are water and oil viscosity. The characteristic length (L_c) consider countercurrent imbibition, different boundary conditions and sample geometry, and it is represented in **Eq. 10**, where V is the bulk volume, A is the area of the face open to imbibition and X_A the distance of the face to the no-flow boundary.

$$L_c = \sqrt{\frac{V}{\sum_{i=1}^n \frac{A_i}{X_i A_i}}} \dots \dots \dots \quad (10)$$

In addition, the geometric mean of oil and water viscosities attempts to address the viscosity assumptions raised by Mattax and Kyte (1962). However, this viscosity correlation is empirical, and Zhang, Morrow, and Ma (1996) noticed that their air-liquid results did not correlate with oil-water systems. Hence, correlation in Eq. 9 does not apply when gas is the wetting phase because imbibition is much slower than the values predicted by the geometric mean of viscosities. Regardless, the lack of correlation of air-liquid systems, Zhang, Morrow, and Ma (1996) experimentally corroborated by using Berea sandstone cylindrical cores that, for different viscosity ratios, boundary conditions and lengths, close correlation was achieved using the scaling group in Eq. 9.

It is important to notice that both scaling methods (Eq. 8 and 9) are for strongly water-wet systems and do not consider changes in wettability and IFT. Also, both methods accounted for variation in rock properties by the use of Leverett microscopic radius (**Eq. 11**) (Leverett 1939).

Taking the work done by Ma, Morrow, and Zhang (1995), Fischer, Wo, and Morrow (2008) defined characteristic lengths for different boundary conditions and flow regimes shown in **Table 2**, after Fischer, Wo, and Morrow (2008). They used spontaneous imbibition data from Berea sandstone to match their correlations and predictions with close agreement. Also, they concluded that for all open faces boundary condition, the most

common laboratory setup for imbibition experiments (Cylindrical - All-faces-open), oil recovery can be estimated by a mix of radial and spherical flow.

Table 2. Flow regimes and characteristic lengths for scaling imbibition data.

Boundary Condition	Flow Regimes	Characteristic Length (L_c)
Open-end-open	Linear	$L_c = l$
Two-ends-open	Radial	$L_c = \frac{d}{2\sqrt{2}}$
Cylindrical (All-faces-open)	Complex	$L_c = \frac{ld}{2\sqrt{d^2 + 2l^2}}$
Sphere	Radial (3D)	$L_c = \frac{d}{2\sqrt{3}}$

Gupta and Civan (1994) and Guo, Schechter, and Baker (1998) worked in addressing the fact that the scaling group proposed by Ma, Morrow, and Zhang (1995) did not consider pore surface wettability; hence, they introduced the effect of wettability in the scaling group as the cosine of the contact angle. This case represented better a wide variety of reservoirs which wettability ranges from oil to water-wet. The dimensionless time was modified as presented in **Eq. 12**.

$$t_D = t \sqrt{\frac{k}{\phi} \frac{\sigma \cos \theta}{\mu_o \mu_w} \frac{1}{L_c^2}} \dots \dots \dots \quad (12)$$

where θ is then contact angle and all other parameters the same as in Eq. 9. Gupta and Civan (1994) used experimental data from previous studies such as Mattax and Kyte (1962) and Cuiec, Bourbiaux, and Kalaydjian (1994) to show improved correlation amongst the imbibition recovery for samples with different rock properties, boundary conditions and sizes. This correlation was successfully used in sandstones (Mattax and Kyte 1962) and low-permeability chalk (Cuiec, Bourbiaux, and Kalaydjian 1994). On the other hand, Guo, Schechter, and Baker (1998) used low permeability naturally-fractured Spraberry Trend Area siltstones with significantly lower imbibition rates than Berea sandstones.

Next, Zhou et al. (2002) performed countercurrent imbibition experiments with low permeability diatomite cores using CT scan methods. They emphasized that imbibition rate has a strong correlation with wetting and non-wetting phase viscosities, and the viscosity ratio between wetting and non-wetting fluids can vary in several orders of magnitude. In fact, they concluded that the imbibition rate slows and saturation patterns become progressively diffuse when viscosity ratio increases. Thus, the authors presented a modified scaling group that incorporates mobility ratio in the dimensionless time, which is shown in **Eq. 13**.

$$t_D = t \sqrt{\frac{k}{\phi L_c^2}} \sqrt{\lambda_{rw}^* \lambda_{rmw}^*} \frac{1}{\sqrt{M^*} + \frac{1}{\sqrt{M^*}}} \quad \dots \dots \dots \quad (13)$$

$$\lambda_r^* = \frac{k_r^*}{\mu} \quad \dots \dots \dots \quad (14)$$

$$M^* = \frac{\lambda_{rw}^*}{\lambda_{rnw}^*} \dots \dots \dots \dots \dots \quad (15)$$

where λ_r^* (**Eq. 14**) is the characteristic mobility for the phases and M^* (**Eq. 15**) is the characteristic mobility ratio. This scaling group is based under the assumption that capillary pressures and relative permeability are similar for all experiments, and it considers the end-point fluid phase mobility and mobility ratio in the imbibition rate. However, it does not directly take into the account the wettability as Gupta and Civan (1994) and Guo, Schechter, and Baker (1998) expressions, whereas it is considered in the mobility ratio, which depends on the viscosity of the fluids and the wettability of the system.

A few years later, Li and Horne (2005) and Li and Horne (2006) theoretically developed a scaling expression for imbibition experiments that considered all the previous parameters such as permeability, shape, size, boundary conditions, wetting and non-wetting relative permeability, porosity, wettability and IFT as well as the effect of gravity. In previous correlations, it was always assumed the gravitational forces were negligible due to the strongly water-wetness of the rock. However, when dealing with different wettability and reducing IFT by the addition of chemical additives, capillary forces may not be neglected as stated by Schechter, Zhou, and Orr Jr (1994). The dimensionless time is shown in **Eq. 16**.

$$t_D = c^2 \frac{k k_{re}^* P_c^*}{\phi \mu_e} \frac{S_{wf} - S_{wi}}{L_a^2} t \quad \dots \dots \dots \quad (16)$$

where c is a parameter that relates the ratio of gravitational to capillary forces and it is calculated using **Eq. 17** to **Eq. 22**, k and k_{re}^* are the absolute permeability and the relative permeability pseudo function associated with the non-wetting phase relative permeability at S_{wf} (k_{ro}^*) and the water phase relative permeability at S_{wf} (k_{rw}^*). P_c is the capillary pressure at S_{wf} , μ_e is the effective viscosity of the non-wetting phase and wetting phases and L_a is the characteristic length.

$$c = \frac{b_o}{a_o} \quad \dots \dots \dots \quad (17)$$

where a_o and b_o are constants representing the capillary and gravitational forces respectively, and they can be found as linear correlation (Eq.17) of the imbibition rate (R) and the reciprocal of the spontaneous imbibition recovery fluids-rock systems. In addition, constants a_o and b_o can be calculated using Eq. 18 to 22, where M_e^* varies depending the type of imbibition; for cocurrent movement, **Eq. 21** is used whereas for countercurrent imbibition, **Eq. 22** applies. Finally, if constants a_o and b_o are determined by the linear correlation using experimental results, capillary pressures and global mobility can be calculated using **Eq. 23** and **24**.

$$q_w = a_o \frac{1}{R} - b_o \quad \dots \dots \dots \quad (18)$$

where a_o and b_o are defined as follows:

$$a_o = \frac{AM_e^*(S_{wf} - S_{wi})}{L} P_c^* \quad \dots \dots \dots \quad (19)$$

$$b_o = AM_e^* \Delta \rho g \quad \dots \dots \dots \quad (20)$$

where M_e^* is represented as for cocurrent and countercurrent imbibition respectively,

$$M_e^* = \frac{k k_{re}^*}{\mu_e} = \frac{M_w^* M_{nw}^*}{M_{nw}^* - M_w^*} \quad \dots \dots \dots \quad (21)$$

$$M_e^* = \frac{M_w^* M_{nw}^*}{M_w^* + M_{nw}^*} \quad \dots \dots \dots \quad (22)$$

$$P_c = \frac{1}{S_{wf} - S_{wi}} \frac{a_o}{b_o} \Delta \rho g L \quad \dots \dots \dots \quad (23)$$

$$M_e^* = \frac{b_o}{A \Delta \rho g} \quad \dots \dots \dots \quad (24)$$

The authors used experiment results from Schechter, Zhou, and Orr Jr (1994) to confirm their model. Li and Horne (2005) and Li and Horne (2006) confirmed Schechter, Zhou, and Orr Jr (1994) observations that imbibition rate can increase even when IFT is reduced by the addition of gravitational forces in their dimensionless time equation.

Another important contribution was the introduction of the linear correlation of imbibition rate to the reciprocal of the recovery, verified using experimental data. Lastly, it is valuable to notice that without taking into account the wettability, relative permeability, initial fluid saturation and gravitational forces impact, Li and Horne (2005) and Li and Horne (2006) scaling group would look like the one proposed by Mattax and Kyte (1962) and modified by Ma, Morrow, and Zhang (1995).

Most recently, Schmid and Geiger (2012) derived a scaling group for imbibition that attempted to incorporate all the information in the two-phase Darcy model. It relates the cumulative water imbibed to the normalized pore volume by using analytical solutions of the Darcy equation for spontaneous imbibition avoiding the use of fitting parameters. The dimensionless time is shown in **Eq. 25**.

$$t_D = \left[\frac{Q_w(t)}{\phi L_c} \right]^2 = \left[\frac{2A}{\phi L_c} \right]^2 t = \tau_c t \quad \dots \dots \dots \quad (25)$$

where $Q_w(t)$ is the cumulative water imbibed (**Eq. 26**), ϕ is the porosity and L_c is the characteristic length.

$$Q_w(t) = \int_0^t q_w(0, t) dt = 2At^{\frac{1}{2}} \quad \dots \dots \dots \quad (26)$$

A is a parameter that depends on the fluid-rock system characteristics as defined in **Eq. 27**.

where $D(S_w)$ is the capillary dispersion coefficient of the fluid phases and $F(S_w)$ is the fractional flow for countercurrent imbibition. Finally, τ_c is the parameter that takes into account the effect of capillary properties and the physical dimensions (Schmid and Geiger 2012). The authors showed the close correlation of several published experimental data with different lengths, material, initial water content and viscosity ratios. Because the model was derived from Darcy equation, it can also be used to predict if Darcy flow model applies for representing spontaneous imbibition in porous media. This may be very useful to address the validity of Darcy flow in ultra-low permeability reservoirs. However, contrary to the model proposed by Li and Horne (2005) and Li and Horne (2006), this scaling group assumes only water-wet systems, so does not consider changes in wettability and neglects the effect of gravitational forces.

Currently, there is only one study in the literature performing laboratory data scaling for spontaneous imbibition experiments in unconventional liquid reservoirs. Wang et al. (2016) scaled laboratory experiments from Bakken cores with permeability of 0.0015 to 0.096 md and porosity from 4 to 8%. The authors applied analytical models to scale laboratory imbibition data to a field scale in fractured shale formations by using the dimensionless time proposed by Mattax and Kyte (1962) and modified by Ma, Morrow, and Zhang (1995). Four cases were analyzed by varying the presence of induced and natural fractures to address the impact of fracture density. Besides the assumptions adopted by (Mattax and Kyte 1962) when developing the dimensionless time (t_D) in Eq.

7, the authors assumed that t_D has the same value in a lab core as in the field, at the time half of the oil has been displaced from the rock. The authors concluded that, to economically produce liquid hydrocarbons from Bakken typical well, natural fractures must be present in high densities and connected to hydraulically induced fractures. In addition, they found that oil production rates obtained considering the imbibition process were significantly greater than typical rates achieved by primary production in Bakken formations. However, the authors did not consider the effect of wettability on the scaling models as in the model developed by Gupta and Civan (1994) and Guo, Schechter, and Baker (1998) (Eq. 12).

In summary, in the literature there are several studies attempting to scale imbibition experiments in conventional reservoirs. Each of them has its assumptions and limitations. In this investigation, some of the described scaling groups will be evaluated to match experimental results originated from this work and compared to address their validity in ULR.

CHAPTER III

METHODOLOGY *

This study investigates the interaction of completion fluids and unconventional liquid reservoirs when chemical additives are added. In addition, it addresses the effect of wettability, IFT, adsorption and imbibition on recovering hydrocarbons from liquid-rich shale cores from the Wolfcamp, Bakken, Eagle Ford and Barnett formations. These objectives are achieved by performing contact angle, zeta potential, adsorption and IFT measurements, as well as spontaneous imbibition and core-flooding experiments, at reservoir conditions, monitored by computer tomography (CT) methods. In addition, this methodology seeks to address the interactions between rock lithology and different surfactant groups and their impact on oil recovery. Hence, this chapter describes a novel

* Parts of the methodology presented in this chapter have been reprinted from:

“Wettability, Oil and Rock Characterization of the Most Important Unconventional Liquid Reservoirs in the United States and the Impact on Oil Recovery” by J.O. Alvarez and D.S. Schechter. URTEC Paper 2461651. Copyright 2016 by the Unconventional Resources Technology Conference (URTEC). Reproduced with permission of URTEC. Further reproduction prohibited without permission.

“Impact of Surfactants for Wettability Alteration in Stimulation Fluids and the Potential for Surfactant EOR in Unconventional Liquid Reservoirs” by J.O. Alvarez, A. Neog, A. Jais and D.S. Schechter. SPE Paper 169001. Copyright 2014 by the Society of Petroleum Engineers (SPE). Reproduced with permission of SPE. Further reproduction prohibited without permission.

“Wettability Alteration and Spontaneous Imbibition in Unconventional Liquid Reservoirs by Surfactant Additives” by J.O. Alvarez and D.S. Schechter. SPE Reservoir Evaluation & Engineering. Volume 20. Issue 1. Copyright 2017 by the Society of Petroleum Engineers (SPE). Reproduced with permission of SPE. Further reproduction prohibited without permission.

“Potential of Improving Oil Recovery with Surfactant Additives to Completion Fluids for the Bakken” by J.O. Alvarez, I. W. Rakananda Saputra and D.S. Schechter. Energy & Fuels. Volume 31. Issue 6. Copyright 2017 by American Chemical Society (ACS). Reproduced with permission of ACS. Further reproduction prohibited without permission.

set of correlated experiments to evaluate and compare the efficiency of surfactants in altering wettability and recovering hydrocarbons from unconventional liquid reservoir core (Alvarez and Schechter 2016b).

Rock Petrophysical Characterization

Characterizing the samples used in this study is vital to understanding wettability and oil recovery mechanisms. ULR petrophysical properties such as permeability, porosity, and pore size distribution as well as X-Ray Diffraction Analysis (XRD) analyses from the Wolfcamp, Bakken, Eagle Ford and Barnett core were determined to characterize the unconventional rock (Alvarez and Schechter 2016c).

X-ray diffraction analysis

ULR Lithology was determined by x-ray diffraction analysis (XRD); samples were disaggregated with a mortar and pestle, grounded in a micronizing mill to approximately 40 microns, packed into sample holders and analyzed on a Rigaku MiniFlex 600 X-Ray Diffractometer. The X-Ray tube was operated at 40 kV and 15 mA and completed scans were interpreted and quantified using "Whole Pattern Profile Fitting" with refinement based on ICDD/NIST/FIZ databases.

Total organic carbon analysis

In order to determine organic matter, ULR total organic carbon (TOC) was measured. Samples were cleaned and crushed to pass through a 50-mesh screen and dried at 60 °C overnight to remove any excess moisture. Then, 100 mg of material was placed in a filtering crucible and acidized with 19% hydrochloric acid to remove the inorganic carbon. Next, the acidized material was filtered and rinsed with deionized water and dried overnight 60 °C. Finally, total carbonate weight percent was determined by weight loss between raw and acidized material. The material was then analyzed on a LECO C230 Carbon Analyzer to determine TOC content.

Scanning electron microscopy

Energy Dispersive x-ray Spectroscopy was used to confirm the mineralogy of the samples. The samples were mounted so that an unaltered interior surface was exposed, then coated with ionized gold using a backscatter shadow method.

Mercury injection capillary pressure

Mercury injection capillary pressure (MICP) analysis provided porosity, permeability to air and median pore-throat radius. Samples were extracted with toluene followed by methanol until clean. Then, the extracted solutions were exposed to fluorescence and silver nitrate tests to verify that samples were clean. To mitigate the effect of micro fractures on matrix properties, the core material was crushed and sieved. The material bigger than 35 mesh was used for the analyses. All samples were dried in a

convection oven at 100 °C for 24 hours. Next, samples were weighed and analyzed on the AutoPore IV device. Mercury was injected in 118 pressure increments up to a pressure of 60,000 psia. For pore size calculations, the Washburn equation (Washburn 1921) was used with mercury contact angle of 140° and IFT of 480 mN/m.

Fluid Characterization

Fluid properties such as API gravity, TAN, TBN and interfacial tension (IFT) were measured to characterize crude oils and brines (Alvarez and Schechter 2016c). Also, stability tests as prescreening tools for selecting the most stable chemical additives at reservoir conditions are described.

Total acid number and total base number

Total acid number (TAN) and total base number (TBN) of oil samples from Bakken, Eagle Ford, Wolfcamp and Barnett were analyzed in the 905 Titrando by Metrohm Titrator. For TAN, 0.1M KOH in isopropanol was used as titrant with a solution of 3 grams of oil and 60 ml of solvent (toluene, isopropanol, and water with a volume ratio of 500:495:5). For TBN, the solvent used was glacial acetic acid and toluene with a volume ratio of 1:1, and 0.1M HCl in isopropanol as titrant in 3 grams of oil and 60 ml of solvent was used.

Oil and brine density determination

Densities of oil and brine from Bakken, Eagle Ford, Wolfcamp and Barnett were analyzed in Anton Paar DM 4100 M density meter at room ambient and reservoir temperature and atmospheric pressure. The sample was dispensed in the device and the reading was taken when the reservoir temperature was stabilized.

IFT experiments

IFT experiments were performed using a Dataphysics OCA 15 Pro apparatus by the pendant drop method and a Grace Instruments M6500 Spinning Drop Tensiometer by spinning drop method at reservoir temperature using reservoir crude oil, brine and surfactants at the same concentrations as in the contact angle experiments. The pendant drop method is very reliable for IFT values higher than 1 mN/m; for lower values spinning drop method is used. These experiments will also help select proper surfactant type and concentration. Pendant drop bottoms up method aided by a video-based optical measurement system, as shown in **Fig. 5**, consisted on dispensing oil from the capillary needle into a frac fluid solution and measuring IFT when the drop leaves the needle. In addition, to verify low IFT values (less than 1 mN/m) a spinning drop tensiometer was used. Then, an oil drop was inserted inside the sample tube previously filled with frac fluid and rotated to deform the drop and calculate drop diameters. In both methods performed, density of the Wolfcamp, Bakken, Eagle Ford and Barnett crudes and frac fluids at reservoir temperature was used to calculate IFT. Error bars are assigned based on the experiment confidence level with upper and lower bounds of 0.2 mN/m. Using the same

solutions as those used in the CA and zeta potential experiments, IFT is determined as follows:

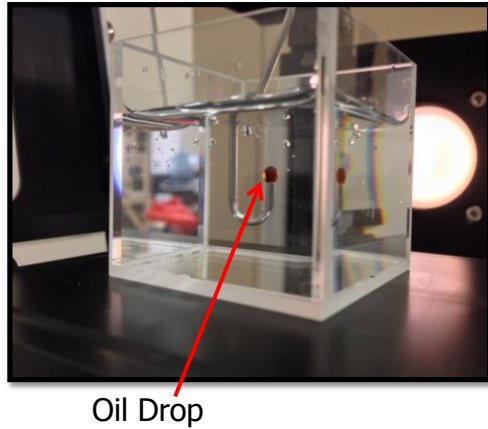


Figure 5. Experimental setup for measuring IFT. Reprinted with permission from Alvarez et al. (2014).

- a. Aqueous solutions, with and without surfactants, were placed inside a quartz cuvette and heated until reservoir temperature was reached.
- b. Crude oil from Wolfcamp, Bakken, Eagle Ford and Barnett wells was dispensed through a j-shaped capillary needle facing upwards into the aqueous solution. The experiment was recorded using a high-resolution camera and the frame that captured the moment when the drop was about to detach from the needle was used for analysis.
- c. Using the DSA software and the density at reservoir temperature of the oil and aqueous solutions, IFT values were calculated by fitting the drop shape profile to the Laplace equation.

Chemical additives stability tests

Stability tests were performed to select the most stable chemical additives at reservoir temperature for further experiments such as CA, zeta potential and IFT experiments. An aqueous solution of brine and chemical additives was mixed and kept at reservoir temperature for several days. In the same way, to test the emulsion tendency of these surfactants, the same solutions were mixed with dead crude oil at equal volumes and kept in the environmental chamber at reservoir temperature. The surfactant solutions that showed visible stability at reservoir temperatures were used in CA, zeta potential and IFT experiments.

In addition, to evaluate the possible impact of dopant in the aqueous solutions, a solution of distilled water, 4 wt.% KI and 2 gallons per thousand gallons (gpt) of surfactants were mixed and kept at reservoir temperature for 10 days. Moreover, to test the emulsion tendency of these surfactants, the same solutions were mixed with dead crude oil from Wolfcamp, Bakken, Eagle Ford and Barnett wells, at equal volumes, and kept in the environmental chamber for 10 days at reservoir temperature.

The conduction of further measuring experiments of contact angle, zeta potential and interfacial tension by selecting the most stable surfactant at the reservoir temperature is the stability experiment. Stable surfactants are picked by the stability experiment, especially when the surfactant is mixed with salt solution, because the salt solution might be unstable after addition of surfactants (Alvarez and Schechter 2016a).

Wettability Measurement Experiments

Original and altered wettability were measured by performing contact angle experiments between the oil and shale rock into the aqueous solution using the captive bubble method at reservoir conditions. This method gives a quantitative value to address original wettability and subsequent alteration by chemical additives. In addition, an exact CA value can be obtained to determine capillary pressures. Due to ULR petrophysical properties of ultralow permeability and low porosity, it is very difficult to flow any kind of fluids into the matrix. Consequently, other wettability measurement methods such as Amott-Harvey and USBM are impractical for micro and nano-Darcie permeability. The contact angle method requires only a smooth surface, which can be easily obtained in ULR cores. Even though contact angle measurements among oil, rock and air gives an indication of wettability, to represent reservoir conditions, contact angle is measured using oil, water and the rock. These experiments serve to determine original ULR wettability and to find proper surfactant type and concentration. In addition, to further qualitatively evaluate wettability changes and determine surface and surfactant charges, zeta potential experiments were used. Aqueous solutions and finely crushed trims from the ULR of study are mixed to measure the stability of the thin liquid film on the rock surface. This stability can give an indication of the water wetness of the sample.

Contact angle experiments

CA measurements were performed on a Dataphysics OCA 15 Pro device using the captive bubble method with the aid of a video-based optical measurement system. The

apparatus consists of the imaging system, dispensing system, and the heating system, all controlled by a drop shape analyzer (DSA) software. ULR rock wettability was determined by oil-rock CA in the presence of an aqueous solution with and without surfactants. Different surfactant types were tested at concentrations of 0.2, 1 and 2 gpt.

Rock trims from Wolfcamp, Bakken, Eagle Ford and Barnett wells, at different depths that in many cases represent siliceous and carbonate strata as shown, were cut and polished to minimize measurement errors due to surface roughness. Samples were cleaned with toluene and methanol to remove any contamination due to the preservation process. Then, trims were aged in well Wolfcamp, Bakken, Eagle Ford and Barnett oil at reservoir temperature for more than 6 months. The procedure is described below and illustrated in

Fig. 6:

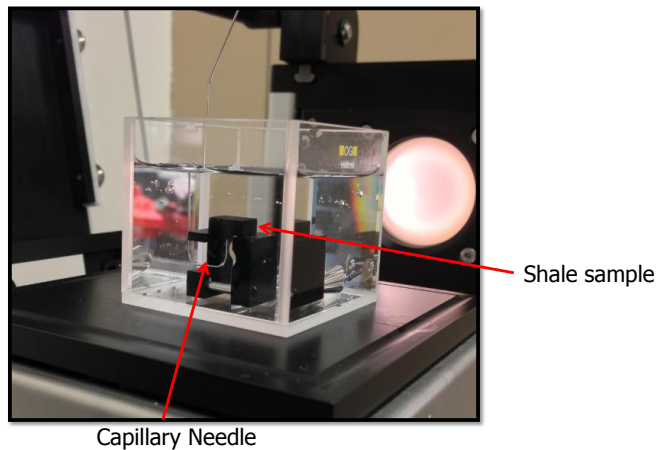


Figure 6. Experimental setup for measuring contact angle. Reprinted with permission from Alvarez et al. (2014).

- a. Aqueous solutions, with and without surfactants, were placed inside a quartz cuvette, and heated until reservoir temperature was reached using a temperature control unit of the heating system on the Dataphysics OCA 15 Pro device.
- b. Shale sample was placed on the holder inside the cuvette with temperature stabilized aqueous solution.
- c. Crude oil from Wolfcamp, Bakken, Eagle Ford and Barnett wells was dispensed throughout a j-shaped capillary needle such that the oil drop is pointing upwards onto the rock surface. Both the rock surface and the oil drop are in contact with the aqueous solution.
- d. The oil drop was slowly attached to the shale sample and enhanced video-image digitalization technique was used to measure the contact angle between the oil and shale surface.
- e. To assure symmetry of the drop shape, the angles measured on both sides of the drop should be as similar as possible ($\pm 1^\circ$).

In order to achieve repeatability and consistency of the measurements, five to seven trials for each sample were performed. Error bars are assigned based on the experiment confidence level with upper and lower bounds of 3 degrees.

Zeta potential experiments

Zeta potential measurements were performed on a NanoBrookTM ZetaPALS apparatus using the phase analytical light scattering (PALS) method. Aqueous solutions were tested to address the stability of surfactant solution films on the shale rock surface. The experiments were performed with the same surfactants and concentrations as those used for the CA experiments. The zeta potential device measures the electrophoretic velocity of the particles in the solution, calculates electrophoretic mobility from the electrophoretic viscosity, and finally evaluates zeta potential (Alvarez and Schechter 2017). The experimental steps are described next:

- a. Aqueous solutions were triple filtered by the aid of an Acrodisc syringe filter and placed in the measuring vial.
- b. Rock trims from Wolfcamp, Bakken, Eagle Ford and Barnett well, at two different depths from siliceous and carbonate layers, were finely crushed and passed through a 45- μm ASTM 325 sieve.
- c. For rock-brine measurements, 1 mg of crushed rock powder was added to 10 ml filtered solution in the vial, whereas for oil-brine solutions, 0.1 ml of crude oil was added to 10 ml of filtered solution.
- d. Aqueous and rock solutions were sonicated using QSonica ultrasonic processor probe at a frequency of 40 Hz for 1 minute. The sonicated solution was left to stabilize by letting it sit for 5-10 minutes so the heavy

insoluble particle could settle down. The waiting time was typically 24 hours for oil-brine measurements.

- e. The mixed solution was placed in the device and the electrode was inserted completely into the vial to measure zeta potential values.

Zeta potential measurements were conducted with frac water with and without surfactants and rock samples, as well as oil-water and oil-surfactant solutions. The pH values for all solutions were constantly monitored and their amounts remained constant during the experiments varying from 6.1 to 7.6 depending of the surfactant and brine studied. In addition, Zeta potential measurements are very sensitive to sample preparation and procedures; hence, special care must be taken when performing these experiments to assure repeatability and consistent results. Error bars are assigned based on the experiment confidence level with upper and lower bounds of 2 mV.

Surfactant Adsorption Experiments

Surfactant adsorption into the ULR during imbibition experiments is measured to establish the concentration in which surfactant remains effective. Surfactant absorbance at known concentrations are used to match surfactant samples that are taken with time during imbibition experiments. Using these concentration tests, curves of surfactant concentrations versus time are reported to address surfactant adsorption in different ULR.

This study also helps to determine the effect of lithology and oil type in chemical additive adsorption.

Surfactant adsorption on the ULR rock surface, as a function of time, is measured by calculating the concentration of the surfactant using an UV-Vis Spectrophotometer. A Hitachi U-4100 UV-Vis-NIR spectrophotometer is used with cuvette made from quartz to be able to project UV light through efficiently. The spectrophotometer is capable of producing light with specific wavelength, which will be shined through two solutions: the reference and sample solution. Water, with no surfactant additive added, is used as reference solution, while the sample solution is the surfactant solution from both calibration curve and adsorption experiment. Surfactant molecules present in the sample solution adsorb the light shined through them. According to Beer-Lambert Law (Ingle and Crouch 1988), the amount of light adsorbed is linearly related to the amount of surfactant molecule, where in this case is the surfactant concentration. Different molecules present in the solution show strong adsorption of light on different wavelength, which comes as an advantage, since it helps differentiate distinct substances in the solution. However, since the wavelength adsorbed most by the surfactant molecule is not known, a calibration curve must be built to: first, find the most adsorbed wavelength of each surfactant used by comparing wavelength scan results of different surfactant concentration, and second, build the calibration curve to correlate the amount of light adsorbed on that wavelength to the surfactant concentration in the solution. The wavelength scan is done by using a range of wavelengths (190 – 300 nm) through different solution with various surfactant concentration. Error bars are based on the UV-Vis spectrophotometer precision of 0.05

light absorbance for the range of wavelength utilized in the experiments. This error is used when calculating surfactant adsorption (Alvarez, Saputra, and Schechter 2017).

For the adsorption measurement, siliceous and carbonate ULR samples from wells in the Wolfcamp, Eagle Ford and Bakken are cleaned by soaking them first in toluene then methanol, for 3 days and 2 days consecutively, then vacuum-dried for 3 days. The cleaned samples are crushed then sieved through mesh N.50 resulting in rock particles with the size less than 300 μm . Rocks and surfactant solutions at 2 gpt are mixed in a 1:20 weight ratio at room temperature and are then put into a sealed beaker. Aqueous solution samples are taken at different times from 10 minutes to 24 hours. Before measuring the light adsorption of each time step, the solution is filtered through a 20 μm syringe filter to remove the rock particle from the solution, hence stopping the adsorption reaction and reducing the noise on the UV-Vis reading. Finally, using the calibration curve for each surfactant, surfactant dynamic adsorption is calculated at each time step using **Eq. 28** (Alvarez, Saputra, and Schechter 2017).

$$\theta_A = \frac{(\phi_{surf}^i - \phi_{surf}^f) * V_{surf} * \rho_{surf} * 10^5}{w_{rock}} \dots \dots \dots \quad (28)$$

where θ_A is the amount of surfactant, ϕ_i surf and ϕ_f surf the initial and final surfactant concentrations, respectively, V_{surf} and ρ_{surf} the surfactant volume and density, respectively, and W_{rock} the weight of rock.

Spontaneous Imbibition Experiments

Preserved and aged cores are submerged in water or oil at reservoir temperature to evaluate wettability and measure fluid imbibition. Because liquids cannot flow through these low porosity and ultralow permeability rocks, spontaneous imbibition experiments are used to gauge the wetting state of the rock and the possibility of water and/or oil to imbibe in these micro pores. Sidewall cores from Bakken, Eagle Ford, Wolfcamp and Barnett are used inside a modified Amott cell at reservoir temperature. Two types of spontaneous imbibition experiments were performed. First, preserved cores were weighted, measured and submerged in water or oil for 2 months at reservoir temperature. This first set of experiments was designed to validate original wettability results from contact angle and zeta potential methods.

On the second scheme of experiments, cores aged in oil for 6 months were submerged in an aqueous solution of distilled water and potassium iodide (KI) at 4 wt.%, as dopant to increase the contrast between oil and water on the CT scanner, for 10 days. During this period, cores were scanned periodically to assess water imbibition with time. In addition, weight and average core CT numbers were used to determine imbibition and oil recovery. This second type of experiments were performed to investigate and compare the capability of different surfactants in imbibing ultralow permeability ULR cores. Initially, spontaneous imbibition experiments were carried out to qualitatively investigate the capability of different types of surfactants of imbibing ultralow permeability shale cores. Cores were aged for 4 months in the well-oil at reservoir temperature. Then, cores were submerged in anionic and nonionic surfactant solutions at a concentration of 3 gpt to

test oil production by free imbibition. After noticing oil produced by imbibition, this procedure was refined to address changes in densities, fluid movements and imbibition, as well as rate of recovery and ultimate recovery.

In order to visualize the movement of the fluid as it penetrates into liquid rich shale samples, CT methods were used. I designed a modified Amott cell capable of being used on the CT scanner and allowing the core to be placed horizontally to trace radial fluid imbibition towards the center of the core. The modified Amott cell is shown in **Fig. 7** and consists in a glass structure with a graduated measuring scale on the top to trace oil production with time. On the bottom of the cell, a Plexiglas base is used to place horizontally the cores. Clamps and screws are aluminum made to be used on the CT scanner (Alvarez and Schechter 2017).

Received cores were in pseudo-preserved state, tightly wrapped in plastic foil and kept in sealable individual bags. After removing plastic foils, cores were immediately submerged in oil from Wolfcamp, Bakken, Eagle Ford and Barnett well at reservoir temperature for six months to reconstitute them with the missing liquid hydrocarbons due to sample handling. Occasionally, air/gas was released from the cores, so the containers were bled off to preserve their integrity. Frac fluid solutions were prepared with 4 wt.% KI brine and different surfactants at 2 gpt. Frac fluid without surfactant was also used to compare effectiveness in penetrating ULR cores. Spontaneous imbibition experiments were performed in an Memmert UF1060 oven at reservoir temperature. The general experimental procedure is provided as follows:



Figure 7. Modified Amott cell for spontaneous imbibition experiments. Reprinted with permission from Alvarez and Schechter (2017)

- a. Selected 1-inch cores from similar depths and lithology were weighed using a high precision weighing balance and measured using Vernier calipers.
- b. The core was scanned on the modified Amott cell before the cell was filled with liquids.
- c. Initial wettability of the core was determined by CA measurements using Dataphysics OCA 15 Pro apparatus.
- d. The core was placed in the modified Amott cell with the frac fluid solution after both the cell and fluid were equilibrated to reservoir temperature.
- e. The modified Amott cell was immediately scanned and marked this scan as t=0 h.

- f. The modified Amott cell was placed in an environmental chamber at reservoir temperature.
- g. CT scans were taken at different time intervals from 0 hour up to 10 days.
- h. Oil production was monitored periodically using a graduated scale on the modified Amott cell.
- i. At the end of the experiment, the core was weighted and scanned without fluids in the cell.
- j. Final wettability of the core was determined by CA measurements using Dataphysics OCA 15 Pro apparatus.

In addition, to test the impact of mineralogy on oil recovery with different surfactant types, siliceous and carbonate cores were used. Moreover, to address different surfactant group (head charges) behaviors, I selected the surfactants that performed the best in CA, zeta potential and IFT experiments. Aqueous solutions were a mix of distilled water and the selected surfactants at 2 gpt. Also, 4 wt.% KI was added to the solution as dopant to increase contrast between the oil and imbibing fluid on the CT scanner. Spontaneous imbibition experiments in frac fluid without surfactant were also carried out to compare surfactant additive effectiveness in recovering oil from ULR cores.

CT scan technology was used to gauge fluid imbibition into the liquid rich shale cores. Modified Amott cells were scanned using a Toshiba Aquilion TSX-101A CT scanner. Helical scans were set on 135 kV and 350 mA with a rotation time of 1 second and a slice thickness of 0.5 mm with intervals between each slice of 0.3 mm. In addition,

images obtained from the CT scanner were analyzed using an open source image processing software called ImageJ to address changes in CT numbers, measured in Hounsfield units (HU), related to fluid imbibition. Then, penetration magnitude was calculated to quantify the fluid movement into the core with time based on the initial average CT number (CT_{base}) and the average CT number at a time 't' (CT_t), as defined in Eq. 29 by Alvarez et al. (2014).

$$\text{Penetration Magnitude} = CT_t - CT_{\text{base}} \quad \dots \quad (29)$$

Core Flooding Experiments

This part of the research is focus on evaluate and expand on the ability of different groups of surfactants, added to completion fluids, on improving oil recovery in ULR by experimentally simulating the fracture-treatment, at reservoir conditions, to represent surfactant imbibition in an ULR core fracture during a soaking and flowback. In the pressure-imbibition experiment, the core displacing system was used to characterize the penetration of surfactants in the fractures of unconventional oil reservoir during fracturing. A core-flooding system to represent surfactant penetration in ULR fractures during a frac job was used. Saturated ULR side-wall cores were longitudinally fractured and loaded into an aluminum-carbon composite core-holder. Different types of surfactants were tested as well as slickwater without surfactants to address their effectiveness in penetrating into the fractures and recovering oil from ULR core. These solutions were injected through the

fractures at reservoir conditions. Then, a soak and produce scheme was used to simulate fracture-treatment and flowback. Initial and final core wettability was determined by contact angle and changes in IFT were measured by pendant drop method. To better understand fluid movements and dynamically visualize fluid penetration in real time, the experiments were performed on the CT scanner. Oil recovery was measured with time to compare surfactant efficacy in imbibing the rock and expelling oil. **Fig. 8** shows the experimental instrument setup, which consists of five components: the injection system, the core flood cell, Toshiba Aquilion TSX-101A CT scanner, the production system, and the data acquisition system.

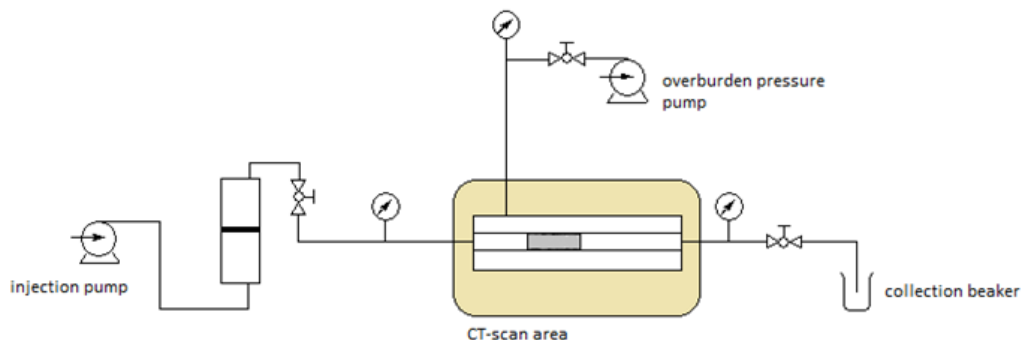


Figure 8. Schematic of the experimental core-flooding system. Reprinted with permission from Alvarez et al. (2014)

Core flooding experiments were performed with artificially cleaved ULR core to simulate a fracture or a set of fractures before loading the sample in the core holder as showed in **Fig. 9**. The actual experimental setup used for the experiments is shown on **Fig. 10.**

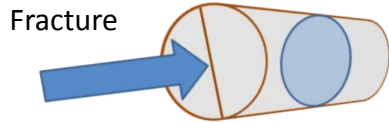


Figure 9. Schematic of the artificially fractured shale cores.

Aqueous solutions with and without surfactants were used to assess the effectiveness of chemical additives in recovering hydrocarbons from ULR core. Also, 4 wt. % KI was added to the solution as dopant to increase the contrast between the oil and imbibing fluid on the CT scanner.



Figure 10. Experimental setup for core-flooding experiments in ULR.

General experimental procedures are provided as follows:

- a. Selected 1-inch cores from similar depths and lithology were weighed using a high precision weighing balance and measured using Vernier calipers.
- b. Initial wettability of the core was determined by CA measurements using Dataphysics OCA 15 Pro apparatus.
- c. A selected aged 1-inch core was fractured by a chisel and hammer to create a fracture along the core representing a hydraulic fracture in the reservoir.
- d. The core was loaded into the 1-inch core holder and scanned. A rubber sleeve was used to separate the overburden fluid and injection fluid.
- e. Overburden pressure was applied at 500 psi above reservoir pressure.
- f. The injection lines were assembled to the loaded core holder, and the pre-flooded core was scanned.
- g. The fracturing fluid prepared in an accumulator was injected at reservoir pressure through the core holder. Once the fluid came out the other end, the pressured fluid was then sealed using a back-pressure regulator. At this moment, the soaking period begins.
- h. CT scans were taken at different time intervals from 0 hour (immediately after flooding) up to 72 hours.
- i. After 72 hours, the system is open to production by reducing the back-pressure regulator constrains. At this moment, the flowback period begins.

- j. Oil production is measured with time for a period of 8 hours. Then, the test is terminated.
- k. The core holder was disassembled, and the core was taken out to measure the post-flooding weight of the core.
- l. Final wettability of the core was determined by CA measurements using Dataphysics OCA 15 Pro apparatus.

As in the spontaneous imbibition experiments, the penetration magnitude was calculated to quantify the fluid movement by Eq. 29.

Scaling Imbibition Results

Scaling methods were used to evaluate imbibition rates and dimensionless scaling groups to correlate laboratory imbibition data and predict oil recovery at well scale in the Eagle Ford. At laboratory scale, capillary forces dominate the imbibition process and consequently oil recovery. However, at field scale, hydrocarbon production is driven by pressure difference between the reservoir and the wellbore and oil recovery can be improved by imbibition when capillary forces are reversed from negative to positive values.

Wettability and IFT measurements as well as oil recovery profiles from imbibition experiments are utilized to calculate imbibition rates and generate normalized production rate curves for three different field-used surfactant types. Imbibition rates are used to

demonstrate surfactant efficacy in recovering hydrocarbons from ULR core over slickwater alone whereas normalized production rate curves are utilized to compare laboratory to field production profiles. Improved oil recovery by imbibition is obtained from scaling spontaneous imbibition laboratory data to the field using the scaling model proposed by Ma, Morrow, and Zhang (1995) (Eq. 9) as well as the one by Gupta and Civan (1994) and Guo, Schechter, and Baker (1998) (Eq. 12). After evaluating both dimensionless time profiles, we selected the latter dimensionless model because represented better our experimental results because besides IFT it considered the effect of wettability alteration in the scaling model as wettability is a fundamental parameter on the Young-Laplace equation (Eq. 1). Next, Fischer, Wo, and Morrow (2008) defined characteristic lengths (L_c) for different boundary conditions and flow regimes. For our experimental case, we selected the cylindrical (all-faces-open) case as defined in Eq. 30, where d is the core diameter and l is the core length. We assumed that all characteristic length calculations in this paper follows all-face-open scenario.

$$L_c = \frac{ld}{2\sqrt{d^2+2l^2}} \quad \dots \dots \dots \dots \quad (30)$$

Similarly, for the field scale dimensionless group, we used Eq. 12, but considering field parameters as shown in Eq. 31, where $t_{D(field)}$ is the dimensionless time in the field; $t_{(field)}$ is the field time; $L_{c(field)}$ is characteristic length in the field.

$$t_{D(field)} = t_{(field)} \sqrt{\frac{k}{\emptyset}} \frac{\sigma \cos \theta}{\sqrt{\mu_o \mu_w}} \frac{1}{L_{c(field)}^2} \quad \dots \dots \dots \dots \quad (31)$$

Because for all our experiments we used sidewall cores and oil collected from same reservoir as our filed data, we assume that the permeability, porosity, IFT and wettability as well as water and oil viscosities are similar between laboratory and field. In addition, to properly upscale laboratory data, the dimensionless time for laboratory core and in the field are assumed to be the same at all time, and by applying the imbibition scaling model to both lab and field data, the characteristic length of the field is calculated using Eq. 32 (Wang et al. 2016).

$$t_{(field)} = t_{(laboratory)} \frac{L_{c(field)}^2}{L_{c(laboratory)}^2} \dots \dots \dots \quad (32)$$

The calculated field characteristic length is used to predict the distance of frac-water imbibition into reservoir matrix, which can determine the cumulative oil production for imbibition at field scale. Thereby, the predicted field cumulative oil production by imbibition obtained from Eq. 33, where Q is the predicted cumulative oil production for spontaneous imbibition, *Oil Recovery* is obtained from experiment measurements, A is total area of opened fractures, S_o is initial oil saturation, d is distance that water penetrates the formation.

$$Q = \text{Oil Recovery} \times A \times S_o \times d \dots \dots \dots \quad (33)$$

Since the t_D values for a laboratory core and field are same, estimated normalized field production rate curve dominated by imbibition has the same shape as normalized production rate obtained in laboratory. We calculated normalized production rate from oil recovery data that was measured in laboratory using Eq. 34 and Eq. 35, where q is

production rate, t time, q_n is the normalized production rate and q_{max} the maximum production rate in spontaneous imbibition experiments. Considering oil accumulation achieved from Eq. 33, field production rate can be estimated.

$$q = \frac{\nabla \text{Oil Recovery}}{\nabla t} \quad \dots \dots \dots \quad (34)$$

$$q_n = \frac{q}{q_{max}} \quad \dots \dots \dots \quad (35)$$

Finally, by considering completion method, reservoir geometry, and initial oil saturation from ULR real-data, we estimated the field production rate under several induced fracture spacing scenarios. This new approach based on dimensionless scaling time allows us to calculate the characteristic length of field, key parameter to predict the distance of surfactant imbibition into the matrix and consequently oil recovery. Also, by considering completion method, reservoir geometry, and initial oil saturation from ULR-well real-data, we estimated the field production rate under several induced and natural fracture spacing scenarios corroborating that fracture density and rock-fluid interactions are key parameters for oil recovery in these ULR.

In summary, this innovative correlated set of experiments was designed to evaluate the surfactant potential of improving oil recovery in ultralow permeability and low porosity rocks. The results obtained by this experimental methodology is used for scaling up and simulating flowback after stimulation in ULR.

CHAPTER IV

ROCK, OIL AND WETTABILITY CHARACTERIZATION *

Rock wettability dominates fluid flow and influences rock-fluid interaction affecting oil recovery. Siliceous and carbonate cores from the Wolfcamp, Bakken, Eagle Ford and Barnett are used to investigate original wettability of these unconventional liquid reservoirs (ULR). In addition, we carefully analyze the relation of rock mineralogy, oil type and total organic content (TOC) to wetting affinity.

Original wettability from ULR cores is quantified initially by contact angle (CA), and zeta potential experiments are utilized to assess the stability of thin water films on the shale rock surface and its correlation to wettability. Petrophysical properties such as permeability, porosity and pore size distribution using mercury injection capillary pressure (MICP), XRD, total organic carbon analyses and scanning electron microscopy (SEM) images, as well as oil properties like IFT, API gravity, and oil total acid and basic number are measured to further understand wettability states from these ULR (Alvarez and Schechter 2016c).

* Parts of the rock, oil and wettability characterization presented in this chapter have been reprinted from “Wettability, Oil and Rock Characterization of the Most Important Unconventional Liquid Reservoirs in the United States and the Impact on Oil Recovery” by J.O. Alvarez and D.S. Schechter. URTEC Paper 2461651. Copyright 2016 by the Unconventional Resources Technology Conference (URTEC). Reproduced with permission of URTEC. Further reproduction prohibited without permission.

Finally, spontaneous imbibition experiments are performed to investigate wetting affinity and fluid penetration in ULR cores. Using modified Amott cells, preserved and cleaned cores are submerged in water or oil to gauge wetting affinity by measuring fluid imbibition. Moreover, time-lapse, computed tomography (CT) determined penetration magnitude. Lastly, the potential of water imbibition as a technique for improving oil recovery during hydraulic fracturing ULR is investigated by submerging aged cores in water to represent soaking during shut-in of the well after stimulation.

The results and observations from the experiments performed are discussed on this Chapter. First, lithology, TOC and petrophysical properties for ULR cores from Bakken, Eagle Ford, Wolfcamp and Barnett are presented. Second, oil properties and IFT results are studied. Third, original ULR wettability is addressed by CA and zeta potential experiments. Finally, wettability and fluid penetration in ULR is studied by spontaneous imbibition experiments monitored by CT methods.

Rock Petrophysical Characterization

In this section ULR mineralogy, TOC, porosity, permeability and pore size radius is studied using X-ray diffraction, total organic carbon analysis, scanning electron microscopy and mercury injection capillary pressure analyzes. Liquid rich shale cores as well as dead oil from different producing wells in Bakken, Eagle Ford, Wolfcamp and Barnett are used. Rock analyses use sidewall cores that are 1-inch in diameter and 1.5 to 3-inches in length. Moreover, companion cores are used to avoid inconsistency in the

experiment results. **Table 3** shows play, well, rock sample depth and reservoir temperature for tested samples.

Table 3. ULR rock sample sources and depths. Reprinted with permission from Alvarez and Schechter (2016c)

ULR	Well	Sample	Depth (ft)	ULR	Well	Sample	Depth (ft)
Bakken Reservoir Temperature (220 °F)	Bk-1	1	9620	Barnett Reservoir Temperature (165 °F)	Br-1	1	6060
		2	9630			2	8018
		3	9635			3	8582
		4	9640			4	8700
	Bk-2	1	10765		Br-2	1	6896
		2	10770			2	7017
		3	10775			3	7030
		4	10780			4	7616
Eagle Ford Reservoir Temperature (218 °F)	EF-1	1	13030	Wolfcamp Reservoir Temperature (165 °F)	W-1	1	7790
		2	13040			2	7830
		3	13125			3	7835
		4	13135			4	7880
	EF-2	1	14185			5	7910
		2	14220		W-2	1	8335
		3	14245			2	8370
		4	14250			3	8385
						4	8425

X-ray diffraction and total organic carbon analysis

X-ray diffraction and total organic carbon analysis experiments are conducted to evaluate the nature of the rocks analyzed as well as the lithological variability of ULR with depth. Determine the mineralogical composition of ULR pay zones is critical to select completion fluids that improve water imbibition and favor oil recovering when fracturing the formation (Alvarez and Schechter 2016a). XRD and TOC results for Bakken and Eagle Ford are in **Table 4**.

XRD results for Bakken wells show different lithologies from the two wells analyzed. Well Bk-1 is more siliceous with higher content of quartz whereas well Bk-2

show higher content of dolomite as carbonate dominated. These samples are taken from Middle Bakken (Bk-1) and Three Folks (Bk-2) units showing low TOC values and 25 to 30 wt.% of mainly illite and mica clays. On the other hand, Eagle Ford samples from two wells are more consistent in lithology with all samples tested showing higher carbonate contents at different depths and 20 to 30 wt% of clay content; in addition, TOC values are higher than Bakken, especially in well EF-2. For both reservoirs, illite/smectite content is elevated as an indication of immature clay system.

Table 4. XRD and TOC results for Bakken and Eagle Ford. Reprinted with permission from Alvarez and Schechter (2016c)

Well / Sample	Bk-1/1	Bk-2/1	EF-1/1	EF-1/2	EF-1/3	EF-1/4	EF-2/1	EF-2/2	EF-2/3	EF-2/4
Mineral Composition (wt%)										
Quartz	53	14	15	17	13	10	15	15	16	15
Clays	29	26	31	35	33	24	20	19	23	25
Calcite	3	0	46	40	44	59	59	58	54	52
Dolomite	4	51	2	1	1	1	0	2	1	1
Feldspar	9	9	1	3	5	1	1	1	1	2
Pyrite	2	0	5	4	4	5	5	5	5	5
Relative Clay (%)										
Illite/mica	69	60	60	65	59	59	60	59	61	54
Illite/Smectite	13	7	40	35	25	26	30	37	32	33
Kaolinite	4	11	0	0	7	10	3	1	2	4
Chlorite	14	22	0	0	9	5	7	3	5	9
TOC (wt%)	0.7	1.1	3.3	4.0	3.5	3.9	5.6	5.2	5.5	5.4

Rock properties for Wolfcamp and Barnett are represented in **Table 5**. Both Wolfcamp wells have variable mineral composition with depth changing from siliceous to carbonate in different strata. In addition, clay content is below 30 wt% and mostly illite and mica. Moreover, Wolfcamp shows relative high TOC values like Eagle Ford. Finally,

Barnett samples show consistent low clay content and low illite/smectite proportions with mixtures in similar proportions of quartz and calcite/dolomite and lower TOC values than Wolfcamp and Eagle Ford.

Table 5. XRD and TOC results for Wolfcamp and Barnett. Reprinted with permission from Alvarez and Schechter (2016c)

Well / Sample	W-1/1	W-1/2	W-1/3	W-1/4	W-1/5	W-2/1	W-2/3	Br-1/1	Br-1/2	Br-2/3
Mineral Composition (wt%)										
Quartz	40	13	46	41	8	20	48	48	43	46
Clays	40	15	13	27	11	28	27	8	22	8
Calcite	2	46	2	13	15	31	13	35	18	38
Dolomite	2	19	22	6	64	14	6	6	7	6
Feldspar	7	4	17	10	1	5	11	2	8	1
Pyrite	9	3	0	3	1	2	3	1	2	1
Relative Clay (%)										
Illite/mica	75	74	70	72	78	69	67	91	90	76
Illite/Smectite	25	26	30	28	22	31	33	0	0	24
Kaolinite	0	0	0	0	0	0	0	11	5	0
Chlorite	0	0	0	0	0	0	0	0	5	0
TOC (wt%)	5.0	3.4	5.5	5.7	3.0	4.7	4.3	1.7	4.7	2.5

Scanning electron microscopy imaging

Selected samples from the four plays are imaged using SEM; results are in **Fig. 11** for Bakken and Eagle Ford and in **Fig. 12** for Wolfcamp and Barnett. For Bakken (Fig. 11, top), the SEM images confirm XRD results showing siltstones at 500X optical zoom and presence of chlorite, mica and illite in a siltstone at 2000X. Moreover, Eagle Ford SEM images (Fig. 11, bottom) show calcareous rocks with siltstones, as XRD results, at 600X and the micritic calcite matrix with small dissolution vugs (squares) and rare foram fossils at 2000X.

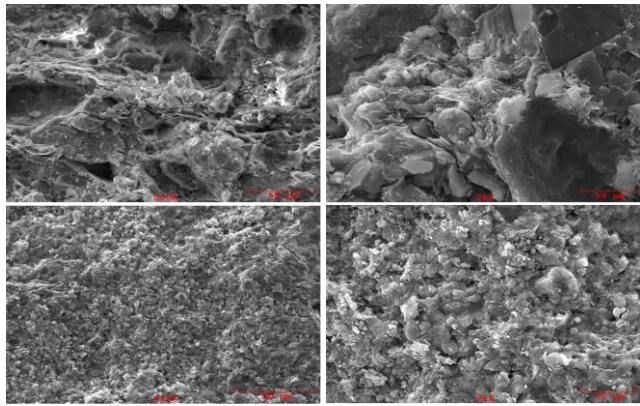


Figure 11. SEM images for sample Bk-1/1 (top) and sample EF-2/1 (bottom). Reprinted with permission from Alvarez and Schechter (2016c).

In addition, Wolfcamp images (Fig. 12, top) represent slightly calcareous siltstones at 750X optical zoom and a siltstone with traces of dolomite (squares 1, 2 and 4) and clay (square 2) at 3000X. Finally, Barnett SEM image at 1000X zoom shows a calcareous siltstone with traces of pyrite in square 1 and chlorite/kaolinite in squares 2 and 3. The detailed view at 3000X for Barnett shows chlorite and mica in square 1 and pyrite frambooids in square 2 surrounded by slightly calcareous siltstone.

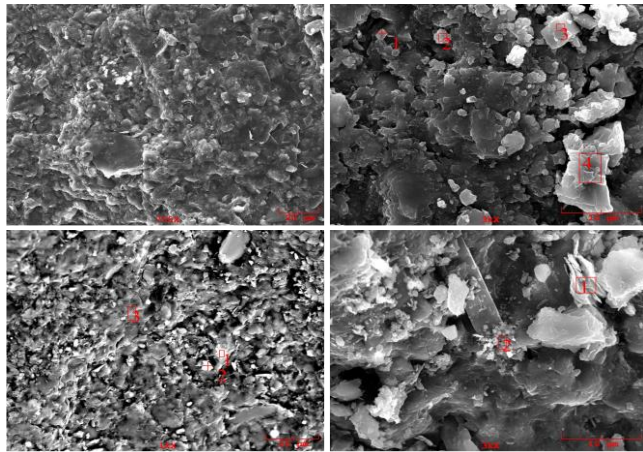


Figure 12. SEM images for sample W-1/2 (top) and sample Br-2/ 2 (bottom). Reprinted with permission from Alvarez and Schechter (2016c).

Mercury injection capillary pressure results

Mercury injection capillary pressure analyzes are performed to have an indication of the petrophysical properties of these ULR. To determine pores size distributions and porosities, the device applies several levels of controlled pressures to the porous sample immersed in mercury. The pore size is inversely proportional to the pressure applied to intrude the mercury in the sample. **Fig. 13** shows the normalize pore size distribution for eight ULR samples from Bakken, Eagle Ford, Wolfcamp and Barnett. All samples represent a unimodal distribution except well Bk-1/1 from Bakken, which has a bimodal pore size distribution. This is an indication that well Bk-1 has larger pores and/or has micro fractures as well as matrix distributions. On the other hand, all other samples show unimodal distributions, so the pores size reported is expected to be the matrix pore size. In addition, Wolfcamp shows the lowest pore size distribution closely followed by Eagle Ford, Barnett and Bakken.

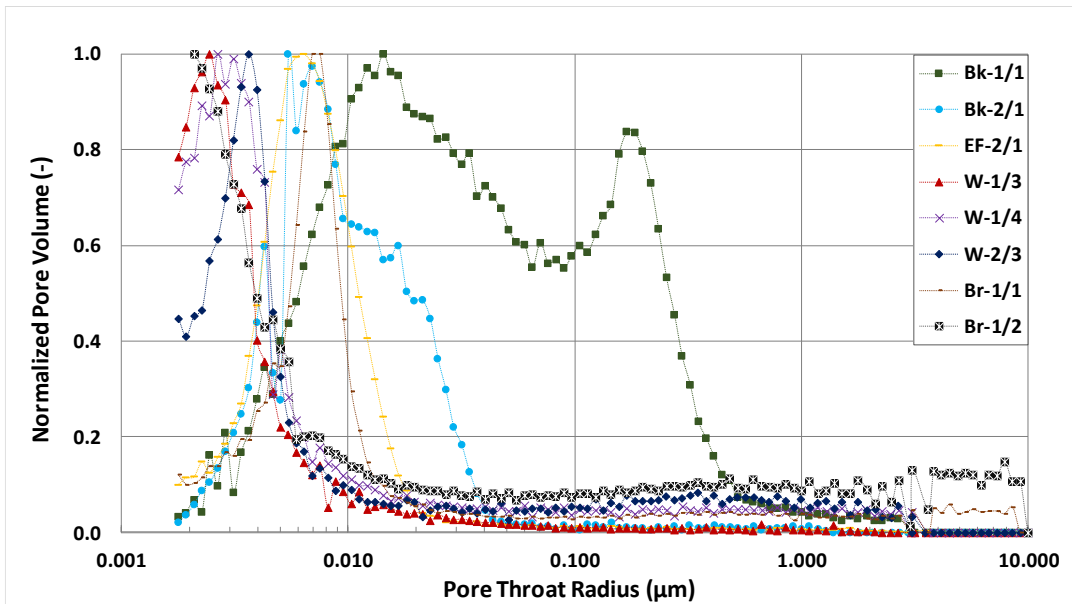


Figure 13. Normalized pore size distributions for Bakken, Eagle Ford, Wolfcamp and Barnett. Reprinted with permission from Alvarez and Schechter (2016c).

The experiment also records the amount of mercury injected with respect to the bulk volume giving accurate values of porosity, bulk and grain density; in addition, permeability to air can be calculated using the Swanson's equation (Swanson 1981). **Table 6** shows the results of porosity, permeability to air, grain and bulk density as well as mean pore radius from the four formations studied. A common denominator for the wells analyzed is their low porosities with values ranging from 6 to 11 % with most values between 6 to 8 %. Moreover, permeability values are also very low in the micro and nano Darcy range with Eagle Ford and Wolfcamp evidencing the lowest numbers among the four. Next, grain densities are shown ranging from 2.55 to 2.75 g/cc which correlates with rock main mineral densities and proportions given by XRD analyzes (quartz (2.65 g/cc), calcite (2.71 g/cc), dolomite (2.85 g/cc) illite (2.66 g/cc), mica (2.80 g/cc)). Bulk densities

are lower because they consider air density related by porosity values. Finally, median pore throat radius from these wells shows nanopore sizes, which are common in these types of reservoirs. This small pore radius makes capillary forces significant dominating fluid displacement in the porous media.

Table 6. Petrophysical properties for Bakken, Eagle Ford, Wolfcamp and Barnett.
Reprinted with permission from Alvarez and Schechter (2016c)

Well / Sample	Bk-1/1	Bk-2/1	EF-2/1	W-1/3	W-1/4	W-2/3	Br-1/1	Br-1/2
Porosity (%)	10.8	6.5	8.6	6.8	6.4	6.2	7.8	6.1
Permeability to air (μD)	23.03	0.41	0.47	0.16	0.25	0.18	1.05	0.75
Grain Density (g/cc)	2.72	2.75	2.52	2.59	2.63	2.73	2.63	2.55
Bulk Density (g/cc)	2.43	2.58	2.31	2.41	2.46	2.56	2.43	2.39
Median pore throat radius (μm)	0.034	0.010	0.007	0.003	0.004	0.005	0.008	0.007

In addition, Swanson air permeability is cross-plotted with porosity values in **Fig. 14**. Wolfcamp wells show the lowest values for permeability and porosity while Bakken display different relationship varying by well. Barnett wells show similar permeability varying porosities at different depths. Regardless the small data set; there is a visible trend of increasing permeability as porosity of the sample increments in Barnett and Bakken samples. Now that ULR rock properties have been identified and differentiated, oil properties are studied next to address rock-fluid interactions.

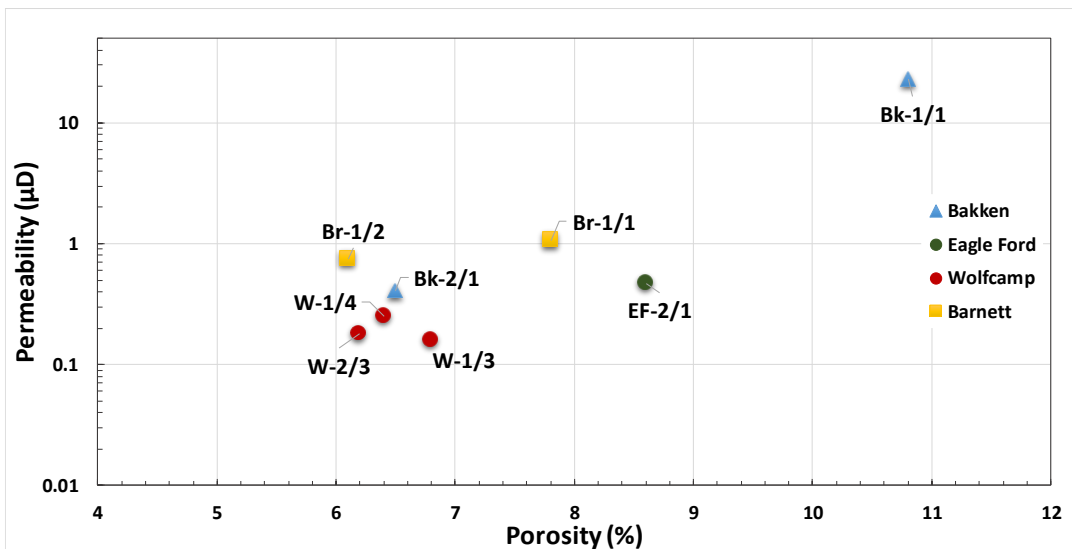


Figure 14. Cross plot for permeability and porosity for Bakken, Eagle Ford, Wolfcamp and Barnett. Reprinted with permission from Alvarez and Schechter (2016c).

Fluid Characterization

Fluid properties are equally important as rock properties to understand rock-fluid interactions as they are related to wettability and capillary pressures. This section covers the oil characterizations from wells in Bakken, Eagle Ford, Wolfcamp and Barnett. Total acid and base numbers as well as API densities are measured. In addition, IFT between water and oil is determined at reservoir temperature.

Oil total acid number, total base number and densities

Oil total acid number, total base number and densities influence rock original wettability (Buckley, Liu, and Monsterleet 1998). Hence, investigating these parameters is crucial to understand fluid behavior as well as rock-fluid interactions in ULR. Measured

crude oil properties from wells in Bakken, Eagle Ford, Wolfcamp and Barnett are shown in **Table 7**. Using titration methods, TAN and TBN is determined. Bakken oil has higher acid number but the difference between TAN and TBN is not very marked. On the other hand, Eagle Ford oil is more basic as well as Barnett 1 and 2, and Wolfcamp shows more basicity but with a small difference when compared to TAN. Regarding oil densities, all samples can be ranked as light oils at reservoir temperature.

Table 7. Oil properties for Bakken, Eagle Ford, Wolfcamp and Barnett. Reprinted with permission from Alvarez and Schechter (2016c).

ULR	Bakken	Eagle Ford	Wolfcamp	Barnett 1	Barnett 2
TAN (mg KOH/ g oil)	0.36	0.02	0.09	0.27	0.10
TBN (mg KOH/ g oil)	0.23	0.61	0.12	0.55	0.57
API (°) @ 70 °F	35.08	57.4	31.4	30.9	30.2
API (°) @ Res. Temp	37.30	58.7	32.4	37.5	35.8

IFT measurements

Using the pendant drop method, IFTs between water and crude oil from Bakken, Eagle Ford, Wolfcamp and Barnett are measured at reservoir temperature. As represented in **Fig. 15**, Eagle Ford has the highest IFT among the group; then, Wolfcamp, Barnett and Bakken show similar IFT values. Oil-water IFT is a very important parameter to follow when addressing IOR in unconventional reservoirs. As shown in the Young-Laplace equation (Eq. 1), IFT is directly proportional to capillary pressure and its original value and possible alteration is fundamental in favoring oil recovery by spontaneous imbibition (Alvarez et al. 2014, Alvarez and Schechter 2016a, 2017). IFT can be altered by adding

proper surfactants to completion fluids favoring imbibition. In the next section, we address ULR wettability as the other parameter in the Young-Laplace equation that can modify capillary pressure as well as the relation of oil and rock properties in ULR original wetting state.

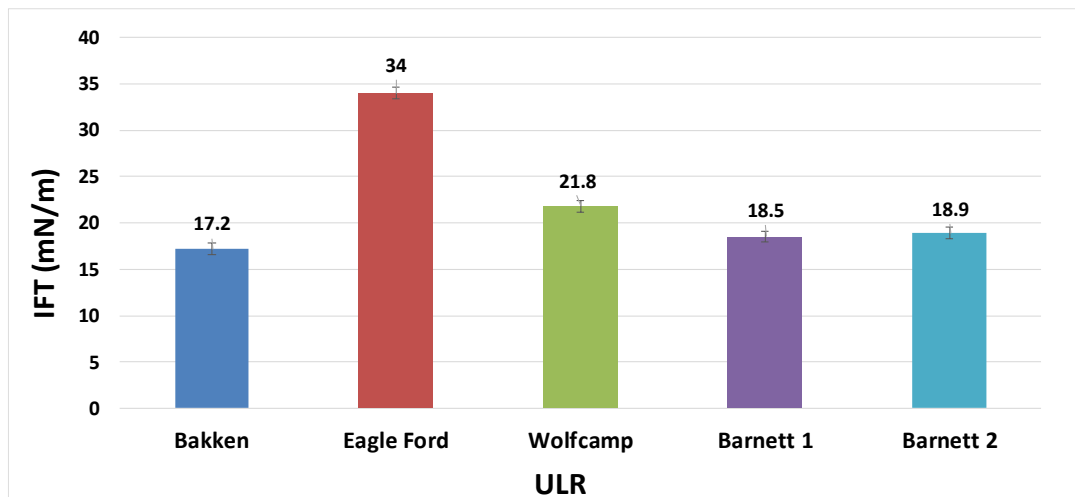


Figure 15. Oil-water IFT for Bakken, Eagle Ford, Wolfcamp and Barnett. Reprinted with permission from Alvarez and Schechter (2016c).

Wettability Measurement Experiments

In this section, I investigate original wettability of different wells from Bakken, Eagle Ford, Wolfcamp and Barnett by contact angle and zeta potential measurements.

Contact angle results

Original rock wettability is measured by CA experiments using the captive bubble method. CA measurements are performed in several samples from different wells in Bakken, Eagle Ford, Wolfcamp and Barnett formations as described in Table 3. To

accurately represent the phases interacting in the reservoir, oil from the ULR and its corresponding shale sample are used in water solutions at reservoir temperature. In these water-oil-rock systems, in which water is the denser fluid, the rock is water-wet when the contact angle between water and solid goes from 0°-75°, intermediate-wet from 75°-105°, and oil-wet from 105°-180° (Anderson 1986a). Advancing CA results from Bakken and Eagle Ford are in **Fig. 16**. All measurements show an intermediate-wet state for Bakken and Eagle Ford samples; however, Eagle Ford samples are more inclined towards oil-wetness than Bakken. One plausible explanation for this behavior is the amount of TOC present in both formations in which Eagle Ford has marked higher TOC values than Bakken. The presence of organic matter as organic pores in the samples favors oil-wetness. Regardless elevated Eagle Ford TOC values, these samples show intermediate-wet behaviors that are driven by the mixture of water-wet inorganic matter and oil-wet organic matter. In addition, Eagle Ford's TBN is notably higher than TAN (Table 7), this affect acid/base and ion-binding interactions as XRD analyzes from Eagle Ford show a mostly carbonate rock and the positively charged carbonate surface is more attracted to bind with acidic oil compounds. Hence, there is less oil-rock attraction affecting original wettability to lean towards intermediate and mild oil-wet rather than strong oil-wetness. Even though Bakken core mineralogy varies from well Bk-1 as siliceous to Bk-2 as carbonate, oil TAN and TBN are very similar diminishing the effect of lithology and ion-binding interactions. In this case, organic matter, clay content and especially high oil densities for Bakken samples might favor asphaltenes precipitation that induces the observed intermediate-wetness.

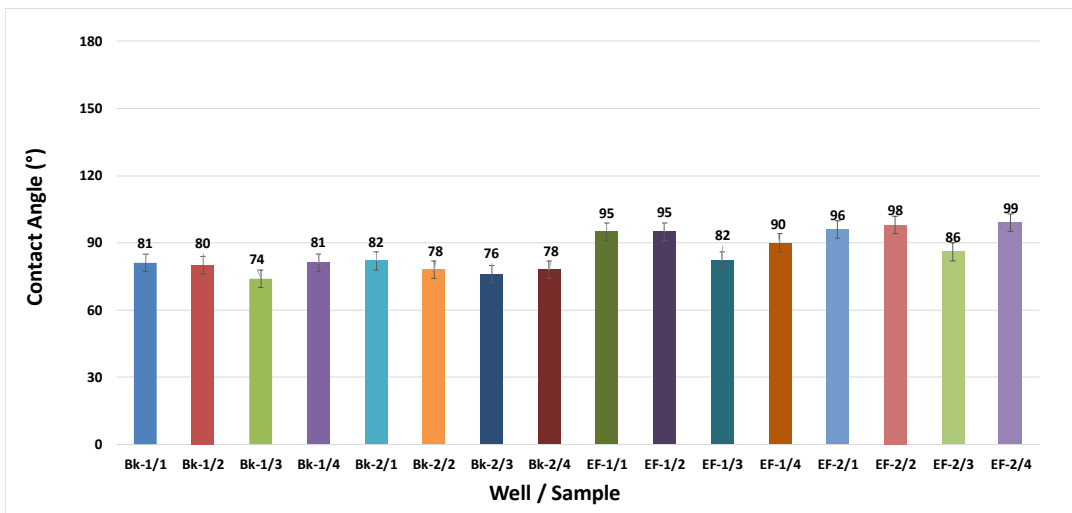


Figure 16. Original wettability for Bakken and Eagle Ford. Reprinted with permission from Alvarez and Schechter (2016c).

Wolfcamp and Barnett original wettability for two wells at different depths is illustrated in **Fig. 17**. Wolfcamp samples show oil-wet towards intermediate-wetness, and, from the ULR studied, Wolfcamp is the formation with the highest CA as indication of rock's oil preference. A mixture of high TOC values and high oil density might explain Wolfcamp oil to intermediate-wet behavior. The interaction of acidic and basic compounds in the oil also can determine this mild affinity to oil as TAN and TBN are very small and similar in value. This similarity of TAN and TBN relegates the effect of electrostatic interactions between ULR surface and oil compounds reason why original wettability is not affected by changes in lithology of the samples. On the other hand, Barnett wettability measurements are showing an intermediate-wet formation for the mostly siliceous samples. Higher TBN compared to TAN for both Barnett wells suggests acid/base and ion-binding interactions that favor oil-wetness regardless low TOC values.

In addition, higher CA values are found in samples Br-1/2 and Br-1/4 and Br-2/4, which have remarkably higher TOC values than other samples from the same formation.

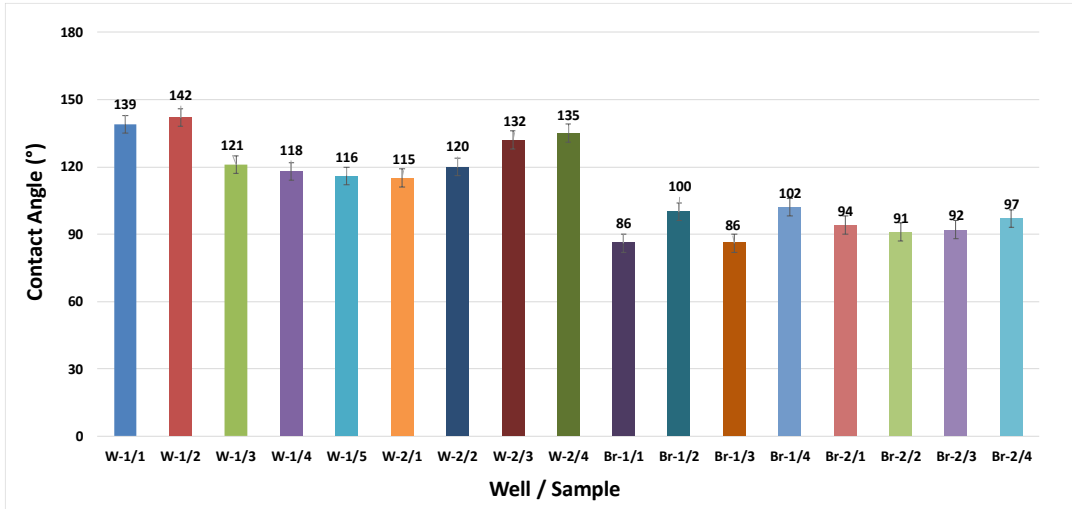


Figure 17. Original wettability for Wolfcamp and Barnett. Reprinted with permission from Alvarez and Schechter (2016c).

In order to analyze the relation of TOC to wetting affinity, CA measurements for Bakken, Eagle Ford, Wolfcamp and Barnett samples are cross-plotted with TOC values. **Fig. 18** shows a trend for the analyzed samples in which higher TOC values give more oil affinity to ULR rock shifting its wettability towards oil-wet. Due to its wetting affinity, organic matter is responsible of giving oil-wetness to the rock, and the higher its amount in the rock, the higher the rock affinity to oil.

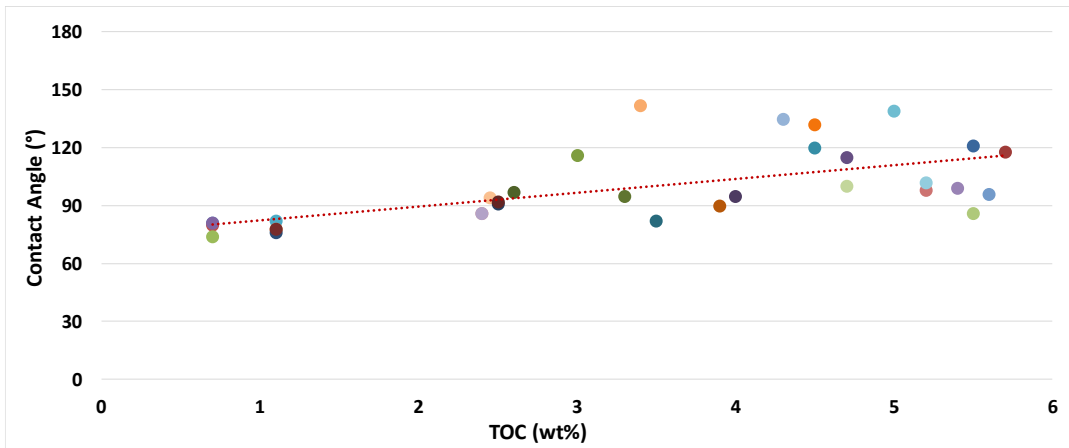


Figure 18. Original wettability for Bakken, Eagle Ford, Wolfcamp and Barnett samples vs. TOC. Reprinted with permission from Alvarez and Schechter (2016c).

In addition, the relation of rock mineralogy and wettability is studied in **Fig. 19**. The results do not show a visible trend between rock dominant lithology, siliceous or carbonate, and CA measurements. Both cores types have intermediate-wet behavior as well as inclinations towards oil or water-wet. Hence, our findings indicate that ULR original wettability is affected by TOC but not by lithology.

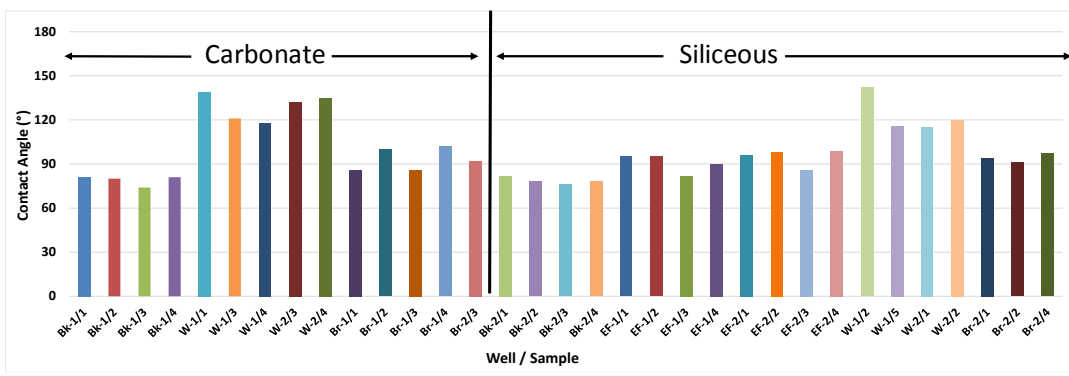


Figure 19. Original wettability for Bakken, Eagle Ford, Wolfcamp and Barnett samples grouped by lithology. Reprinted with permission from Alvarez and Schechter (2016c).

In summary, original wettability for the ULR studied is mostly intermediate towards oil-wet with Wolfcamp showing the most oil-wetness. These findings are consistent with the scarce information in the literature summarized in Table 1 in which most the wettability studies claim intermediate-wetness for ULR. These values are determined not only by CA, but also by other wettability methods as NMR and Amott-Harvey Index, regardless their application on ultra-low permeability reservoirs. The main reason for this neutral wettability in ULR is the presence of water-wet inorganic pores and oil-wet organic pores that create a balance in the wetting forces. In addition, original wetting affinity is influenced by rock-fluid interactions where oil type and surface mineralogy play an important role. Oils with higher TBN tend to shift original wettability of siliceous rocks towards oil-wetness and higher TAN numbers affect carbonate rocks better. In addition, higher TOC values increase the amount of organic matter in the rock giving more oil-wet original wettability. Hence, to fully understand original wettability in ULR wettability, rock and oil properties must be studied to determine possible correlations with the rock and oil affinity. The results show that increasing TOC values shift original wettability towards a more oil-wet behavior whereas lithology does not seem to have a direct impact in wetting affinity. To characterize further original wettability in ULR, zeta potential experiments are discussed next.

Zeta potential results

Original wettability is also investigated using zeta potential measurements. Aqueous solutions of water and finely crushed trims samples from the same wells and

depths as CA experiments are used to gauge wetting affinity. The main goal of these measurements is to address stability of thin liquid film on the rock surface. This stability can give an indication of sample water-wetness. Commonly, solutions with zeta potential values greater than +30 mV or lower than -30 mV are defined as stable whereas values between -30 to +30 mV are acknowledged as unstable. Zeta potential measurements for Bakken, Eagle Ford, Wolfcamp and Barnett formations are shown in **Fig. 20**. The results advice that all analyzed samples have values less than -30 mV suggesting unstable water films. These results can be interpreted as intermediate and even oil-wet behaviors due to the low double layer repulsion between the rock and water film represented as their low electrical potential.

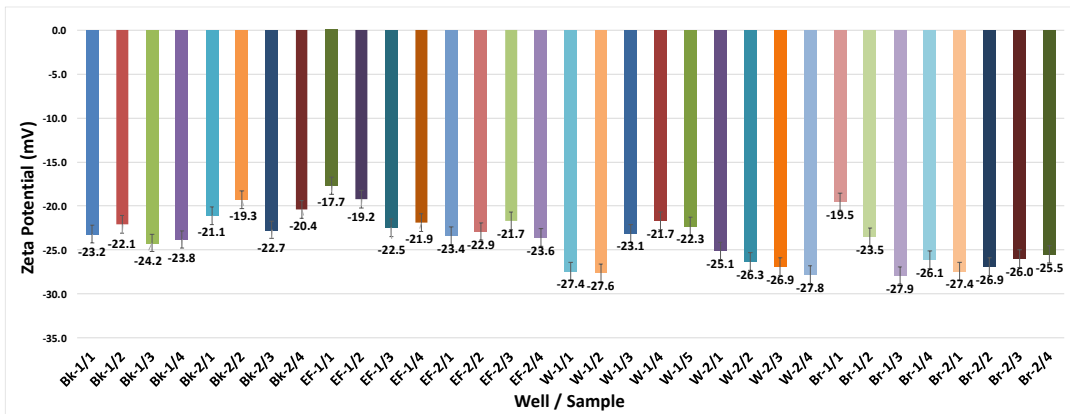


Figure 20. Zeta potential results for water-rock system in wells from Bakken, Eagle Ford, Wolfcamp and Barnett. Reprinted with permission from Alvarez and Schechter (2016c).

Consistent with CA measurements, zeta potential values for Bakken, Eagle Ford, Wolfcamp and Barnett show intermediate-wet as original wettability as thin water films

in the rock behave unstably. CA and zeta potential results clearly define original wettability for these four ULR as intermediate and oil-wet. On the next section, we address the validity of these findings in dynamic wettability measurements by spontaneous imbibition experiments in ULR cores.

Original Wettability Determination by Spontaneous Imbibition Experiments

Monitored by CT Scan Methods

Spontaneous imbibition experiments are the most reliable method to measure wettability in these low porosity and ultralow permeability liquid rich shales. To that end, two types of experiments are performed. First, ULR original wettability is extensively studied by submerging several cores from Bakken, Eagle Ford, Wolfcamp and Barnett formations in oil or water, at reservoir temperatures, to gauge their wetting affinity and consequent imbibition. In addition, to investigate further the changes inside the ULR rocks before and after imbibition, CT scan methods are used to quantitatively measure oil and water penetration magnitudes or imbibition. The second type of experiments addresses the potential of water imbibition with time in oil-aged cores as a technique of improving oil recovery when fracturing ULR. Aged cores are submerged in water for ten days to represent soaking during shut-in of the well after stimulation and oil recovery is periodically measured. Next, we describe the results of the first type of experiments when cores are submerged in oil.

Spontaneous imbibition of oil into ULR cores

Cores from Bakken, Eagle Ford, Wolfcamp and Barnett are submerged in oil from the same formation inside an environmental chamber to guarantee reservoir temperature. Initial weight and average CT numbers are recorded to address changes at the end of the experiments. After two months, samples are weighted and scanned and the volume imbibed is calculate using oil and water densities. The results are represented in **Table 8**. The main observation from oil imbibition experiments is that all formations let oil spontaneously imbibe into the cores regardless, lithology, petrophysical characteristics and oil type. This confirms the results from previous sections in which CA and zeta potential measurements show intermediate and oil-wet behaviors. When the results are analyzed by ULR, Bakken cores show low percentage of pore volume imbibed with values ranging from 18 to 21%. Imbibition results are consistent with wettability values for Bakken, which have the lowest CA along with Barnett samples. This confirms Bakken intermediate affinity to oil compared to other ULR.

Table 8. Oil spontaneous imbibition experiment results. Reprinted with permission from Alvarez and Schechter (2016c)

ULR	Well / Sample	Penetration magnitude (HU)	Δ Weight (gr)	Volume imbibed (ml)	Pore volume (ml)	% Pore volume imbibed
Bakken	Bk-1/1	49	0.389	0.490	2.697	18.1
	Bk-1/3	52	0.487	0.614	3.520	17.4
	Bk-2/1	51	0.209	0.264	1.277	20.7
	Bk-2/3	44	0.168	0.211	1.231	17.1
Eagle Ford	EF-1/2	95	1.036	1.444	3.155	45.8
	EF-1/4	116	1.041	1.451	3.497	41.5
	EF-2/1	133	1.235	1.721	2.284	75.8
	EF-2/2	139	1.140	1.602	2.567	62.4
Wolfcamp	W-1/3	46	0.599	0.731	1.690	43.3
	W-1/4	48	0.607	0.740	1.625	45.5
	W-2/1	50	0.756	0.922	1.465	62.9
	W-2/3	51	0.787	0.959	1.660	57.8
Barnett	Br-1/1	51	0.080	0.099	0.730	13.6
	Br-2/3	69	0.070	0.087	0.722	12.0

Moreover, Eagle Ford and Wolfcamp cores show higher oil imbibition among the group with values from 41 up to 76% of pore volume imbibed. All samples from these formations are intermediate towards oil-wet as determined in CA experiments and confirmed by spontaneous imbibition. Also, Eagle Ford elevated changes in penetration magnitude is because oil is visible replacing gas and/or air from the cores in much more amount than samples from other ULR. This is clearly observed in **Fig. 21**, and it is attributed to the preservation technique used to store Eagle Ford cores before they were handled to our laboratories.



Figure 21. Oil imbibition of Eagle Ford core at $t=0$ h (left) and at $t=1$ h (right).
Reprinted with permission from Alvarez and Schechter (2016c).

Lastly, spontaneous imbibition results for Barnett show low percentage of pore volume imbibed with values of 12 and 13.6% for both wells. Same as in Bakken cores, CA results for these two Barnett samples are intermediate towards water-wet. This wetting state affect capillary pressure and diminish oil capability to imbibe the pores. Hence, wettability is the most important factor driving oil imbibition in these ULR. To track changes inside the cores, CT scan methods are used. Positive penetration magnitudes value in all ULR cores analyzed (Table 8) corroborate oil imbibition. This is because oil has higher CT numbers (approximately -180 HU) than air and gas (around -1000 HU), so when oil replaces air inside the rock the difference in CT numbers is a positive number. Selected CT images before and after spontaneous imbibition experiments for Bakken, Eagle Ford, Wolfcamp and Barnett are shown in **Fig. 22**. Positive changes in CT numbers suggest oil imbibition in cores and the replacement of a fluid with lower CT number (air/gas) by another with higher CT number (oil). Cores from all ULR studied show visible changes in colors from red and green (lower CT numbers) to dark/light blue and purple (higher CT numbers). In addition, images also illustrate the level of core heterogeneity in which laminations as well as vugs and other features are present in ULR samples. These

heterogeneities prevent fluid flow to be concentric towards the core center as fluids are penetrating the samples unevenly by passing through zones with lower permeability.

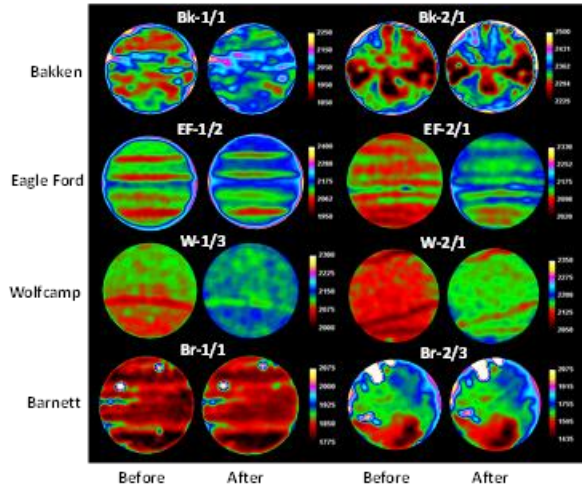


Figure 22. CT images for core slices from Bakken, Eagle Ford, Wolfcamp and Barnett under oil imbibition. Reprinted with permission from Alvarez and Schechter (2016c).

In summary, liquid hydrocarbons are capable to imbibe ULR cores up to 75% of the pore volume demonstrating affinity for oil as wettability indicator of intermediate and oil-wetness. These results are consistent and correlated with CA and zeta potential measurements. In addition, CT scan images show oil penetration into the liquid rich shales by displacing air from the pores. Next, wettability is also addressed by submerging ULR in water to gauge water imbibition.

Spontaneous imbibition of water into ULR cores

Following the same procedure as the previous section, companion cores from the same ULR wells and depths as oil imbibition experiments are submerged in water inside an oven at reservoir temperature for a period of 2 months. After recording initial and final weight and average CT numbers, water penetration is calculated. The results are shown in

Table 9. Consistent with wettability results from CA and zeta potential in which all ULR studied present intermediate-wet behavior, water imbibed in all cores analyzed regardless formation, location or lithology. Cores from Bakken, Eagle Ford, Wolfcamp and Barnett not only let oil imbibe but also water into their pores by capillary forces confirming intermediate wetting affinity. When analyzing the results by unconventional formation, Bakken cores suggest higher imbibition by water than oil with percentage of water imbibed of 62 to 66% of the pore volume in contrast to almost 21% by oil. These findings are persistent with CA measurements where wettability is intermediate towards water-wet and invariable for all cores from the two wells.

Table 9. Water spontaneous imbibition experiment results. Reprinted with permission from Alvarez and Schechter (2016c)

ULR	Well / Sample	Penetration magnitude (HU)	Δ Weight (gr)	Volume imbibed (ml)	Pore volume (ml)	% Pore volume imbibed
Bakken	Bk-1/1	66	1.888	1.888	2.897	65.2
	Bk-1/3	55	1.685	1.685	2.697	62.5
	Bk-2/1	26	0.714	0.714	1.231	57.9
	Bk-2/3	30	0.756	0.756	1.181	63.9
Eagle Ford	EF-1/2	52	0.6708	0.671	3.491	19.2
	EF-1/4	43	0.3645	0.365	3.352	10.9
	EF-2/1	66	0.184	0.184	1.835	10.0
Wolfcamp	W-1/3	36	0.175	0.175	1.388	12.6
	W-2/1	22	0.106	0.106	1.147	9.2
Barnett	Br-1/1	59	0.170	0.170	0.730	23.3
	Br-2/3	42	0.254	0.254	1.630	15.6

In the same line, and contrary with oil imbibition results, Eagle Ford and Wolfcamp samples show much lower water imbibition as well as penetration magnitudes compared to oil. In the previous section, it is shown that oil imbibe Eagle Ford and Wolfcamp cores up to 76% of the pore volume whereas water only imbibe up to 20% in the best case with an average of 11%. These results are a clear indication that samples from Eagle Ford and Wolfcamp have higher affinity to oil than water, which is also confirmed by CA measurements. Nevertheless, the presence of organic and inorganic matter make water able to imbibe the cores but in lower quantities. Then, Barnett imbibition numbers also show slightly higher imbibition by water than oil coherent with CA measurements.

CT scan images from selected cores showing changes in densities related by CT numbers are illustrated in **Fig. 23**. All cores show a distinct increase in CT numbers before

and after imbibition by water with higher changes for Bakken and Barnett cores. CT numbers are increasing because water is replacing air/gas or oil from the cores that have lower CT numbers than water. Hence, positive variations imply water imbibition into the cores by capillary forces. In addition, as Fig 22, heterogeneities are observed which favor water flow inside specific areas of the cores. These heterogeneities are common in ULR and must be considered when designing production strategies.

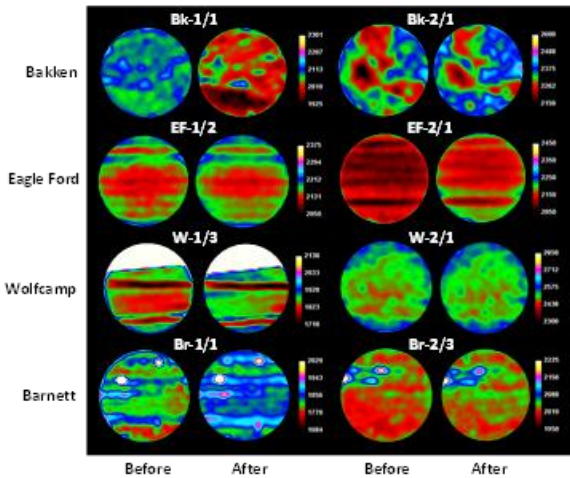


Figure 23. CT images for core slices from Bakken, Eagle Ford, Wolfcamp and Barnett under water imbibition. Reprinted with permission from Alvarez and Schechter (2016c).

In short, water imbibition in Bakken, Eagle Ford, Wolfcamp and Barnett cores is possible due to the mixed wettability exhibited by these ULR. Formations with intermediate towards water-wet results (Bakken and Barnett) have higher water penetration whereas formations with intermediate towards oil-wet values (Eagle Ford and Wolfcamp) show lower water penetration and higher oil imbibition. This capability of

either water or oil to imbibe ULR can be used to improve oil recovery when fracturing the formation. To study the potential of water imbibition and oil recovery in oil saturated ULR cores, spontaneous imbibition experiments that represent the soaking process in the reservoir after stimulation are discussed in the next section.

Spontaneous Imbibition Experiments in Aged ULR Cores

Using cores aged for 4 months at reservoir temperature, we investigate the potential of water to displace oil from ULR samples by spontaneous imbibition experiments. Core dimensions and petrophysical properties shown in Table 6 from Bakken, Eagle Ford, and Wolfcamp samples are used to calculate original oil in place (OOIP). To reproduce a stimulation treatment with a soaking period, experiments are performed for 10 days. Using modified Amott cells, oil recovery is noted with time and reported as function of the OOIP as shown in **Fig. 24**. Spontaneous imbibition results show oil recoveries from 2.8 to 7.8 % of the OOIP. Bakken sample Bk-1/1 has the highest recovery due to its intermediate towards water-wetness as well as its higher permeability compared to other samples. The lowest recovery factors are exhibited by samples from Wolfcamp and Eagle Ford because of their intermediate towards oil-wet wetting affinity. In these ULR cores, oil is replaced by water due to wettability, which favors positive capillary pressure that permits water to imbibe the cores. Then, oil is displaced from the surface by gravity forces due to density difference between oil and water. In addition, from Fig. 14 oil recovery begins only few hours after water gets in contact to the cores.

Nevertheless, all oil recovery values are below 10% of the OOIP suggesting the necessity of another factor that can alter core wettability and shift wetting affinity to more water-wet behaviors.

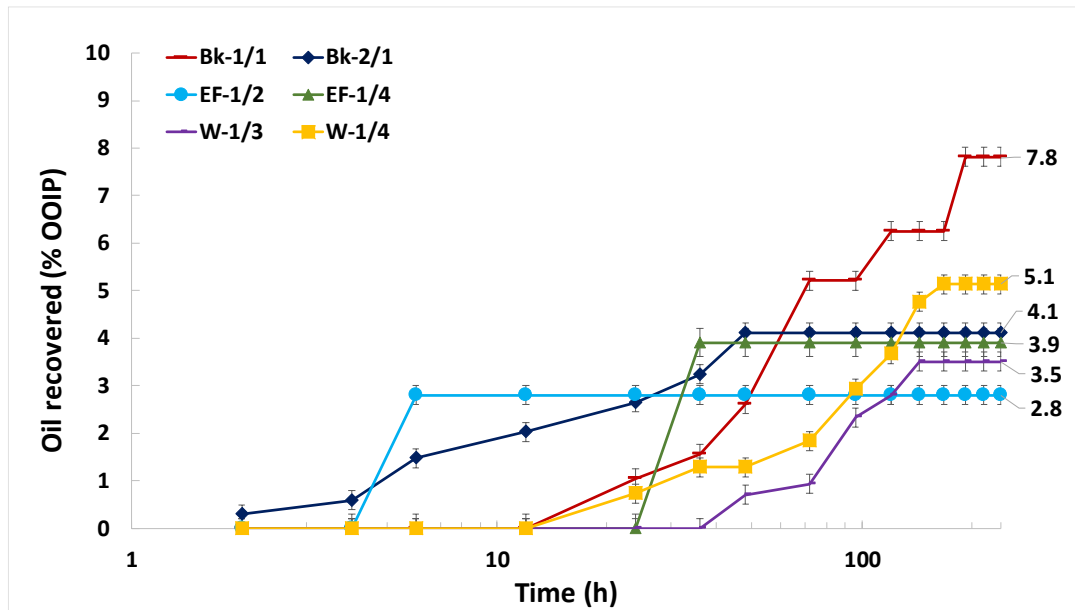


Figure 24. Oil recovered by spontaneous imbibition as percentage of OOIP vs. time for Bakken, Eagle Ford and Wolfcamp cores.

Modified Amott cells are periodically CT scanned to see fluid movement inside the cores with time and track water imbibition into the ULR samples. The difference between water and oil CT numbers allows us to see fluid movement inside the cores as well as cores heterogeneities. To that end, oil CT number is close to -180 HU whereas water-dopant solution CT number is approximately 800 HU. Hence, due to the nature of the dopant used, water imbibition in ULR is encountered when changes in CT numbers are positive in value. CT images at different times during spontaneous imbibition

experiments for cores from Bakken, Eagle Ford and Wolfcamp are shown in **Fig. 25**. Core slice images show changes in CT numbers from low to high values. The variation in colors from red to green and green to dark/light blue is an evidence of water penetration into the core and its consequent oil expulsion. In addition, as observed before, CT images show core heterogeneities that restrict water penetration to be concentric towards the core center. Consequently, water is imbibing into the cores unevenly penetrating zones with better rock properties. Even though, heterogeneities affect fluid flow, a positive change in CT number is observed confirming that water is imbibing the ULR samples displacing oil in the process.

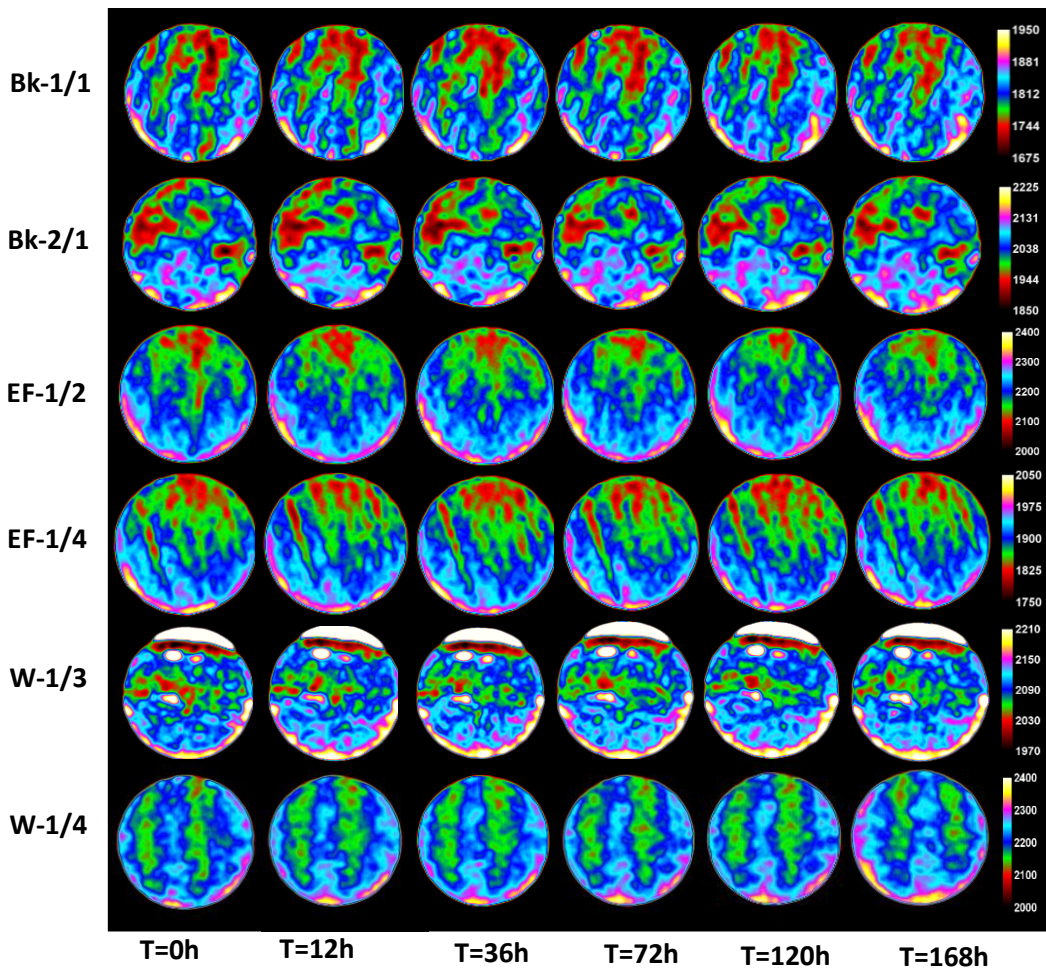


Figure 25. CT images for core slices from Bakken, Eagle Ford and Wolfcamp.
Reprinted with permission from Alvarez and Schechter (2016c).

Nevertheless, as represented in **Table 10**, oil recoveries values from spontaneous imbibition experiments in aged ULR cores are below 8 % of the OOIP. In addition, penetration magnitudes and water imbibition are very modest suggesting that a high percentage of the OOIP is not produced by spontaneous imbibition. This can be explained by the fact that wettability is not shifted towards a moderate and strong water-wet state. In fact, having intermediate and oil-wet behaviors in these ULR rocks makes capillary

pressures negative in sign suppressing water to efficiently imbibe the cores. Only core intermediate-wetness allows capillary pressure to be positive in sign and permits water to penetrate the rock and displace oil in countercurrent movement as evidenced in **Fig 26**.

Table 10. Spontaneous imbibition experiment results. Reprinted with permission from Alvarez and Schechter (2016c)

ULR	Well / Sample	Penetration magnitude (HU)	Δ Weight (gr)	N _b ⁻¹ (-)	Oil Recovered (% OOIP)
Bakken	Bk-1/1	9	0.09	938	7.8
	Bk-2/1	7	0.08	5516	4.1
Eagle Ford	EF-1/2	8	0.01	8452	2.8
	EF-1/4	7	0.02	9984	3.9
Wolfcamp	W-1/3			1109	
	W-1/4	7	0.02	5	3.5
		13	0.05	8611	5.1

As shown, imbibition is responsible of recovering oil in these ULR cores by replacing oil in the matrix by water. In order to assess further the type of forces that are contributing to water imbibition and corroborate the type of fluid movement, the inverse Bond number (Eq. 7) is used. This ratio of gravity to capillary forces determines which force is a dominant, gravitational force as cocurrent flow or capillary force as countercurrent flow. Table 9 shows high inverse Bond numbers for ULR cores from Bakken, Eagle Ford and Wolfcamp. In fact, all inverse Bond numbers are decidedly greater than 5, which confirms that capillarity is responsible of fluid movement and spontaneous imbibition of water into the rocks and fluid flow occurs counter currently, corroborating what was observed in Fig. 16. Capillarity is the main force driving oil production in these experiments because of the inverse effect of pore radius as stated in

the Young-Laplace equation (Eq. 2). As defined in Eq. 2, the smaller the pores, the higher the capillary pressure; hence, capillarity dominates fluid flow. Consequently, ULR with ultralow permeability exhibit high inverse Bond numbers as a clear indication that capillary forces are more important than gravitational forces in controlling imbibition.



Figure 26. Cores Bk-2/1 (left), EF-1/2 (center) and W-1/4 (right) under spontaneous imbibition experiment. Reprinted with permission from Alvarez and Schechter (2016c).

In summary, imbibition experiments performed on aged cores from Bakken, Eagle Ford and Wolfcamp show the potential of recovering oil by them soaking in water, which represents the completion fluid, for a period of 10 days. Moreover, oil recovery is consistent with water penetration observed by CT scan methods and capillary pressure dominates imbibition.

Finally, analyzed ULR show mixed lithology with organic matter, small pore sizes, low porosity, and ultralow permeability as well as oil and intermediate-wet wetting affinity. Due to ULR petrophysical properties, commercial recovery of hydrocarbons depends on multistage fracture treatments in horizontal wells. Stimulation techniques use water and additives as completion fluid to open fractures and transport proppants to the reservoir. Completion fluids are typically composed of water (more than 99 wt.%),

chemical additives (1 wt.%). This study is focused only on the potential of water without chemicals in imbibing shale cores and the results confirm that potential. However, to improve further oil recovery from ULR when fracturing the formation, wettability modifiers, such as surfactants, can be add to completion fluids to alter wettability, reduce IFT and consequently improve water imbibition. On the next chapter surfactant effectiveness in altering wettability and IFT is evaluated using core and oil samples from Bakken, Eagle Ford, Wolfcamp and Barnett.

CHAPTER V

WETTABILITY AND IFT ALTERATION BY SURFACTANTS *

In this chapter, the surfactant capability of altering wettability and reducing IFT is studied using several surfactant types and concentrations. Initially, surfactant stability with brine and oil is studied as a prescreening tool for further experiments. Next, wettability alteration is quantitatively measured at reservoir temperature by contact angle methods and qualitatively measured by zeta potential experiments. Then, the interfacial tension between crude oil and fracturing fluid solution under reservoir temperature was measured using the pendant drop or spinning drop method.

Contact angle, zeta potential and IFT experiments are performed on different core and oil samples from the Wolfcamp, Bakken, Eagle Ford, and Barnett formations. Also,

* Parts of the wettability and IFT alteration by surfactants presented in this chapter have been reprinted from:

“Impact of Surfactants for Wettability Alteration in Stimulation Fluids and the Potential for Surfactant EOR in Unconventional Liquid Reservoirs” by J.O. Alvarez, A. Neog, A. Jais and D.S. Schechter. SPE Paper 169001. Copyright 2014 by the Society of Petroleum Engineers (SPE). Reproduced with permission of SPE. Further reproduction prohibited without permission.

“Wettability Alteration and Spontaneous Imbibition in Unconventional Liquid Reservoirs by Surfactant Additives” by J.O. Alvarez and D.S. Schechter. SPE Reservoir Evaluation & Engineering. Volume 20. Issue 1. Copyright 2017 by the Society of Petroleum Engineers (SPE). Reproduced with permission of SPE. Further reproduction prohibited without permission.

“Altering Wettability in Bakken Shale by Surfactant Additives and Potential of Improving Oil Recovery during Injection of Completion Fluids” by J.O. Alvarez and D.S. Schechter. SPE Paper 179688. Copyright 2016 by the Society of Petroleum Engineers (SPE). Reproduced with permission of SPE. Further reproduction prohibited without permission.

“Potential of Improving Oil Recovery with Surfactant Additives to Completion Fluids for the Bakken” by J.O. Alvarez, I. W. Rakananda Saputra and D.S. Schechter. Energy & Fuels. Volume 31. Issue 6. Copyright 2017 by American Chemical Society (ACS). Reproduced with permission of ACS. Further reproduction prohibited without permission.

these experiments serve as a screening process when several surfactants are tested. The results from this chapter are analyzed according to the capability of surfactants of altering wettability of the rock from its original state towards water-wet and reducing IFT without reaching ultralow values.

Surfactant Stability and Emulsion Tendency Test

Chemical additives stability tests were initially performed with seven different surfactants: two anionic, two nonionic and two blended (nonionic-cationic and nonionic-anionic) surfactants and a complex nanofluid (CNF). These chemical additives are currently offered and used by service companies in hydraulic fracture operations in the Permian Basin. For this study and based on stability test results, some of these surfactants were used in the subsequent experiments. The description of the surfactants used is in

Table 11.

Table 11. Surfactant properties

Surfactant	Primary Components	Concentration (wt.%)	pH	Specific Gravity
Anionic A	Methyl alcohol	40-70	5.8-7.2	0.866 - 0.892
	Proprietary sulfonate	10-30		
Anionic B	Methyl alcohol	10-30	4.7-5.7	0.974 - 0.999
	Proprietary Sulfonate	7-13		
Nonionic A	Branched alcohol oxyalkylate	10-30	5.0-7.0	0.997 - 1.027
Nonionic B	2-Butoxyethanol	10-30	7.2-9.3	0.964 - 0.989
	Methyl alcohol	10-30		
	Petroleum naphtha	1-5		
Nonionic-Cationic	Ethoxylated isodecyl alcohol	10-30	7.0 - 9.0	1.016 - 1.046
	Quaternary ammonium compound	5-10		
	Quaternary ammonium compound	1-5		
Nonionic-Anionic	Methyl alcohol	60-90	6.3-7.3	0.823 - 0.848
	Proprietary ethoxylated alcohol	7-13		
	Proprietary sulfonate	5-10		
CNF	Isopropyl Alcohol	10-30	6.8-8.3	0.953 - 0.956
	Citrus Terpenes	10-30		
	Proprietary	10-20		

Surfactant solutions, during 10 days in an oven at reservoir temperature, were visually investigated to assess surfactant stability; the results after 10 days are shown in **Fig. 27 (top)**. From the seven surfactants tested, surfactants Anionic B and Nonionic B exhibited poor aqueous stability. In addition, emulsion tendency tests for the same surfactants and oil from the Wolfcamp are illustrated in **Fig. 27 (bottom)**.

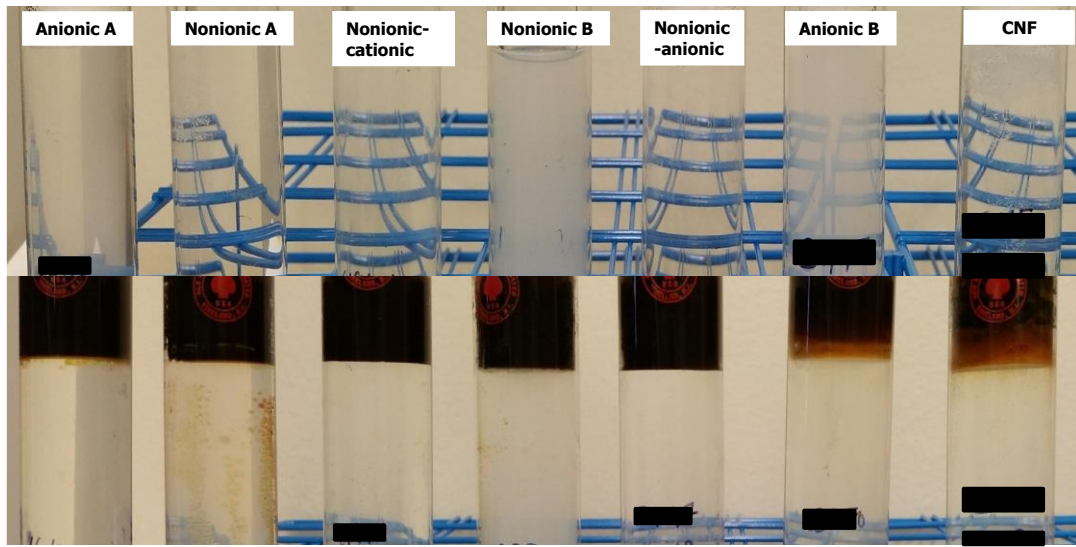


Figure 27. Stability test at 2 gpt (top) for surfactant solutions and emulsion tendency test for surfactant solutions and crude oil (bottom).

After 10 days, surfactant Anionic B still showed emulsions. This was caused by surfactant inability to aggregate the oil drops dissolved into the micelles to favor coalescence and further migration to the oil phase. In addition, surfactant Nonionic A was not completely capable of moving all oil droplets to the oil phase, giving a suboptimal phase separation; but more importantly, surfactant Anionic B and CNF showed emulsions on the interface. Emulsion tendency tests for oil from the Bakken, Eagle Ford, and Barnett formations were also carried out with similar results. Based on the stability test results as a preliminary screening technique, I selected surfactants Anionic A, Nonionic A, Nonionic-cationic, Nonionic-anionic and CNF for the CA, zeta potential and IFT experiments.

Wettability Alteration Results in Unconventional Liquid Reservoirs

The results and observations from the wettability alteration experiments performed are discussed on this section. In order to evaluate the performance of surfactants in altering wettability the same formulation and concentrations are used in samples from the Wolfcamp, Bakken, Eagle Ford, and Barnett formations.

Wettability alteration results in the Wolfcamp formation

Sidewall ULR cores from wells W-1 and W-2 on the Permian Basin, Texas, USA, were used. Cores were 1-inch diameter with total organic carbon (TOC) of 5 to 6 wt. %, measured on a LECO C230 Carbon Analyzer. Porosity ranged from 6 to 7 %, permeability to air from 100 to 160 nD for carbonate cores and 200 to 250 nD for siliceous cores, and median pore radii of 0.004 microns, all measured by mercury injection capillary pressure analysis (MICP). Depth varied from 7820 to 7890 ft. for well W-1 and from 8320 to 8380 ft. for well W-2. **Table 12** shows the XRD analysis from well W-1 at three different depths and well W-2 at one depth. In well W-1, samples from depths of 7850 to 7890 ft. had higher siliceous content, so I called these siliceous samples. On the other hand, samples from depths ranging from 7790 to 7815 ft. were predominately carbonaceous and I addressed them as carbonate samples. For well W-2, at the depth analyzed, samples were predominately siliceous.

Table 12. Lithological composition of rock samples from Wolfcamp wells W-1 and W-2

Well / Sample (Depth)	W-1 / 1 (7876 ft.)	W-1 / 2 (7880 ft.)	W-1 / 3 (7790 ft.)	W-2 / 1 (8370 ft.)
Mineral (wt. %)				
Quartz	42	41	13	48
Clays	26	27	16	27
Calcite	12	13	46	13
Dolomite	6	6	19	6
Feldspar	11	11	4	11
Pyrite	3	2	2	3
Relative Clay (%)				
Illite/mica	95.2	95.8	94.3	94.2
Smectite	4.8	4.2	5.7	5.8
Kaolinite	0	0	0	0
Chlorite	0	0	0	0

Dead crude oil from well W-1 had a black color with density of 0.82 g/cm³ and 32.4° API at reservoir temperature of 165 °F. Moreover, using a Metrohm 905 Titrando apparatus, oil total acid number (TAN) and total base number (TBN) were determined. TAN and TBN values for Wolfcamp oil are 0.09 and 0.12 mg KOH/g oil, respectively. CA and zeta potential measurements for well W-2 were also performed using crude oil from well W-1, which is from the same area and reservoir.

Wolfcamp contact angle measurements results

The results for CA experiments for well W-1 at depths 1 and 2 (siliceous samples) described on Table 12, are shown in **Fig. 28** and **Fig. 29**. To have a baseline to compare wettability alterations and to address original wettability, CA measurements were performed with water without surfactants. The Frac Water bar represents the initial core

wettability. For both depths, initial wettability was oil and intermediate-wet. This mixed wettability is characteristic of ULR due to the mixture of water-wet inorganic pores and oil-wet organic pores. As discussed in chapter 4, these findings are consistent with other studies in which wettability is measured by NMR methods (Odusina, Sondergeld, and Rai 2011), Amott-Harvey methods (Wang et al. 2012) and contact angle methods (Alvarez et al. 2014, Morsy and Sheng 2014, Alvarez and Schechter 2016a).

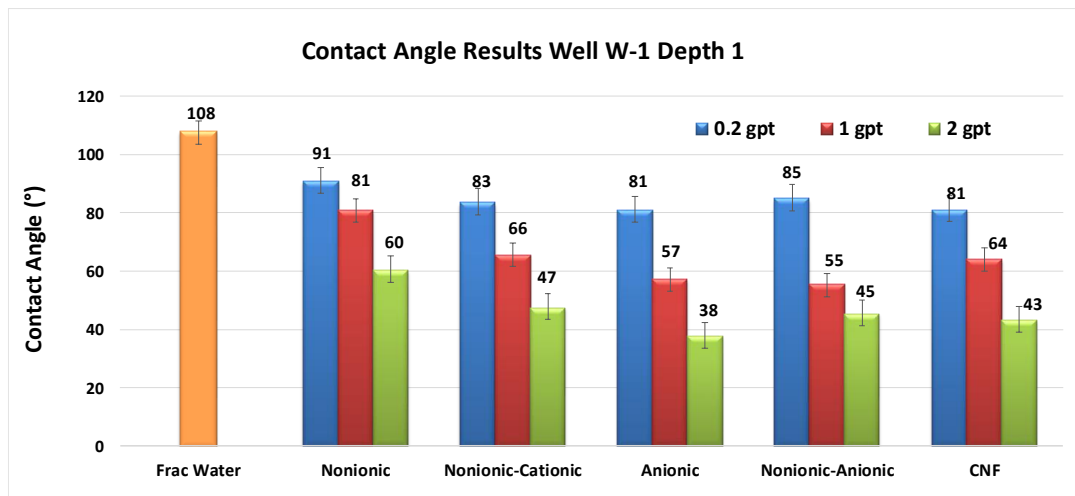


Figure 28. Contact angle results for well W-1 at depth 1.

From the CA results, adding surfactants to frac water reduced the oil's contact angle with the shale surface, and, in concentrations of 1 and 2 gpt, surfactants can shift wettability from oil and intermediate-wet to water-wet. In addition, at the same concentrations, anionic surfactant performed better in reducing CA than nonionic surfactants. This was also evidenced on the nonionic-anionic surfactant in which the contribution of anionic surfactant helped to change wettability in greater amount than the

nonionic and nonionic-cationic surfactants. Anionic surfactant changed CA in higher amount followed very close by the CNF and then, nonionic-anionic and then nonionic-cationic, and nonionic surfactants. In fact, for both depths, anionic surfactant at 2 gpt altered CA in more than 70 degrees (Alvarez and Schechter 2016a).

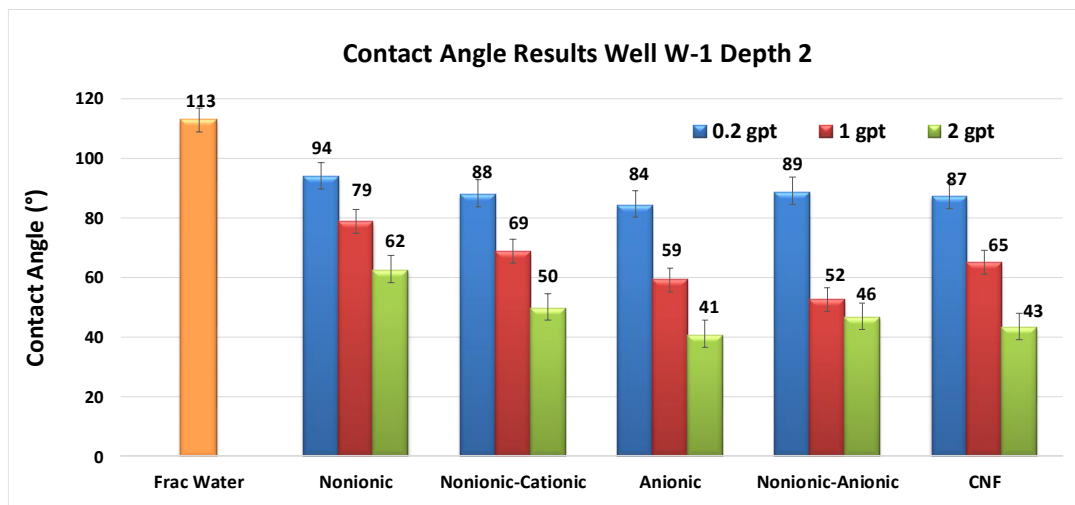


Figure 29. Contact angle results for well W-1 at depth 2.

These results are consistent with the hypothesis that the better performance of anionic surfactants over mixtures of nonionic surfactants is due to electrostatic forces. Thus, the negatively charged heads on anionic surfactant presumably interact with the positively charged oil molecules, mostly based compounds, adsorbed to the siliceous rock surface, which is considered negatively charged (Buckley, Liu, and Monsterleet 1998), forming ion-pairs. Then, the layer of oil in the rock surface is desorbed as ion-pairs forming micelles and transported due their hydrophobicity to the oil phase.

CA experiment results for well W-1 at depth 3, (carbonate samples) are shown in **Fig. 30**. The initial sample wettability was also oil to intermediate-wet as expressed by the frac-water value of 111° . Moreover, as surfactant concentration increased, carbonate ULR sample wettability shifted to water-wet for all surfactants for concentrations of 1 and 2 gpt; however, contrary to the siliceous samples, surfactant nonionic-cationic performed slightly better than the CNF and better than the nonionic-anionic blend, and the anionic surfactant, by reducing CA further. We suggest that nonionic-cationic surfactant has the best efficacy due to electrostatic interactions between positively charged nonionic-cationic surfactant heads and negatively charged oil compounds, mostly acid compounds, attached to positively charged carbonate surfaces. Consequently, oil molecules were stripped from the carbonate surface, thereby altering wettability to a water-wet state. Similarly, negatively charged surfactants such as anionic and nonionic-anionic blends lacked these electrostatic interactions, changing CA in lesser amounts by hydrophobic interactions. In addition, the presence of nonionic surfactant in the nonionic-anionic blend improved its efficacy as compared to the anionic surfactant alone, and poor results exhibited by surfactant nonionic were attributed to the absence of ethoxylated alcohol groups, which are proven more effective in wettability alteration. Moreover, it is important to note that the TAN and TBN crude oil from well WC-1 were measured and the values were 0.09 and 0.12 mg KOH/ g oil, respectively. These results suggested that the Wolfcamp oil is slightly more basic, but the difference between TAN and TBN is minimal. Hence, electrostatic interactions are largely governed by rock charges as distinguished by different lithologies.

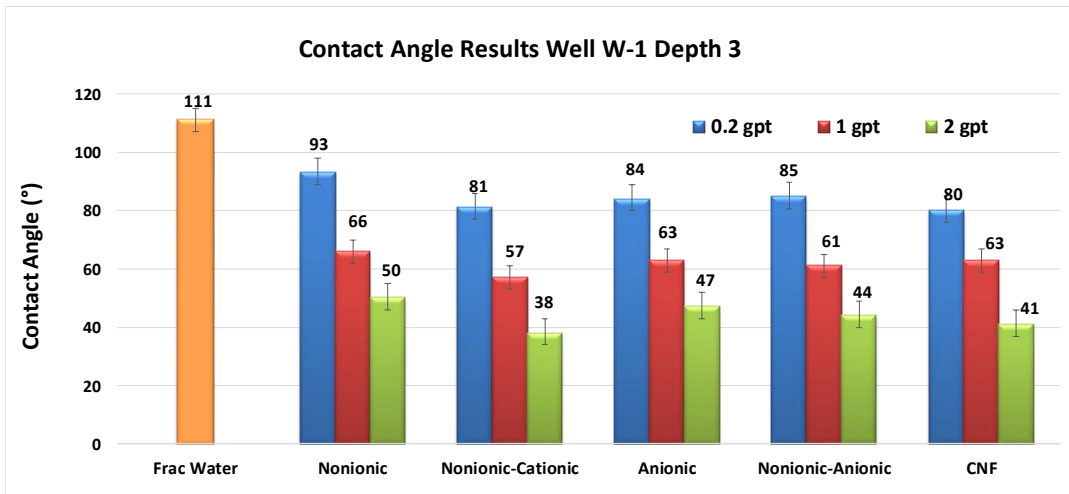


Figure 30. Contact angle results for well W-1 at depth 3.

Results for CA measurements for well W-2 at depth 1 are shown in Fig. 31. As shown in Table 12, W-2 samples were mostly siliceous. Initial sample CA, representing its original wettability was 110° . Hence, the original wetting affinity of this siliceous core was oil towards intermediate-wet. Then, as surfactant concentrations increased from 0.2 gpt to 2 gpt, CA values were reduced, changing wettability from intermediate and oil-wet to water-wet, especially at concentrations of 2 gpt. In addition, anionic surfactant performed better in altering wettability than CNF, nonionic and nonionic blended surfactant. However, due to the amount of anionic surfactant that the nonionic-anionic blend had, surfactant nonionic-anionic performed better than other nonionic and blended surfactants. These results found in well W-2 are consistent with the ones in siliceous samples for well W-1 (depths 1 and 2).

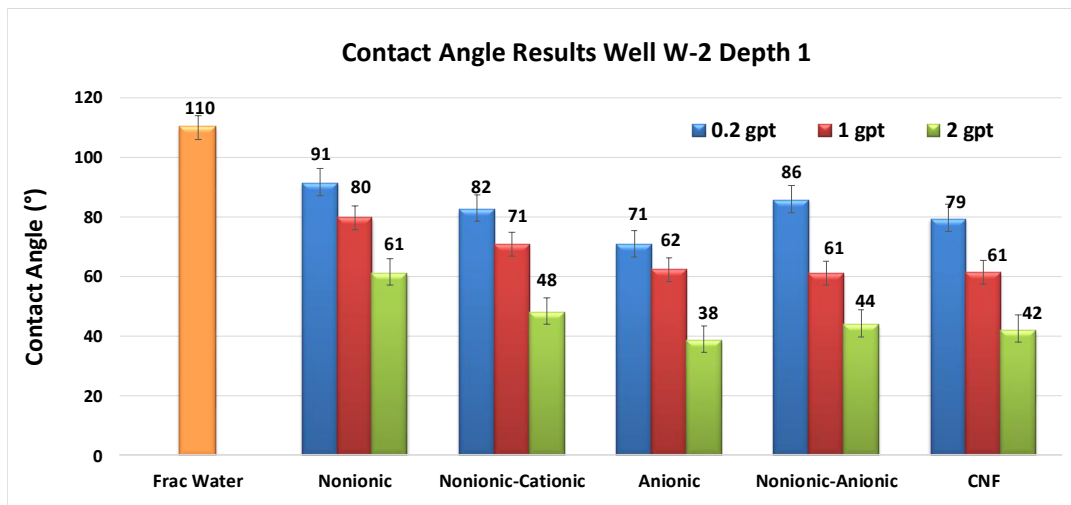


Figure 31. Contact angle results for well W-2 at depth 1.

In summary, anionic surfactant reduced more CA in siliceous cores whereas surfactant nonionic-cationic performed better in carbonate cores. CNF showed slightly better performance in carbonate formations, but also performed well in siliceous samples. These findings suggest that lithology and surfactant type have a direct impact on surfactant efficacy of altering rock wettability on the analyzed Wolfcamp cores. Next, wettability alteration is studied using zeta potential experiment measuring the stability of the thin water film on the liquid rich shale surface for well W-1.

Wolfcamp zeta potential measurements results

The five surfactants tested in CA experiments, at the same concentrations, oil and rock samples from well W-1, at depths 1 and 3, are used in zeta potential experiments. **Fig. 32** shows the zeta potential measurements for siliceous samples (depth 1). Frac-water values for Wolfcamp siliceous trims showed unstable water films, which are read as

intermediate or oil-wetting affinity. However, when surfactant additives were added, film stability increased in absolute values, indicating wettability alteration and better rock affinity for water solutions. In addition, as surfactant concentrations increased, higher absolute zeta potentials were encountered and surfactant anionic A showed slightly more stability than nonionic and nonionic blends. These findings are consistent with previous wettability measurements as CA results also showed more water-wetness as surfactant concentrations increased and anionic surfactant performed better in reducing CA in these siliceous samples.

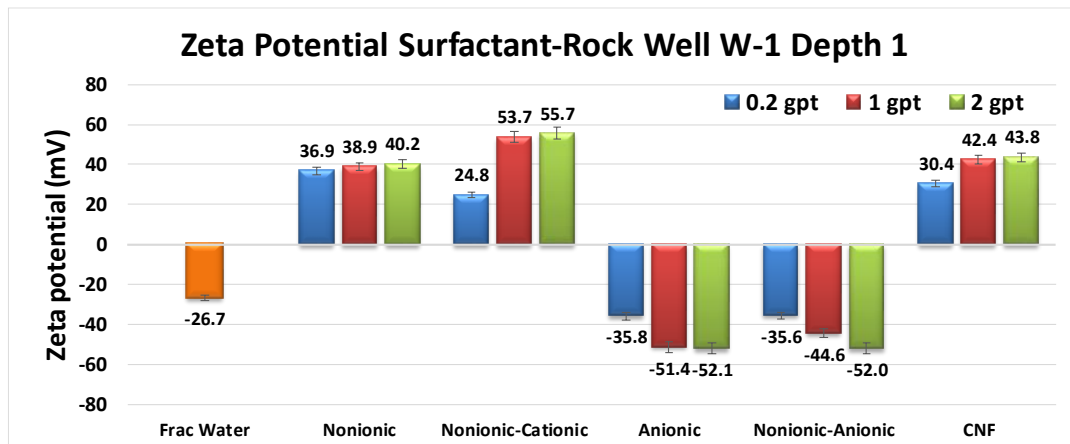


Figure 32. Zeta potential results for well W-1 depth 1 water-rock system.

Zeta potential results for well W-1, carbonate samples (depth 3) are shown in Fig. 33. Rising trends in zeta potential absolute values as surfactant concentrations increased were repeated in carbonate cores as well as the observations that frac water results did not show stable values. However, two differences appeared compared to the siliceous samples. First, zeta potential value for carbonate samples (depth 3) in frac water was considerably

less negative than the siliceous cores due to the positive charges of carbonate rocks. Second, surfactant type performance changed from one lithology to another. In carbonates samples, surfactant nonionic-cationic reached higher absolute zeta potential values than anionic surfactant, showing better stability, which is coherent with the trends observed from contact angle experiments.

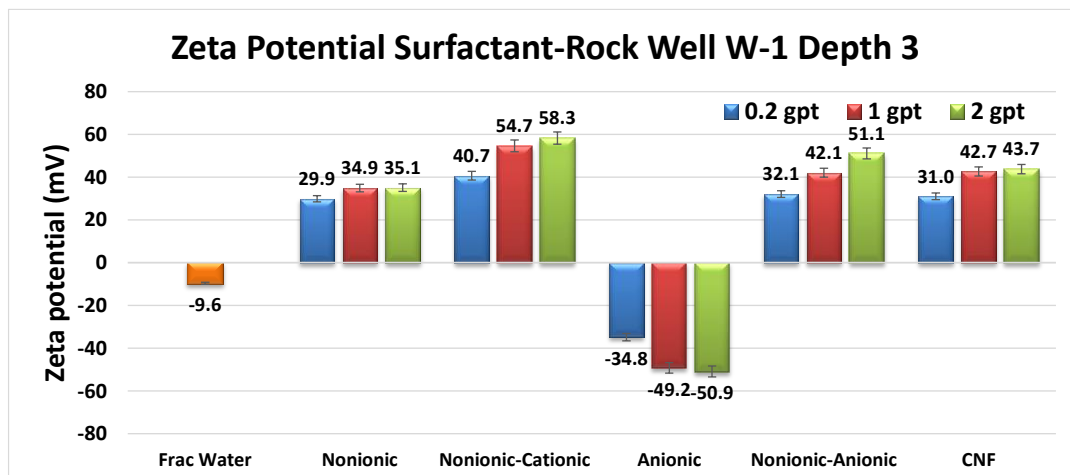


Figure 33. Zeta potential results for well W-1 depth 3 water-rock system.

For both depths analyzed, surfactant and CNF solutions at concentrations of 2 gpt showed very stable films with values higher than ± 40 mV, which is an indication of a water-wet behavior. These results are coherent with CA experiments in which all surfactants tested at 2 gpt alter wettability from oil and intermediate-wet to water-wet. In addition, zeta potential values for water-oil system (**Fig. 34**) showed better stability for surfactants than frac water alone. The increase in the absolute zeta potential value as surfactant concentration increases is an indication of higher stability and stronger impact

on the electric surface charge at the surfactant-oil interface, which facilitated IFT reduction by oil solubilization in surfactant solution (Alvarez and Schechter 2016a).

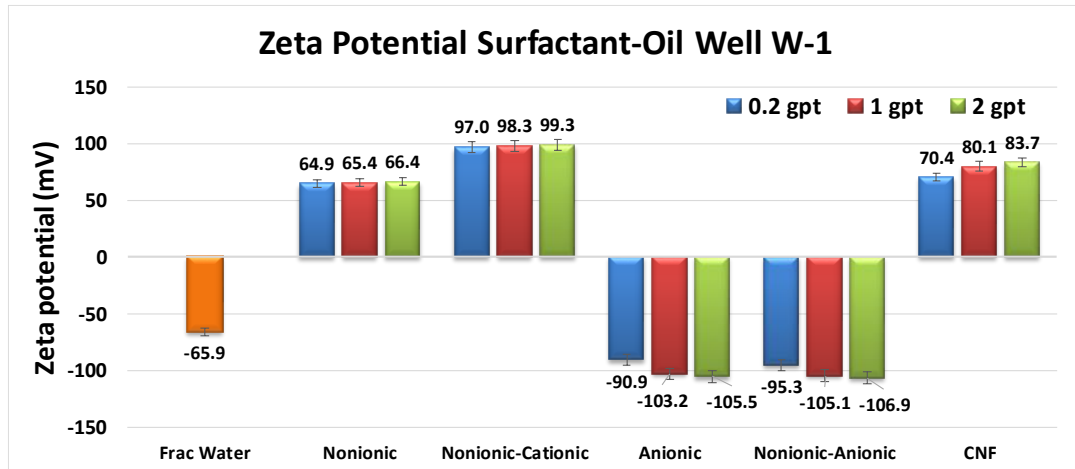


Figure 34. Zeta potential results for well W-1 water-oil system.

Zeta potential values for surfactant-rock and surfactant-oil confirmed also the nature of the surfactant analyzed. The positive contribution of the cationic compounds on the nonionic-cationic surfactant (quaternary ammonium salt) as well as a proprietary and undisclosed by the chemical provider component in nonionic surfactant and CNF made them both positive in zeta potential values; in contrast, negatively charged compounds in anionic and nonionic-anionic surfactants gave them negative zeta potential values. Lastly, zeta potential results reinforced previous observations that electrostatic interactions, due to different surfactant and rock surface charges, may play an important role in wettability alteration in these ULR cores, as surfactants are capable in altering wettability from oil and intermediate to water-wet.

Wettability alteration results in the Eagle Ford formation

Core plugs and trims were received from the liquid rich portion of the Eagle Ford play. The samples were taken from well EF-1 at depths from 13,000 to 13,150 ft. and EF-2 at depths from 14,150 to 14,300 ft. Cores are 1-inch in diameter and 1.5 to 2.5-inches in length with porosities from 9 to 12 %, permeability to air of 100-300 nD, and median pore radii of 0.007 microns, all measured by MICP. Moreover, samples have total organic carbon (TOC) from 5.9 to 6.5 wt. %, measured on a LECO C230 Carbon Analyzer. XRD analysis for wells EF-1 and EF-2 at four different depths is provided in **Table 13** and shows carbonate as the predominant lithology present for the samples tested.

Table 13. Lithological composition of rock samples from wells EF-1 and EF-2

Well / Sample (Depth)	EF-1 / 1 (13043 ft.)	EF-1 / 2 (13122 ft.)	EF-2 / 1 (14185 ft.)	EF-2 / 2 (14250 ft.)
Mineral (wt.%)				
Calcite	60.2	53.9	58.5	53.9
Dolomite	0.9	1.1	0.0	1.0
Quartz	15.4	14.8	14.6	14.8
Clays	15.8	21.7	18.7	21.7
Pyrite	4.1	4.4	4.7	4.4
Plagioclase	2.6	3.0	2.7	3.0
Marcasite	1.0	1.1	0.0	1.1
Relative Clay (%)				
Illite/mica	60	59	60.3	54.2
Illite/Smectite	30	37	29.8	32.8
Kaolinite	3	1	2.3	4.5
Chlorite	7	3	7.6	8.5

Crude oil from well EF-2 is used with density of 0.72 g/cm³ and 52.61° API at testing temperature of 180 °F. Oil total acid number (TAN) and total base number (TBN)

is determined by titration methods in a Metrohm 905 Titrando apparatus. TAN and TBN values are 0.02 and 0.61 mg KOH/g oil, respectively. This suggests that Eagle Ford oil is more basic than acidic. CA and zeta potential measurements for well EF-1 were also performed using crude oil from well EF-2, which is from the same area and reservoir.

Eagle Ford contact angle measurements results

The results for CA experiments, performed in Eagle Ford cores from wells EF-1 and EF-2, as described on Table 13, are shown in **Fig. 35** to **Fig. 38**. CA measurements with brine without surfactants (Frac-water) are performed to define original core wettability and to provide a baseline for wettability alteration. It is observed from the frac-water contact angles that the initial state of wettability of all the samples was intermediate-wet. These results are consistent with other researchers who measured Eagle Ford original wettability by NMR methods (Odusina, Sondergeld, and Rai 2011) and contact angle methods (Alvarez and Schechter 2016c, Morsy and Sheng 2014, Nguyen et al. 2014).

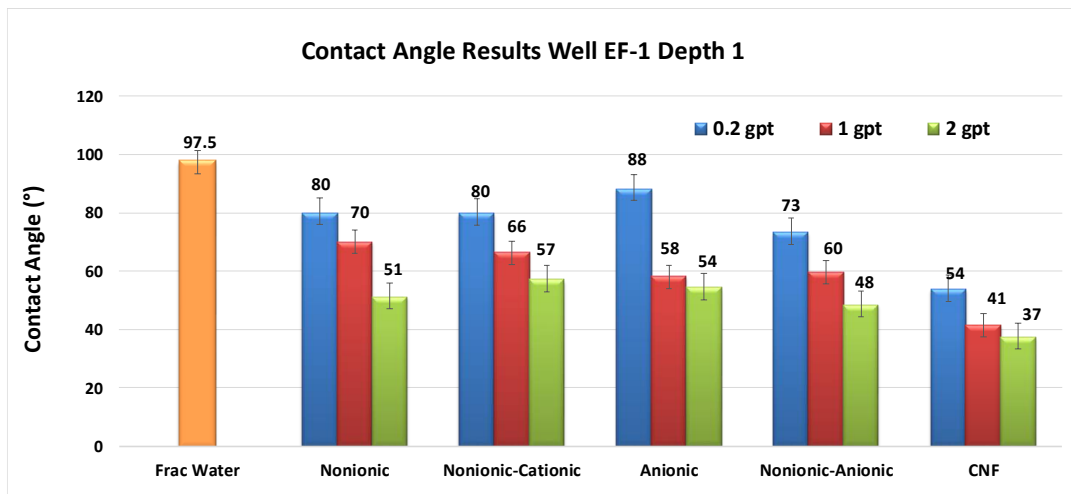


Figure 35. Contact angle results for well EF-1 at depth 1.

Experiments with surfactants and CNF suggested that all surfactants could alter the wettability of samples towards a more water-wet state at a concentration of 1 and 2 gpt, though the degree of alteration was different for different formulations.

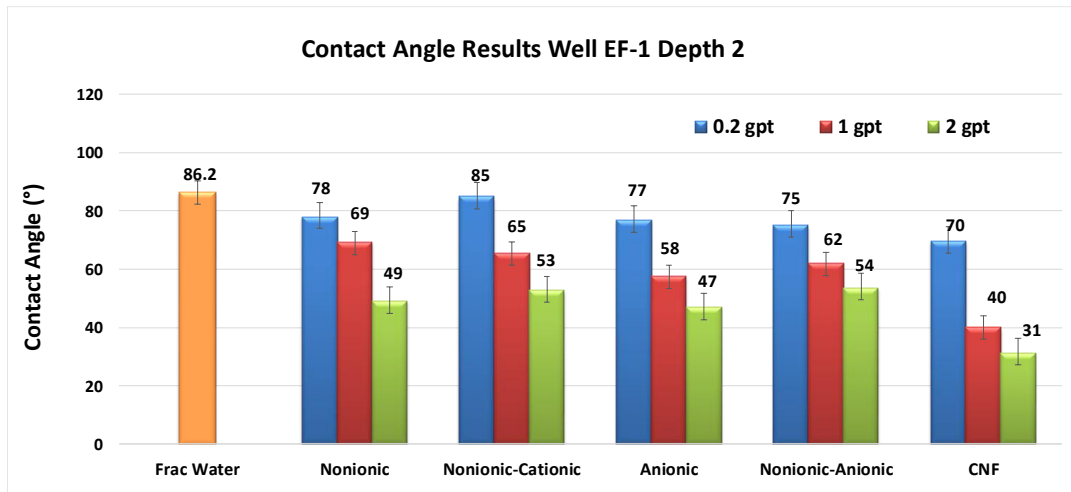


Figure 36. Contact angle results for well EF-1 at depth 2.

Besides, the contact angles decreased with increasing surfactant concentration. For both wells at all depths tested, CNF showed superior performance in terms of reducing contact angle of the rock surface and promoting a more water-wet state followed by anionic surfactant. Among the blended surfactants, the predominantly anionic-nonionic performed better compared to the more nonionic-cationic implying anionic and nonionic components of surfactants had a stronger effect on wettability of the rocks tested.

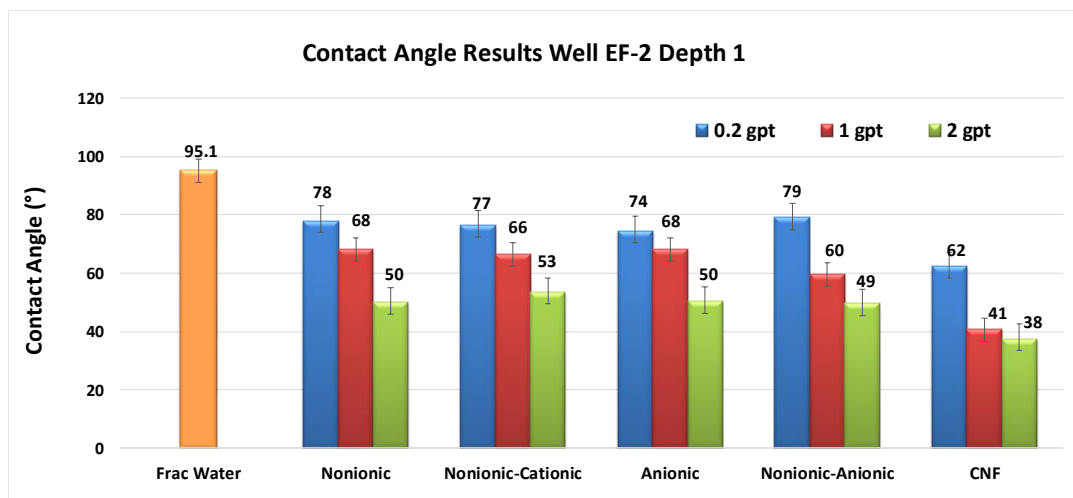


Figure 37. Contact angle results for well EF-2 at depth 1.

This improved performance of CNF and anionic and anionic blend surfactants is attributed to the hypothesis that electrostatic interactions are formed between negatively charged surfactant heads and the mostly basic Eagle Ford oil. As described before in the methodology section, Eagle Ford oil TAN and TBN values are 0.02 and 0.61 mg KOH/g oil, respectively. The higher TAN suggest a basic oil that is more prone to interact with

negatively charged ions such as the ones on additive CNF and anionic surfactants. These interactions favor oil detachment from the rock surface.

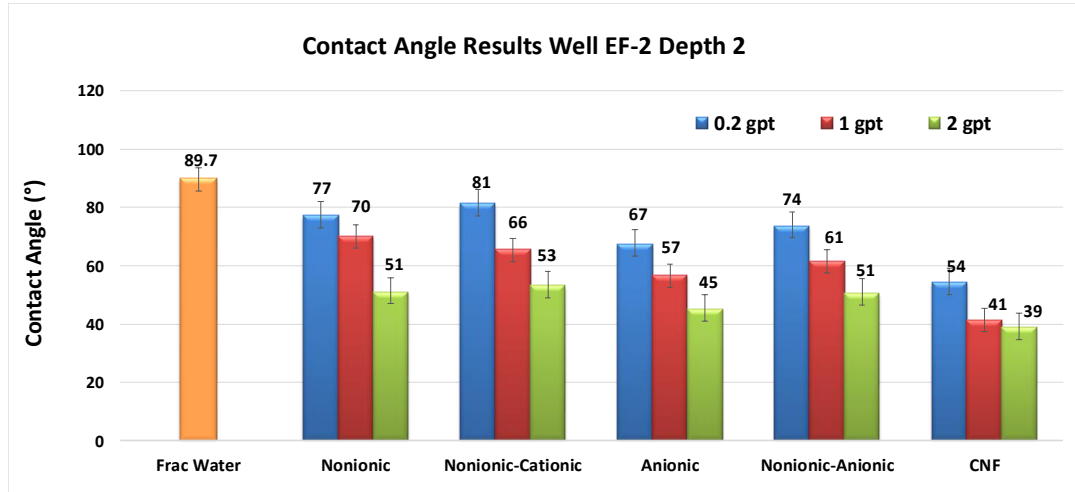


Figure 38. Contact angle results for well EF-2 at depth 2.

In summary, all surfactant additives used on CA experiments shows the capability of altering wettability at concentrations utilized in the field from 1 and 2 gpt. Negatively charged surfactants alter wettability largely. The charges of the surfactant solutions as well as the stability of the water films on the Eagle Ford rock is studied next on the zeta potential experiments.

Eagle Ford zeta potential measurements results

The five surfactants tested in CA experiments, at the same concentrations, oil and rock samples from well EF-2, at depths 1 and 2, are used in zeta potential experiments. Results obtained from zeta potential tests for samples are shown in the **Fig. 39** and **Fig.**

40. Zeta potential values for frac-water suggest that the rock surface-brine are negatively charged when no surfactant additives are added. As can be inferred by comparing the values for water and surfactants, it is evident that the double layer is more stable in the case of surfactants as the magnitude of zeta potential increases.

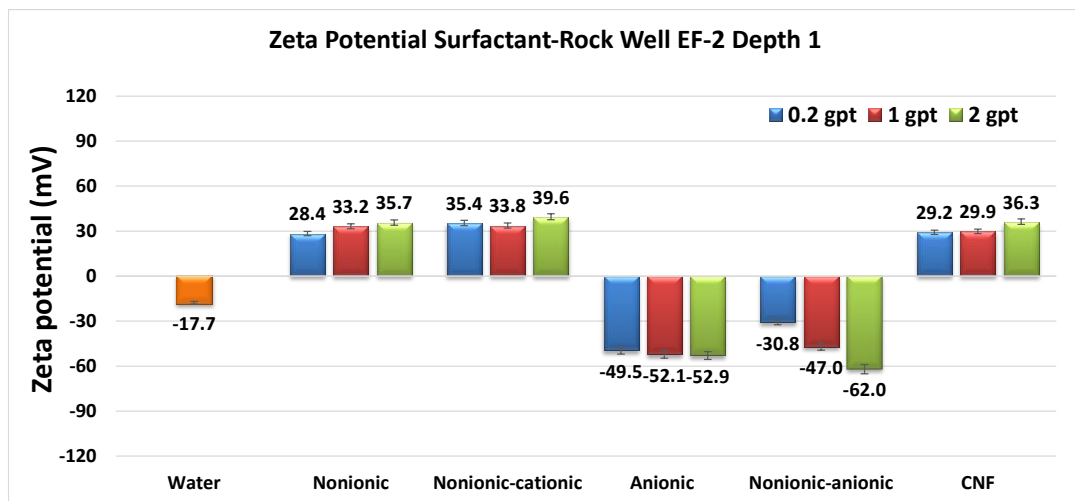


Figure 39. Zeta potential results for well EF-2 depth 1 water-rock system.

The layer stability represented as higher absolute zeta potential values can be interpreted more water-wet as surfactant concentrations are increased. However, the nature of the film depends on the type of surfactant employed. All the surfactants with anionic components such as anionic and nonionic-anionic formed negatively charged films while surfactants nonionic, nonionic-cationic formed a positively charged film as well as CNF. Besides, the strength of the film increased by increasing surfactant concentration, which agrees with the trends observed from contact angle experiments.

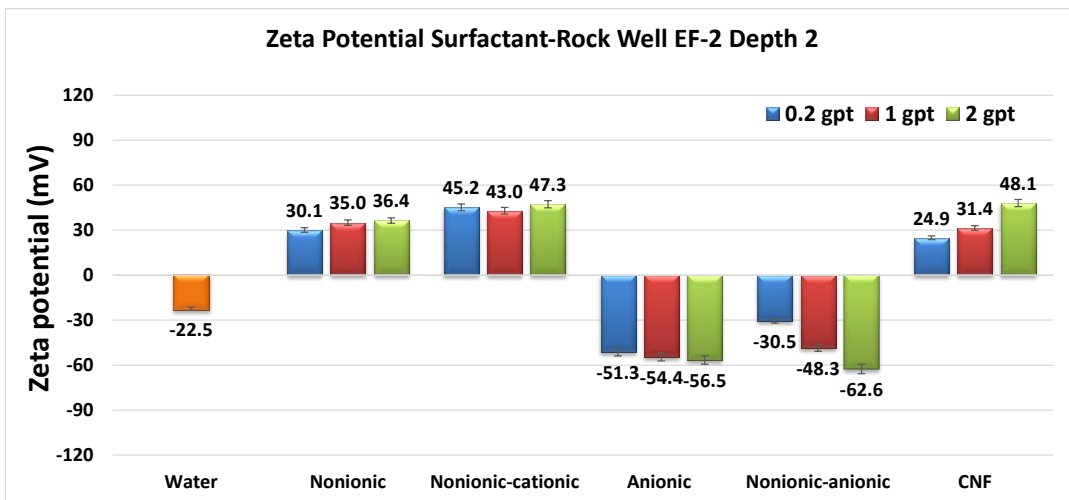


Figure 40. Zeta potential results for well EF-2 depth 2 water-rock system.

As shown in Table 13, Eagle Ford samples tested are predominantly carbonaceous in lithology; negatively charged components in anionic and nonionic-anionic surfactants adsorb readily onto the rock surface and form a thicker film, which is evident from the higher magnitude of negative zeta potentials compared to the positive ones. Thus, it is safe to say surfactants with anionic components adsorbed better on to the carbonate rock surface than the nonionic surfactant. However, at this time no definitely conclusions could be made on the results obtained until I evaluate surfactant adsorption on these rocks that will be addressed in the next chapter. For now, I observed that the formation a stable double layer around the rock due to surfactant adsorption might play a key role in wettability alteration by surfactants while it is important to consider other factors such as ion-pair formation and desorption of adsorbed oil surface-active agents, which explain the wetting changes.

Lastly, **Fig. 41** shows the increase in the absolute zeta potential value as surfactant concentration increases is an indication of higher stability and stronger impact on the electric surface charge at the surfactant-oil interface, which facilitated IFT reduction by oil solubilization in surfactant solution.

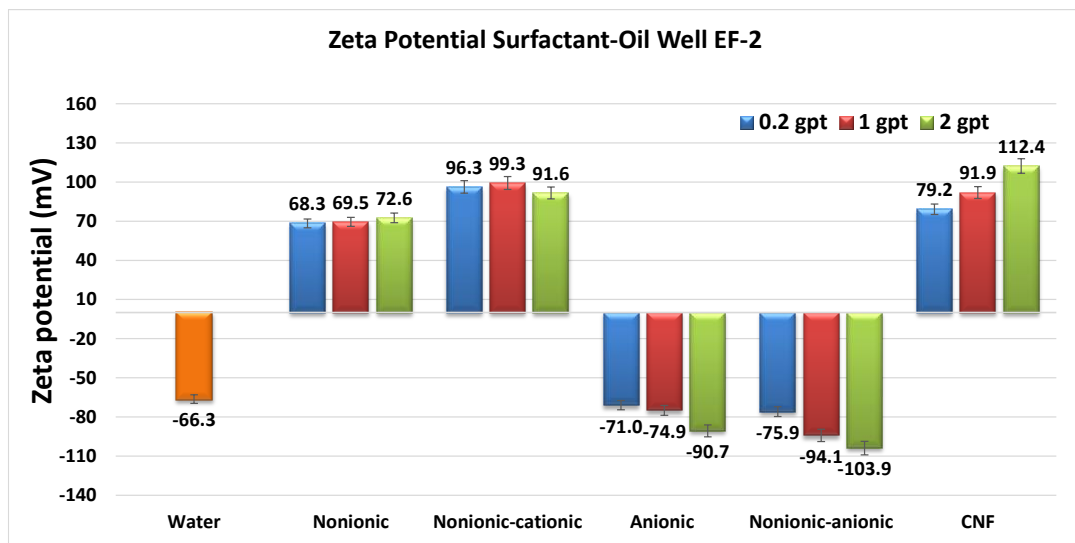


Figure 41. Zeta potential results for well EF-2 water-oil system.

In summary, zeta potential values for surfactant-rock and surfactant-oil systems in the samples tested from the Eagle Ford were higher in absolute value in solutions with surfactant additives implying stronger aqueous films as an indication of water wetness. This effect increased with increasing surfactant concentration.

Wettability alteration results in the Bakken formation

Cores from Bakken, North Dakota, USA, were used. 1-inch diameter cores were cut with a core air drill from preserved 4-inch cores from wells Bk-1 (depths from 9,500

to 10,000 ft.) and Bk-2 (depths from 10,500 to 11,000 ft.). Mineralogical composition by XRD analyses from both wells at the studied depths are listed in **Table 14**. Lithology data indicates that well Bk-1 is mainly siliceous in composition whereas well Bk-2 is more carbonate. This information is vital to understand surfactant efficacy and wettability alteration mechanisms that are dependent on ULR mineral composition. In addition, Bakken dead crude oil is used with density of 0.7936 g/cm³ and 37.30° API at 180 °F.

Table 14. Lithological composition of rock samples from wells Bk-1 and Bk-2

Well / Sample (Depth)	Bk-1 / 1 (9620 ft.)	Bk-1 / 2 (9635 ft.)	Bk-2 / 1 (10765 ft.)
Mineral (wt.%)			
Quartz	53	49	14
Clays	29	19	26
Calcite	3	26	0
Dolomite	4	3	51
Feldspar	9	2	9
Pyrite	2	1	0
Relative Clay (%)			
Illite/mica	69	67	60
Illite/Smectite	13	8	7
Kaolinite	4	9	11
Chlorite	14	16	22

Moreover, using a Metrohm 905 Titrando apparatus, oil total acid number (TAN) and total base number (TBN) were determined. TAN and TBN values for the Barnett oil are 0.36 and 0.23 mg KOH/g oil, respectively. CA and zeta potential measurements for wells Bk-2 were also performed using crude oil from well Bk-1 which is from the same area and reservoir.

Bakken contact angle measurements results

CA experiments are performed in two different wells in the Bakken area. **Fig. 42** and **Fig. 43** show CA measurements for well Bk-1 at depths 1 and 2, respectively, and the changes on CA from original wettability by different surfactants and CNF. To have a baseline to compare wettability alterations and to address original wettability, CA measurements are performed with water without surfactants. This value is represented in Fig. 42 and Fig. 43, where it can be evidenced an initial oil-wet towards intermediate-wet behavior from the well Bk-1 due to its initial CA of 121° and 118° for depths 1 and 2.

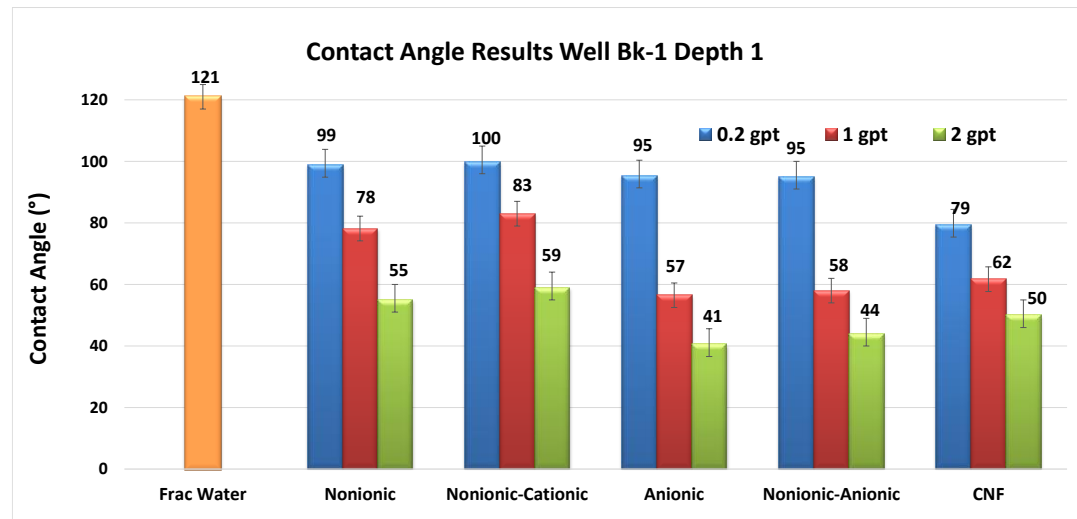


Figure 42. Contact angle results for well Bk-1 at depth 1.

The CA results in well Bk-1 demonstrate that surfactant and CNF additives shift wettability in Bakken samples as their concentration increase from oil-wet to water-wet. In fact, surfactants and CNF additives at concentrations of 1 and 2 gpt are capable of changing CA from 40 to 80° . Moreover, anionic surfactants are more effective in changing

CA from well Bk-1 samples than nonionic, nonionic-cationic and CNF additives. We suggest that that electrostatic interactions govern surfactant performance where the negatively charged anionic surfactant heads interact with the positively charged mostly basic oil compounds that are adsorbed to the siliceous rock surface.

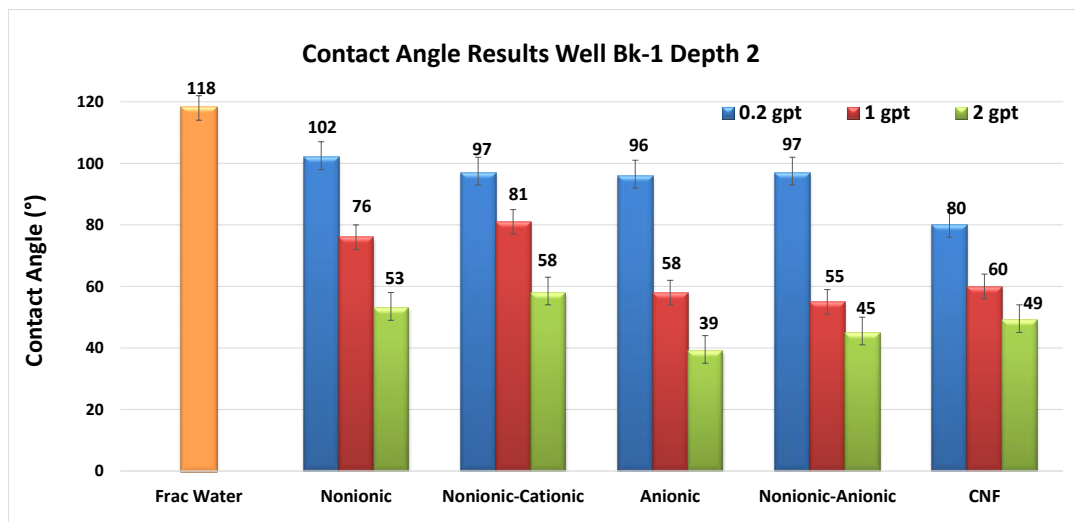


Figure 43. Contact angle results for well Bk-1 at depth 2.

As presented in Table 14, well Bk-1, at both depths analyzed, has mainly siliceous mineralogical composition; this gives negative charges to the rock surface in which oil is attached. The oil compounds that bear positive charges and are attracted and absorbed by the surface polarity along with the presence of organic matter mixed in the samples give the rock an oil-wet behavior (Buckley, Liu, and Monsterleet 1998). Anionic surfactant heads and the attached oil on the rock surface form ion-pairs. These ion-pairs are desorbed from the surface in the form of micelles and transported to the oil phase due their hydrophobicity (Alvarez and Schechter 2016a).

CA results for well Bk-2 are shown in **Fig. 44**. In this case, well Bk-2 is mainly carbonate as shown in Table 14, and its original wettability is calculated as oil-wet towards intermediate-wet defined by the CA of 122°. As in well Bk-1, when surfactants and CNF concentration are raised, Bakken samples change their wettability to water-wet, specifically at concentrations of 1 and 2 gpt. However, contrary to well Bk-1, CNF and surfactant nonionic-cationic perform better, by reducing the CA to lower values, than anionic surfactant. CNF and surfactant nonionic-cationic have positive charges, which are attracted to the negatively charged oil molecules, mostly acid compounds, attached to the positively charged carbonate surface. We hypothesized that these electrostatic forces aid ion-pair formation of oil and CNF molecules by forming micelles to strip oil from the surface and move it to the oil phase. By the same principle, anionic surfactant negatively charged heads are repelled from the surface, performing not as well as CNF or nonionic and blended surfactants. Moreover, in both wells, we propose that nonionic surfactants alter wettability by surfactant adsorption, driven by hydrophobicity, in which the oil layer adsorbed to the shale surface forms a double layer with the hydrophobic surfactant tails; hence, the hydrophilic surfactant heads face the solution, altering wettability and creating a water-wet zone.

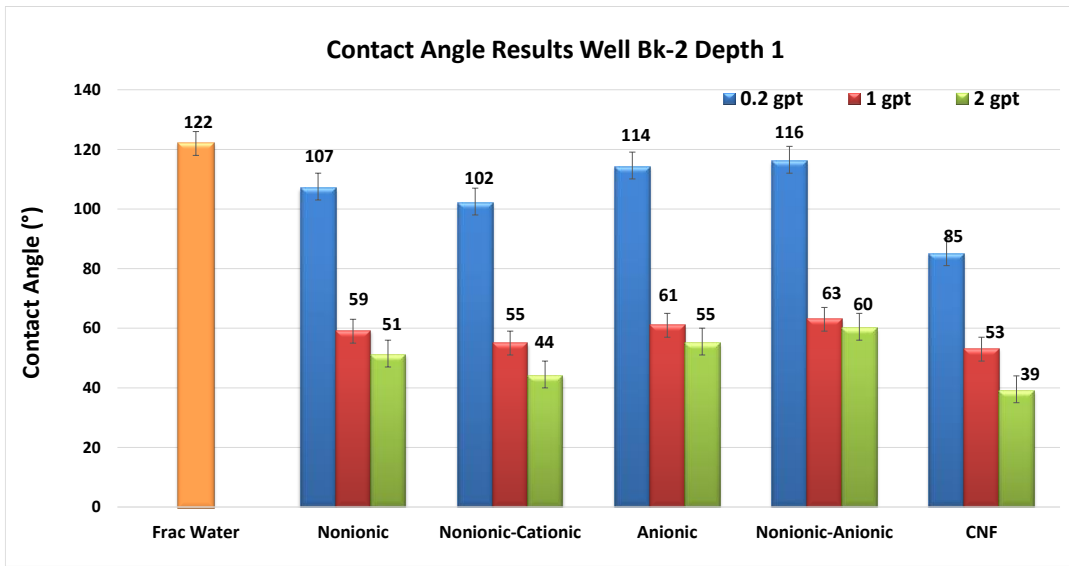


Figure 44. Contact angle results for well Bk-2 at depth 1.

In summary, for both wells studied, original wettability is oil towards intermediate-wet, regardless of their mineralogical composition. These findings are consistent with other Bakken wettability studies such as Shuler et al. (2011), Wang et al. (2012), Nguyen et al. (2014) and Wang et al. (2016). This wetting preference is characteristic of Bakken as ULR due to the mixture of water-wet inorganic pores and oil-wet organic pores. Moreover, at field-used concentrations of 1 gpt and 2 gpt, surfactants and CNF are capable of altering wettability towards water-wet in all the Bakken samples tested and their efficacy depends on surfactant type and mineral composition. To evaluate further wettability alteration, zeta potential experiments are discussed next.

Bakken zeta potential measurements results

Surfactants and CNF zeta potential measurements results for well Bk-1 and well Bk-2 are shown in **Fig. 45** and **Fig. 46**, respectively. Aqueous solutions without chemical additives show an unstable water film on the rock surface, determined as zeta potential values between -30 and +30 mV, which can be interpreted as an oil or intermediate wetting preference. Then, as surfactant and CNF additives are added to the aqueous solutions in increasing concentrations, zeta potential values are higher in absolute number as evidence of more stable water films and, consequently, more water-wetness. These results are consistent with CA measurements in which surfactants and CNF additives changed wettability from oil-wet to water-wet.

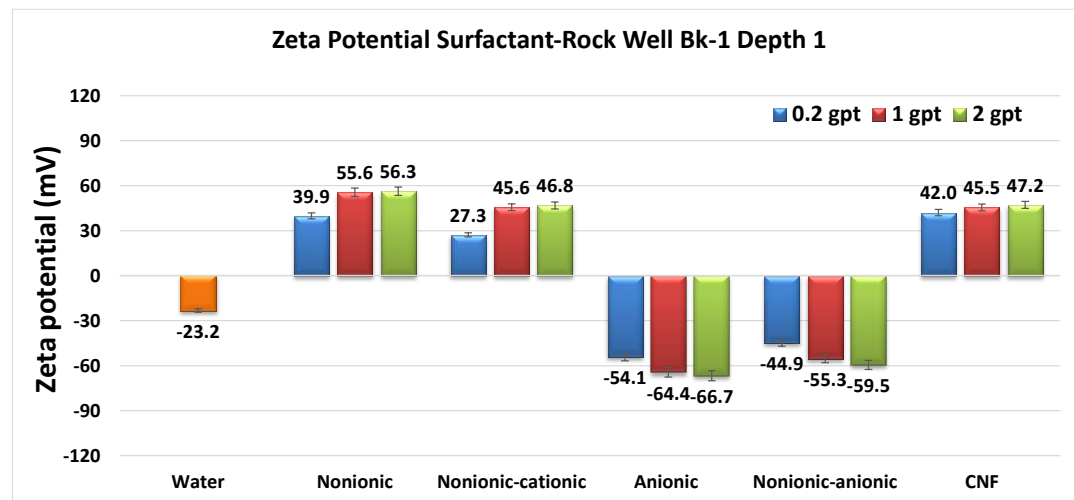


Figure 45. Zeta potential results for well Bk-1 depth 1 water-rock system.

When each well is analyzed separately, well Bk-1 (Fig. 45) shows higher absolute values for anionic surfactants compared to nonionic and blended surfactants and to CNF

due to the electrostatic interactions driven by rock-fluid charges. In addition, all surfactants and CNF at concentrations of 1 and 2 gpt show zeta potential values higher than 45 mV. On the other hand, well Bk-2 (Fig. 46) shows higher zeta potential absolute values for nonionic surfactants, and CNF, compared to anionic surfactants which is consistent with CA findings due to electrostatic attractions of CNF and repulsions of anionic surfactants (Alvarez and Schechter 2016a).

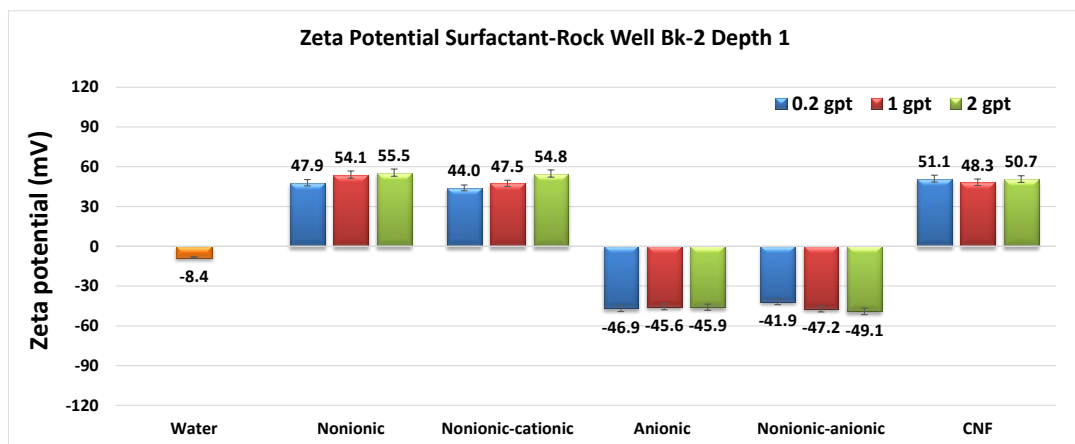


Figure 46. Zeta potential results for well Bk-2 depth 1 water-rock system.

In addition, the stability of aqueous solutions, with and without surfactants and CNF, and Bakken oil is also studied by zeta potential experiments as shown in **Fig. 47**. The lowest value is observed in the solution without chemical additives, water. Then, as surfactant concentrations increase, solutions have higher absolute values, an indication of better stability. Moreover, this electric potential on the aqueous solution-oil interface favors IFT reduction and subsequent wettability alteration. Finally, zeta potential results for surfactant-rock and surfactant-oil can also give an indication of the nature of the

chemical additives analyzed as well as the rock charges. Anionic surfactants exhibit negative values whereas nonionic surfactants and CNF show positive numbers and siliceous rocks have more negative zeta potential values than carbonate samples. These different charges in nature help to explain the role of electrostatic forces in wettability alteration, which are evidenced by CA results shown in the previous section.

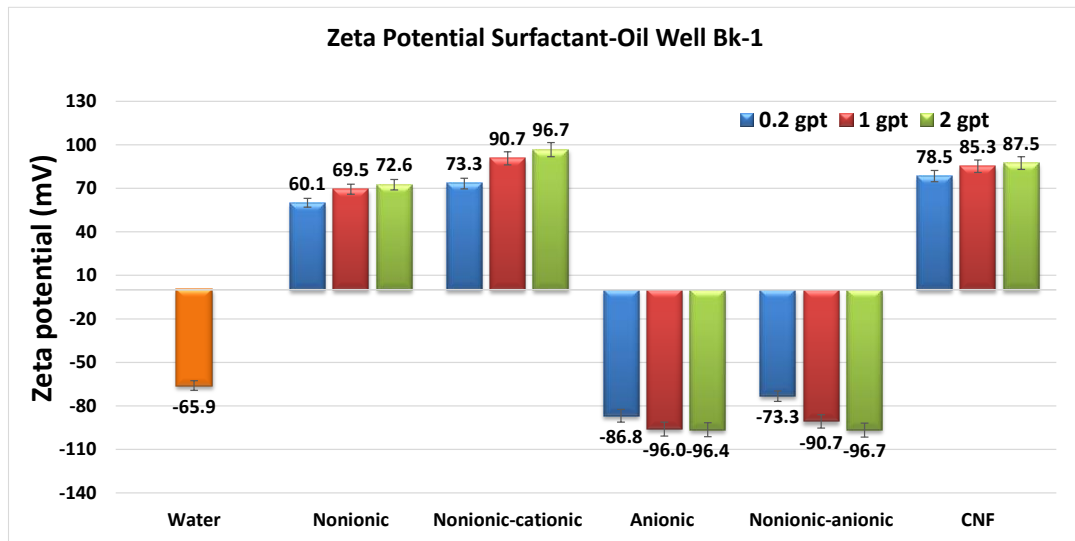


Figure 47. Zeta potential results for well Bk-1 water-oil system.

In summary, consistent with CA, zeta potential results show higher absolute values for solutions with surfactants and CNF than water alone as evidence of more stable water films, and consequently, more water-wetness, especially at concentrations of 1 and 2 gpt.

Wettability alteration results in the Barnett formation

The ULR cores that we used are from depths around 6000 ft. to almost 9000 ft. They are preserved side-wall cores, 1-inch diameter and 1.5 to 2.5-inches in length with

porosities from 6 to 8 %, permeability to air of 750-1050 nD, and median pore radii of 0.007 microns, all measured by MICP. Moreover, samples have total organic carbon (TOC) from 1.7 to 2.5 wt. %, measured on a LECO C230 Carbon Analyzer. XRD analysis for wells Br-1 and Br-2 at three different depths is provided in **Table 15** and shows siliceous as the predominant lithology present for the samples tested.

Table 15. Lithological composition of rock samples from wells Br-1 and Br-2

Well / Sample (Depth)	Br-1 / 1 (6060 ft.)	Br-1 / 2 (8018 ft.)	Br-2 / 1 (7030 ft.)
Mineral (wt.%)			
Quartz	48	43	46
Clays	8	22	8
Calcite	35	18	38
Dolomite	6	7	6
Feldspar	2	8	1
Pyrite	1	2	1
Relative Clay (%)			
Illite/mica	91	90	76
Illite/Smectite	0	0	24
Kaolinite	11	5	0
Chlorite	0	5	0

Dead crude oils used were from the same wells as the cores with a viscosity of 30.0 cp and a density of 0.8080 g/cc at 165 °F and 37.74° API for Well Br-1, and 40.5 cp and a density of 0.8054 g/cc at 165 °F and 35.77° API for Well Br-2. Moreover, using a Metrohm 905 Titando apparatus, oil total acid number (TAN) and total base number (TBN) were determined. TAN and TBN values for the Bakken oil are 0.27 and 0.55 mg KOH/g oil, respectively, for well Br-1, and 0.10 and 0.57 mg KOH/g oil, respectively, for well Br-2.

Barnett contact angle measurements results

For well Br-1 depths 1 and 2 contact angle results are shown in **Fig. 48** and **Fig. 49**, respectively. Frac water bars in the plots represent the experiments performed without adding any surfactant to test the original contact angle of the cores before altering wettability.

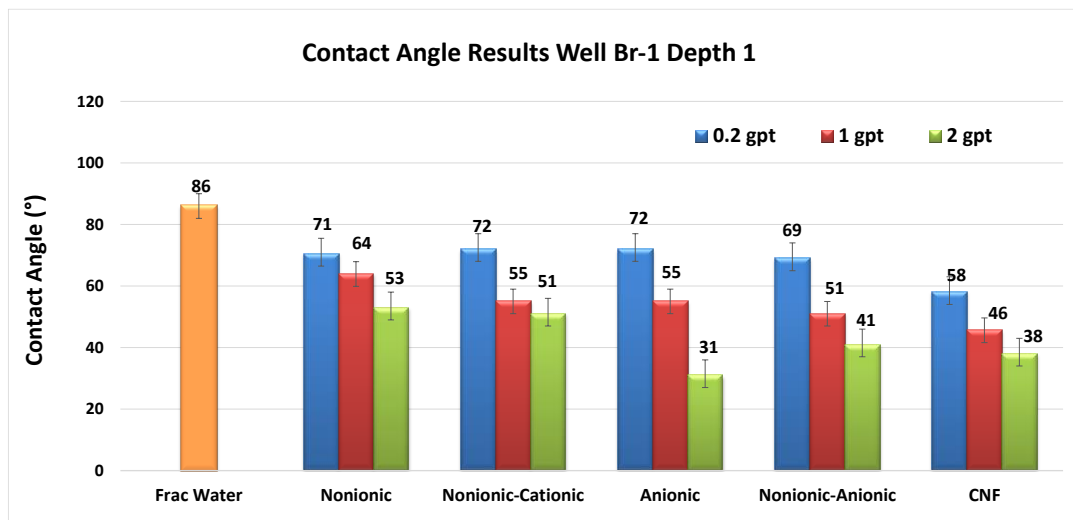


Figure 48. Contact angle results for well Br-1 at depth 1.

From contact angle measurements without surfactant, we obtained that all samples are initially intermediate-wet ranging from 86 to 100°. At the two depths tested, almost all surfactant concentrations of 1 and 2 gpt can vary wettability in shale samples from intermediate-wet towards water-wet. Also, lower contact angles, which represent more water-wet behavior, were obtained using anionic surfactants than CNF, nonionic and mixed surfactants, at the same concentrations.

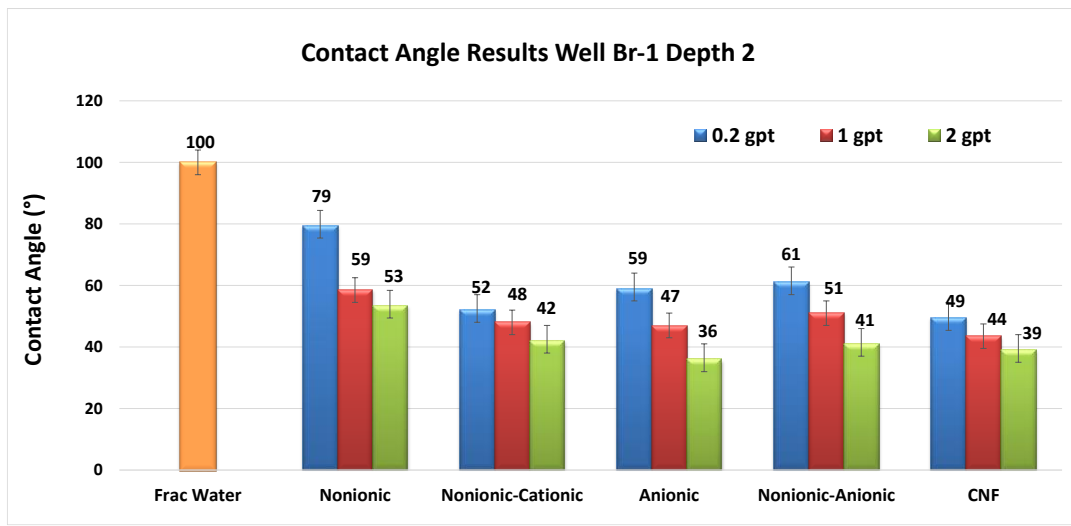


Figure 49. Contact angle results for well Br-1 at depth 2.

The results for well Br-2 depth 1 are shown in **Fig. 50**. Frac water bars showed that cores are intermediate-wet. For all depths, water-wet behavior was reached using anionic surfactant at all concentrations, when nonionic surfactant needed higher concentrations (1 gpt and in some cases 2 gpt) to shift wettability towards strong water-wet behavior. Overall, anionic surfactant decreased more contact angle than CNF, nonionic and mixed surfactants (Alvarez et al. 2014).

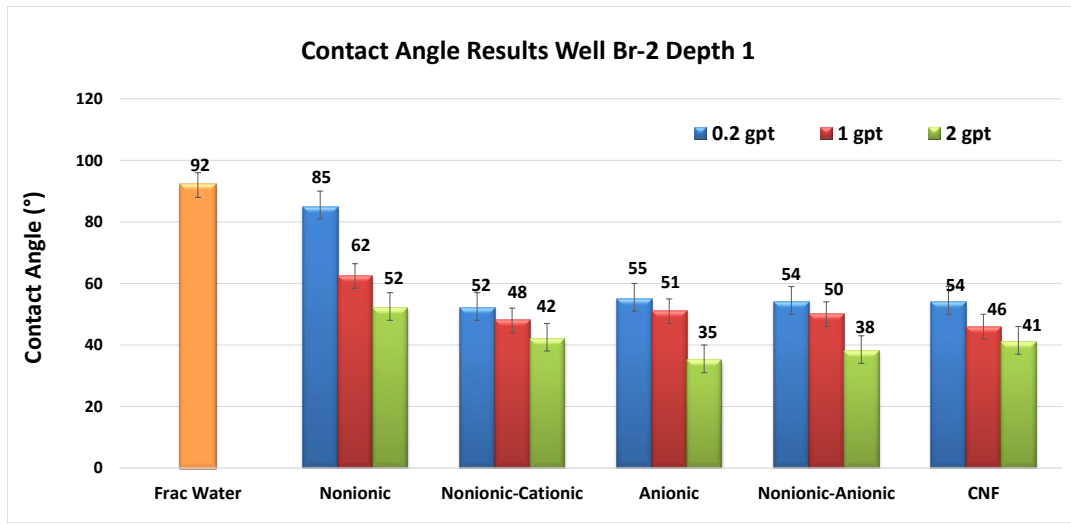


Figure 50. Contact angle results for well Br-2 at depth 1.

In summary, anionic surfactant showed better capability to shift wettability from oil to intermediate-wet towards water-wet than CNF, nonionic and mixed surfactants at field used concentrations of 1 and 2 gpt in these mainly siliceous rocks.

IFT Alteration Results in Unconventional Liquid Reservoirs

The results and observations from the IFT alteration experiments performed are discussed on this section. To evaluate fluid-fluid interactions and the performance of surfactants in altering IFT the same formulation and concentrations, as in contact angle and zeta potential experiments, are used in crude oil samples from the Wolfcamp, Bakken, Eagle Ford, and Barnett formations.

IFT alteration results in the Wolfcamp formation

IFT measurements are performed using dead oil from Well W-1 and the same surfactants and concentrations tested in CA and zeta potential experiments at reservoir temperature (165 °F). IFT results are in **Fig. 51** in which Frac water values represent the aqueous solutions without surfactants. Initially, frac water and oil have an IFT of 21.8 mN/m. This value is significantly reduced by adding surfactants at field concentrations of 1 and 2 gpt. Surfactants, as amphiphilic compounds, align themselves at the oil-water interface lowering IFT. These molecules are placed at the interface such that the hydrophobic tails interact with the hydrophobic oil phase, and the hydrophilic heads interact with the hydrophilic phase, thus lowering potential energy. For the observed results, anionic surfactant has better performance in reducing IFT than nonionic and mixed nonionic surfactants. In fact, at concentrations of 2 gpt, anionic surfactant reduces IFT in one order of magnitude less than the other surfactants tested followed by CNF. In addition, due to its anionic contribution, the nonionic-anionic surfactant decreased IFT greater than the nonionic-cationic surfactant. Moreover, surfactant efficacy in decreasing IFT depended also on the surfactant nature. This improved efficacy of the anionic surfactant in decreasing IFT is attributed to the presence of sulfonates as part of their composition, which are functional groups with the general formula R-SO₃⁻ on its formulation. Sulfonates are complex molecules with an anionic polar head and a non-polar component tail, giving them the so-called amphoteric property that make them excellent surfactants. These sulfonates will stabilize the emulsion of the oil in the water, which can be appreciated by a reduction of IFT (Alvarez and Schechter 2017).

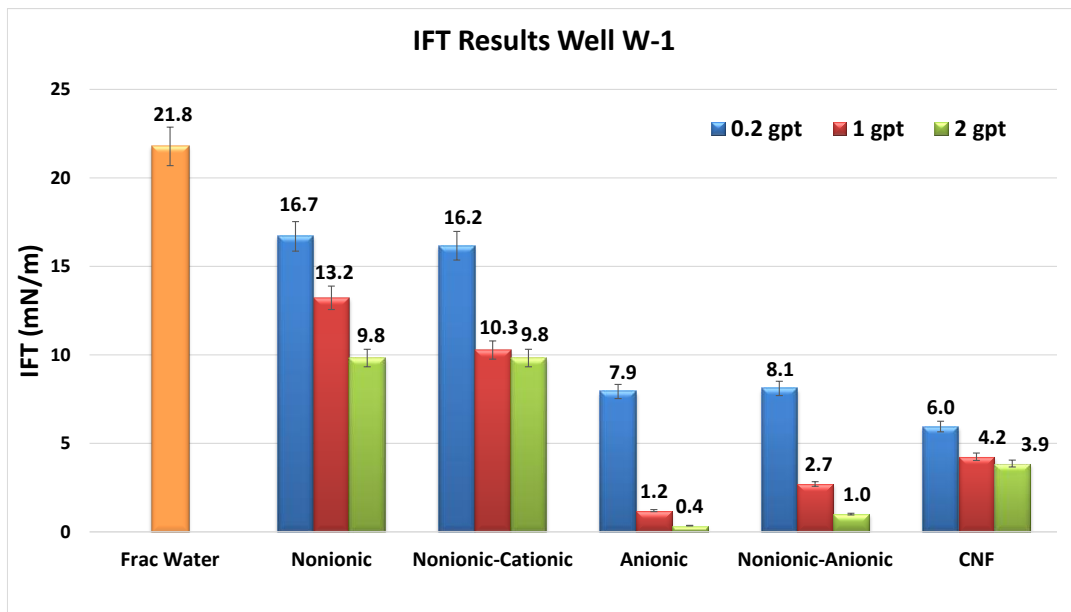


Figure 51. IFT results for Well W-1.

Furthermore, the slightly basic character of Wolfcamp well W-1, as determined by its TAN and TBN of 0.09 and 0.12 mg KOH/g oil, respectively, favored negatively charged surfactants (anionic surfactants) to interact better with positively charged basic oil molecules and reduce IFT in higher amounts.

Previous studies hypothesized that IFT reduction favors micellar solubilization mechanism to alter wettability (Kumar, Dao, and Mohanty 2008). In capillary pores, especially in this ULR where pore size is very small (0.004 microns), the aqueous phase initially imbibes the pores due to IFT reduction. Then, the oil film on the rock surface is solubilized by surfactant solution stripping oil from the surface altering wettability from oil-wet to water-wet. In our experiments, anionic surfactant show better performance decreasing IFT than nonionic and mixed nonionic surfactants, this is consistent with CA angle results in which anionic surfactant alters wettability in greater value. Hence, we

suggest that a combination of electrostatic interactions and IFT reduction is responsible of altering wettability from oil and intermediate-wet to water-wet in these ULR cores. As shown before, in ULR, surfactants can be used to reduce IFT to favor water imbibition; however, IFT should be decreased low enough to let water imbibe into the pore and expel oil as countercurrent flow, without reaching ultralow values which might favor oil redeposition on the surface and water movement outwards the matrix due to ultralow capillary pressure.

IFT alteration results in the Eagle Ford formation

Interfacial tension was measured at 180 °F for the oil-aqueous solution interface using the pendant drop method. Initial oil/frac-water IFT was found to be 34.0 mN/m. **Fig. 52** shows the variation in oil-aqueous solution IFT with increasing surfactant concentrations. IFT reduction by surfactants is achieved due to their amphiphilic nature. These molecules align themselves at the oil-water interface and reduce its potential energy by aligning the tail group with the hydrophobic oil phase and head group with the hydrophilic water phase.

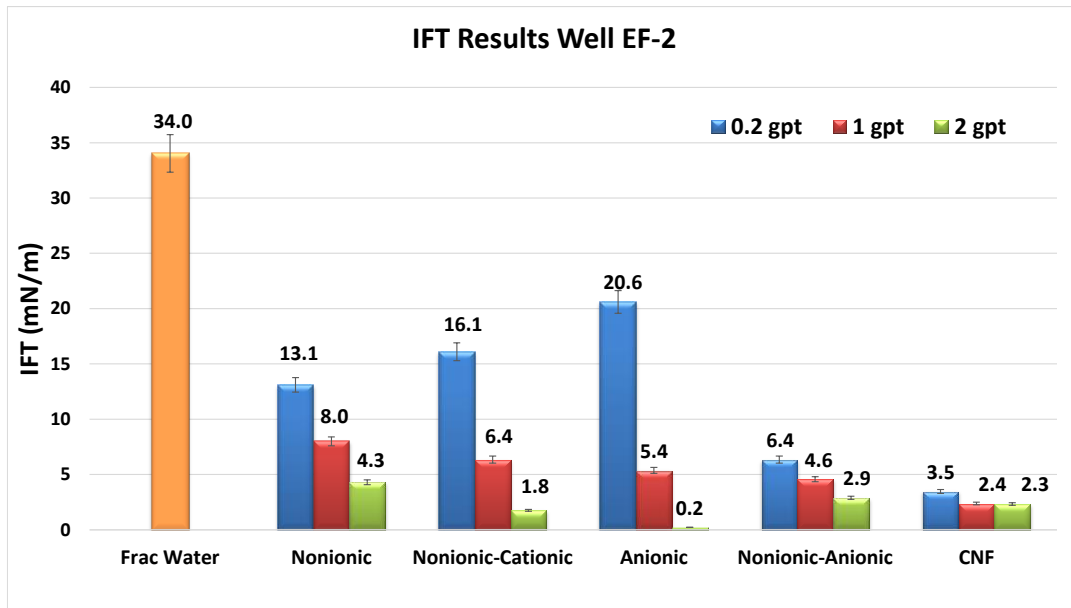


Figure 52. IFT results for Well EF-2.

All surfactants reduced interfacial tension at the oil-water interface as the value of IFT reduced with increasing surfactant concentration. Anionic surfactants reduced the IFT the most. I attribute the better performance of anionic surfactants to the presence of sulfonate in its formulation. These sulfonates, as polar compounds, can stabilize the oil-water emulsion and consequently reduce IFT. Blended surfactants and CNF followed the pure anionic surfactant. In addition, as described before in chapter 4, Eagle Ford oil TAN and TBN values are 0.02 and 0.61 mg KOH/g oil, respectively. The higher TAN suggest a basic oil that is more prone to interact with negatively charged ions such as the ones anionic surfactants. These interactions favor molecules alignment at the oil-water interface potential energy and consequently reducing IFT.

IFT alteration results in the Bakken formation

IFT reduction by chemical additives was tested using Bakken oil and the same surfactants and CNF as those used in the CA and zeta potential experiments, and the results are shown in **Fig. 53**. Original IFT between water and Bakken oil has an initial value of 17.2 mN/m. Then, as surfactants and CNF additives are added to the solution, IFT values drastically decrease, in some cases up to two orders of magnitude. IFT reduction by surfactants is achieved by increasing the number of surfactant molecules on the interface. Due to amphiphilic nature and to lower potential energy, the molecules are aligned on the interface facing the different phases decreasing IFT. In addition, the results show that anionic surfactants are more effective in reducing IFT than CNF and nonionic surfactants. This better performance of anionic surfactants is due to the sulfonates on their formulation. Sulfonates, as polar compounds, favor the migration of amphiphilic molecules to the interface, reducing IFT.

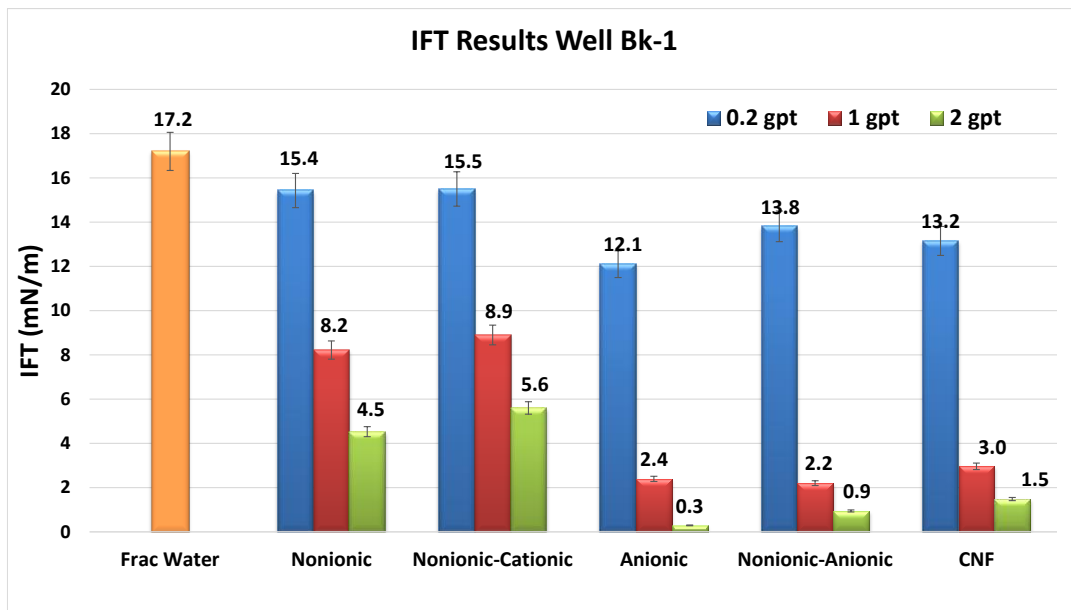


Figure 53. IFT results for Well Bk-1.

IFT reduction also aids wetting affinity alteration by reduction of capillary forces. Hence, chemical additives that reduce IFT improve aqueous phase imbibition in the capillary pores. Once inside the pores, surfactant and CNF solutions can form micelles and alter wettability to water-wet by desorbing the oil attached to the pore surface. In the CA experiments for well Bk-1, anionic surfactants show better performance in changing CA than CNF and nonionic surfactants. As explained before, this behavior is due to rock-fluid electrostatic interactions; however, the fact that anionic surfactants also reduce IFT more than other chemical additives favors surfactant solubilization into the rock, improving aqueous solution imbibition in the pores to change wettability. Thus, we believe that rock-fluid interactions as electrostatic interaction and fluid-fluid interactions as IFT reduction combined are responsible for shifting wettability from oil-wet to water-wet in these Bakken cores. IFT reduction aiding surfactant solubilization also explains why CNF,

even when having more positive charges, are capable of changing wettability in oil-wet siliceous cores. Due to IFT reduction, CNF solution enters the pores and then, by surfactant coating based on hydrophobicity, a double layer is formed giving the water-wet behavior. Moreover, in well Bk-2, CNF and surfactant nonionic-cationic alter CA in higher amounts than nonionic and anionic surfactants, aided by electrostatic interactions and low IFT values. Hence, a combination of electrostatic interactions and IFT reductions contribute to wettability alteration and water imbibition (Alvarez and Schechter 2016a).

In summary, anionic surfactants showed higher IFT reduction, closely followed by CNF, then by blended and nonionic surfactants. IFT alteration reduces capillary pressure and helps wettability alteration. These results correlate with the findings in the CA and zeta potential experiments.

IFT alteration results in the Barnett formation

IFT experiments for Barnett crude oil from wells Br-1 and Br-2 were also performed using the same previous different surfactants at reservoir temperature (165 °F) with three concentrations (0.2, 1 and 2 gpt). For oil from well Br-1, the results are in **Fig. 54**. Anionic surfactants reduced IFT in higher values than blended, CNF and nonionic surfactants (Alvarez et al. 2014).

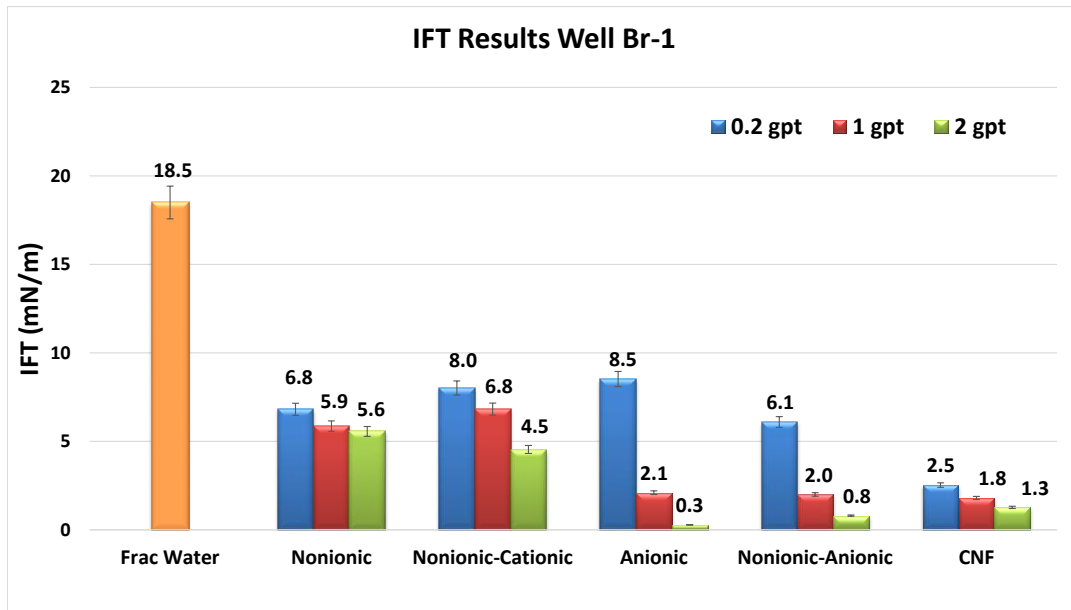


Figure 54. IFT results for Well Br-1.

In Fig. 55 are the results of IFT experiments for oil from well Br-2 in which anionic surfactant perform better than blended, CNF and nonionic surfactants at field concentrations of 1 and 2 gpt.

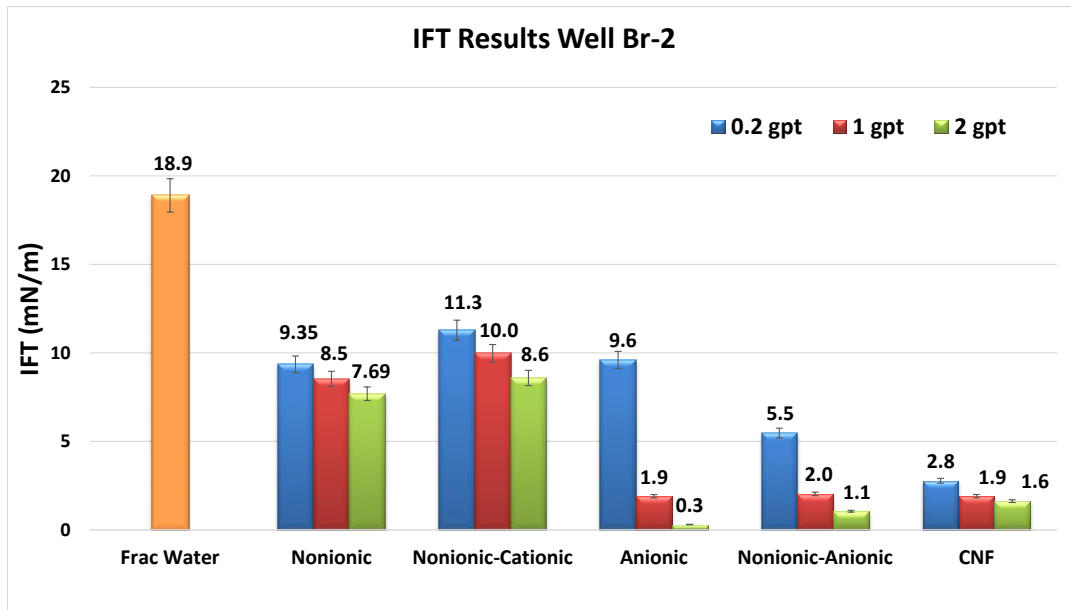


Figure 55 . IFT results for Well Br-2.

In short, anionic surfactants reduce IFT in higher degree than blended, CNF and nonionic surfactant; however, the reduction at field used concentration of 2 gpt was very similar for almost all the cases. We believe that a balance between wettability alteration and IFT reduction by surfactants should be reached at the time of designing a fracturing job in ULR, so when surfactants change wettability, capillarity pressure does not decrease very much to prevent imbibed fluids drain from the matrix.

As seen in the IFT results, the surfactants and CNF used in these experiments reduce IFT to low values (10 - 0.2 mN/m), decreasing capillary pressure and favoring water imbibition in the small pores. These chemical additives were carefully selected to avoid having ultra-low water-oil IFT that may induce oil redeposition on the sample surface and water movement from the pores due to reduced capillary pressures. A surfactant's capability to reduce IFT plays an important role in wettability alteration.

Aided by IFT reduction, surfactant solutions imbibe ULR pores by reducing the capillary pressure and then, in contact with the rock surface, wettability alteration takes place through either electrostatic interactions or hydrophobic forces, depending on rock mineralogy and surfactant type. In ULR, where pore sizes are very small (0.003 -0.006 microns for ULR tested samples), IFT reduction favors water imbibition in the pores. Solubilizing the oil attached to the rock surface alters the wettability. This is the main reason why all surfactants tested, regardless of their charge and rock lithology, altered wettability at field concentrations. Their efficacy varied over surfactant and rock type, but the capability of reducing IFT low enough to imbibe the pores gave the possibility of altering the wettability even further by cleaning or coating the rock surface. However, contrary to conventional EOR techniques such as surfactant flooding, ultralow IFT values should be avoided to prevent oil redeposition on the shale surface due to ultralow capillary pressure. For the results obtained, we suggest that wettability alteration in ULR, is not only influenced by electrostatic and hydrophobic interaction, but also by moderately reduced IFT due to ultra-small pores sizes.

CHAPTER VI

SURFACTANT ADSORPTION *

In the previous chapters, I performed petrophysical and wettability characterization of ULR cores from the Wolfcamp, Bakken, Eagle Ford, and Barnett formations. These analyses showed low porosity and ultralow permeability, and different rock lithologies. The main objective of this chapter is to determine the amount of surfactant adsorption when in contact with ULR. Surfactant adsorption onto ULR rocks is studied by using ultraviolet-visible (UV-Vis) spectroscopy. Calibration curves for surfactant solutions are determined by relating surfactant concentration to light absorbance. The curves are used to calculate the amount of surfactant adsorption and its implications in wettability alteration and oil recovery.

Surfactant Adsorption Results in Unconventional Liquid Reservoirs

Surfactant adsorption experiments are performed with the same surfactants shown in Table 11 and the procedure explained in Chapter III. These experiments serve as a complementing part of investigating rock-fluid interactions as the effect of surfactants in

* Parts of the surfactant adsorption results presented in this chapter have been reprinted from: "Potential of Improving Oil Recovery with Surfactant Additives to Completion Fluids for the Bakken" by J.O. Alvarez, I. W. Rakananda Saputra and D.S. Schechter. Energy & Fuels. Volume 31. Issue 6. Copyright 2017 by American Chemical Society (ACS). Reproduced with permission of ACS. Further reproduction prohibited without permission.

altering the wetting behavior of unconventional liquid reservoirs and their effectiveness in improving effective ultimate recovery as well as the extent of surfactant loss by adsorption during imbibition of completion fluids.

The surfactant light adsorption curves were constructed using wavelength scans (190 to 300 nm) at different surfactant concentrations from 0.5 to 3 gpt. Light adsorption values for surfactant anionic A are shown in **Fig. 56**.

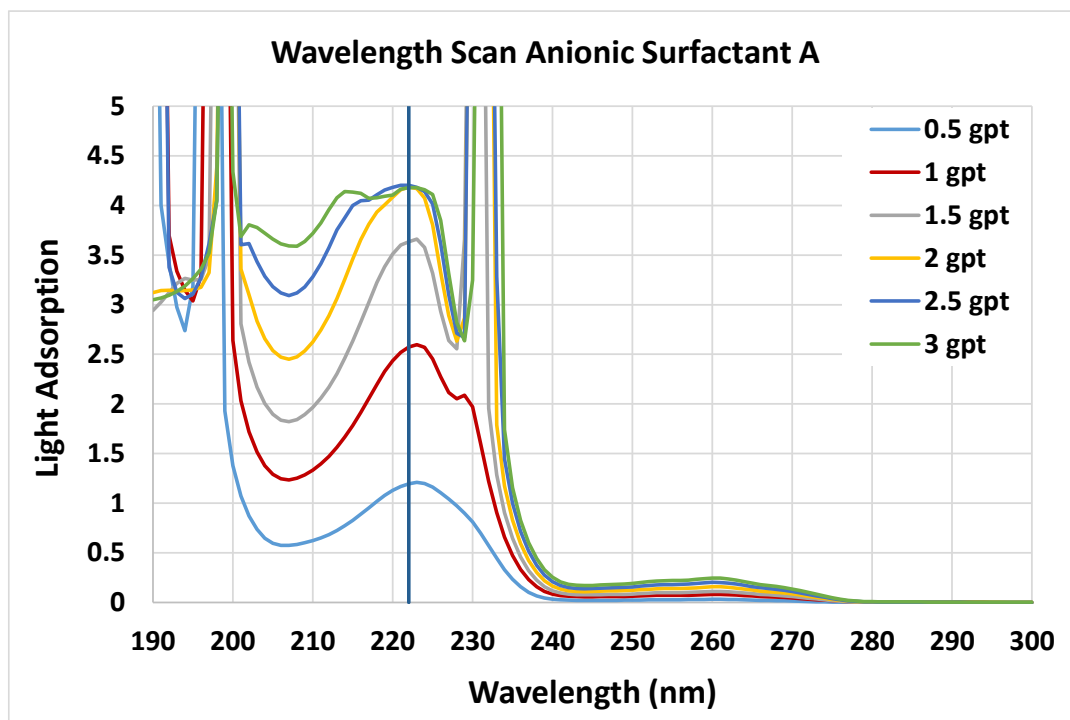


Figure 56. Light adsorption for surfactant Anionic A.

Similarly, the surfactant light adsorption curve for surfactant CNF at different surfactant concentrations from 0.5 to 3 gpt is shown in **Fig. 57**.

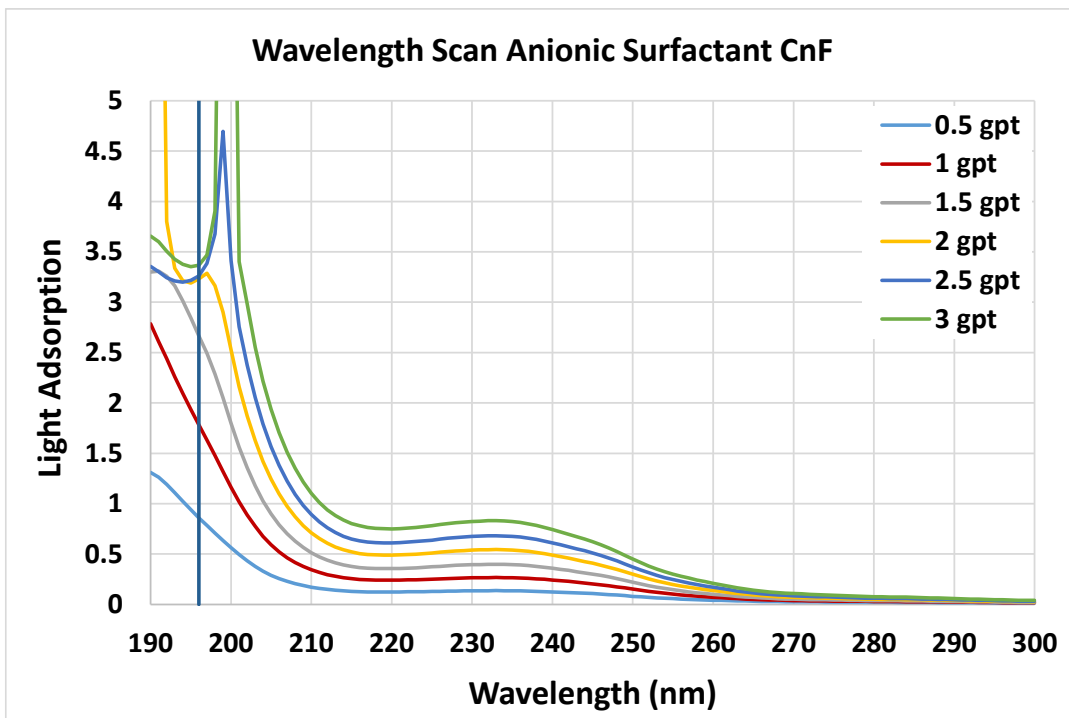


Figure 57. Light adsorption for surfactant CNF.

The light adsorption curves, and consequently the calibration curves, for nonionic and nonionic-cationic surfactants are not available because these two surfactants are not detected by the wavelength scan of the UV-Vis machine, even with an increased range of 800 nm. The UV-Vis machine limits the detection of particles within certain quantities or within particle sizes that are greater than the wavelength used. I hypothesize that this limitation caused the nonionic and nonionic-cationic surfactants to be “invisible” in the machine. Either there is an insufficient amount of substance to be detected or the size of the substance is simply too small to be detected.

Based on the wavelength scans done on various surfactant concentrations, the light adsorption-surfactant concentration calibration curves for surfactants Anionic A and CNF (Table 11) can be seen on **Fig. 58**.

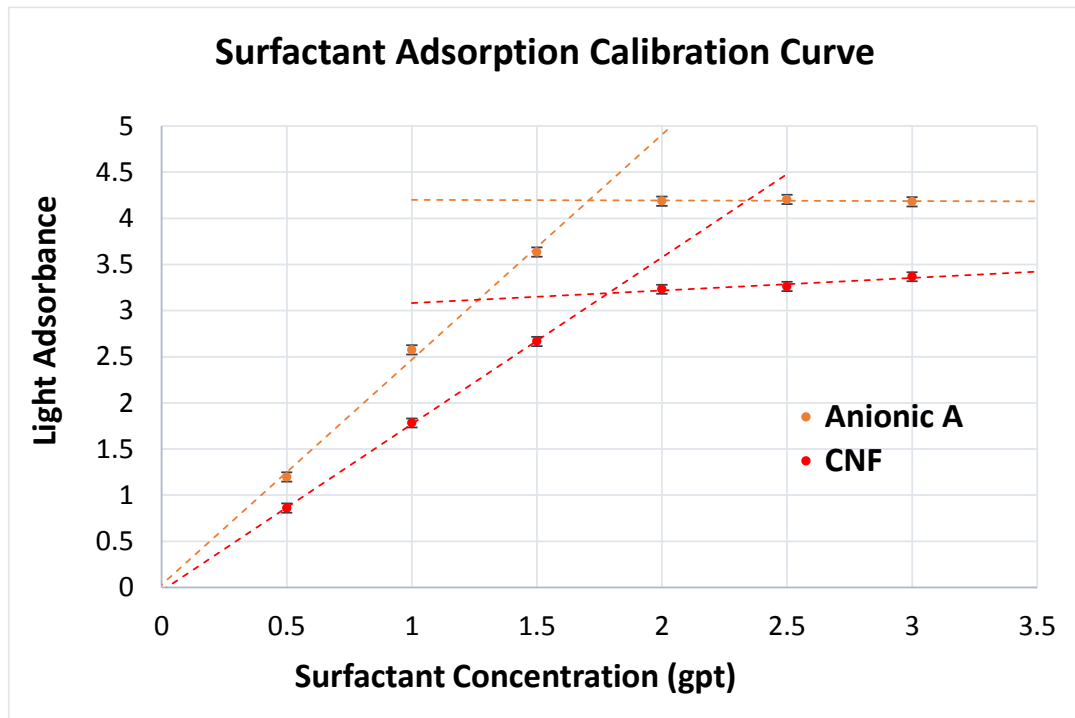


Figure 58. Calibration curves for surfactants Anionic A and CNF.

Looking at the calibration curves for both surfactants, there is an indication of the critical micelle concentration (CMC) as there are two trend lines observed. Higher surfactant concentration or high amount of surfactant molecules tends to cause the molecules to attach with each other, forming a micelle, which has different light adsorption property from the individual surfactant molecule, hence the two different trend lines. We suggest that observing CMC from wavelength scan could be used as a

verification method that the chosen peak is caused by the surfactant molecules rather than any other molecule in the solution. The CMC features observed in CA and IFT show a change of trend between 1 and 2 gpt. The CMC results from the UV-VIS spectroscopy ranges between 1.5 to 2 gpt. By matching these two CMC features, it can be concluded that the chosen peaks, 222 nm for surfactants Anionic A and 196 nm for CNF, are accurate.

Surfactant adsorption results in the Wolfcamp formation

For the adsorption measurement, Wolfcamp samples from well W-1, as described in Table 12, were used. Dynamic surfactant adsorption measurement results for surfactants anionic A and CNF on samples W-1/1 and W-1/3 are shown on **Fig. 59** and **Fig. 60**, respectively. As time progresses, the surfactant adsorption onto the rock increases with time following a Langmuir type profile. As reported in table 12, core samples from well W-1 have different lithologies depending on depth. To that end, samples from section W-1/1 are mostly siliceous with quartz content of more than 40 wt.%, clays 26 wt.% and 18 wt.% of calcite and dolomite. Adsorption profiles on Fig 59 show a larger adsorption for surfactant anionic A over CNF. At the end of the experiment, surfactant Anionic A showed an adsorption capacity of 14.3 mg/g of rock; whereas CNF showed final adsorption of 9.2 mg/g of rock. The expected results for this experiment was a higher adsorption by CNF over surfactant Anionic A. However, we hypothesize that the amount of carbonaceous content plus the clays present on the sample influenced the results favoring anionic surfactant adsorption.

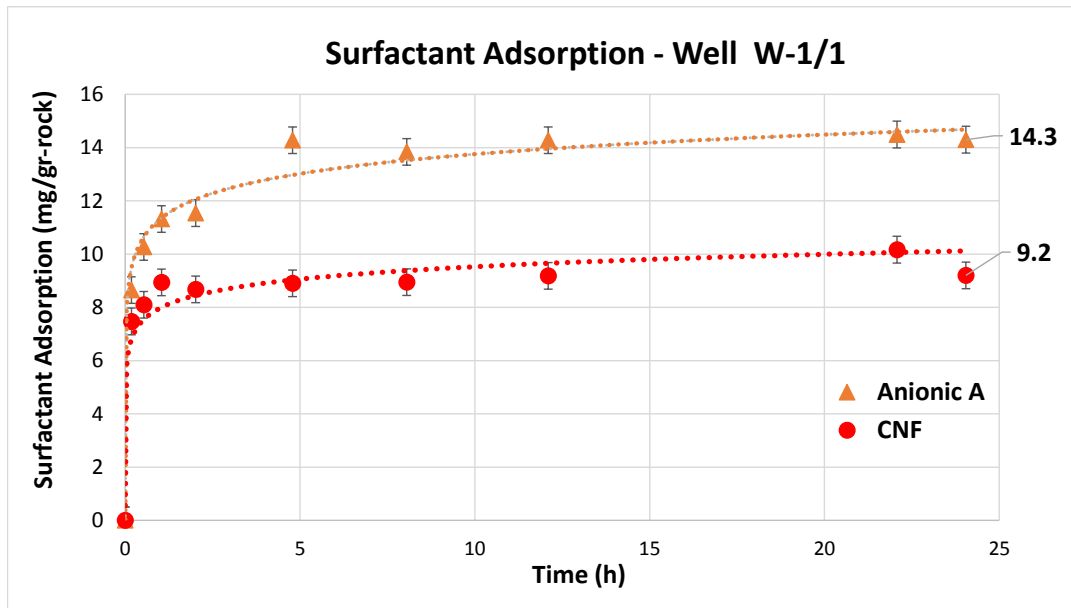


Figure 59. Surfactant adsorption measurement with time of well W-1/1.

Samples from the interval W-1/3 (Table 12) are mostly carbonates with more than 65 wt.% of calcite and dolomite. As shown on Fig. 60, adsorption profiles for surfactant anionic A are larger than CNF. Surfactant anionic A had a final adsorption capacity of 14.8 mg/g of rock whereas CNF showed a final adsorption of 7.8 mg/g of rock. This larger adoption by the surfactant Anionic A is due to the electrostatic interactions between negatively charged surfactant heads and the positively charged rock surface, as determined by the zeta potential measurements.

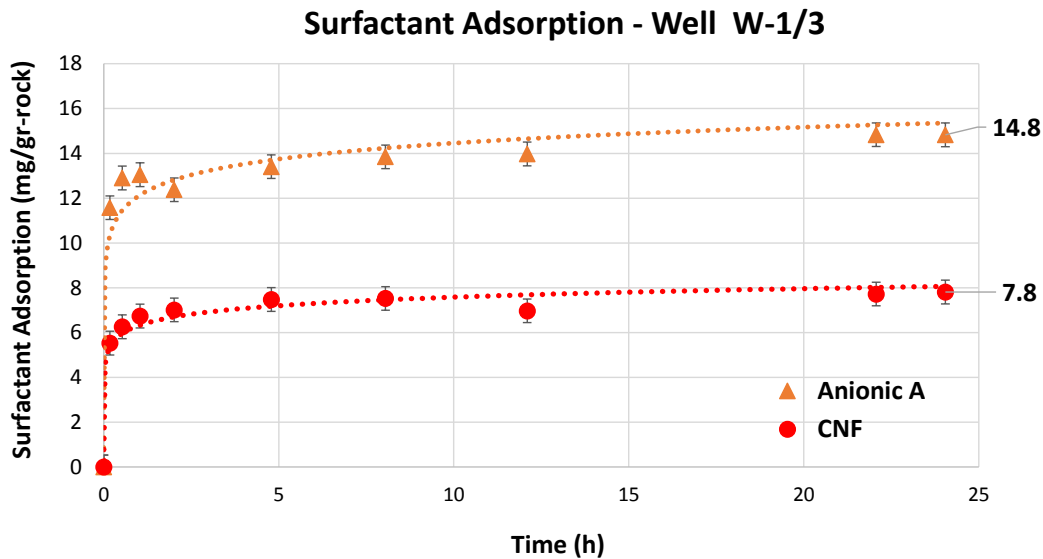


Figure 60. Surfactant adsorption measurement with time of well W-1/3.

Surfactant adsorption results in the Bakken formation

For the adsorption measurement, siliceous and carbonate Bakken samples from wells Bk-1 and Bk-2, as described in Table 14, were used. Dynamic surfactant adsorption measurement results for surfactants anionic A and CNF on wells Bk-1 and Bk-2 core are shown on **Fig. 61** and **Fig. 62**, respectively. An increasing amount of surfactant adsorbed on the rock as time progresses verifies the premise that the surfactant is adsorbed on the rock.

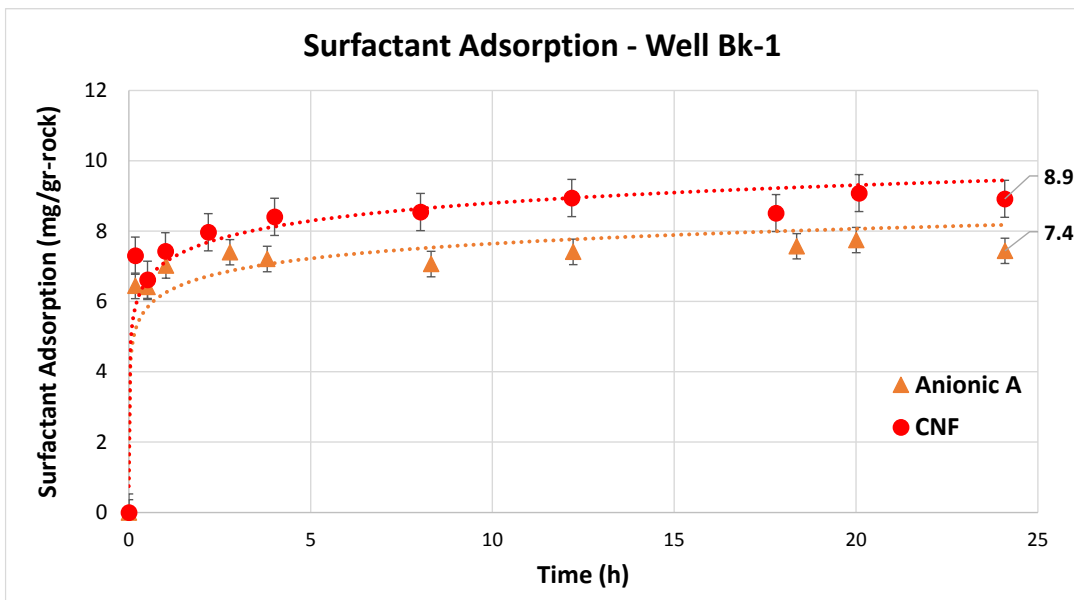


Figure 61. Surfactant adsorption measurement with time of well Bk-1.

Comparing the two surfactants on well Bk-1 (Fig. 61), CNF and anionic A surfactants adsorbed in similar quantities in the early stage (up to three hours) of the 24-hour experiment time, while CNF is adsorbed more later. At the end of the experiment, surfactant Anionic A showed an adsorption capacity of 7.4 mg/g of rock, whereas CNF showed final adsorption of 8.9 mg/g. I hypothesize that these results are observed due to the interaction between the different charges carried by both the surfactant and the rock. The more siliceous well Bk-1 core contains more negative charge on its surface, with the anionic A surfactant carrying more negative charge than CNF as determined by the zeta potential measurements (Fig. 45). A repelling force occurs between them restricting the amount of surfactant adsorbed on its surface (Alvarez, Saputra, and Schechter 2017).

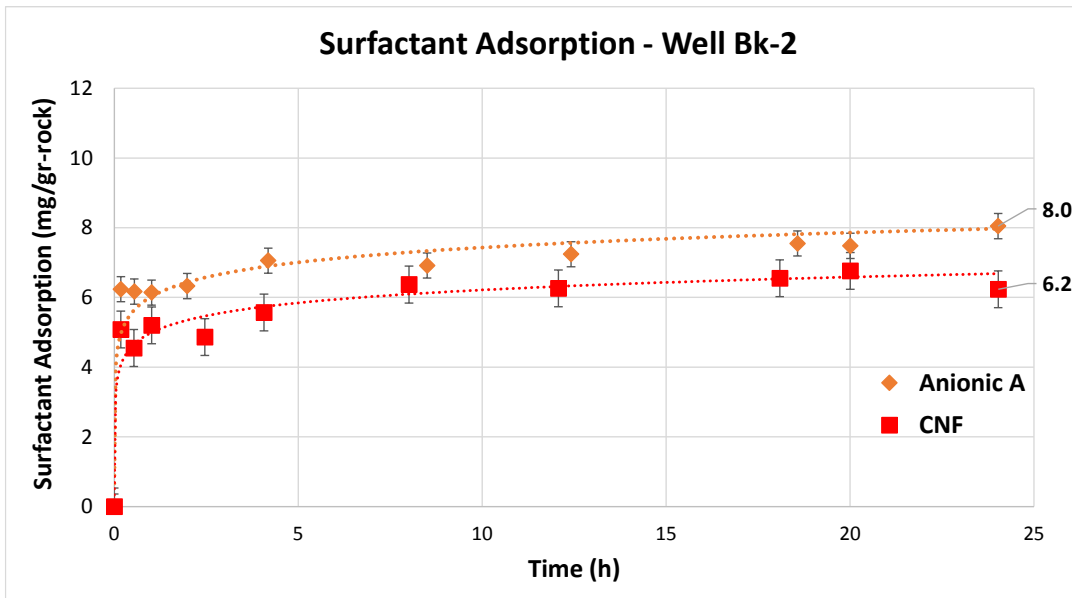


Figure 62. Surfactant adsorption measurement with time of well Bk-2.

On the other hand, the results observed on the more carbonate well Bk-2 (Fig. 62) showed a different trend where surfactant anionic A adsorbed more than CNF, even at early stages of the experiments. At the end of the experiments, surfactant anionic A shows an adsorption of 8.0 mg/g whereas CNF adsorbs 6.2 mg/g. Carbonate core from well Bk-2 has more positive charge on the surface, thereby, it attracts more negatively charged particles on its surface. This means more anionic surfactant is adsorbed since anionic surfactant bears a greater negative charge as compared to CNF, as shown by the zeta potential results (Fig. 46). Both Fig. 61 and 62 indicate a Langmuir-type adsorption mechanism on these Bakken ULR rocks. Moreover, the results for both wells and surfactants confirm the effects of lithology and surfactant type on adsorption and, consequently, surfactant efficacy (Alvarez, Saputra, and Schechter 2017). These findings

are also consistent with CA and zeta potential measurements where lithology impacted surfactant wettability alteration performance.

Surfactant adsorption results in the Eagle Ford formation

Adsorption measurements were performed in samples from Well EF-2 depth 1, as described in Table 13. Dynamic surfactant adsorption measurement results for surfactants anionic A and CNF, on sample EF-2/1 are shown on **Fig. 63**. As in the Bakken cores results, an increasing amount of surfactant adsorbed on the rock as time progresses, verifying the premise that the surfactant is adsorbed on the rock.

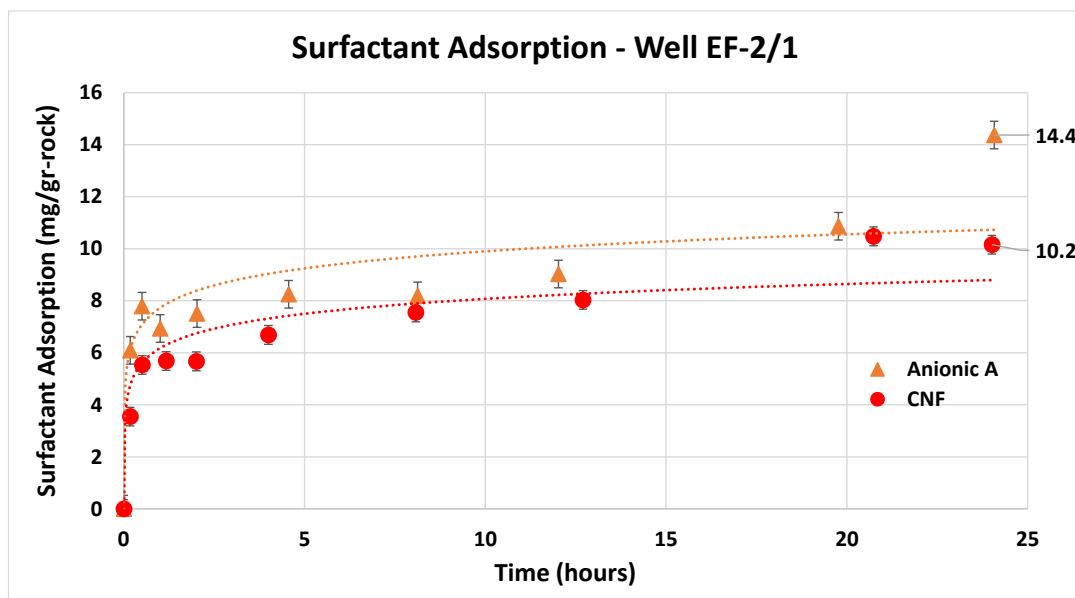


Figure 63. Surfactant adsorption measurement with time of well EF-2-1.

As shown in Table 13, the mineralogical composition of sample EF-2/1 is mainly carbonate with more than 58 wt.% calcite. When comparing the two surfactants on sample

EF-2/1 (Fig. 63), there is obviously greater adsorption by negatively charged surfactant Anionic A, with a final adsorption of 14.4 mg/g of rock, whereas the positively charge CNF showed final adsorption of 10.2 mg/g of rock. Consistent with the Bakken results, a trend points out the interaction between the different charges carried by both surfactants and the carbonate rock. Carbonate cores have more positive charges on the surface, thereby, it attracts more negatively charged particles on its surface. This means more anionic surfactant is adsorbed since anionic surfactant bears more a greater charge as compared to CNF as shown in the zeta potential results (Fig. 39). Fig. 63 also indicates a Langmuir-type adsorption mechanism on this Eagle Ford rock.

Finally, putting these results in the perspective of field application, adsorption measurement contributes to the estimation of the amount of surfactant needed in a well treatment. Surfactants with higher adsorption will require higher additive quantities compared to the less-adsorbed surfactant. This is because adsorption would reduce the amount of surfactant available in the fluid, to either alter the wettability or reduce the IFT in deeper part of the reservoir. Using CNF in well Bk-1, or any well with more siliceous lithology, would require more surfactant than using an anionic surfactant since it would be more adsorbed on the rock. On the contrary, injecting anionic surfactant in well Bk-2 or any well carbonate-rich rock lithology would consume more surfactant compared to CNF surfactant. These findings give valuable insights on surfactant selection and well treatment design in terms of rock lithology and surfactant type. In the next chapter, we investigate spontaneous imbibition in ULR and its relation to wettability and IFT alteration as well as surfactant adsorption.

CHAPTER VII

SPONTANEOUS IMBIBITION EXPERIMENTS MONITORED BY CT SCAN

TECHNOLOGY *

In the previous sections, I observed the efficacy of surfactants in altering wettability and reducing IFT in rock and oil samples from Wolfcamp, Bakken, Eagle Ford, and Barnett formations. In addition, I discussed that chemical additives performance and adsorption varied with surfactant, oil and rock types. In this chapter, I address the validity of these findings and how they are related to imbibition and oil recovery. To that end, aged unconventional siliceous and carbonate ULR cores were submerged in aqueous solutions, with and without surfactants at reservoir temperature, to evaluate wettability changes, core fluid penetrations and the associated oil recoveries.

* Parts of the spontaneous imbibition experiments monitored by CT scan technology presented in this chapter have been reprinted from:

“Impact of Surfactants for Wettability Alteration in Stimulation Fluids and the Potential for Surfactant EOR in Unconventional Liquid Reservoirs” by J.O. Alvarez, A. Neog, A. Jais and D.S. Schechter. SPE Paper 169001. Copyright 2014 by the Society of Petroleum Engineers (SPE). Reproduced with permission of SPE. Further reproduction prohibited without permission.

“Wettability Alteration and Spontaneous Imbibition in Unconventional Liquid Reservoirs by Surfactant Additives” by J.O. Alvarez and D.S. Schechter. SPE Reservoir Evaluation & Engineering. Volume 20. Issue 1. Copyright 2017 by the Society of Petroleum Engineers (SPE). Reproduced with permission of SPE. Further reproduction prohibited without permission.

“Altering Wettability in Bakken Shale by Surfactant Additives and Potential of Improving Oil Recovery during Injection of Completion Fluids” by J.O. Alvarez and D.S. Schechter. SPE Paper 179688. Copyright 2016 by the Society of Petroleum Engineers (SPE). Reproduced with permission of SPE. Further reproduction prohibited without permission.

“Potential of Improving Oil Recovery with Surfactant Additives to Completion Fluids for the Bakken” by J.O. Alvarez, I. W. Rakananda Saputra and D.S. Schechter. Energy & Fuels. Volume 31. Issue 6. Copyright 2017 by American Chemical Society (ACS). Reproduced with permission of ACS. Further reproduction prohibited without permission.

Spontaneous Imbibition Experiments in the Barnett Formation

At the early stages of this research project, the idea of producing oil from this ultralow permeability and low porosity ULR cores was full of doubts and skepticisms. Hence, on the Barnett Formation, spontaneous imbibition experiments were performed to qualitatively investigate the capability of anionic and nonionic surfactants of imbibing ultralow permeability shale cores. Cores were aged for four months in the well-oil at reservoir temperature. Then, I submerged the cores in Anionic and Nonionic surfactant solutions at a concentration of 3 gpt to see if oil can come out of them by free imbibition. This setup was very rudimentary and it only mean was to confirm a proof-of concept and advance to more sophisticated ways to evaluate imbibition by surfactants additives.

In order to back up our theory that spontaneous imbibition is in fact taking place at early stages; we submerged aged cores into frac-fluid solutions containing anionic and nonionic surfactant at reservoir temperature. We observed that for the core Br-2/3 in anionic surfactant, in less than 24 hours, several oil drops came out of the core; this is shown in **Fig. 64**.

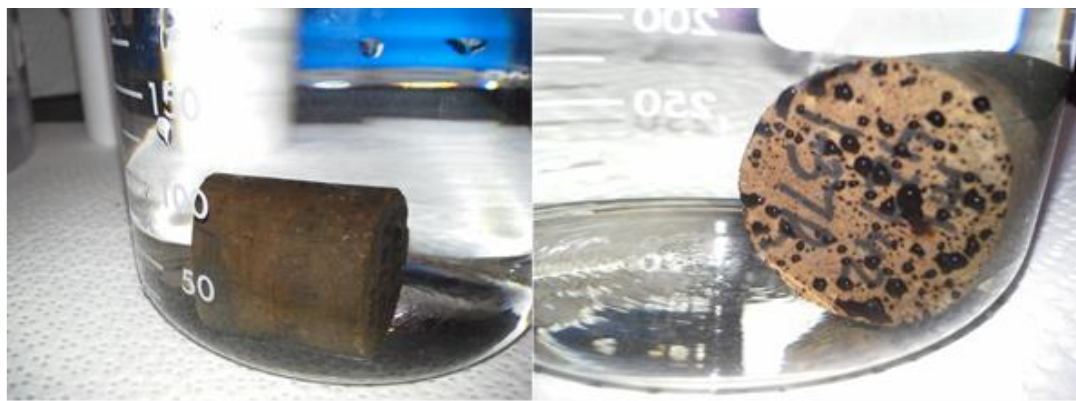


Figure 64. Core Br-2/3 before (left) submerging in anionic surfactant and after 24 hours (right). Reprinted with permission from Alvarez et al. (2014).

Also, a companion core from Br-2/3, which was submerged in nonionic surfactant, recovered oil but about one third of the amount recovered by the core in anionic surfactant showing almost none oil drops in the core (**Fig. 65**). These observed oil recoveries from shale cores demonstrating spontaneous imbibition opened further discussions for enhanced oil recovery potential in shale formations (Alvarez et al. 2014).

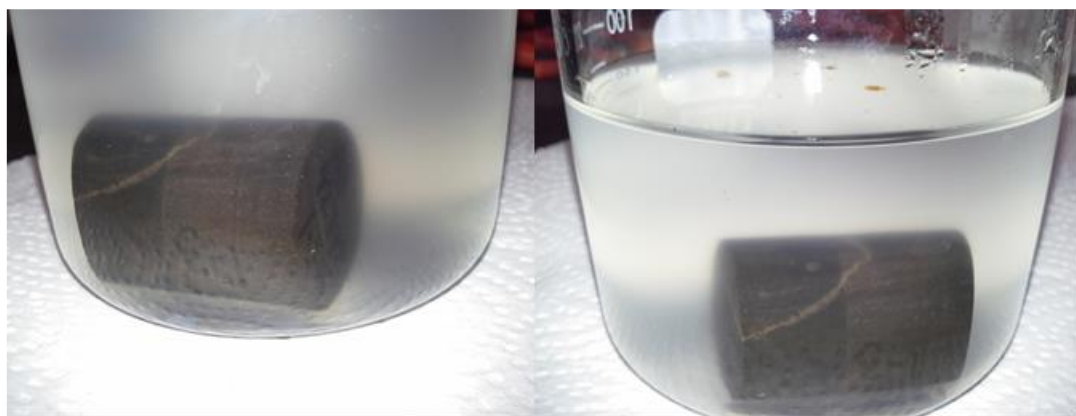


Figure 65. Core Br-2/3 before (left) submerging in nonionic surfactant and after 24 hours (right). Reprinted with permission from Alvarez et al. (2014).

After confirming a proof-of-concept regarding spontaneous imbibition in ULR, more detailed experiments were designed in order to capture changes in densities, fluid movements and imbibition as well as rates of recovery and ultimate recovery using modified Amott cells and CT scan technology.

Spontaneous Imbibition Experiments in the Wolfcamp Formation

Spontaneous imbibition experiments in ULR use siliceous cores from the Permian Basin. The experiments are conducted at reservoir temperature in an environmental chamber. All cores are from the same well, and they were aged in oil from the well at reservoir temperature (165 °F) for more than six months to reconstitute them with the missing liquid hydrocarbons due to sample handling. To confirm results repeatability, all experiments are performed twice on different cores from the same depth range. Moreover, aged unconventional siliceous and carbonate cores were submerged in aqueous solutions, with and without surfactants at reservoir temperature, to evaluate wettability changes, core fluid penetrations and the associated oil recoveries.

Initial core properties and type of fluid used for these experiments are shown in **Table 16**. These values were used to calculate original oil in place (OOIP) in cores. Moreover, porosities and initial water saturation (S_{wi}) value of 0.1 were provided by the core supplier and confirmed using mercury intrusion and extrusion analysis. To determine the initial wettability of the cores, CA measurements were performed on the samples.

Table 16. Initial core properties for Wolfcamp spontaneous imbibition experiments

Core	Diameter (in)	Length (in)	Porosity (%)	Initial CA (°)	Type of Fluid
1	0.980	1.59	6.4	139.2	Anionic A
2	0.979	1.48	6.4	131.4	Anionic A
3	0.982	1.70	6.5	139.8	Nonionic-Cationic
4	0.982	1.54	6.5	137.6	Nonionic-Cationic
5	0.973	1.78	6.5	139.1	Frac-Water
6	0.974	1.96	6.8	142.4	Anionic A
7	0.981	2.13	6.5	126.2	Anionic A
8	0.981	1.81	6.5	138.8	Nonionic-Cationic
9	0.984	2.04	6.5	135.6	Nonionic-Cationic
10	0.980	1.45	6.5	132.0	Frac-Water

At the beginning of the experiments, initial wettability measurement results showed cores with wettability of oil-wet towards intermediate-wet due to the extended aging period. Next, cores were submerged in different fluids as specified in Table 16. To address different surfactant types and their interactions with different rock lithologies, aqueous solutions of brine and surfactants anionic A and nonionic-cationic, at a concentration of 2 gpt, as well as brine alone were used. Regarding rock lithology, cores 1 to 5 were taken from Depth 1 and they were mostly siliceous with quartz as the predominant lithology (more than 40 wt.%), as shown in **Table 17**. Conversely, cores 6 to 10 were extracted from Depth 2 (Table 17) and there were predominately carbonate (more than 60 wt.%). Finally, to guarantee repeatability of our results, spontaneous imbibition experiments were performed twice with brine and surfactants on different cores and different lithologies from the same well.

Table 17. Lithological composition of rock samples from well W-1

Depth	1 / (7876 ft.)	2 / (7790 ft.)
Mineral (wt. %)		
Quartz	42	13
Clays	26	16
Calcite	12	46
Dolomite	6	19
Feldspar	11	4
Pyrite	3	2
Relative Clay (%)		
Illite/mica	95.2	94.3
Smectite	4.8	5.7

First, siliceous cores were evaluated, so cores 1 to 5 were submerged in aqueous solutions with and without surfactants as described in Table 16. The use of surfactant in spontaneous imbibition experiments accelerate oil recovery as shown in **Fig. 66**, for three of the five evaluated cores, in which oil was produced from core 1 (Anionic A) in less than 12 hours. Then, core 3 (Nonionic-cationic surfactant) began to expel oil at 36 hours. Lastly, core 5 (Frac water) began to produce oil at 48 hours. Similar behaviors were encountered for core 2 (Anionic A), core 4 (Nonionic-cationic surfactant). This faster oil production caused by imbibition in core 1 compared to cores 3 and 5 is explained by the fact that anionic surfactant changes wettability in the core faster due to its lower IFT which favors the imbibition of the aqueous phase into the core changing wettability faster, as showed in the IFT section of this manuscript. This change in wettability shifts capillary pressure from negative to positive mobilizing oil with the help also of gravity forces. In addition, because surfactant solution is imbibing into the core, its concentration is

increasing along the core walls favoring a countercurrent movement as evidenced in Fig. 66, Core 1, at t=12 hours (Alvarez and Schechter 2017).

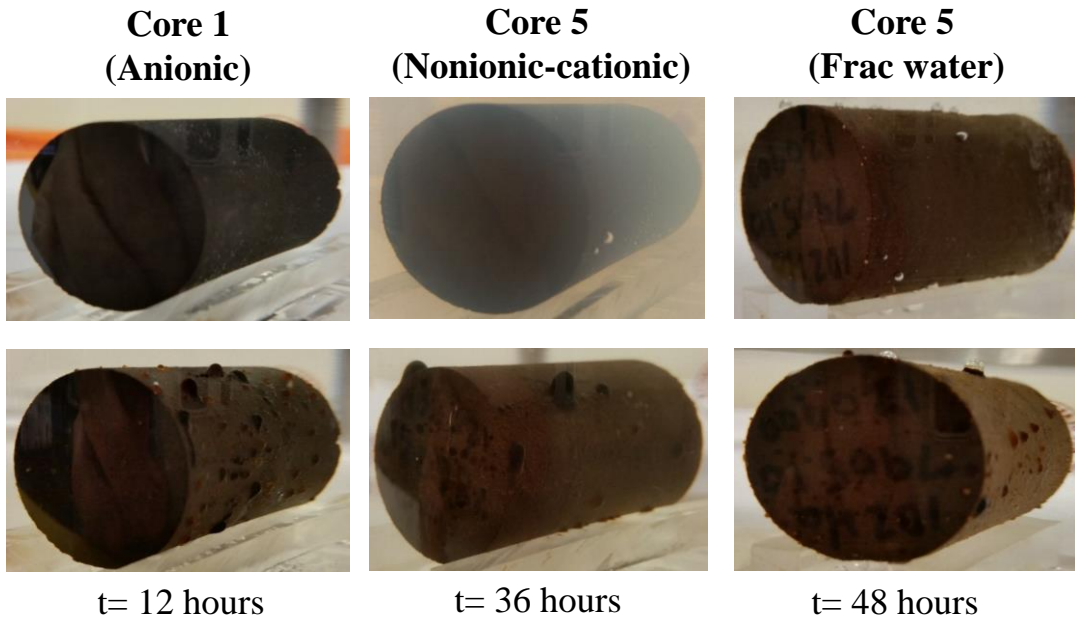


Figure 66. Cores at the beginning of the spontaneous imbibition experiments (up) and when oil begins to be expelled from the cores (bottom). Reprinted with permission from Alvarez and Schechter (2017).

The oil produced from the cores was recorded using the graduated cylinder on the top of the modified Amott cell and these values were plotted as a function of the OOIP with time as shown in **Fig. 67**. Four main observations can be drawn for these oil recovery profiles. First, surfactant solutions recovered up to four times more hydrocarbons than brine alone. Second, oil recovery in cores submerged in surfactants expelled oil faster than cores submerged in frac-water. Third, surfactant anionic A performed better than surfactant nonionic-cationic in these siliceous cores. Lastly, almost all the oil expelled by

the cores was recovered in less than 5 days. The first three observations described are consistent with the CA, zeta potential and IFT results explained in previous sections. The ability of surfactants in altering wettability and reducing IFT affected capillary pressure (Eq. 1) by changing its sign from negative to positive, due to wettability alteration, and moderately lowering its value, due to IFT reduction. This change in capillary pressure favored aqueous solution imbibition into the cores and consequently oil production. Hence, cores in surfactant solutions produced faster and more oil than cores in only brine. Conversely, imbibition in core 5 (frac-water) was very limited and oil was marginally produced by gravity forces driven by fluid density differences. Moreover, the better recovery obtained by surfactant anionic A also agreed with the CA and IFT results. In siliceous cores, anionic surfactants altered wettability in greater amount as evidenced by a lower CA and reduced IFT in higher degrees without reaching ultralow IFT values. This efficacy of anionic surfactant in altering wettability and reducing IFT was corroborated in spontaneous imbibition experiments reinforcing our theory that electrostatic interactions played an important role in wettability alteration and further imbibition.

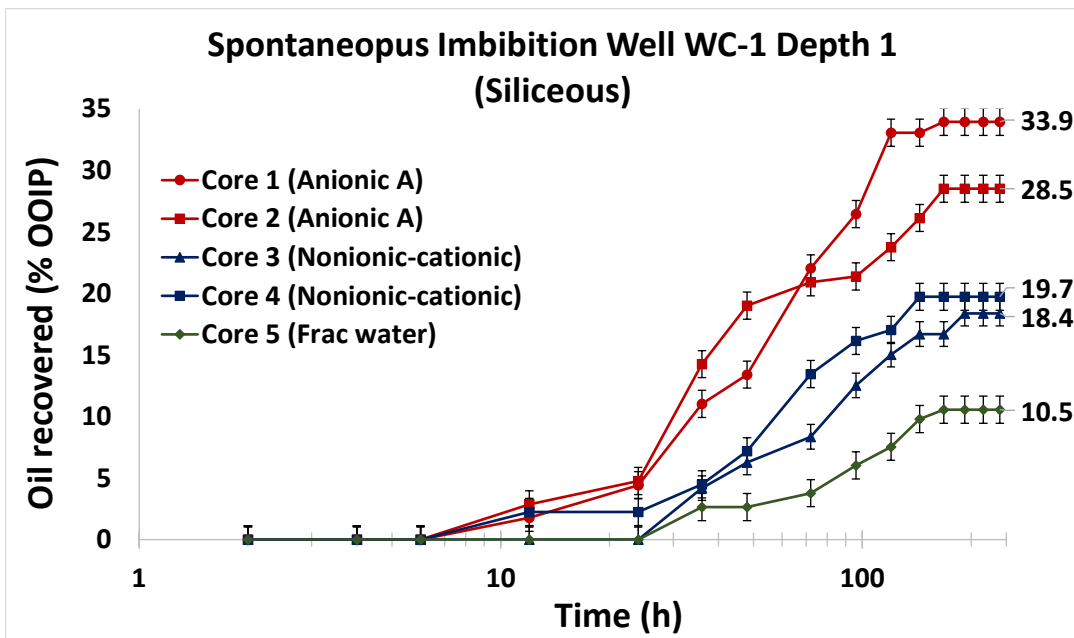


Figure 67. Oil recovered for well WC-1, depth 1 (siliceous) by spontaneous imbibition.

The fourth observation gave us insights on imbibition rates, as determined by oil recovery profile slopes, and the role of IFT and wettability in recovering hydrocarbons from these liquid rich shale rocks. In the first 30 hours, approximately, imbibition rates were governed by IFT reductions. This was due to the immediate fluid-fluid interactions between oil and aqueous solution. IFT reductions decreased capillary forces, and gravity forces mobilized oil. Later in time, wettability alteration began to dominate, as surfactant solution diffused into the rocks surface, and a faster fluid movement was evidenced due to the change in capillary force sign. Hence, when both wettability and IFT were altered, oil was recovered in a determined period, which in our case was close to 4-5 days. In the end, the cores in surfactant anionic A (Cores 1-2) recovered 28.5-33.9 % of the OOIP,

followed by surfactant nonionic-cationic (Cores 3-4) with 18.4-19.7 % OOIP. The core submerged in frac-water (core 5) managed to recovery only 10.5 % of the OOIP.

Next, carbonate cores for well WC-1 were also tested using the same surfactants and concentration. As shown in **Fig. 68**, like the siliceous cores results, carbonate cores submerged on aqueous solutions containing surfactant recovered oil faster and in greater amounts than core in brine alone due to wettability alteration and IFT reductions, which modified capillary forces and improved oil recovery. However, contrary to siliceous core surfactant performance, carbonate cores showed higher oil recovery in samples submerged in surfactant nonionic-cationic. These results are consistent with CA measurements for carbonate cores in which surfactant nonionic-cationic reduced CA better than anionic surfactants in carbonate trims. I suggest that electrostatic interactions between negatively charged oil compounds attached to the carbonate surface were stripped from the rock by positively charged heads on nonionic-cationic surfactant. This changed wettability faster and more effectively than surfactant anionic A, and consequently the capillary forces, favoring imbibition and oil recovery. This behavior was also observed on the imbibition rates (oil recovery profile slopes). In Fig. 68, after 50 hours, surfactant nonionic-cationic showed steeper slopes compared to the slopes for surfactant anionic A, demonstrating better wettability alteration. In addition, the IFT reduction effect can be seen in the first 50 hours. Surfactant anionic A recovered oil faster due to higher IFT reduction, but as soon as wettability alteration dominated oil production, the oil recovery profile changed to favoring the nonionic-cationic surfactant. Nevertheless, IFT reduction by surfactant nonionic-cationic was enough for the aqueous solution to imbibe small pores and

solubilize the oil inside them, favoring wettability alteration and oil recovery. This corroborates the importance of proper combination of wettability alteration and IFT reduction in promoting water imbibition from these liquid rich shale cores.

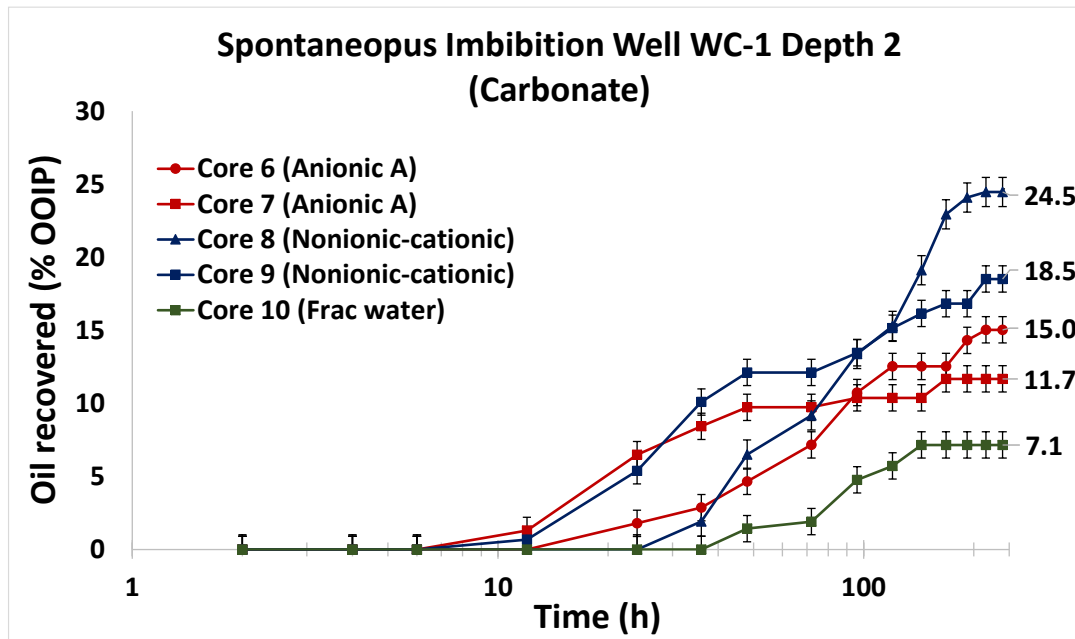


Figure 68. Oil recovered for well WC-1, depth 2 (carbonate) by spontaneous imbibition.

At the end of the experiments, cores in surfactant nonionic-cationic (Cores 8-9) recovered 24.5-18.5 % of the OOIP, followed by surfactant anionic A (Cores 6-7) with 11.7-15.0 % OOIP, and the core submerged in frac-water (core 10) recovered only 7.1 % of the OOIP. Finally, due to lower carbonate core permeability (100 to 160 nD) compared to siliceous cores (200 to 250 nD), final oil recovery in carbonate cores was generally lower than in siliceous cores (Fig. 67). Permeability differences between siliceous and

carbonate cores directly impacted oil recovery where higher permeability allowed hydrocarbons to flow better outside the core.

To monitor spontaneous imbibition into the ULR cores, CT scan images were taken at different times. CT technology enable us to look at fluid movement periodically and relate these changes in CT numbers to fluid imbibition. Due to the use of KI as a dopant, we can better differentiate between oil and frac fluids. In our experiments, oil CT number is close to -100 HU whereas frac fluids CT number is around 800 HU. This marked CT number difference allows us to see changes when frac fluids imbibe into the cores and fill part of pore volume originally occupied by oil. Consequently, imbibition is represented by positive changes in CT number (Alvarez and Schechter 2017). CT scan images at progressive times for cores 1-5 (siliceous cores) during spontaneous imbibition experiments are shown in **Fig. 69**. Consecutive images for cores submerged in surfactant solutions (cores 1-4) showed visible changes in colors as CT numbers increased with time. Color changes from blue to green and yellow to red demonstrate water penetration inside the cores, and consequently oil displacement. Conversely, the core in frac-water without surfactant showed small color variations from blue to green and small changes on the core periphery with time, indicating limited water imbibition. These observations qualitatively agreed with oil recovery (Fig. 67) in which cores submerged in surfactant solutions produced up to three times more than the core in frac-water alone, confirming our theory that oil recovery increases when water imbibition is promoted by wettability and IFT alteration.

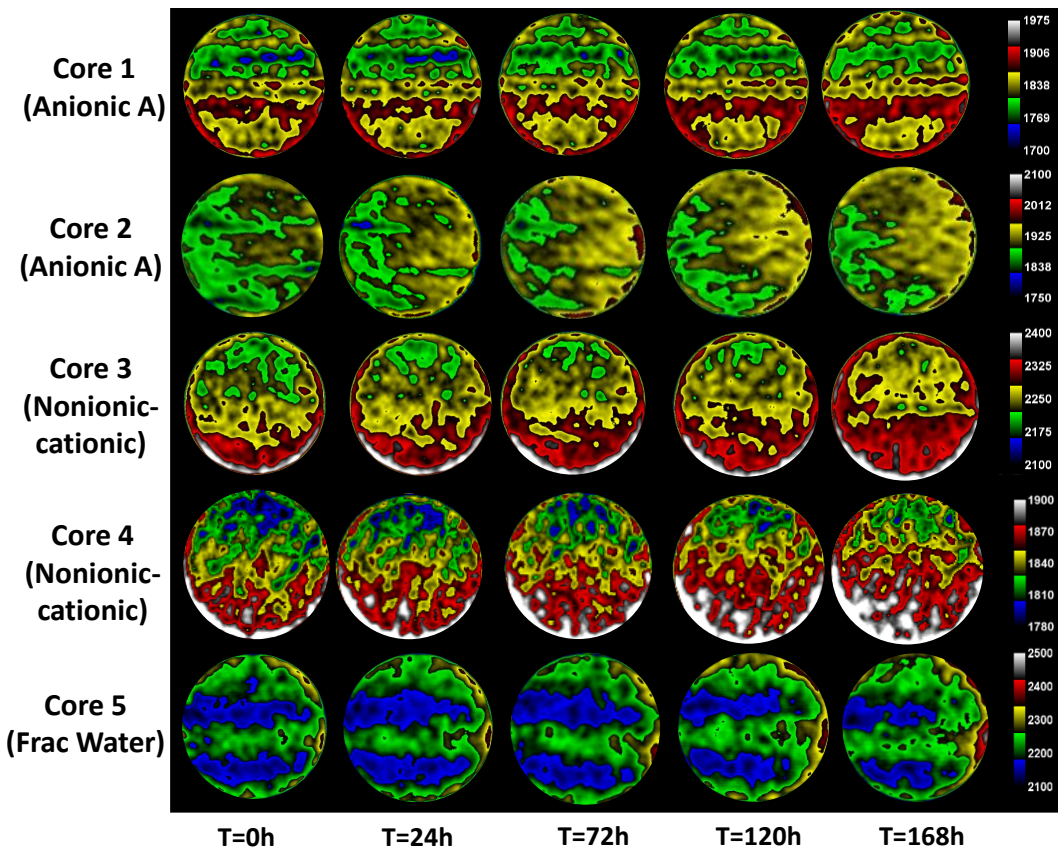


Figure 69. CT images for well WC-1, depth 1 (siliceous).

Similarly, CT scan images with time for cores 6-10 (carbonate cores) during spontaneous imbibition experiments are shown in **Fig. 70**. Just as in siliceous cores, CT images for carbonate cores showed clear changes in cores submerged in surfactant solutions (cores 6-9) with noticeable color variations from green to yellow and yellow to red. These changes indicated an increase in CT number, interpreted as water imbibition. On the other hand, core 10 (frac-water) showed inferior water imbibition compared to cores 6-9 as represented by small changes in colors. Results shown in Fig 10 correlate with cores 6 to 10 oil recovery performance (Fig. 68). Higher water penetration in cores 6

to 9 led to higher oil recovery for cores in surfactant solutions, and lower imbibition in core 10 resulted in lower oil recovery.

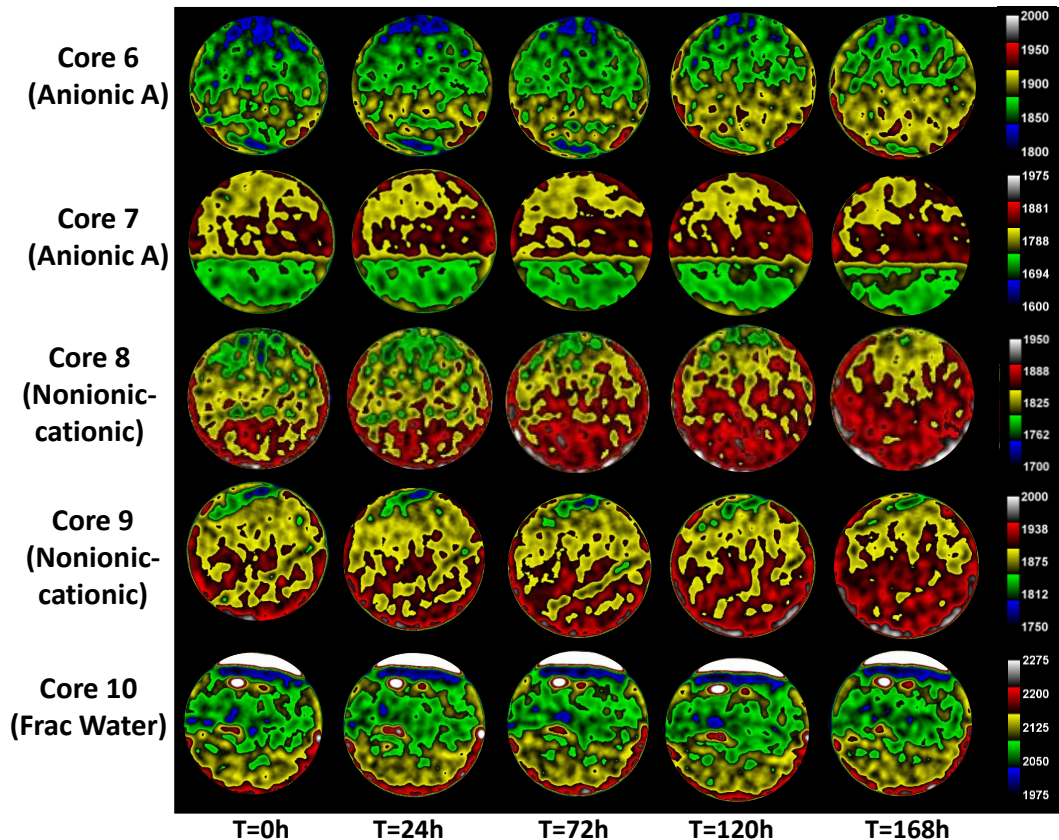


Figure 70. CT images for well WC-1, depth 2 (carbonate).

Fluid flow was not radially homogeneous towards the core center, and it greatly relied on core heterogeneities such as bedding planes and natural fractures. This can be inferred from Fig. 69 and Fig. 70. These heterogeneities are very common in unconventional liquid reservoirs and, in many cases, dominate oil production in shale systems. In addition, they present an important challenge when upscaling methods are

applied to translate laboratory results to the field. Hence, we observed that imbibing fluids move throughout less resistance pathways inside the core, displacing hydrocarbon during the flow. Moreover, during the experiments, fluid countercurrent movement was evidenced where oil was expelled from the core surface as completion fluid imbibed due to changes in capillary pressure. Nevertheless, cores submerged in surfactant solutions showed visible changes in CT numbers indicating better imbibition compared to cores in frac-water, regardless of core lithology. This is consistent with oil recovery results (Fig. 67 and Fig. 68) and demonstrates that altering rock wettability and fluid IFT by the addition of surfactants improved the water penetration into the rock matrix, which consequently increased oil recovery.

Spontaneous imbibition experiment results are summarized in **Table 18** and **Table 19**. The cores used from Wolfcamp well WC-1 on the Permian Basin showed different penetration magnitude values, calculated using Eq. 29. For siliceous cores (cores 1-5), penetration magnitudes are seemingly higher for samples exposed to surfactant solutions than core submerged in water alone with the highest penetration by cores in surfactant anionic A. Similarly, carbonate cores (cores 6-10) showed higher imbibition by surfactant additives, but the highest penetration magnitude was evidenced by surfactant nonionic-cationic. These results qualitatively agree with oil recoveries by different surfactants and different lithologies, and corroborated our hypothesis that rock surface and surfactant charges play a vital role in imbibition and hydrocarbon production where electrostatic and hydrophilic rock-fluid interactions must be considered. Table 18 also shows changes in rock wettability, as determined by CA, before and after spontaneous imbibition

experiments. Cores in surfactant solutions changed their wettability from oil and intermediate-wet to water-wet; whereas cores submerged in frac-water without surfactant did not change the CA significantly enough to change wettability to water-wet.

Table 18. Wolfcamp spontaneous imbibition experiment results

Core	Type of Fluid	Initial Average CT (HU)	Final Average CT (HU)	Penetration magnitude (HU)	Final IFT (mN/m)	Initial CA (°)	Final CA (°)	Oil Recovery (%OOIP)
1	Anionic A	2066	2101	35	0.9	139.2	56.8	33.9
2	Anionic A	2214	2247	34	0.9	131.4	40.1	28.5
3	Nonionic -Cationic	2399	2425	26	7.4	139.8	59.4	18.4
4	Nonionic -Cationic	2253	2280	27	7.4	137.6	53.7	19.7
5	Frac-Water	2620	2632	12	22.1	139.1	111.9	10.5
6	Anionic A	2203	2225	22	0.9	142.4	46.4	15.0
7	Anionic A	2208	2226	19	0.9	126.2	56.0	11.7
8	Nonionic -Cationic	2231	2262	30	7.4	138.8	51.9	24.5
9	Nonionic -Cationic	2245	2273	27	7.4	135.6	55.1	18.5
10	Frac-Water	2218	2231	13	22.1	132.0	110.7	7.1

The ability of surfactant to alter wettability along with reducing IFT made possible for capillary pressure to shift from negative to positive values as shown in Table 1 and calculated by using Eq. 1. These changes in capillary forces for cores in contact with surfactants favored imbibition and improved oil recovery as demonstrated in the last column of Table 19. On the other hand, cores in frac-water without surfactants were not able to change capillary pressure sign and consequently did not favor imbibition marginally recovering oil only by the aid of fluid densities difference as gravity forces.

Table 19. Wolfcamp capillary pressure and inverse Bond numbers

Core	Type of Fluid	Initial Pc (psi)	Final Pc (psi)	N _b ⁻¹ (-)	Oil Recovery (%OOIP)
1	Anionic A	-1213	36	438	33.9
2	Anionic A	-1060	50	438	28.5
3	Nonionic-Cationic	-1224	273	3629	18.4
4	Nonionic-Cationic	-1183	318	3629	19.7
5	Frac-Water	-1211	-598	10838	10.5
6	Anionic A	-1270	45	594	15.0
7	Anionic A	-1206	36	581	11.7
8	Nonionic-Cationic	-947	331	4774	24.5
9	Nonionic-Cationic	-1145	307	4774	18.5
10	Frac-Water	-1072	-567	14258	7.1

In order to assess the impact of capillary forces with respect to gravity forces in these liquid rich shales from the Permian Basin, the inverse Bond number (Eq. 7) was calculated. The inverse Bond number represents the ratio of capillary forces to gravitational forces and determines when capillary forces drive imbibition as countercurrent flow or when gravitational forces drive it as cocurrent flow. From Schechter, Zhou, and Orr Jr (1994), I learned that when the inverse Bond number is greater than 5, capillary forces are responsible of imbibition. As shown in Table 19, inverse Bond numbers for these unconventional reservoirs with ultralow permeability were clearly greater than 5, which confirmed that capillary forces are the main driving force for aqueous solution imbibition. This observation is corroborated by penetration magnitude and oil recovery exhibited in cores that changed wettability and reduced IFT using surfactants in contrast to cores in frac-water only.

In summary, oil recovery regarding OOIP clearly shows the efficacy of surfactants on improving oil production compared with frac water without surfactants. Moreover, oil recovery in imbibition experiments is driven by the interaction of surfactant solutions and the rock surfaces (solid-liquid interaction as wettability alteration) as well as surfactant solutions and oil interactions (liquid-liquid interaction as IFT alteration). However, the main mechanism favoring imbibition is solid-liquid interaction because wettability must be shifted to water-wet to have a positive capillary pressure that promotes water imbibition into the rock. IFT moderate reduction aids trigger wettability alteration by imbibition into surface pores but its contribution by itself does not guarantee capillary pressure change of sign, but only its reduction. In addition, one of the most important findings of this study was corroborating that ULR lithology and oil type play an important factor in oil recovery. Siliceous cores had higher fluid penetration and oil recovery when anionic surfactants were used, due to electrostatic and hydrophilic rock-fluid and fluid-fluid interactions. Conversely, carbonate shale cores showed better penetration and hydrocarbon recovery when submerged in nonionic-cationic surfactants. Moreover, anionic surfactants reduced IFT better, aided by oil basic tendency, than nonionic and blended surfactants. These results also showed that rock-fluid interactions are the dominant mechanism favoring imbibition. Even though IFT was reduced in higher amounts by anionic surfactants as fluid-fluid interactions, oil recovery was not always higher when anionic surfactants were used. In fact, due to different lithologies and surfactant head charges, wettability was altered better by anionic surfactants in siliceous cores but by nonionic-cationic surfactants in carbonate cores, which affected oil recovery in each case. The surfactant that altered

wettability further was the one that recovered more oil, which leads us to conclude that rock-fluid interactions controlled imbibition and fluid flow. Hence, rock lithology and oil type should be considered and studied to select the proper surfactant additive for completion fluids to maximize oil recovery after stimulation.

Spontaneous Imbibition Experiments in the Eagle Ford Formation

This section presents the spontaneous imbibition results for brine with and without surfactant additives, which include wettability changes, penetration of the fluids into cores and the associated oil recovery. Initial properties of the samples used for these experiments are provided in **Table 20**. Core measurements as well as porosity and initial water saturation (S_{wi}) were used to calculate the OOIP. Porosities, shown in Table 20, and water initial saturations were provided by the core supplier and confirmed using mercury intrusion and extrusion analysis. For this study, initial water saturation used for the calculations was 0.15. Finally, core initial wettability was determined by CA methods as described in previous sections. The results in Table 4 show mostly intermediate towards oil-wet cores.

Table 20. Initial core properties for Eagle Ford spontaneous imbibition experiments

Core	Diameter (in)	Length (in)	Porosity (%)	Initial CA (°)	Type of Fluid
1	0.997	2.288	12.2	104.9	Frac-Water
2	0.999	1.165	12.0	123.2	Frac-Water
3	0.991	2.253	12.2	103.0	Anionic A (A)
4	0.998	1.453	12.0	132.5	Anionic A (A)
5	0.993	2.028	12.2	110.4	Nonionic-Cationic (NC)
6	0.995	1.643	12.0	120.2	Nonionic-Cationic (NC)
7	1.001	2.214	12.2	103.4	Complex Nanofluid (C1)
8	0.995	2.071	12.0	106.1	Complex Nanofluid (C1)
9	0.955	2.070	13.1	100.1	Anionic-Nonionic (AN)
10	0.994	1.953	13.1	96.0	Nonionic-Anionic (NA)
11	0.991	1.819	13.1	98.4	Complex Nanofluid 2 (C2)

Eagle Ford cores from well EF-2 were aged for more than 4 months at reservoir temperature and spontaneous imbibition experiments were conducted at 180 °F. In addition, XRD analysis shows that all cores used have carbonate as the predominant lithology (more than 60 wt.% carbonates). The same surfactants tested in CA, zeta potential and IFT experiments, described in Table 11, Chapter 5, were used at a concentration of 2 gpt. In addition, I added two more surfactants to the set of spontaneous imbibition experiments, their description is in **Table 21**, and the other surfactant properties are in Table 11, Chapter 5.

Table 21. Surfactant properties 2

Surfactant	Primary components	Composition (wt.%)	pH	Specific Gravity
Anionic + Nonionic (AN)	Methyl alcohol	10-30	4.7 - 5.7	0.97 - 0.99
	Proprietary Sulfonate	7-13		
Complex Nanofluid 2 (C2)	Isopropyl alcohol	5-40	5.0 - 8.0	0.96 - 1.01
	Citrus Terpenes	5-15		

Moreover, to guarantee repeatability of our results, experiments with brine and surfactants Anionic A (A), Nonionic-cationic (NC) and CNF (C1) were performed twice on different cores from the same well. To that end, cores 1 and 2 were tested with frac-water, cores 3-4 with anionic surfactant (A), cores 5-6 with nonionic-cationic surfactant (NC), cores 7-8 with CNF (C1), core 9 with surfactant anionic-nonionic (AN), core 10 with surfactant nonionic-anionic (NA) and core 11 with complex nanofluid 2 (C2).

The oil expelled by imbibition from the cores was measured using a graduated cylinder at the top of the modified Amott cells. **Fig. 71** shows oil recovery, as function of the OOIP, with time. After rigorously follow the development of the experiments, we identified three marked stages for oil recovery as shown in Fig. 71. The very first stage (stage 1) shows greater recovery rates in the first 12 hours. In addition, the cores submerged in surfactant solutions begin to produce oil faster than brine alone. These observations are explained by the capability of surfactants of reducing IFT. During early time of the experiments, capillary pressures were still negative because wettability alteration has not taken place yet. However, IFT reduction on aqueous solution-oil

interface decreases capillary pressure, which minimizes resistance of oil to leave the pores and favors gravity forces. The second period (stage 2) shows a different oil recovery slope 12 hours after initiation of the test. As surfactants gradually alter wettability of the core surface, capillary pressures change in sign from negative to positive and imbibition takes place. This is the reason why the oil-recovery profile slope is not as steep. From then, capillarity dominates oil recovery from the core and oil is displaced to the top of the modified Amott cell by density differences. Finally, stage 3 shows that additional oil is marginally recovered after approximately 72 hours of the experiments for most surfactants.

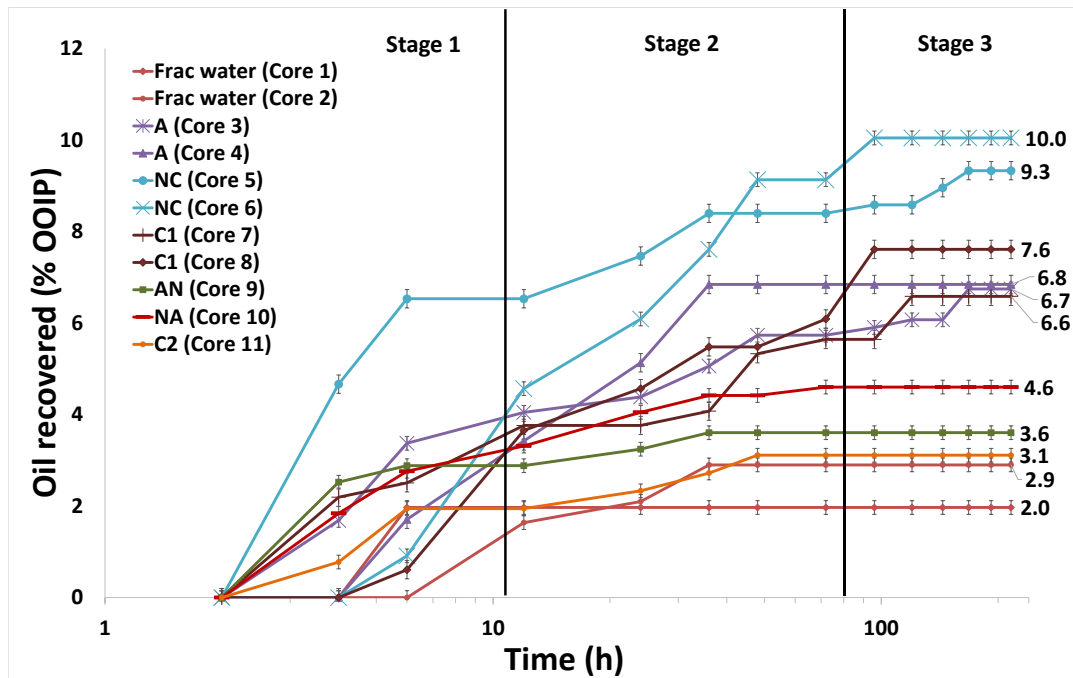


Figure 71. Oil recovered for well EF-2 by spontaneous imbibition.

As shown in Fig. 71, core submerged in frac-water (cores 1-2) recovered only 2.0-2.9 % of the OOIP. This low oil recovery is attributed to the inability of frac-water to alter wettability and reduce IFT. During these experiments, capillary pressures of cores 1 and 2 remain negative and low oil recovery is only favored by brine-oil density differences. On the other hand, the results for cores submerged on surfactant solutions (cores 3-11) show oil recoveries up to 10 % of the OOIP. Maximum recovery was observed for the nonionic-cationic surfactant NC (cores 5-6) which recovered 9.3-10 % of the OOIP. This was followed by the purely anionic surfactant A (cores 3-4) and the complex nanofluid C1 (CNF) (cores 7-8) which recovered 6.7-6.8 % and 6.6-7.6 % OOIP, respectively. These findings correlate well with contact angle and interfacial tension results, which earlier suggested that surfactants A, NC and C1 were better in terms of both wettability alteration and IFT reduction. Among the blended surfactants, the more nonionic-anionic surfactant NA (core 10) recovered 4.6 % of the OOIP while the more anionic-nonionic surfactant AN (core 9) recovered 3.6% of the OOIP. Lastly, complex nanofluid C2 (core 11) recovered the least among the surfactants at 3.1% OOIP.

Oil recovery results are consistent with wettability alteration and IFT reduction in which only aqueous solution with surfactant additives altered wettability and reduced IFT. These alterations favored imbibition by positive capillary forces and displaced oil by gravity forces. Moreover, the highest recovery was observed with surfactant NC compared to surfactants A and C1. This higher recovery suggests that IFT reduction is beneficial only to a certain extent and lowering IFT to very low values would decrease capillary pressure to a point that it would not be the main production driving force in these tight

nanopores. In addition, we speculate that better imbibition performance by a nonionic-cationic surfactant NC brings an indication that electrostatic forces between acidic and negatively charged compounds attached to positively charged carbonate surfaces improve surfactant efficacy of altering wettability inside the core and consequently oil recovery. Conversely, anionic surfactant A and complex nanofluid C1 negative charges, as shown in zeta potential experiments (Fig. 39), might be responsible for lower electrostatic interactions than surfactants NC in these carbonate rocks, which leads to the hypothesis that hydrophobic interactions alter wettability in these cores. Nevertheless, it is very clear that regardless of the wettability alteration mechanism, the cores submerged in surfactant solutions recovered more oil than the ones submerged in brine alone. Hence, it can be deducted that wettability alteration to water-wet helped surfactant fluids penetrate deeper into the rock matrix and solubilize the oil trapped in tight channels, which is produced in a countercurrent fashion as suggested by the slow imbibition rates at the latter part of the experiment. Though the penetration of fluids increases steadily over time, most production was observed in the first 24-36 hours increasing slowly as time progresses. Moreover, only surfactants NC and A as well as CNF C1 could produce additional oil beyond 72 hours which underlines the importance of both wettability alteration and IFT reduction for improved imbibition and oil recovery.

Next, movement of the imbibing fluids was studied using the computer tomography methods. To that end, CT scans were taken at various times during spontaneous imbibition experiments as shown in **Fig. 72**. Color-scale for CT numbers are shown to the right of each set of images and it was varied based on experiment to observe

a better contrast between the oil and aqueous phases. Brighter yellow to orange regions were considered to have a high CT number owing to higher density while purple regions correspond to lower CT number due to lower density compared to the surrounding medium. Change in colors from darker purple to lighter orange/yellow implies the displacement of a low-density medium by a high-density medium, which in this case are oil and aqueous solution, respectively. As described on the methodology section, high aqueous solution CT numbers were achieved by adding KI as dopant.

Initial results obtained with frac-water alone and surfactant based aqueous solutions suggested that the latter exhibited higher fluid penetration or imbibition. Surfactant solutions imbibed into the matrix despite the presence of bedding planes or fractures and drove the low-density oil phase out as is evident by observing the changes in the respective CT scan images. The surfactants that recovered the highest amount of oil (NC, A and C1), also showed the biggest change in colors as represented in cores 3, 5 and 7 from Fig. 72. Core 1 (frac-water) showed minimum changes in color from the initial time up to 9 days. Conversely, cores 3 and 5, anionic and nonionic-cationic surfactant respectively, presented visible changes in CT numbers changing colors from dark violet to light orange/yellow. CNF surfactant C1 also changed color but in lesser amount imbibing along bedding planes. Core 9 (anionic-nonionic surfactant) had a fracture that probably facilitated imbibing fluid movement into the rock matrix as the low-density region to the left of the fracture changed color. Core 10 (nonionic-anionic surfactant) imbibed along the bedding planes that changed color from purple to yellowish orange by

the end of the experiment. Lastly, core 11 also showed evidence of a natural fracture that could probably have facilitated complex nanofluid C2 imbibition into the rock matrix.

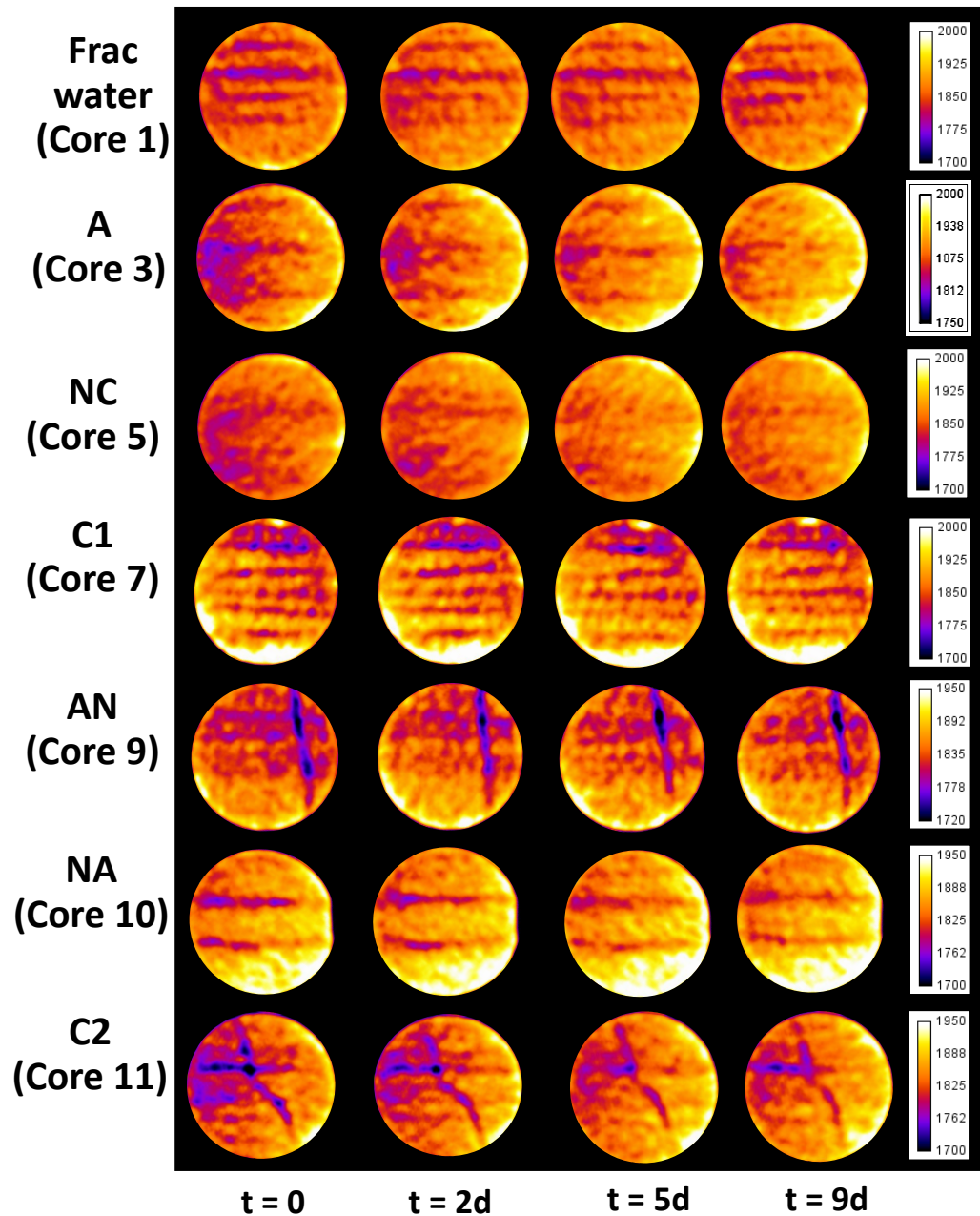


Figure 72. CT images for well EF-2.

These CT scan images gave us two important insights. First, all cores showed bedding planes and cores 9 and 11 also showed small natural fractures. Second, fluid flow inside the core was not radially concentric and homogeneous and depended on core heterogeneity as bedding planes and natural fractures. Thereby, fluid imbibition is not uniform, and it is governed by core heterogeneities, which are very common in liquid rich shale reservoirs. Third, surfactant solutions visually imbibed better into Eagle Ford core than frac-water without surfactants and changes from the initial and final states were more pronounced compared to the frac-water case. This is consistent with oil recovery (Fig. 71) and demonstrates that altering rock wettability and reservoir fluid IFT with surfactant additives improved the penetration of imbibing fluid into rock matrix, which translated into higher oil recovery.

To summarize our spontaneous imbibition results, **Table 22** and **Table 23** show before and after values for CT numbers and contact angles, IFT measurements as well as capillary pressures and final oil recoveries, as function of the OOIP, for all cores tested. Penetration magnitudes of imbibing fluids into the rock and capillary pressures are quantified using Eq. 29 and Eq. 1, respectively, as discussed in the methodology section. Consistent with Fig. 72, cores submerged in surfactant solutions have higher penetration magnitudes or imbibition than brine alone. Surfactants penetrated more into the cores compared to frac-water, which barely reached penetration magnitude values of 7 and 8 HU. Nonionic-cationic surfactant NC penetrated the highest with 18 and 19 HU followed by anionic surfactant A and CNF C1 at 16-17 HU and 15-16 HU respectively. Complex nanofluid C2 penetrated the lowest among surfactants, which was expected due to its poor

wettability alteration potential. Moreover, penetration magnitude values correlated with oil recovery reinforcing the relation of imbibition and hydrocarbon production in these ultralow permeability cores.

Table 22. Eagle Ford spontaneous imbibition experiment results

Core	Type of Fluid	Initial Average CT (HU)	Final Average CT (HU)	Penetration magnitude (HU)	IFT (mN/m)	Initial CA (°)	Final CA (°)	Oil Recovered (% OOIP)
1	Frac-water	1847	1855	8	34.03	104.9	94.7	1.9
2	Frac-water	1816	1822	7	34.03	113.2	93.2	2.9
3	A	1865	1881	17	0.22	103.0	35.8	6.8
4	A	1771	1787	16	0.22	132.5	40.3	6.6
5	NC	1852	1871	19	1.76	110.4	39.9	9.3
6	NC	1765	1782	18	1.76	120.2	36.4	10.0
7	C1	1842	1857	15	2.33	103.4	34.3	6.6
8	C1	1776	1792	16	2.33	106.1	46.4	7.6
9	AN	1827	1840	13	2.89	100.1	39.2	3.6
10	NA	1840	1857	17	4.48	96.0	41.2	4.6
11	C2	1834	1845	11	7.25	98.4	77.5	3.1

Initial CA confirmed the presence of intermediate towards oil-wet core Final CA and IFT showed the capability of surfactant additives to alter wettability to water-wet and reduce oil-water IFT. In addition, final CA suggested that solution without surfactant additives were not able to alter wettability or reduce IFT, which had a direct impact in on capillary pressure. As showed, initially capillary pressures are negative for all cores due to initial wettability states. As the experiments progress and surfactant solutions alter wettability, capillary forces turned positive favoring imbibition and consequently oil recovery as demonstrated on the last column of Table 23. On the other hand, capillary

pressures for cores in frac-water still showed negative values at the end of the experiments, this is the main reason for low penetration and hydrocarbon production.

Table 23. Eagle Ford capillary pressures and inverse Bond numbers

Core	Type of Fluid	Initial Pc (psi)	Final Pc (psi)	Oil Recovered (% OOIP)
1	Frac-water	-363	-116	1.9
2	Frac-water	-556	-79	2.9
3	A	-317	7	6.8
4	A	-953	7	6.6
5	NC	-492	56	9.3
6	NC	-709	59	10.0
7	C1	-327	80	6.6
8	C1	-391	67	7.6
9	AN	-247	93	3.6
10	NA	-147	140	4.6
11	C2	-206	65	3.1

In summary, the results of these correlated set of experiments show that wettability alteration and IFT reduction play a significant role on improving the penetration of stimulation fluid into the rock matrix, which also improve oil recovery. Rock wettability must be shifted from intermediate and oil-wet to water-wet to let capillary forces promote imbibition and release trapped hydrocarbons. In addition, moderate IFT reductions are needed to trigger wettability alteration by pore imbibition. However, contrary to conventional EOR in which IFT is required to be reduced to almost zero, in liquid rich shales, IFT should not be greatly reduced to avoid oil redeposition into the pores and eliminate capillary forces as a driving mechanism. Moreover, rock surface charges as well

as oil and surfactant impact imbibition and oil recovery, thereby they must be considered when choosing the best suitable treatment for the reservoir.

Spontaneous Imbibition Experiments in the Bakken Formation

In Chapter V, I corroborated that adding chemical additives like surfactants and CNF to completion fluids alters wettability of Bakken cores from oil-wet to water-wet and reduces water-oil IFT. These changes in CA and IFT modify capillary pressure to favor spontaneous imbibition. Bakken cores from wells Bk-1 (predominately siliceous) and Bk-2 (predominately carbonate) were aged in Bakken oil for more than 6 months at reservoir temperature to reconstitute them with the missing liquid hydrocarbons due to sample handling. Moreover, spontaneous imbibition experiments were performed in an environmental chamber at 180 °F. For both wells, core dimensions, initial properties, and type of fluid used are in **Table 24**. These values are used to calculate the original oil in place (OOIP) and obtain oil recovery with times as experiments progress. Bakken initial water saturation (S_{wi}) for well Bk-1 is 0.38 and for well Bk-2 is 0.20; we used these values to calculate OOIP. In addition, core initial wetting affinity is measured by CA methods. Table 24 shows that all cores are initially oil-wet due to the extended aging period.

Table 24. Initial core properties for Bakken spontaneous imbibition experiments

Core	Well	Porosity (%)	OOIP (cm ³)	Initial CA (°)	Type of Fluid
1	Bk-1	10.8	1.672	121.0	Water
2	Bk-1	10.8	1.780	120.6	Anionic A
3	Bk-1	10.8	1.797	122.6	Nonionic-cationic
4	Bk-1	10.8	2.183	117.2	CNF
5	Bk-2	6.5	0.945	121.7	Water
6	Bk-2	6.5	0.985	126.7	Anionic A
7	Bk-2	6.5	1.022	120.5	Nonionic-cationic
8	Bk-2	6.5	0.816	119.1	CNF

The first set of experiments is performed with cores from well Bk-1. Cores 1 to 4 are submerged in aqueous solutions with and without surfactants and CNF as specified on Table 24. The concentration used for surfactant and CNF was 2 gpt. Using the graduated cylinder at the top of the modified Amott cells, oil production for all experiments is recorded with time and reported as function of the OOIP. This is shown in Fig. 73 where surfactant Anionic A performed better than CNF and surfactant Nonionic-cationic, and all solutions with chemical additives recover more oil than water alone, which is consistent with CA, zeta potential, and IFT results. Surfactant Anionic A produces more oil from these Bakken siliceous cores because it alters wettability in higher amounts and reduces IFT to lower values. Lower IFT favors water penetration in the nanopores, changing wettability by electrostatic interactions. I suggest that Anionic surfactant heads form ion-pairs with the oil in the pores and strip it from the rock surface. Then, by imbibition, water replaces the oil in-situ, expelling it out of the cores in a countercurrent movement. In the process, capillary pressure not only changes from negative to positive, but also its value is reduced due to IFT alteration. This mobilizes liquid hydrocarbons from the ULR cores

with help from gravitational forces. In the end, the core submerged in surfactant Anionic A recovers 40.6% of the OOIP, followed by CNF with 36.8%, and surfactant Nonionic-cationic with 31.3%. The core submerged in water without chemical additives only recovered 15.9% of the OOIP.

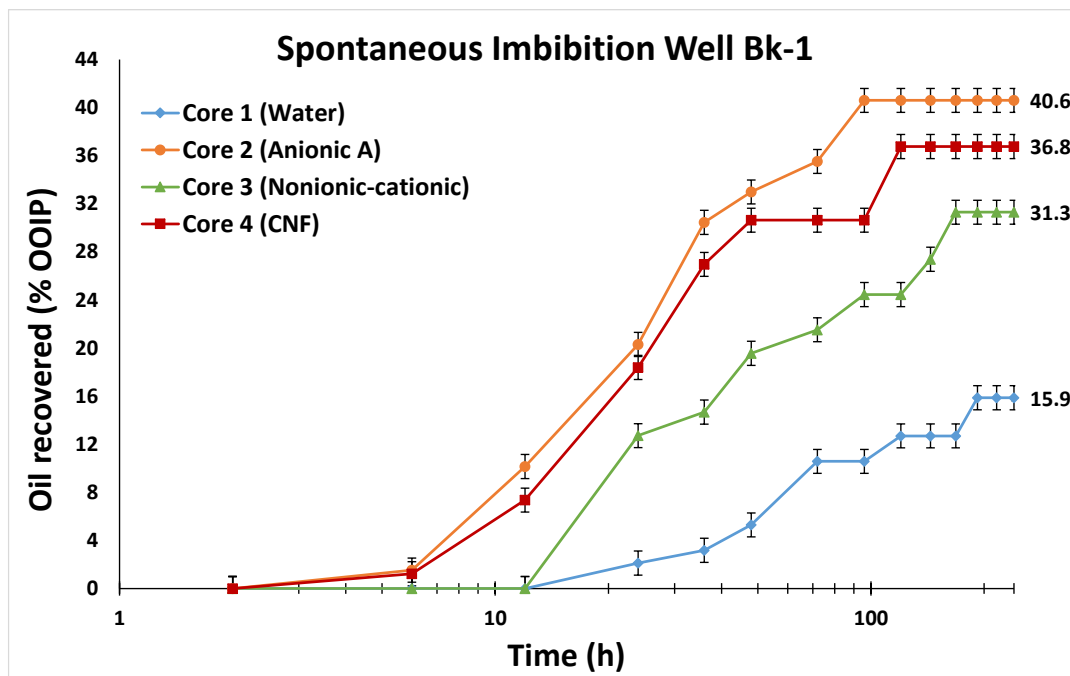


Figure 73. Oil recovered for well Bk-1 (siliceous) by spontaneous imbibition.

In addition, better IFT reduction of surfactant Anionic A and CNF accelerates water imbibition and oil is recovered faster than surfactant Nonionic-cationic and water alone. In fact, surfactant Anionic A and CNF begin to recover oil as soon as 6 hours compared to Nonionic-cationic and water that begin to produce at 24 hours. Finally, it is important to notice the poor performance of water without chemical additives in

recovering oil from Bakken cores. This is because water alone is not capable of shifting wettability and reducing IFT, so oil is only marginally recovered by gravitational forces.

Next, oil recovered in spontaneous imbibition as percentage of OOIP vs. time for well Bk-2 is shown in **Fig. 74** In this case, well Bk-2 has higher carbonate composition, and consistent with CA results, CNF and surfactant Nonionic-cationic perform better than surfactant Anionic A. Positive charges present in CNF and surfactant Nonionic-cationic improve wettability alteration; thus, electrostatic interaction between the negatively charged oil compounds attached to the carbonate and positively CNF heads interact and remove oil from the core surface, favoring water imbibition. In addition, surfactant Anionic A recovers the least among the three chemical additives. This is also due to electrostatic repulsion of negatively surfactant heads and negative charges of the oil attached to the positive core surface (Alvarez and Schechter 2016a).

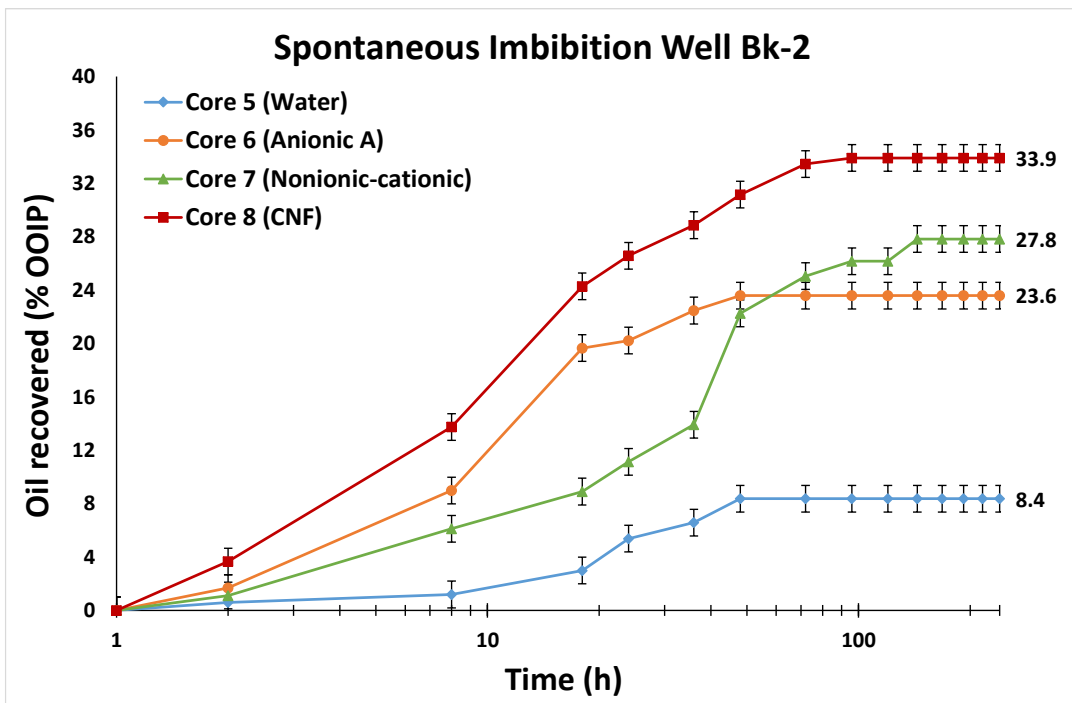


Figure 74. Oil recovered for well Bk-2 (carbonate) by spontaneous imbibition.

The importance of the electrostatic interaction and its impact on oil recovery is clearly seen on the surfactant Nonionic-cationic performance, which regardless of its deficient IFT reduction compared to anionic surfactants, as it recovers more oil than anionic surfactant A due to its positively charge surfactant heads. Moreover, the impact of IFT reduction is shown by the surfactant curves. Anionic A recovers oil faster than Nonionic-cationic because its better IFT reduction, but then, due to electrostatic charges, Nonionic-cationic recovers more oil at the end of the experiments. Consequently, a combination of wettability alteration and IFT reduction is the key for a proper water imbibition and hence liquid hydrocarbon production from these Bakken cores (Alvarez, Saputra, and Schechter 2017).

Lastly, just as well Bk-1, all surfactants and CNF recover more oil than water alone due to wettability alteration and IFT reduction, which favors capillary forces. CNF recovered 33.9 % of the OOIP, followed by surfactants Nonionic-cationic and Anionic A with 27.8% and 23.6%, respectively; whereas, water without chemical additives produced only 8.4% of the OOIP, aided only by gravitational forces. From the obtained results in both wells, we can conclude that the use of chemical additives in completion fluids enhances oil recovery in Bakken cores, but this recovery is highly tied to formation lithology and surfactant type.

Another important information I can obtain from the recovery profiles for wells Bk-1 and Bk-2 is the difference in final oil recovery due to distinct petrophysical properties. As seen in Table 6, Chapter IV, well Bk-1 has higher porosity, permeability, and pore throat radius than those of well Bk-2. This improves recovery by allowing hydrocarbons to flow better outside the core (Alvarez and Schechter 2016a).

Next, CT scan technology is used to monitor spontaneous imbibition in Bakken cores for wells Bk-1 and Bk-2 and correlate the results with oil recovery. Modified Amott cells were periodically scanned to see fluid movement inside the cores with time. Changes in CT numbers can be related to water imbibition using dopants in the aqueous solution, so oil CT number is close to -100 HU whereas completion fluid CT number approximately 800 HU. This considerable difference between water and oil allow us to trace fluid penetration into the cores while water occupies pores originally filled with oil. Hence, due to the dopant type used, water imbibition in Bakken cores is characterized by positive

changes in CT numbers. In fact, the greater the positive change, the more water imbibes the cores and replaces oil.

CT images at different times during spontaneous imbibition experiments for cores from well Bk-1 are shown in **Fig. 75**. Positive changes in CT numbers suggest water imbibition in Bakken cores and the replacement of a fluid with lower CT number (oil) by another with higher CT number (water with dopant). The core in water without chemical additives (core 1) shows small changes in colors with some variations on the core periphery. In contrast, the cores submerged in aqueous solutions with surfactants and CNF (cores 2-4) show clear changes in colors as an indication of water penetration and consequently oil displacement. As shown, core 1 (water) shows limited changes in CT numbers as interpreted by small color variation; thus, water penetration is also meager. Core 2 (Anionic A) changes colors from red/green to dark blue/light blue and then from pink to yellow indicating that CT numbers are increasing inside the core. Moreover, core 3 (Nonionic-cationic) presents similar alteration in CT numbers as colors pass from red to green and dark blue to light blue. Lastly, core 4 (CNF) also visibly changes colors demonstrating water penetration as time progresses when moving from red to green and dark blue to light blue. The trends observed by CT methods, in which cores in solutions with surfactants and CNF have higher positive CT numbers, are consistent with oil recovery (Fig. 73), corroborating the importance of water imbibition and oil displacement in producing liquid hydrocarbons from Bakken cores. Moreover, the low changes in CT numbers, as limited imbibition rates, exhibited by core 1 correlates with its modest oil recovery.

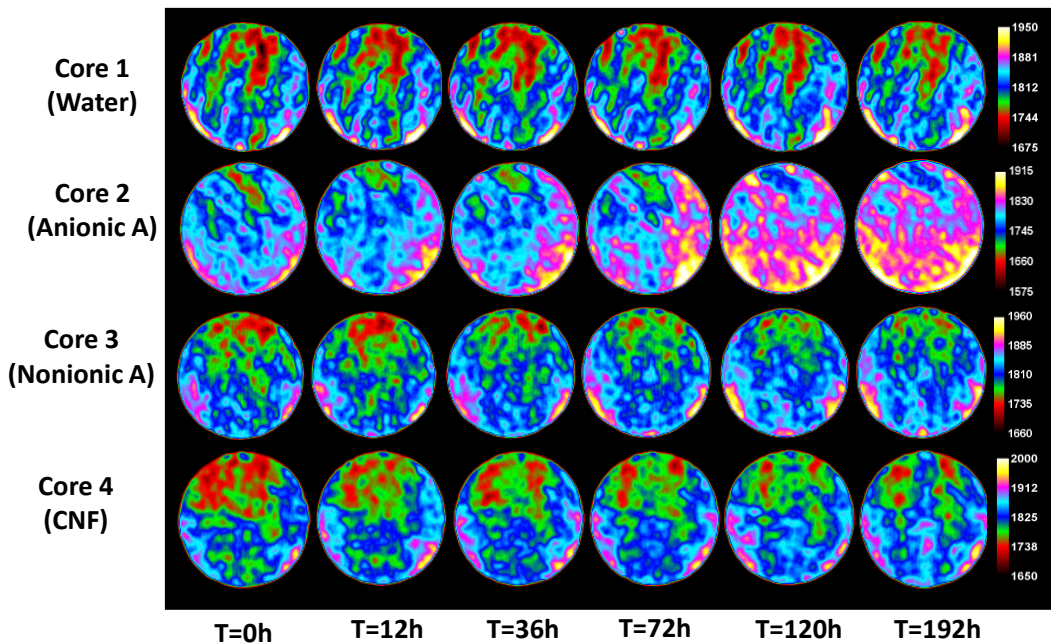


Figure 75. CT images for well Bk-1. Reprinted with permission from Alvarez and Schechter (2016a).

Similarly, fluid penetration in CT images for well Bk-2 can be seen in **Fig. 76**.

Core 5 (water) changes the least among the group cores (cores 5-8) whereas cores 6-8 show noticeable color variations with time. Thus, water imbibition and oil displacement in Bakken samples from well Bk-2 is more effective in the experiments using surfactants and CNF. As shown in Fig 76, core 5 barely changes CT numbers with time (few spots changing from red to green) as evidence of limited imbibition, which is consistent with its poor oil recovery (Fig. 74). On the other hand, as a sign of fluid imbibition, core 6 (Anionic A) presents color changes from red to green, dark blue to light blue, and pink to yellow. Moreover, core 7 (Nonionic-cationic) and core 8 (CNF) exhibit marked variation in colors

increasing CT numbers as the test progresses, changing from dark blue to light blue and pink to yellow in core 7, and red to green, dark blue to light blue, and pink to yellow in core 8. This imminent imbibition of aqueous solutions into the cores identified by CT methods favors oil production and is consistent with oil recovery by CNF and surfactants in well Bk-2 (Fig. 74).

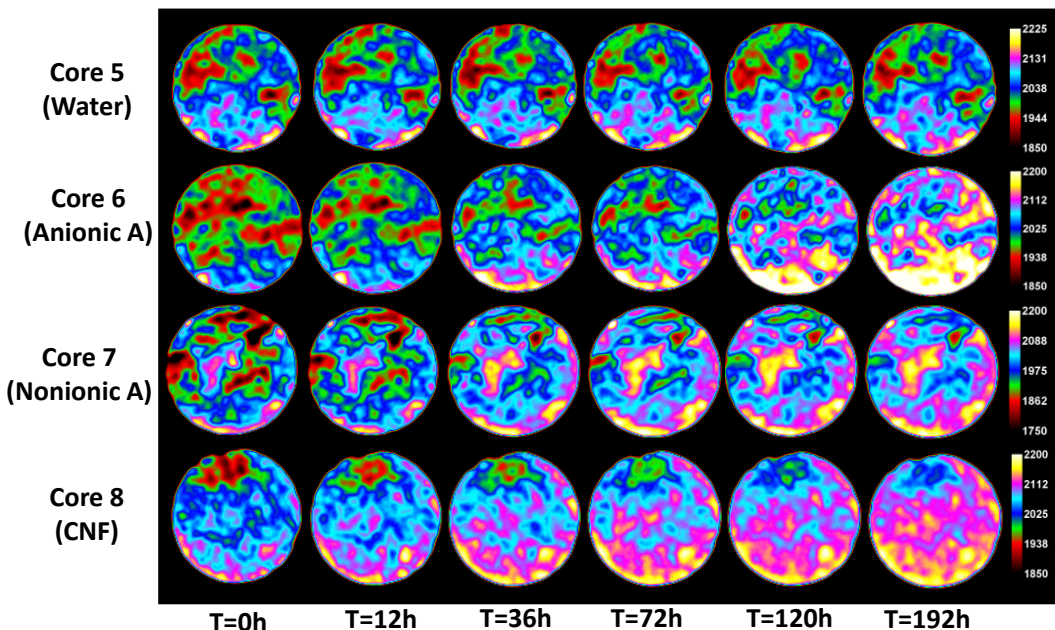


Figure 76. CT images for well Bk-2. Reprinted with permission from Alvarez and Schechter (2016a).

One common characteristic in Figures 75 and 76, when the samples are exposed to the CT scanner, is their core heterogeneity. Rock heterogeneity prevents fluid flow to be concentric towards the core center. In fact, changes in core colors during spontaneous imbibition experiments indicate that imbibing fluids are penetrating the rock unevenly by passing through zones with higher mobility. Also, during these experiments, micro

fractures are created favoring water imbibition and oil expulsion from the matrix. Even though water imbibition may not seem uniform along the cores due to rock heterogeneities, an imbibition profile is observed in our experiments, as positive changes in CT numbers, and more importantly, oil is recovered in higher amounts when using surfactants and CNF additives. Thus, CT scan methods provide reliable means to oversee completion fluid imbibition in Bakken cores, which can be related to hydrocarbon production (Alvarez, Saputra, and Schechter 2017).

The aqueous solution imbibition or penetration magnitude in the cores related by Eq. 29 is shown in **Table 25**. The differences between initial and final core average CT numbers can tell us comparatively the amount of fluid that imbibes in each experiment. The results for well Bk-1 show that core 1 (water alone) has the lowest penetration magnitude whereas cores 2-4, surfactant Anionic A, Nonionic-cationic, and CNF, respectively, have higher values compared to core 1. In fact, core 2 is shows the highest penetration magnitude followed by cores 4 and 3. These results are consistent with oil recovery for well Bk-1 cores. In addition, Table 25 also point out initial and final core weights. Due to water imbibition and oil expulsion, cores are expected to weigh more at the end of the experiments. This is the case for all the cores in well Bk-1; however, cores 2 to 4 have higher changes in weight as an indication of better imbibition, while core 1 has a much lower value due to its limited water imbibition.

Table 25. Bakken spontaneous imbibition experiment results

Core	Type of Fluid	Initial Average Core CT (HU)	Final Average Core CT (HU)	Penetration magnitude (HU)	Initial Weight (gr)	Final Weight (gr)	Initial CA (°)	Final CA (°)
1	Water	1761	1770	9	62.784	62.881	121.0	99.9
2	Anionic A	1762	1789	27	66.695	66.859	120.6	44.5
3	Nonionic -cationic	1760	1782	22	67.351	67.475	122.6	55.1
4	CNF	1767	1791	24	81.370	81.530	117.2	46.1
5	Water	1954	1961	7	46.043	46.126	121.7	109
6	Anionic A	1950	1969	19	49.600	49.727	126.7	49.6
7	Nonionic -cationic	1952	1973	21	51.228	51.349	120.5	51.0
8	CNF	1956	1981	25	40.670	40.808	119.1	43.8

Similarly, to penetration magnitudes for well Bk-1, changes in weight are consistent with oil recoveries. Finally, for well Bk-1, initial and final CA as values for wetting affinity are shown in Table 25. As explained before, all well Bk-1 cores are initially oil-wet, but after the spontaneous experiments cores 2 to 4 change their wettability to water-wet due to the interaction with surfactants and CNF as shown in Fig. 77. On the other hand, core 1 barely changes CA towards intermediate-wet, but it does not reach the water-wet behavior (Fig. 77). The lack of wettability changes in core 1 is the reason why penetration magnitude is the lowest as well as the change in weight; therefore, water imbibition is limited and oil recovery is the lowest among the cores evaluated.

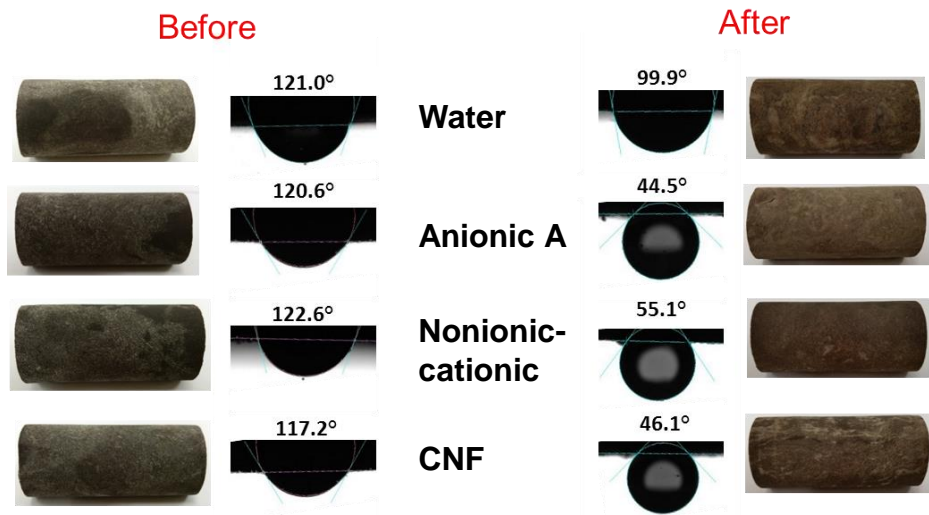


Figure 77. Contact angles before and after spontaneous imbibition experiments for well Bk-1 cores.

Table 25 also shows spontaneous imbibition experiments for well Bk-2, where penetration magnitudes are higher in cores with chemical additives (cores 6-8) and lowest in core 5 (only water). In addition, all cores increased weight as evidence of water imbibition and possible oil displacement, but cores 6 to 8 have higher changes in weight compared to core 5. These results are related to oil recoveries for well Bk-2 in which core 8 recovered more oil and have the highest penetration magnitude and weight change followed by surfactants Nonionic-cationic and Anionic A. Moreover, like well Bk-1, CA measurements before and after the experiments, as shown in Fig. 78, indicate that core 5 (water) does not change its wettability to water-wet whereas cores 6-8 (surfactants and CNF) alter their wetting preference from oil-wet to water-wet.

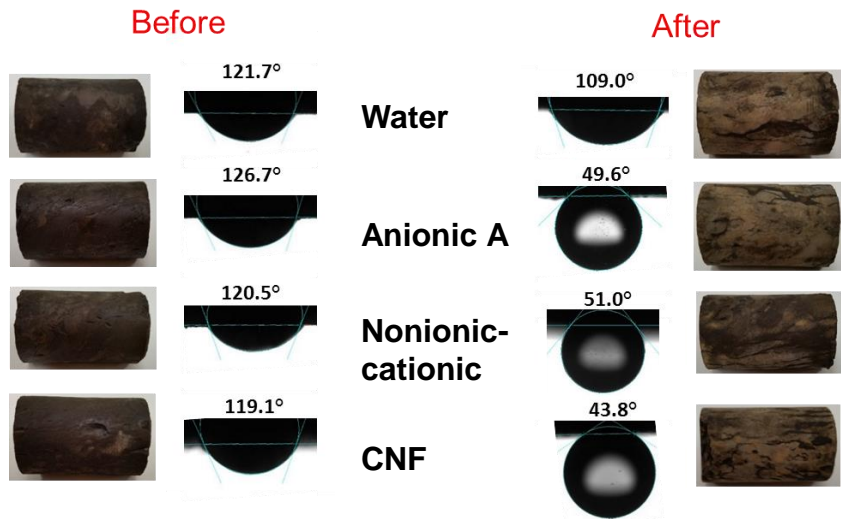


Figure 78. Contact angles before and after spontaneous imbibition experiments for well Bk-2 cores.

The results for both wells show water imbibition by penetration magnitude and wettability changes by CA measurements. These alterations along with changes in IFT are responsible for better oil recovery for the cores in contact to aqueous solutions with surfactants and CNF. To that end, capillary pressures (Eq. 1), before and after the experiments, are calculated using CA, IFT, and pore radius (Table 6) for each core and shown in **Table 26**. For all cores, initial capillary pressures are negative with high values, especially for cores from well Bk-2 with smaller pore radius. Pore radius inversely affects capillary pressure; so, the smaller the pores, the higher the capillary pressure and the more difficult it is to displace oil by imbibition. In fact, in oil-wet systems, spontaneous imbibition does not take place because oil is captured by the matrix, driven by capillarity. When wettability and IFT are altered by addition of surfactants and CNF, capillary pressure not only changes from negative to positive, but also reduces its value low enough

to let the aqueous solution invade the cores and drive oil out in countercurrent movement. Conversely, the lack of alteration in wettability and IFT in the cores 1 and 5 is responsible for their lower oil recovery as compared to the other cores (Alvarez and Schechter 2016a).

Table 26. Bakken capillary pressure and inverse Bond numbers

Well	Type of Fluid	IFT (mN/m)	Initial Pc (psi)	Final Pc (psi)	N _b ⁻¹ (-)	Oil Recovered (% OOIP)
Bk-1	Water	17.2	-76	-25	938	15.9
Bk-1	Anionic A	0.3	-75	2	16	40.6
Bk-1	Nonionic-cationic	4.5				31.3
Bk-1	CNF	1.5	-67	9	85	36.8
Bk-2	Water	17.2	-262	-162	5513	8.4
Bk-2	Anionic A	0.3	-298	6	96	23.6
Bk-2	Nonionic-cationic	4.5		-253	82	27.8
Bk-2	CNF	1.5	-243	31	481	33.9

In addition to capillary pressure, the inverse Bond number (Eq. 7) was calculated to address the ratio of capillary to gravitational forces and to determine if imbibition is driven by gravitational forces as cocurrent flow or driven by capillary forces as countercurrent flow. As shown in Table 26, inverse Bond numbers are significantly higher than 5, which corroborates that the main force propelling spontaneous imbibition in these Bakken cores is capillarity favoring countercurrent flow. In general, due to their ultra-low permeability, ULR have high inverse Bond numbers, which implies that capillary forces are more important than gravitational forces in controlling imbibition.

In summary, for wells Bk-1 and Bk-2, surfactants and CNF clearly show better performance over water alone in altering wettability, as determined by CA and zeta

potential experiments, and decreasing IFT, as measured by IFT experiments. In addition, surfactants and CNF recover more oil, as shown in spontaneous imbibition, and improve water imbibition, as evidenced by CT scan technology. These changes in wettability and IFT in ultra-tight Bakken rocks reverse the sign of and lower capillary pressure values. Surfactants and CNF diffuse into the cores and, by imbibition in a countercurrent movement, displace liquid hydrocarbons and provide higher oil recovery than aqueous solutions without chemical additives. However, from the results obtained, we observe that wettability changes deeply depend on sample lithology. For instance, samples from well Bk-1 are mostly siliceous, and show better wettability alteration, penetration magnitude, and oil recovery when anionic surfactants are present in completion fluids. These interactions are favored by electrostatic rock-fluid interaction as well as IFT reduction. On the other hand, well Bk-2 samples are mainly carbonates, and CNF show better results also aided by electrostatic rock-fluid interaction. Moreover, for both wells, nonionic and blended surfactant change wettability improving oil recovery but not as fast and effective as anionic (well Bk-1) and CNF (well Bk-2), due to smaller IFT changes. These correlated series of experiments proposed demonstrate a way to recover liquid hydrocarbons from Bakken cores by spontaneous imbibition when altering wetting affinity and decreasing IFT using chemical additives such as surfactants and CNF in completion fluids as well as the importance of assessing rock-fluid and fluid-fluid interactions when selecting chemical additives for stimulation treatments (Alvarez and Schechter 2016a).

Finally, this chapter dealt with the effect of flowback surfactants on altering the wettability of the rock as well as reducing oil-water IFT and their combined effect on oil

recovery through spontaneous imbibition. These results have practical implications on the design of chemically compatible and stimulating fluids to improve recovery in ULR. Choosing the appropriate surfactant and proper concentrations can reduce costs and recover additional oil as compared to a conventional stimulation treatment with any surfactant additives. To that end, completion fluid additives and their concentrations should be carefully selected while taking into consideration surfactant, oil and rock type. These can reduce completion costs and improve oil recovery after flowback as compared to adding an unknown chemical that may not effectively promote imbibition into the rock. Moreover, from the spontaneous imbibition experiments results, I observe that most of the oil production occurred during the first 5 days from the start of the experiments. This common trend in oil recovery underline the importance of flowback schedules, such as Huff and Puff that may be beneficial when using surfactant additives. Huff and Puff schemes give completion fluids enough time to imbibe into the shale rock and mobilize additional hydrocarbons as compared to other type of schedules such as Frac and Flow. To confirm these results at reservoir pressures and to reproduce a soak and flowback schedule in ULR, a set of experimental core flooding through induced fractures using surfactant additives are performed and explained in the next chapter.

CHAPTER VIII

CORE FLOODING IMBIBITION EXPERIMENTS MONITORED BY CT SCAN

TECHNOLOGY

In the previous chapters, we observed the efficacy of surfactants in altering wettability and moderately reducing IFT in rock and oil samples from Wolfcamp, Bakken, Eagle Ford, and Barnett formations. The impact on oil production of these alterations was successfully demonstrated by spontaneous imbibition experiments in Chapter VII. Liquid rich shale samples showed higher production when submerged in completion fluids bearing surfactants than slick water alone. Thereby, fracture treatment performance and consequently oil recovery could be improved by adding surfactants to stimulation fluids when soaking-flowback production schedule is applied. In this chapter, I systematically evaluate and expand on the ability of different groups of surfactants, added to completion fluids, on improving oil recovery in ULR by experimentally simulating the fracture-treatment, at reservoir conditions, to represent surfactant imbibition in an ULR core fracture during a soaking and flowback.

A core-flooding system was designed to be combined with the CT-scanner. This integrated system enabled us to dynamically visualize the movement of the fluid as it penetrates the ULR samples in real-time, as well as compare oil recovery performance between surfactants and slickwater without additives. Saturated Wolfcamp side-wall cores were longitudinally fractured and loaded into an aluminum-carbon composite core-holder.

Three different types of surfactants were used, as described in Table 11 and complemented in **Table 27**: anionic A, nonionic-cationic, and complex nanofluid 3 (CNF-3). These surfactants, as well as slickwater without surfactants, were tested to address their effectiveness in penetration into the fractures and recovering oil from ULR cores. These solutions were injected through the fractures at reservoir conditions. Then, a soak and produce scheme was used to simulate fracture-treatment and flowback. Initial and final core wettability were determined by contact angle. Changes in IFT were measured by the pendant drop method.

Table 27. Surfactant properties 3

Surfactant	Primary components	Composition (wt.%)	pH	Specific Gravity
Complex Nanofluid 3 (CNF-3)	Isopropyl alcohol	7-13	6.41	1.00-1.06
	Citrus Terpenes	10-30		
	Sulfonated surfactant	10-30		

Core Flooding Imbibition Experiments Results in ULR

Liquid rich shale cores from the Wolfcamp ULR were used. Sidewall cores had a diameter of 1-inch and a length of 1.5 to 3-inches. All cores were from well W-2, as described in Table 3. TOC content ranged from 4.5 to 5.7 wt.%, which was measured on a LECO C230 Carbon Analyzer. In addition, X-Ray Diffraction (XRD) analysis for the cores used describes core mineralogy as shown in **Table 28**. Samples depths range from

8390 to 8405 ft., and they are predominately carbonaceous with calcite and dolomite contents of more than 50 wt.%.

Table 28. Lithological composition of rock samples from well WC-2

Sample / Depth (ft)	1 / (8405)	2 / (8400)	3 / (8395)	4 / (8390)
Mineral (wt. %)				
Quartz	22	20	24	22
Clays	20	23	20	22
Calcite	36	36	30	32
Dolomite	16	15	19	17
Feldspar	5	4	4	5
Pyrite	1	2	3	2
Relative Clay (%)				
Illite/mica	96.2	96.0	95.5	95.1
Smectite	3.8	4.0	4.5	4.9

Petrophysical analyses, measured by mercury injection capillary pressure (MICP), showed permeability to air from 100 to 200 nD for the carbonate cores, with both having core porosities ranging from 6 to 7%, and median pore radius of 0.005 microns.

Initial core properties and type of fluid used for these experiments are shown in **Table 29**. These values were used to calculate original oil in place (OOIP) in cores. Moreover, initial oil saturation (S_{oi}) value of 0.65 was provided by the core supplier and confirmed using mercury intrusion and extrusion analysis. To determine the initial wettability of the cores, CA measurements were performed on the samples.

Table 29. Initial core properties for Wolfcamp core flooding imbibition experiments

Core	Diameter (in)	Length (in)	Porosity (%)	Initial Weight (gr)	Initial CA (°)	Type of Fluid
1	0.987	2.995	6.3	95.39	131.2	Anionic A
2	0.986	3.465	6.4	105.16	141.0	Nonionic-Cationic
3	0.987	3.587	6.4	110.06	133.6	CNF-3
4	0.986	3.436	6.4	107.99	130.3	Frac-water

Initial wettability measurement results showed cores with wetting affinity of oil-wet to intermediate-wet due to the extended aging period. Then, core-flooding imbibition experiments were performed by varying the type of fluid injected. Due to core ultralow permeability, fluid flow was expected to occur throughout the fractures. However, wettability and IFT alterations induced by surfactants would trigger imbibition on the fractures towards the matrix, improving oil recovery compared to a system injecting slickwater alone. The first part of the experiment aims to reproduce the soaking stage that a well undergoes when a completion fluid is left on the propped fractures for an extended period. To accomplish this, aqueous solutions containing different surfactants at concentration of 2 gpt as well as slick water alone were injected at reservoir conditions of 165 °F and 1500 psi and soaked into the core-flooding system for 72 hours. During the soaking period, CT scan images were taken to assess the penetration magnitude or imbibition of completion fluids inside the core. **Fig. 79** shows the behavior of average change of CT number, or penetration magnitude (Eq. 29), with time in cores 1 to 4. As used in spontaneous imbibition experiments, KI was added as a dopant to better

differentiate between oil and frac fluids. In these experiments, oil CT number is close to -100 HU, whereas frac fluids' CT number is around 800 HU. This marked CT number difference allows me to see changes when frac fluids imbibe into the cores and fill part of pore volume originally occupied by oil. Thereby, imbibition from the fractures to the matrix is represented by positive changes in CT number. The greater the positive change, the more water imbibes the cores.

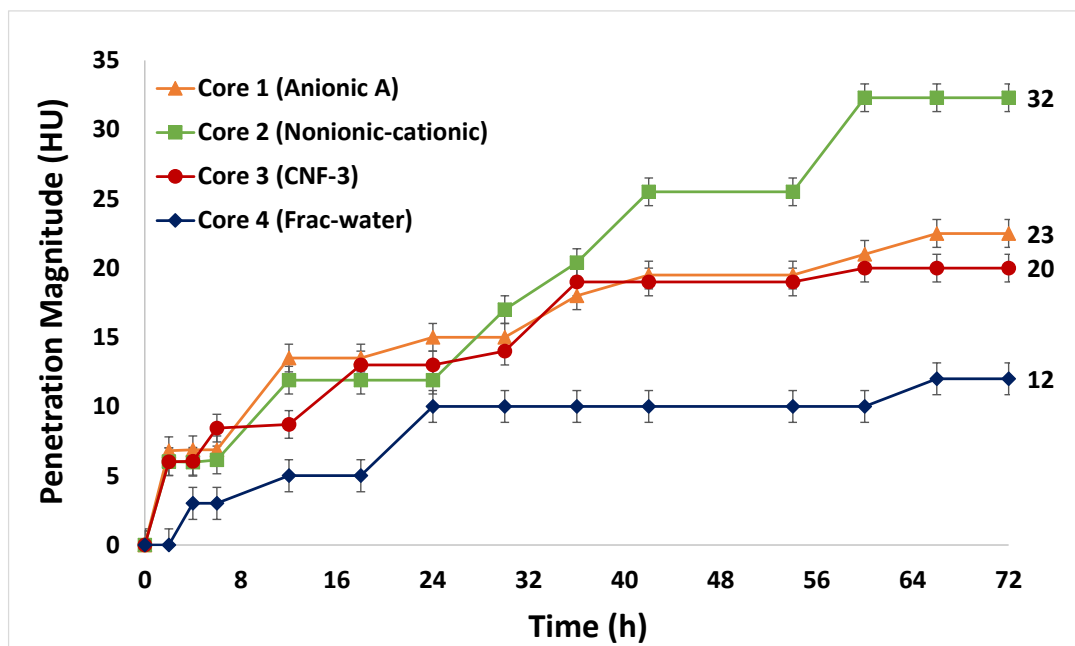


Figure 79. Penetration magnitude for core flooding imbibition experiments.

From Fig. 79, the cores flooded with surfactant solutions (cores 1 to 3) showed higher penetration magnitudes, or changes in CT number, than the core flooded with slickwater alone (core 4). In addition, the highest change in penetration magnitude is observed during the early stages (region 1) of the experiments. The cores submerged in

surfactant solutions have larger changes than brine alone. This trend is consistent with oil production curves obtained in spontaneous imbibition experiments (Chapter VII, Fig. 68) in which oil recovery has its highest rate before the first 12 to 24 hours. This imbibition behavior is due to the fast reduction of water-oil IFT by surfactant additives, as shown in Chapter V. Surfactants solutions have the ability of reducing IFT from initial 21.8 mN/n to 0.4 to 9.8 mN/m. The IFT reduction minimizes capillary pressures, allowing trapped oil in the pores to leave and replaced by a higher CT number fluid (doped aqueous solutions). After 24 hours (region 2), penetration magnitudes still rise, but at lower rates. At this moment, surfactant solutions changed fracture surface wettability, so the capillary pressure sign shifts from negative to positive, allowing imbibition to fully take place. Due to core ultralow petrophysical properties, imbibition driven by wettability alteration is a slower mechanism. Thereby, penetration magnitude profile slope is not as steep as region 1. Finally, region 3 shows constant penetration magnitudes for the rest of the soaking period.

In addition, during the soaking period, the CT scan images were taken to dynamically visualize the movement of the fluid as it penetrates the ULR samples as shown in **Fig. 80**. In each core, the fracture is highlighted as a dotted line. The color-scale for CT numbers are shown to the right of each set of images and it was varied based on experiment to observe a better contrast between the oil and aqueous phases. Brighter yellow to blue regions were considered to have a high CT number owing to higher density, while red to green colors corresponded to lower CT number. Change in colors from

red/green to blue to yellow implies the displacement of a low-density medium (oil) by a high-density medium (doped aqueous solutions).

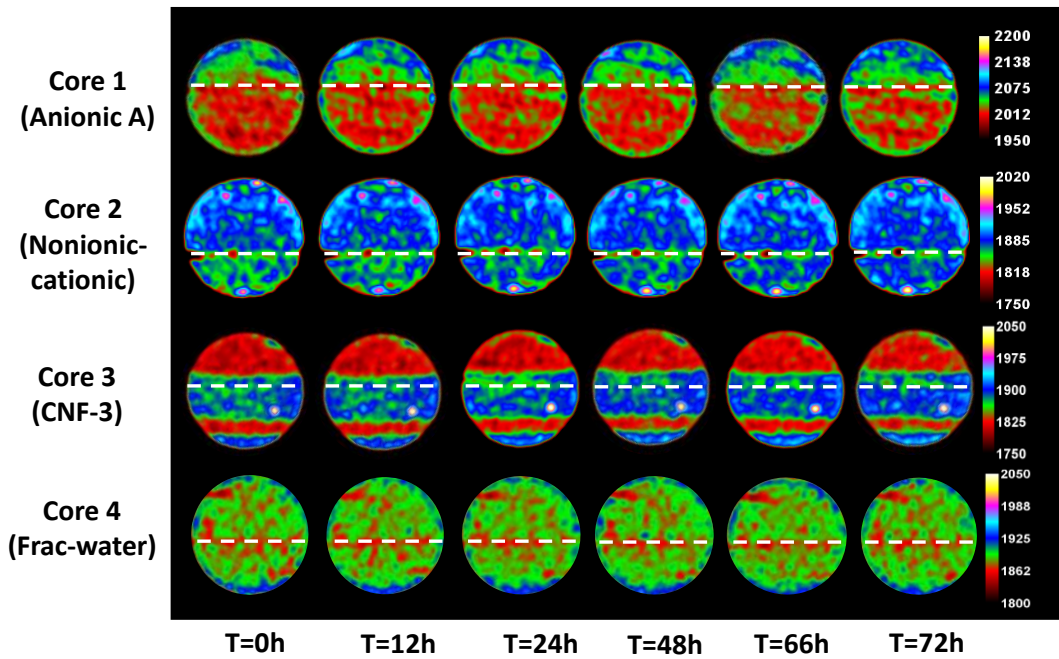


Figure 80. CT images for core flooding imbibition experiments.

Fluid penetration for the four cores evaluated shows interesting insights about imbibition aided by surfactant additives. Cores flooded with aqueous solution with surfactants showed noticeable changes as colors move from red to green (core 1), green to blue (core 2) and red/green to dark/light blue (core 3), representing an increase of CT number and consequently an increase in fluid imbibition into the core. On the other hand, the core flooded with frac-water alone (core 4) showed limited changes in colors as an indication of modest positive changes in CT numbers and limited imbibition. These changes are consistent with the average CT number changing as a function of time as

presented in Fig. 79 in which core 2 (nonionic-cationic) has the higher penetration magnitude followed by cores 3 (CNF-3) and 1 (anionic A), respectively. Conversely, core 4 (frac-water) showed almost no change in CT number and lowest penetration magnitude. Therefore, the use of CT scan technology offers a reliable way to monitor water imbibition into ULR cores, which can be correlated to oil recovery.

In addition, Fig. 80 also show heterogeneities in the cores affecting fluid movements and preferential imbibition to zones of better petrophysical property areas around the fracture. Greater changes in CT numbers occurred not only close to the fractures, but also in layers of presumably better petrophysical properties. In fact, core heterogeneities give very distinct changes in CT numbers. These heterogeneities are common in liquid rich unconventional reservoirs and they are one of the most challenging factors when upscaling laboratory results. Nevertheless, higher changes in CT numbers are clearly evidenced in cores flooded by surfactant solutions than the one flooded with slickwater alone.

Next, after a soaking period of 72 hours, the core flooding system is opened to production for 8 hours. At this stage of the experiment, we reproduced the well flowback where production is greatly dominated by pressure differences between the reservoir and the wellbore.

The oil recovered from the core was collected and measured every 2 hours to address oil recovery as a function of the original oil in place with time. **Fig. 81** shows the actual oil recovered at the end of the experiments. Visual inspection of the recovered hydrocarbon suggests that the oil produced maintains the same composition. There is no

visible indication of higher recovery of lighter oil components, which suggests to us that imbibition is taking place in the average pore size, consisting with large hydrocarbon molecules. To confirm our visual observations, we measured recovered oil density and compared it to initial oil density shown in Table 7 in Chapter IV. Initial Wolfcamp oil density at 70 °F is 31.4 °API and recovered samples showed a density of 30.9 °API. This small change in API gravity confirmed our observations that the oil recovered maintains similar properties as the one stored in the ULR rock pores.

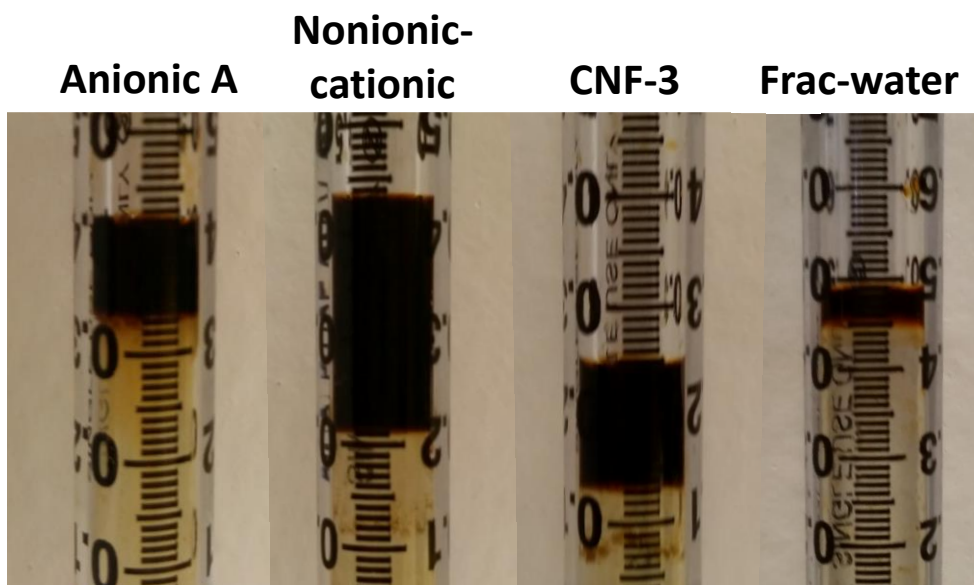


Figure 81. Oil recovered at the end of the core flooding imbibition experiments.

In addition, using the values in Table 29 and initial oil saturations as well as the oil recovered in each experiment, we calculated the oil recovered as a function of the OOIP for the flowback period. This is shown in **Fig. 82** where surfactant nonionic-cationic performed better than surfactants anionic A and CNF-3. All solutions with chemical

additives recovered more oil than water alone, which is consistent with CA, zeta potential, and IFT results, as well as penetration magnitudes observed by CT scan technology (Fig. 79).

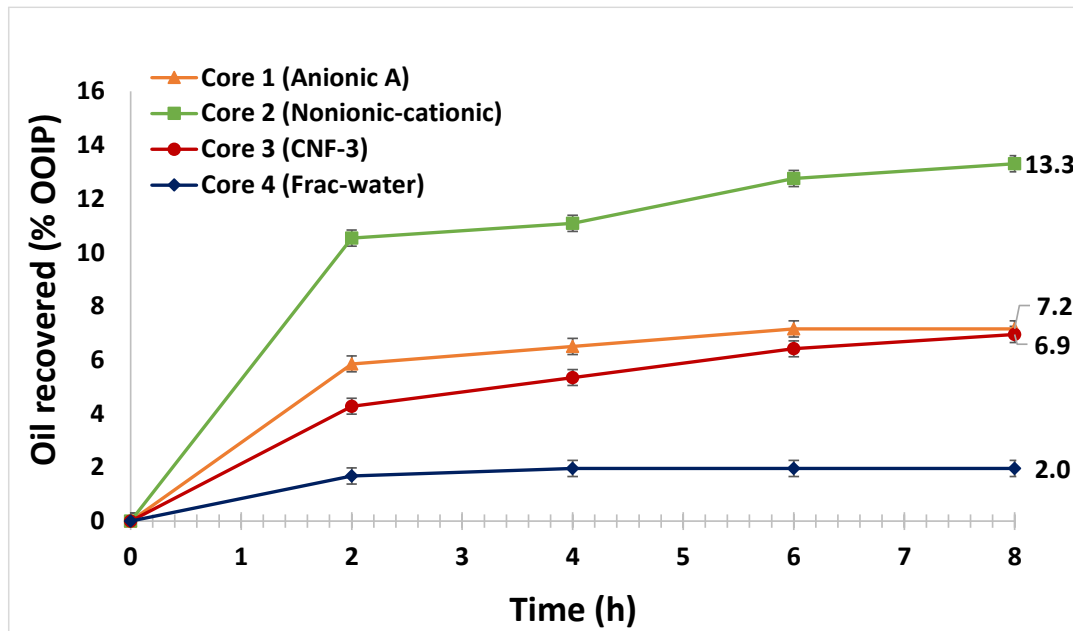


Figure 82. Oil recovered in core flooding imbibition experiments.

As shown in Table 28, the cores used in this section had higher carbonate composition and were consistent with the CA experiments. The nonionic-cationic surfactants altered wettability better than surfactants with anionic compounds, such as anionic A and CNF-3. This is attributed to the electrostatic interactions between the negatively charged oil compounds attached to the carbonate rock and positively charged cationic heads of surfactant nonionic-cationic. The charges interact and remove oil from the core surface, favoring aqueous solution imbibition. In the same way, the repulsion

forces between the negatively charged anionic heads and negative charges of the oil attached to the positive core surface impact surfactants anionic A and CNF-3 oil recovery.

The penetration magnitude and oil production results highlight the role of electrostatic interactions in imbibition and, consequently, oil recovery. In the core flooding experiments, the nonionic-cationic surfactant performed better than anionic A and CNF-3, due to its positively charged surfactant heads recovering more oil and penetrating to a higher extent into the rock, regardless of its moderate IFT reduction compared to the reduction in the more anionic surfactants. Thereby, a combination of wettability alteration and IFT reduction is the key for proper imbibition and oil recovery from these ULR cores. Moreover, it is important to note that the TAN and TBN Wolfcamp crude oil used in these experiments are 0.09 and 0.12 mg KOH/ g oil, respectively. These values suggested that the Wolfcamp oil is slightly more basic, but the difference between TAN and TBN is minimal. Thus, electrostatic interactions are largely governed by rock surface charges as distinguished by different lithologies.

Lastly, all cores flooded with surfactant solutions recover more oil than slickwater alone due to wettability alteration and IFT reduction, which favors capillary forces. Nonionic-cationic surfactant recovered 13.3 % of the OOIP; followed by surfactants Anionic A and CNF-3 with 7.2 % and 6.9 % recovery, respectively; whereas, water without surfactants produced only 2.0 % of the OOIP. From the obtained results, we can conclude that the use of surfactants in completion fluids enhances oil recovery in ULR cores, but this recovery is highly tied to formation lithology and surfactant type.

To investigate the effect of wettability by different surfactant types and slickwater alone, the samples used and their initial and final core wettability, measured as contact angle, are shown in **Fig. 83**. Fig. 83 shows the different wettability states of the samples before and after the core flooding experiments. Initially, all cores showed contact angles of greater than 130 degrees as a clear indication of the oil-wet character. At the end of the experiments, all cores flooded by aqueous solutions with surfactant additives (cores 1 to 3) showed wettability alteration to water-wet with core 2 exhibiting the lowest contact angle as an indication of larger wettability alteration among the three. Conversely, the core flooded with water without surfactant (frac-water) was not capable of shifting wettability from oil-wet to water-wet, showing an intermediate-wet behavior with final contact angle of 93.3 degrees. The lack of wettability changes in core 4 is the reason why penetration magnitude is the lowest; therefore, water imbibition is limited and oil recovery is the lowest for this core among the cores evaluated. These observations confirm the results reached in the wettability alteration chapter (Chapter V) in which it was broadly shown that the use of surfactants altered ULR wettability from oil and intermediate-wet to oil-wet.

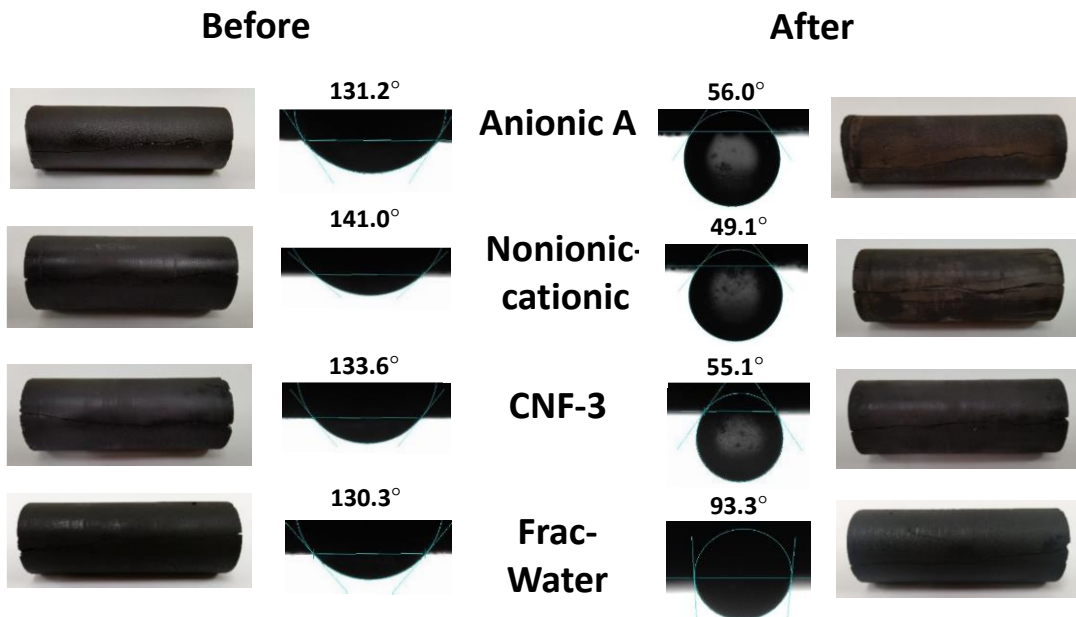


Figure 83. Contact angles before and after core flooding imbibition experiments.

As shown in the wettability alteration chapter (Chapter V, Fig. 30) and Fig. 83, for these carbonate cores, wettability is altered in greater amounts by the nonionic-cationic surfactant (core 2). We suggest that this better nonionic-cationic surfactant performance is due to electrostatic interaction between positively charged nonionic-cationic surfactant heads and negatively charged oil compounds, mostly acidic compounds, attached to the positive charged carbonate surface. These electrostatic interactions favor oil molecules to be stripped from the carbonate surface to the oil phase and consequently altering wettability to a water-wet state. Similarly, cores flooded with anionic surfactant and CNF-3 (cores 1 and 3) changed wettability from oil-wet to water-wet, but in lesser quantities as compared to nonionic-cationic surfactant due to the lack of electrostatic interactions. In this case, negatively charged surfactants anionic A and CNF-3 altered wettability by

hydrophobic interactions, while the oil layer attached to the shale surface forms a double layer with the hydrophobic surfactant tails. Thereby, the hydrophilic surfactant heads face the aqueous solution, altering wettability and creating a water-wet zone.

Table 30 summarizes the experimental results for the four core flooding experiments. Penetration magnitudes compare the amount of fluid that imbibes in each experiment. The results show that core 4 (frac-water) has the lowest penetration magnitude whereas cores 1-3, surfactant Anionic A, nonionic-cationic, and CNF-3, respectively, have higher values compared to the magnitude of core 4. Also, core 2 shows the highest penetration magnitude followed by cores 1 and 3. These results are consistent with final oil recovery. In addition, Table 30 also shows the cores change in weight. Cores are expected to weigh more at the end of the experiments because imbibition replaces a lighter fluid (oil) by a heavier fluid (water), so the change should be positive in magnitude. This is the case for all the cores tested. Moreover, cores 1 to 3 display higher changes in weight as an indication of larger imbibition, while core 4 has a much lower value confirming its limited water imbibition. Consistent to the obtained penetration magnitudes results, changes in weight also show correlation with oil recoveries.

Table 30. Core flooding imbibition experiment results

Core	Type of Fluid	Penetration magnitude (HU)	Δ Weight (gr)	Δ CA (°)	Δ IFT (mN/m)	Initial Pc (psi)	Final Pc (psi)	Oil Recovered (% OOIP)
1	Anionic A	23	0.14	75.2	20.9	-845	29	7.2
2	Nonionic cationic	32	0.32	91.2	14.4	-996	281	13.3
3	CNF-3	20	0.19	78.5	17.6	-884	139	6.9
4	Frac-water	12	0.09	37	0	-829	-73	2.0

In addition, changes in CA are also shown in Table 30. Core flooded with nonionic-cationic surfactant (core 2) has the highest change in contact angle, followed by cores 3 and 1 (CNF-3 and anionic A). Conversely, core 4 barely changed the CA, not reaching water-wetness and, consequently, not promoting water imbibition into the core. Changes in IFT are also in Table 30. Surfactant anionic A shows the highest variation among all surfactants tested, followed by CNF-3 and nonionic-cationic surfactants. Wettability alteration results correlates with oil recovery, whereas IFT changes does not correlate. The results indicate that wettability alteration dominates imbibition over IFT reduction in theses ULR. Nevertheless, surfactant capability of moderately reducing IFT is vital to capillary forces reduction and wettability alteration. Surfactants reduce IFT low enough to reduce capillary pressures and let fluids imbibe into the pores and alter wettability by cleaning or coating the rock surface.

Finally, using the Young-Laplace equation (Eq. 1), we calculated capillary pressures. Initially, due to oil-wetness and small pore radius, capillary pressures are negative with large values. Wettability gave the negative sign and pore radius gave the large magnitude value. In fact, in ULR, capillary forces are elevated because the small pore sizes impact oil displacement by imbibition. Then, as wettability is altered and IFT moderately reduced by surfactants (cores 1 to 3), capillary pressures change sign from negative to positive and reduce their magnitude low enough to let the aqueous solutions invade the matrix from the fractures and expel oil out to the fractures in a countercurrent movement. Contrarily, frac-water alone (core 4) is not capable of altering either

wettability, or IFT barely affected highly negative capillary pressures. Hence, the oil recovery is lower as compared to the recovery by the other cores.

In summary, this chapter evaluated and expanded on the ability of different groups of surfactants added to completion fluids on improving oil recovery in ULR by experimentally simulating the fracture-treatment, at reservoir conditions, to represent surfactant imbibition in an ULR core fracture during a soaking and flowback. A core-flooding system was designed to be combined with the CT-scanner. This integrated system enabled us to dynamically visualize the movement of the fluid as it penetrates the ULR samples in real-time as well as compare oil recovery performance between surfactants and slickwater without additives. Core-flooding results showed that aqueous solutions with surfactants had higher imbibition and recovered more oil from liquid-rich cores compared to slickwater alone. The soaking-flowback production schedule aided by surfactant additives could recover up to 13.3% of the original oil in place (OOIP), whereas slickwater without additives only recovered up to 2.0 % of the OOIP. These results are consistent with wettability and IFT alteration measurements. For the results obtained, we can conclude that the addition of surfactants to completion fluids and the use of a soaking-flowback production scheme can improve oil recovery by wettability alteration and IFT reduction, maximizing well performance after stimulation.

These findings also give an interesting insight in the importance of surfactant additives on the soaking and flowback schedules. By using CT scan technology, during the soaking period, we confirmed that aqueous solutions with surfactant additives could penetrate more the ULR matrix from the fractures than slickwater alone. Then, during the

flowback stage, oil was recovered with time in larger amounts when surfactant solutions were flooded instead of water alone. In addition, we observed that imbibition as penetration magnitude increased with time, and it reached its maximum close to 72 hours of soaking. These suggest that soaking time may be needed when using surfactants in completion fluids to allow imbibing fluids to penetrate the fractured rock and improve oil recovery. Thereby, these findings give important understanding for designing completion fluid treatments and flowback schedules for ULR. Field trials are recommended, but rock lithology, heterogeneity, and surfactant type must be considered to successfully scale up laboratory results, which will be discussed in the next chapter.

CHAPTER IX

SCALING LABORATORY DATA TO THE FIELD

As demonstrated in the previous chapters, in several of our laboratory studies, the effectiveness of fracture treatments in increasing oil recovery can be improved when proper surfactants are added to completion fluids, thereby altering wettability, moderately reducing interfacial tension (IFT), and consequently improving water imbibition. As the final step for this investigation, we systematically evaluate imbibition rates and dimensionless scaling groups to correlate laboratory imbibition data and predict oil recovery at field scale in unconventional liquid reservoirs.

A novel correlated set of laboratory experiments, specially designed for ULR, is used to gather the required data for scaling spontaneous imbibition experiments performed in sidewall cores. Wettability and IFT measurements as well as oil recovery profiles from imbibition experiments are utilized to calculate imbibition rates and generate normalized production rate curves for three different field-used surfactant types. Imbibition rates are used to demonstrate surfactant efficacy in recovering hydrocarbons from ULR core over slickwater alone; whereas normalized production rate curves are utilized to compare laboratory to field production profiles. Next, dimensionless time scaling models are used to study normalized oil recovery. Finally, by applying the imbibition scaling model to both lab and field data, the characteristic length of the field is calculated and used to predict field scale production rate. Also, by considering completion method, reservoir geometry,

and initial oil saturation from ULR well real-data, we estimated the field production rate under several induced and natural fracture spacing scenarios corroborating that fracture density and rock-fluid interactions are key parameters for oil recovery in these ULR.

Scaling Laboratory Data to the Field in the Eagle Ford Formation

The results obtained for the spontaneous imbibition experiments for Eagle Ford (Chapter VII, Fig. 71) were used to scale laboratory data to field scale. Different dimensionless time scaling models were used to study normalized oil recovery and to address their validity in ULR. These sets of normalized oil recovery vs dimensionless time curves were plotted to investigate the best scaling model for spontaneous imbibition in ULR. **Fig. 84** shows the oil recovered as a function of the OOIP vs. dimensionless time defined by Ma, Morrow, and Zhang (1995) (Eq. 9).

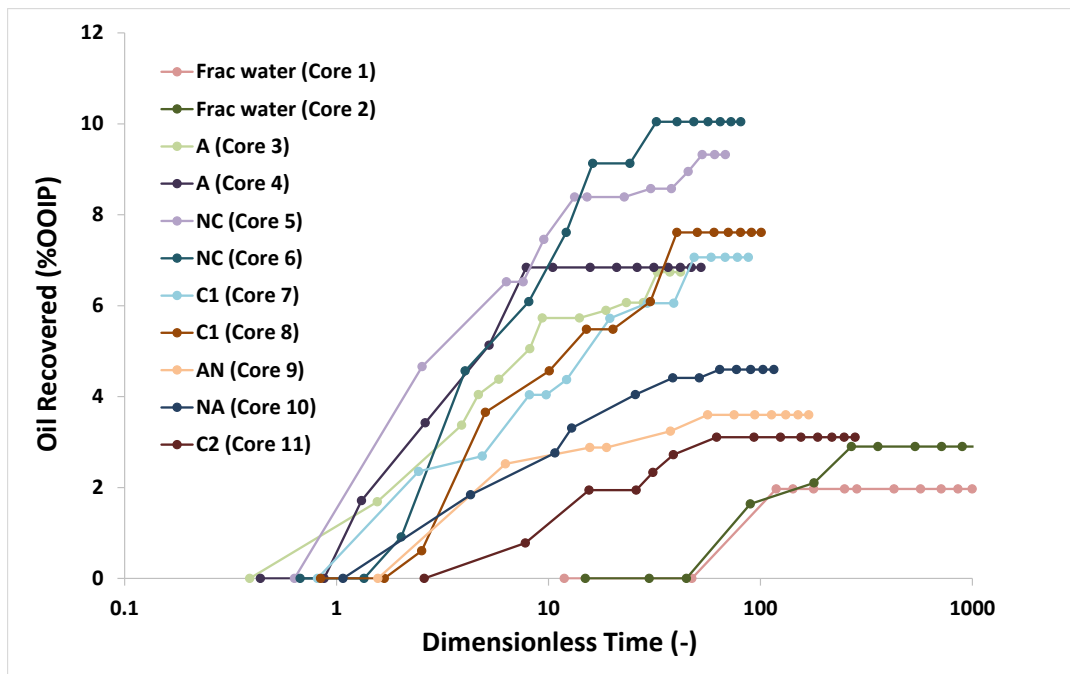


Figure 84. Oil recovery vs. dimensionless time for Eagle Ford using scaling group by Ma, Morrow, and Zhang (1995).

The curve profiles were like the laboratory results (Fig. 71), but the curves needed to be normalized to assess the dimensional scaling group validity in our data set. **Fig. 85** shows the normalized oil recovery and dimensionless time for the Ma, Morrow, and Zhang (1995) scaling group.

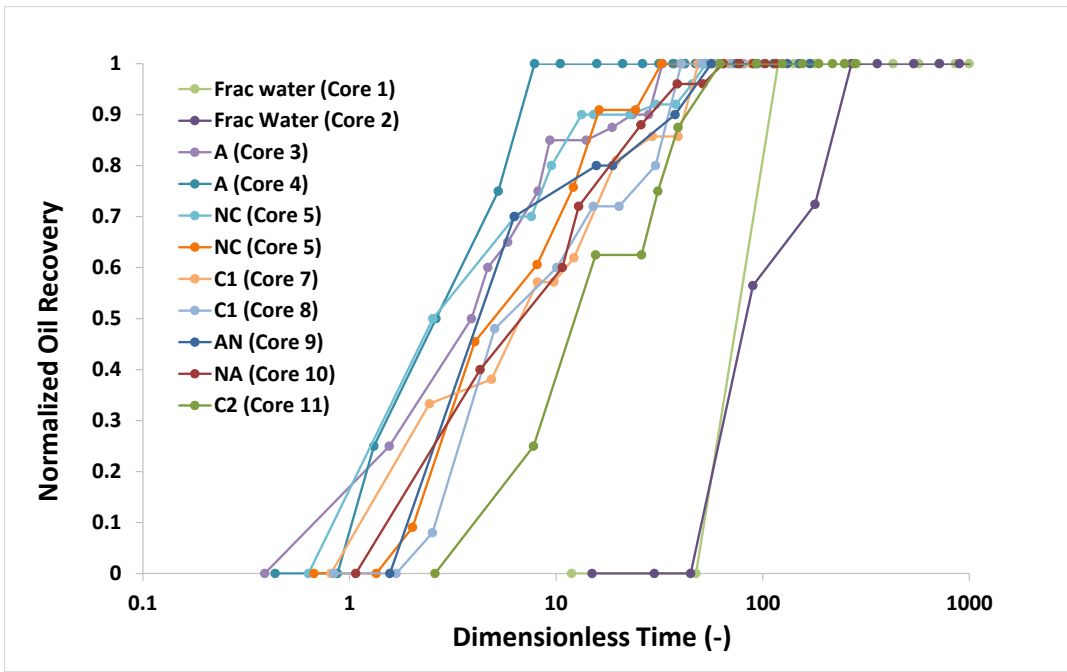


Figure 85. Normalized oil recovery vs. dimensionless time for Eagle Ford using scaling group by Ma, Morrow, and Zhang (1995).

The normalized plot grouped better the laboratory results improving their correlation for scaling to field production. However, frac water curves (Cores 1 and 2) demonstrated poor grouping to the scaling group, so the data scaled spans almost two log cycles. This wide span is a result of a wettability alteration that is not considered by Ma, Morrow, and Zhang (1995) (Eq. 9). The scaling number proposed by the equation considers that the system is very strongly water-wet (VSWW). As demonstrated in Chapter IV, ULR showed initial wettability of oil and intermediate-wet; hence, wettability alteration to achieve imbibition is a fundamental parameter to consider when scaling laboratory data.

Next, we analyzed the same Eagle Ford data using the scaling number proposed by Gupta and Civan (1994) and Guo, Schechter, and Baker (1998) (Eq. 12). This group

considers wettability proportional to dimensionless time. **Fig. 86** shows the oil recovered as function of the OOIP vs. dimensionless time and **Fig. 87** shows the normalized oil recovery versus dimensionless time as defined by Gupta and Civan (1994) and Guo, Schechter, and Baker (1998).

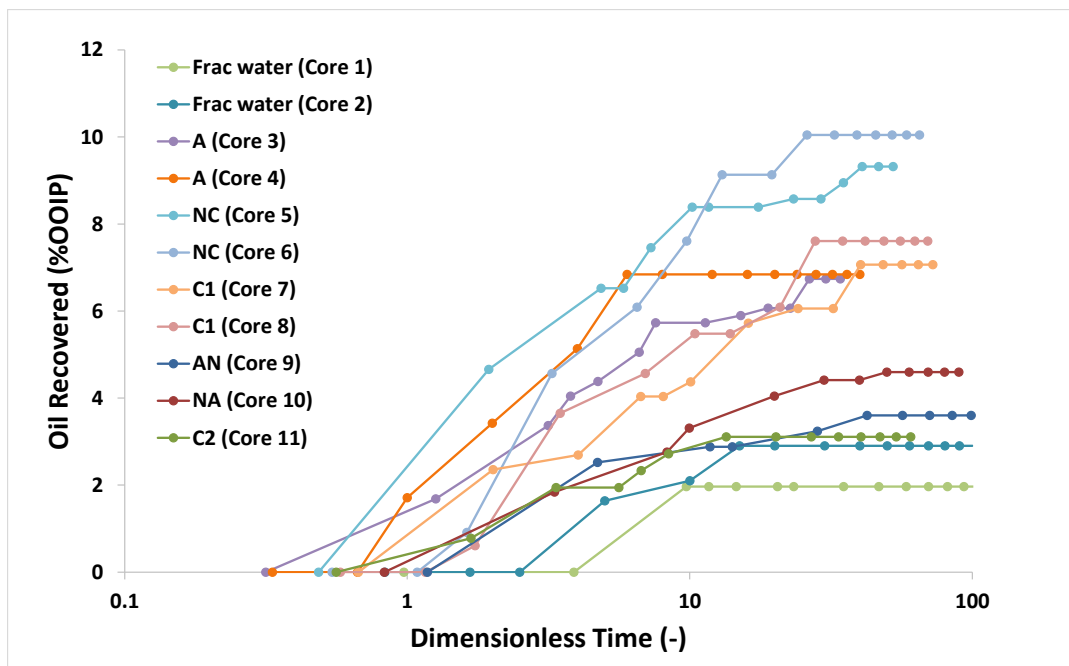


Figure 86. Oil recovery vs. dimensionless for Eagle Ford using scaling group by Gupta and Civan (1994) and Guo, Schechter, and Baker (1998).

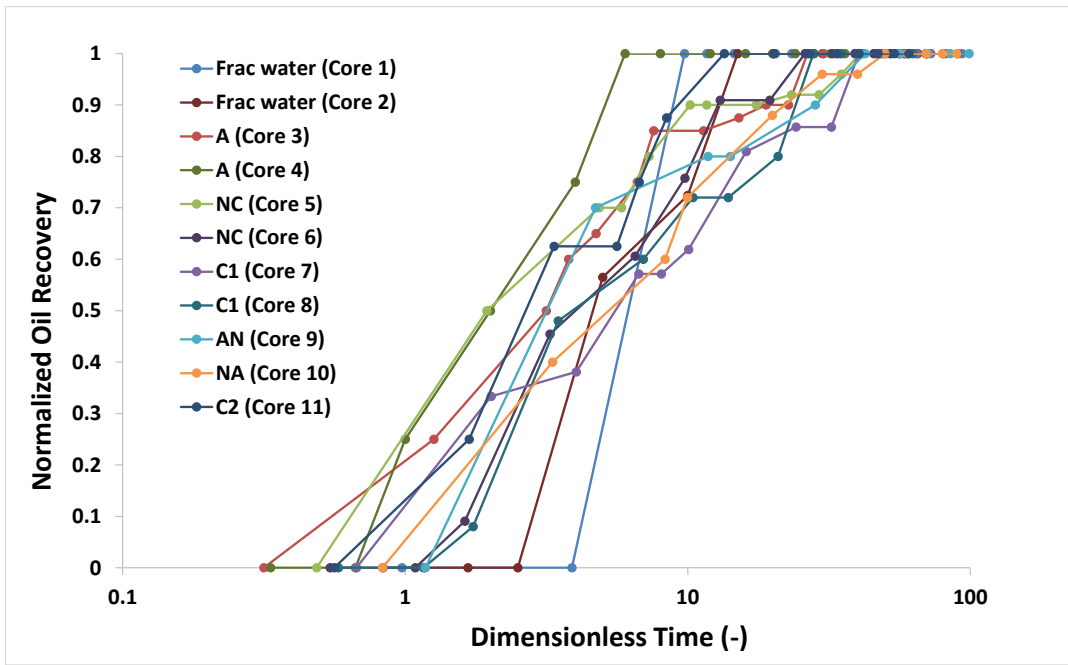


Figure 87. Normalized oil recovery vs. dimensionless time for Eagle Ford using scaling group by Gupta and Civan (1994) and Guo, Schechter, and Baker (1998).

When using the scaling number proposed by Gupta and Civan (1994) and Guo, Schechter, and Baker (1998), we first observed the data spread for the normalized oil recovery narrowed down from a span of two log cycles (Fig 85) to approximately one log cycle (Fig. 87), an indication of a better correlation as compared to the scaling number proposed by Ma, Morrow, and Zhang (1995). In addition, after comparing two scaling methods with and without contact angle, the results show that contact angle plays a critical role for dimensionless time.

Finally, after evaluating both dimensionless time profiles, we selected the latter dimensionless model, (Gupta and Civan (1994) and Guo, Schechter, and Baker (1998)). This model better represented our experimental results by considering not only IFT, but

also the effect of wettability alteration in the scaling model, as wettability is a fundamental parameter in the Young-Laplace equation (Eq. 1).

Based on our assumption that the dimensionless time for laboratory and the field are the same at all times, well production profiles due to imbibition has the same shape as that of the laboratory production curve. Hence, we generated production curves for Eagle Ford cores 1 to 11 using the oil recovery data measured in the laboratory (Fig. 71) and Eq. 34 and Eq. 35. **Fig. 88** shows production rates for spontaneous imbibition experiments. Moreover, the area under the production rate curve is the total oil recovered.

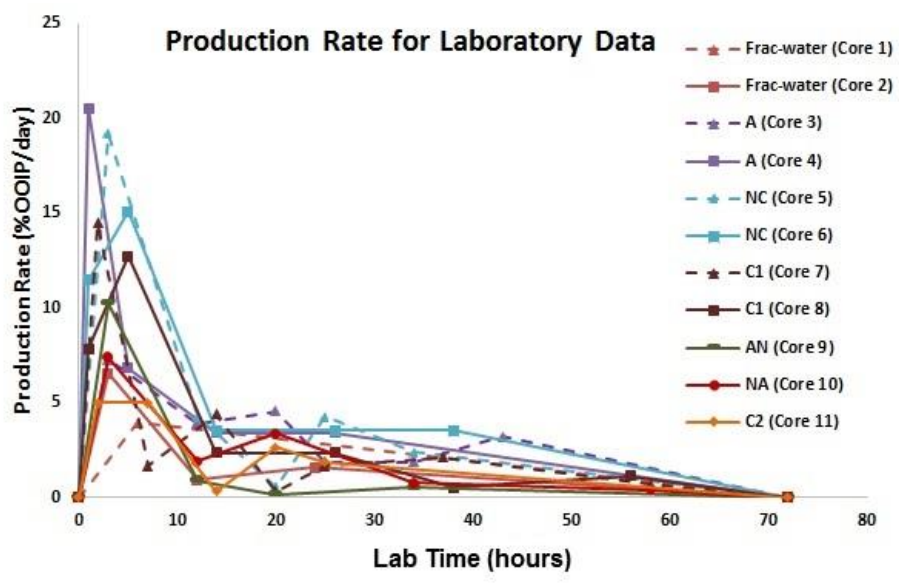


Figure 88. Production rates for the Eagle Ford spontaneous imbibition experiments.

As shown in Fig. 88, production rates reached maximum value within very short durations. After approximately 12 hours, production rates decreased nearly 70% of their maximum. These production rate curves are like actual production rate curves observed

on the field. As shown in Fig. 71, stage 1 exhibits larger production rates in the first 12 hours as surfactant solution penetrates the core surface due to a decrease in IFT. At stage 2 (after 12 hours), wettability alteration takes place and production rates are relatively stable because capillary pressure sign changed and remained nearly constant. By stage 3 (after 70 hours), the production rates decreased to almost zero due to the size of core samples.

Upscaling data from the laboratory to the field was done using the experimental data from cores 2, 4, 6, and 8. We chose these cores to compare the impact of production profiles by using different surfactant types and slickwater alone. For spontaneous imbibition experiments, the average end time of high production was 10 hours. Using core dimensions in Table 20, the characteristic lengths of core samples were calculated using Eq. 30 and shown in **Table 31**. In addition, field characteristic lengths were calculated using Eq. 31.

Table 31. Characteristic core lengths for the Eagle Ford

Core	Type of Fluid	$L_{c(Lab)}$ (cm)	$L_{c(field)}$ (cm)
2	Frac-water	0.767	79.722
4	A	0.806	83.780
6	NC	0.821	85.362
8	C1	0.846	87.924

For the scaling process, we assumed that the induced fractures form one layer of equal-sized cube matrix blocks along both sides of the hydraulic fracture as shown in **Fig. 89**. We also assumed that the imbibition process only happens in the opened blocks. Field scale spontaneous imbibition can be equivalent to spontaneous imbibition for these cube

matrix blocks surrounded by aqueous solution. Therefore, the side length of these matrix blocks can be obtained based on $L_{c(field)}$, which was used to determine the total well-oil production by spontaneous imbibition.

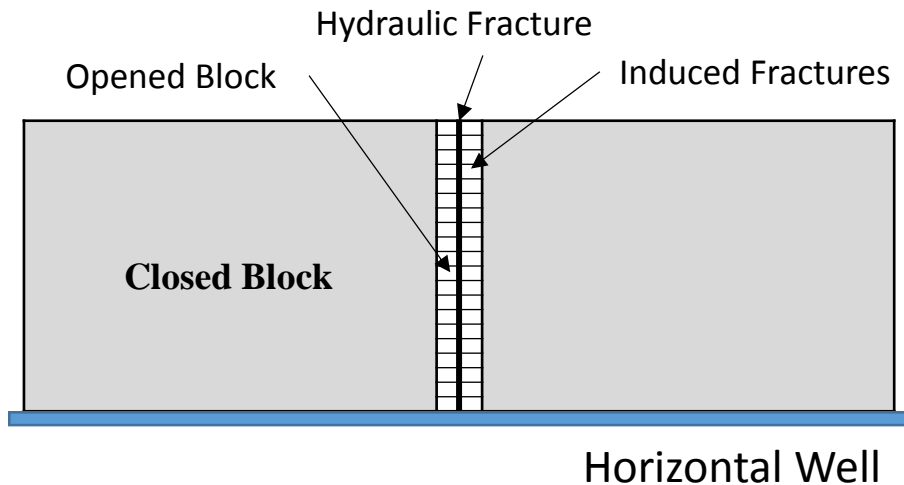


Figure 89. Distribution of induced fractures and hydraulic fractures along the horizontal well.

To test different completion scenarios and hydraulic fracture geometries, four cases were considered. Hydraulic fracture height was 200 ft. for all cases and **Table 32** illustrates the number of stages, number of hydraulic fractures (HF) per stage, and fracture half-length for the four cases.

Table 32. Completion methods and fracture geometries

Case	Number of Stages	Number of HF per stage	HF Half-length (ft.)
1	15	2	200
2	15	4	200
3	15	4	400
4	30	4	400

After carefully analyzing field production data from the same Eagle Ford area as the samples tested, we observed that the production rate decreased to less than 30% of maximum production after one year and then to a very low value after five years of production. Thereby, we decided to predict five years of production rates for all cases.

Fig. 90 shows the field production rate curves for all cases.

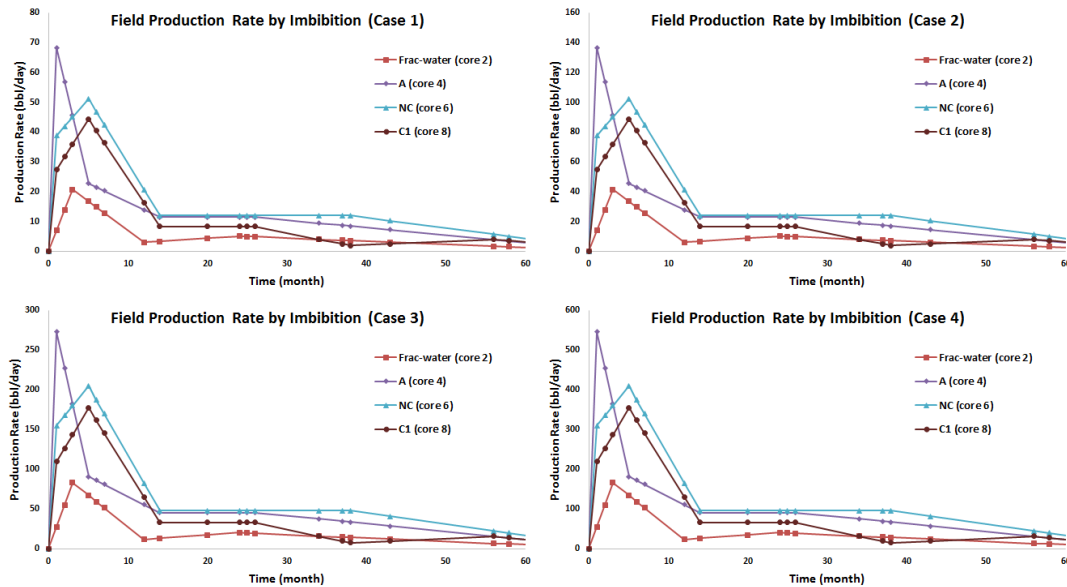


Figure 90. Predicted field production rates by imbibition from scaling laboratory data in the Eagle Ford.

Upscaled field production data shows that surfactant Anionic A has the highest peak, and its production rate decreased rapidly. The high initial production is due to the capability of surfactant Anionic A in reducing IFT. Then, surfactant NC dominates imbibition because its capability in altering wettability largely than surfactants with anionic compounds. Lastly, all cores submerged in surfactant solutions showed higher field production rates than the production rates from cores in slickwater alone.

Moreover, as fracture geometries increased from case 1 to 4, production rates also increase. Production rates driven by imbibition show the impact of surfactants in oil recovery. In fact, imbibition aided by surfactants increased oil production rate by 50 bbl/day in case 1 to almost to 375 bbl/day in case 4. These findings highlight the importance of imbibition and corroborate that fracture density and rock-fluid interactions are key parameters for oil recovery in these ULR. The results showed that the close presence of induced fractures to the hydraulic fracture results in economic production rates, and the use of surfactants could effectively improve oil recovery in fractured ULR.

Cumulative field oil production dominated by imbibition was calculated using Eq. 33 and listed for all cases in **Table 33**. Surfactant NC (core 6) achieved the highest cumulative oil production for all four cases, which matched the experiments results. As total opened fracture area increased (from case 1 to case 4), the predicted oil accumulation for imbibition also increased. This rising trend in oil production as fracture density increases is due to the improved oil recovery by imbibition because of a higher area of contact with the rock surface by the aqueous solutions.

Table 33. Cumulative field oil production by imbibition for the Eagle Ford

Core	Type of Fluid	Cumulative Oil Production (bbl)			
		Case 1	Case 2	Case 3	Case 4
2	Frac-water	6,614	13,228	26,455	52,910
4	A	16,400	32,800	65,600	131,200
6	NC	24,530	49,059	98,119	196,237
8	C1	19,141	38,282	76,563	153,127

Until now, the upscaling results obtained correspond to the amount of oil that would be recovered by altering wettability and IFT to favor imbibition of completion fluids in a soaking and flowback completion scheme. However, the oil produced by pressure differences between the reservoirs and wellbore also contributes significantly to total oil production. Hence, total well-oil production is the contribution of both fluid flow driven by pressure difference and imbibition. We used real-field production data, retrieved from IHS Energy database, of the wells from the same county as core sample as a base case for the pressure difference contribution. Therefore, as shown in **Fig. 91**, production rates are the sum of the actual field production data and the oil recovered by imbibition in each case.

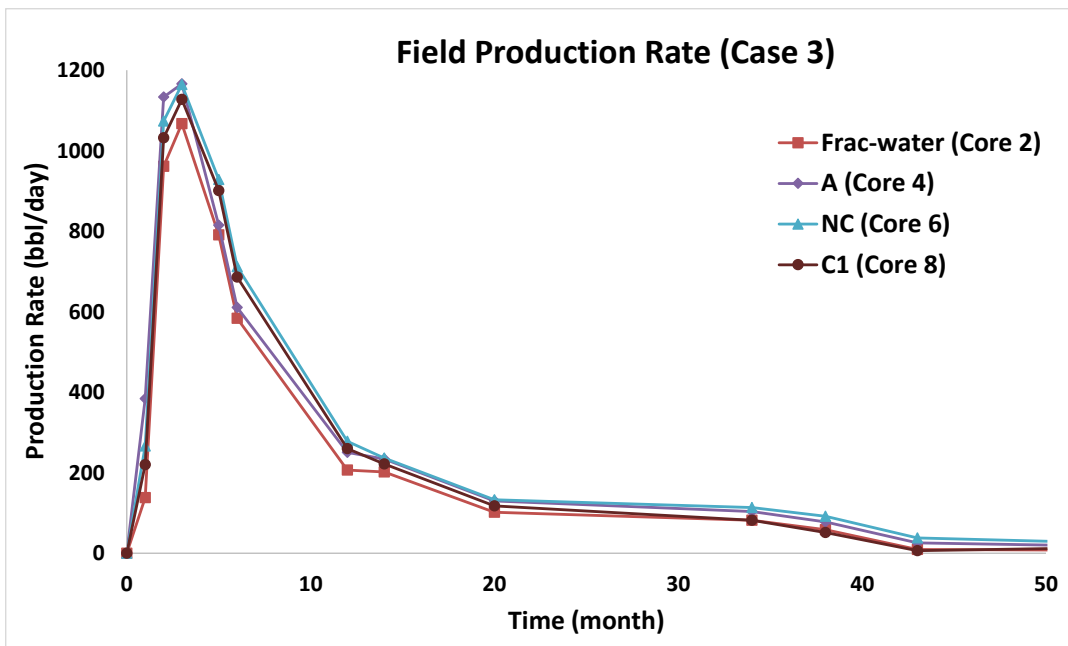


Figure 91. Predicted Eagle Ford field production using case 3.

Considering actual field production data and scaled laboratory imbibition results, the predicted production rates for these three surfactant types and slick water are generated. Surfactant NC achieved the largest increment in production rate followed by surfactants A and C1. By comparing the best surfactant (NC) to frac-water alone, the upscaling results indicate that maximum well production rates could be increased by almost 20%.

Scaling Laboratory Data to the Field in the Wolfcamp Formation

The experimental results obtained by the spontaneous imbibition experiments for Wolfcamp (Chapter VII, Fig. 67) were used to scale laboratory data to the field. As done

with data collected from Eagle Ford experiments, **Fig. 92** shows the Wolfcamp oil recovered as function of the OOIP versus dimensionless time defined by Ma, Morrow, and Zhang (1995) (Eq. 9) which does not consider wettability alteration in its equation.

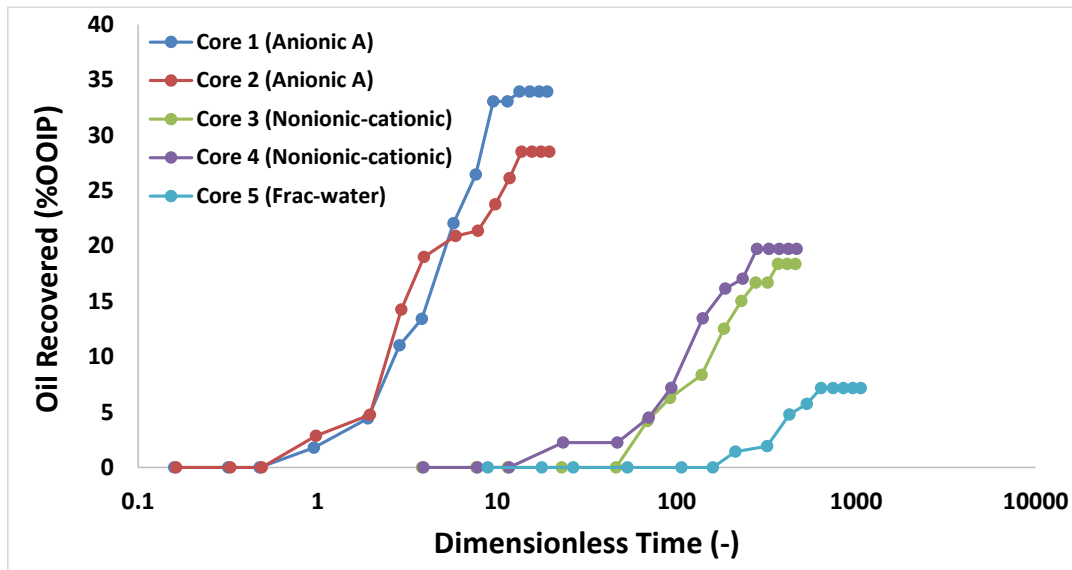


Figure 92. Oil recovery vs. dimensionless time in spontaneous imbibition experiments for Wolfcamp using scaling group by Ma, Morrow, and Zhang (1995).

Fig. 92 shows the difference in imbibition rates for different groups of surfactants and slickwater without surfactants. In order to assess the dimensional scaling group validity in our data set, we also plot the normalized oil recovery and dimensionless time for the Ma, Morrow, and Zhang (1995) scaling group in **Fig. 93**.

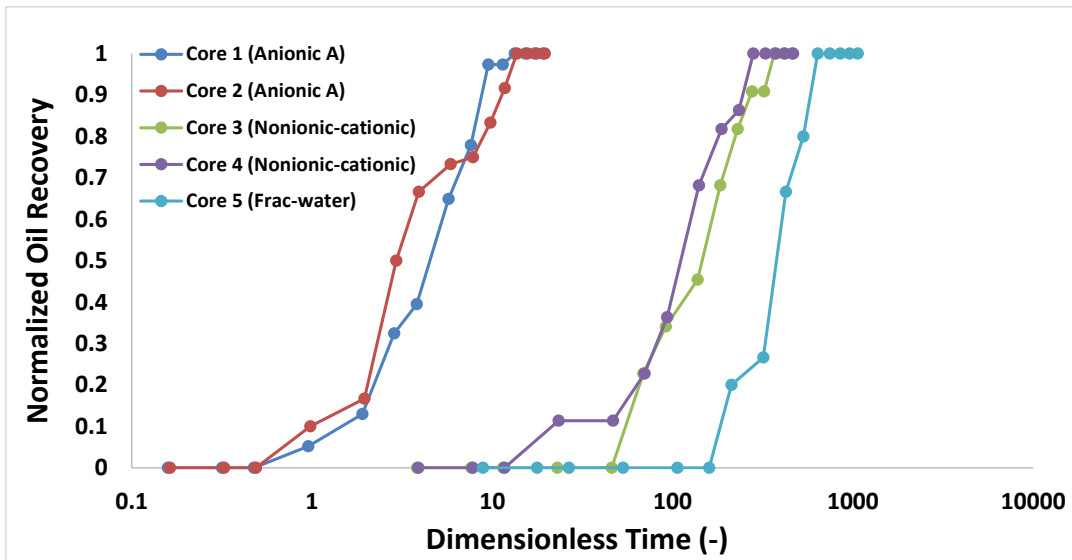


Figure 93. Normalized oil recovery vs. dimensionless time for Wolfcamp using scaling group by Ma, Morrow, and Zhang (1995).

The normalized plot grouped better the laboratory results for surfactant nonionic-cationic and frac-water; however, it does not group the surfactant Anionic A results as closely as desired. This raises a possibility that the scaling group proposed by Ma, Morrow, and Zhang (1995) does not fully represent the experimental data with a span of almost three log cycles.

Next, we analyzed the same Wolfcamp data using the scaling number proposed by Gupta and Civan (1994) and Guo, Schechter, and Baker (1998) (Eq. 12) which considers wettability alteration in its formulation. **Fig. 94** shows the oil recovered as function of the OOIP vs. dimensionless time. **Fig. 95** shows the normalized oil recovery and dimensionless time defined by Gupta and Civan (1994) and Guo, Schechter, and Baker (1998).

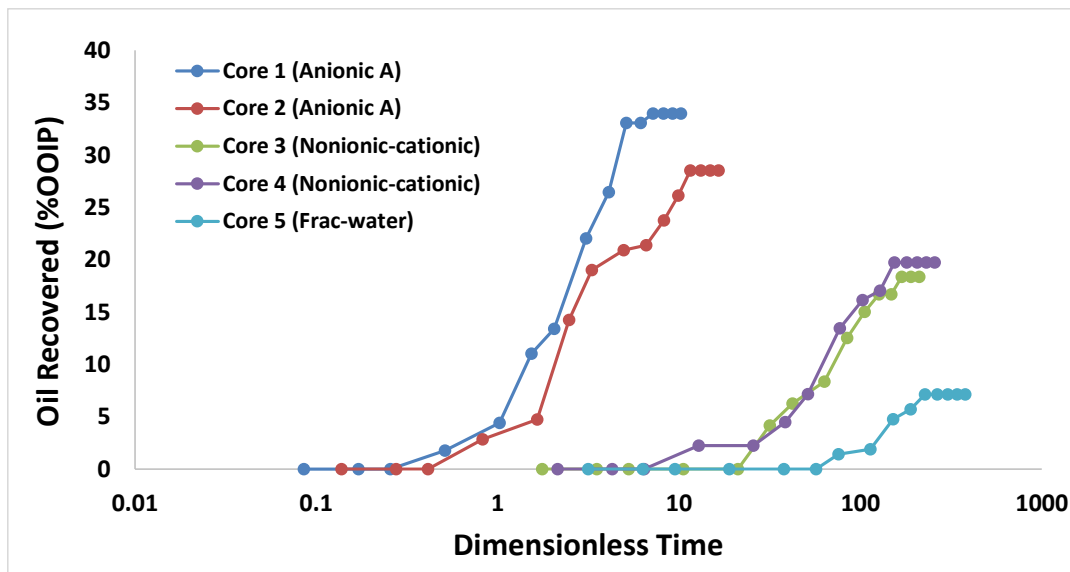


Figure 94. Oil recovery vs. dimensionless time for Wolfcamp using scaling group by Gupta and Civan (1994) and Guo, Schechter, and Baker (1998).

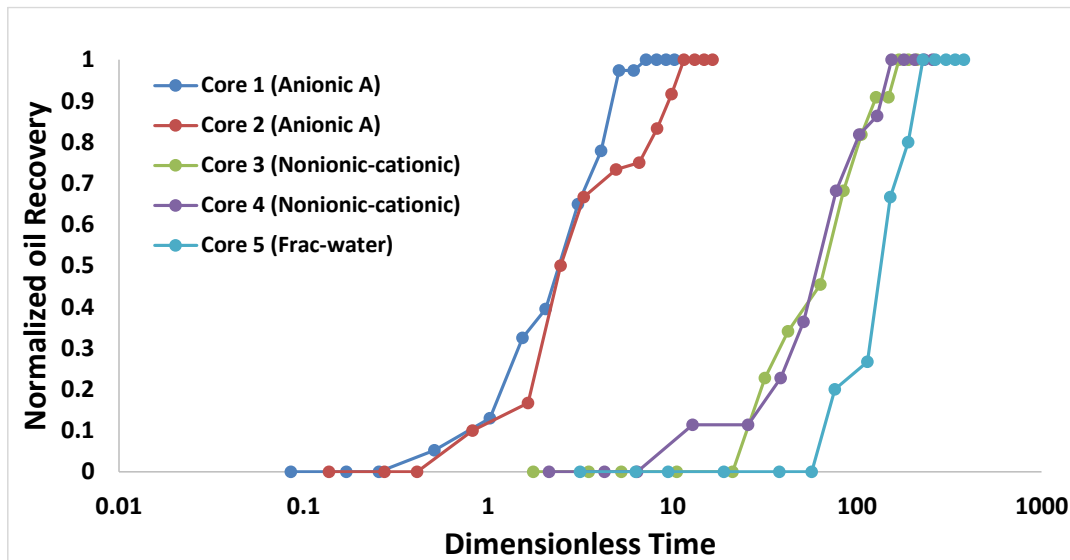


Figure 95. Normalized oil recovery vs. dimensionless time for Wolfcamp using scaling group by Gupta and Civan (1994) and Guo, Schechter, and Baker (1998).

The scaling number proposed by Gupta and Civan (1994) and Guo, Schechter, and Baker (1998) reduced the data spread from three log cycles in Fig. 93 to approximately

two log cycles in Fig. 95, showing the importance of considering wettability alteration when scaling laboratory data. In addition, the dimensionless time profiles were faster by approximately half order of magnitude, as the contact angle is considered into the equation due to changes from oil-wet original wettability to more water-wet as measured in the spontaneous imbibition experiments (Chapter VII). After evaluating both dimensionless time profiles, we selected the dimensionless model by Gupta and Civan (1994) and Guo, Schechter, and Baker (1998) to represent our experimental data. **Fig. 96** shows the production rates for the Wolfcamp spontaneous imbibition experiments.

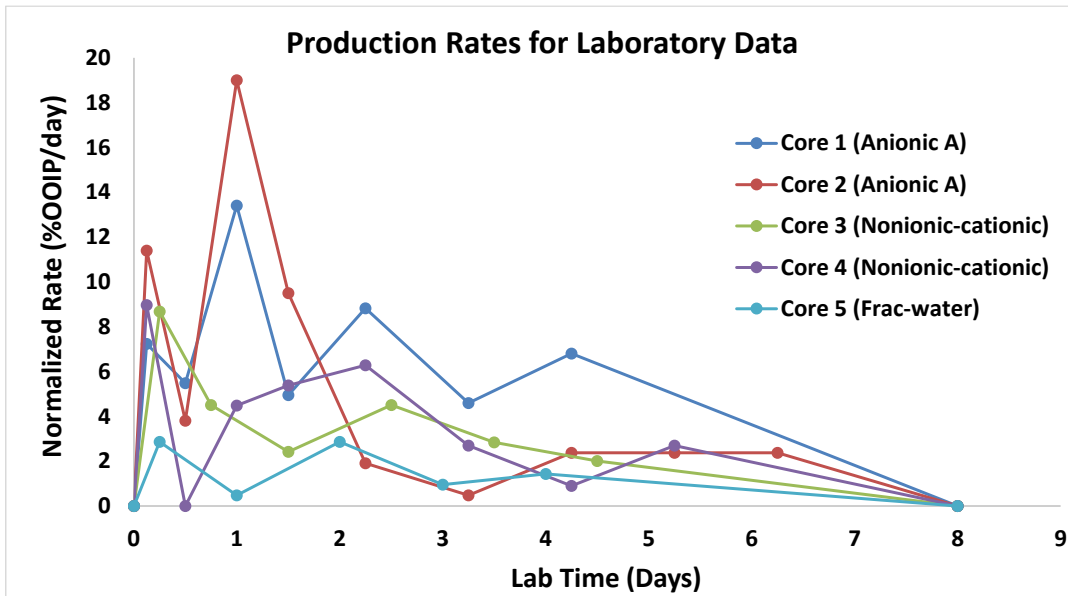


Figure 96. Production rate for the Wolfcamp spontaneous imbibition experiments.

As shown in Fig. 96, production rates reached maximum values after approximately one day. Then, the production rates decreased drastically to nearly 70% of

their maximums. These production rate curves are like actual production rate curves observed on the field.

Upscaling data from the laboratory to the field was done using the experimental data to compare the production profiles by using different surfactant types and frac-water alone. Using core dimensions in Table 16 (cores 1 to 5), the characteristic lengths of core samples were calculated with Eq. 30 and shown in **Table 34**. In addition, field characteristic lengths were calculated using Eq. 31.

Table 34. Characteristic core lengths for Wolfcamp

Core	Type of Fluid	$L_{c(Lab)}$ (cm)	$L_{c(field)}$ (cm)
1	Anionic A	0.807	45.936
2	Anionic A	0.796	45.335
3	Nonionic-cationic	0.816	46.477
4	Nonionic-cationic	0.803	45.740
5	Frac-water	0.794	45.204

Similar as the scaling process for the Eagle Ford, we assumed that the induced fractures form one layer of equal-sized cube matrix blocks along both sides of hydraulic fracture, and assume that the imbibition process only happens in the opened blocks. Field scale spontaneous imbibition can be equivalent to spontaneous imbibition for these cube matrix blocks surrounded by aqueous solution. Hence, the side length of these matrix blocks can be obtained based on $L_{c(field)}$, which is used to determine the total well-oil production by spontaneous imbibition. In the same way, we tested the same four completion scenarios and hydraulic fracture geometries as that in the Eagle Ford section, and shown in Table 22. Finally, the prediction time was limited to five years because after

analyzing field data, we observed that the production rates decreased to less than 30% of maximum production after one year and to a very low value after five years of production.

Fig. 97 shows the field production rate curves for all cases.

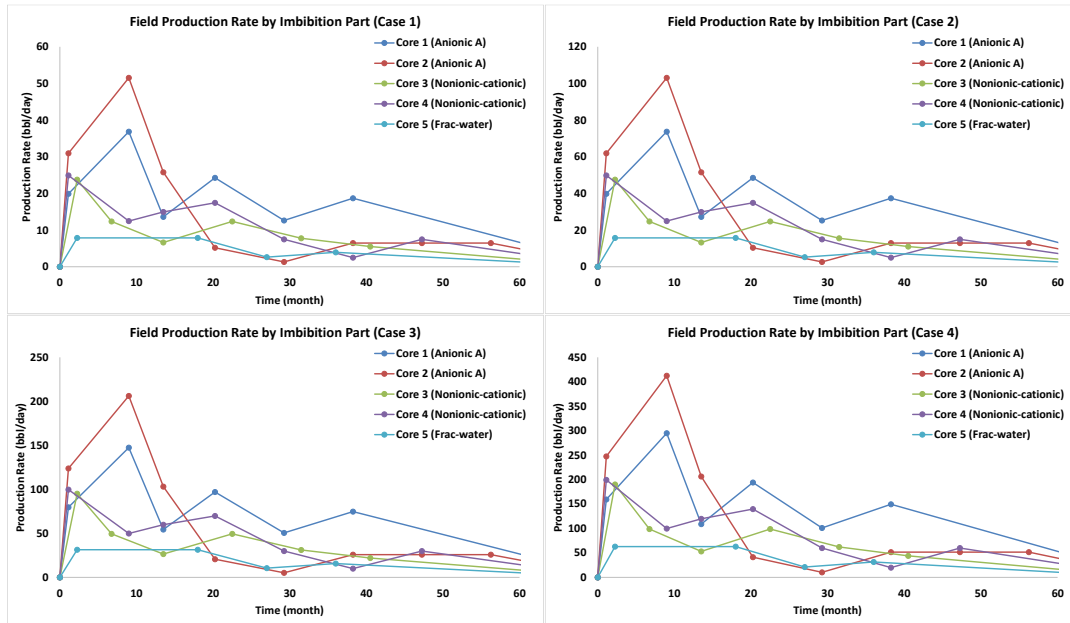


Figure 97. Predicted field production rate by imbibition from scaling laboratory data in the Wolfcamp.

Fig. 97 shows upscaled production for the four cases evaluated. The first observation is that the higher the fracture density, the higher the oil rates. As fracture geometries increase from case 1 to 4, production rates also increase. Thereby, production rates driven by imbibition shows the impact of surfactants in oil recovery. Imbibition aided by surfactants increases in oil production rate of 40 bbl/day in case 1 to almost to 410 bbl/day in case 4. This highlights the importance of contact area for oil recovery on these ULR. The plots also show the highest peak in production rate for surfactant Anionic A,

consistent with the laboratory results explained in Chapter VII, and stressing the impact of wettability and IFT alteration in imbibition and oil recovery. This better performance of surfactant Anionic A is due to its efficacy in altering wettability and reducing IFT better than the nonionic-cationic surfactant. Nevertheless, all cores submerged in surfactant solutions show higher field production rates than the cores in frac-water alone, confirming the role of surfactants in imbibition.

Next, cumulative field oil production dominated by imbibition was calculated using Eq. 33 and listed for all cases in **Table 35**. Surfactant Anionic A (cores 1 and 2) achieved the highest cumulative oil production for all four cases followed surfactant nonionic-cationic surfactant (core 3 and 4). These results match the experiments results obtained in Chapter VII. In addition, as total opened fracture area increased (from case 1 to case 4), the predicted oil accumulation for imbibition also increased, confirming the impact of fracture density on oil recovery.

Table 35. Cumulative field oil production by imbibition for the Wolfcamp

Core	Type of Fluid	Cumulative Oil Production (bbl)			
		Case 1	Case 2	Case 3	Case 4
1	Anionic A	25,190	50,381	10,0761	20,1522
2	Anionic A	20,879	41,759	83,518	167,036
3	Nonionic-cationic	13,576	27,152	54,303	108,607
4	Nonionic-cationic	14,804	29,609	59,217	118,434
5	Frac-water	5,302	10,603	21,206	42,412

Until now, production rates and cumulative oil production values for Wolfcamp shown in Table 35 correspond only to the oil recovered by imbibition as a driven mechanism when a soaking and flowback completion scheme is used. This production is mainly impacted by wettability, IFT alteration, and the rock-fluid interactions between frac fluid and unconventional reservoirs. However, after the well is opened to production, the pressure difference between the reservoirs and the wellbore is the major force that drives oil production. To have a more realistic production profile driven by pressure difference contribution, we used real-field production data, retrieved from IHS Energy database, of the wells from the same county as that of the core samples. Therefore, as shown in **Fig. 98**, production rates are the sum of the actual field production data and the oil recovered by imbibition in each case.

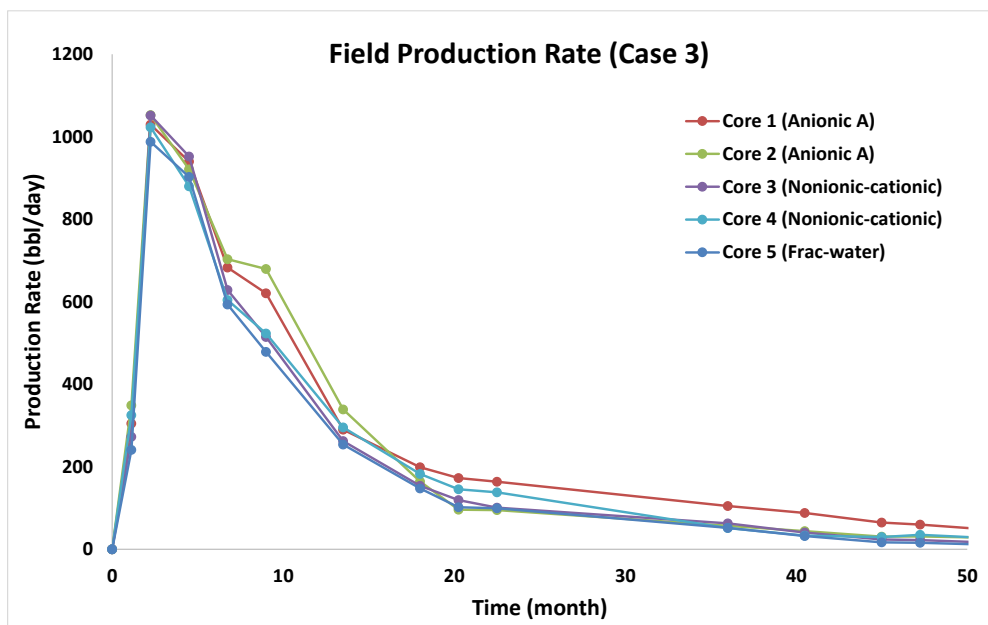


Figure 98. Predicted Wolfcamp field production using case 3

Considering actual field production data and scaled laboratory imbibition results, the predicted production rate for these two surfactant types and frac water are generated. Surfactant anionic A achieved the largest increment in production rate followed by surfactants Nonionic-cationic. By comparing surfactant anionic A to frac water alone, the upscaling results indicate that maximum well production rates could be increased by almost 15%.

In summary, the results of these correlated sets of experiments show that wettability alteration and IFT reduction play a significant role in improving the penetration of stimulation fluid into the rock matrix, consequently improving oil recovery. Rock wettability must be shifted from intermediate and oil-wet to water-wet to let capillary forces promote imbibition and release trapped hydrocarbons. In addition, moderate IFT reductions are needed to trigger wettability alteration by pore imbibition. However, contrary to conventional EOR in which IFT is required to be reduced to almost zero, in liquid rich shales, IFT should not be greatly reduced to eliminate capillary forces as a driving mechanism. Moreover, rock surface charges, oil, and surfactant impact imbibition and oil recover. Thereby, they must be considered when choosing the best suitable treatment for the reservoir.

CHAPTER X

FINAL CONSIDERATIONS, CONCLUSIONS AND RECOMMENDATIONS *

This investigation dealt with the effect of flowback surfactants on altering the wettability of the rock and reducing oil-water IFT and their combined effect on oil recovery through spontaneous imbibition and core flooding experiments. During this research, a set of correlated experiments were designed and executed to evaluate the effects of adding surfactants to completion fluids on fluid imbibition in unconventional liquid reservoirs. This study evaluated surfactant stability on brine and crude oil and adsorption into the ULR rock as well as surfactant efficacy in altering wettability and

*Parts of the conclusions and recommendations technology presented in this chapter have been reprinted from:

“Wettability, Oil and Rock Characterization of the Most Important Unconventional Liquid Reservoirs in the United States and the Impact on Oil Recovery” by J.O. Alvarez and D.S. Schechter. URTEC Paper 2461651. Copyright 2016 by the Unconventional Resources Technology Conference (URTEC). Reproduced with permission of URTEC. Further reproduction prohibited without permission.

“Impact of Surfactants for Wettability Alteration in Stimulation Fluids and the Potential for Surfactant EOR in Unconventional Liquid Reservoirs” by J.O. Alvarez, A. Neog, A. Jais and D.S. Schechter. SPE Paper 169001. Copyright 2014 by the Society of Petroleum Engineers (SPE). Reproduced with permission of SPE. Further reproduction prohibited without permission.

“Wettability Alteration and Spontaneous Imbibition in Unconventional Liquid Reservoirs by Surfactant Additives” by J.O. Alvarez and D.S. Schechter. SPE Reservoir Evaluation & Engineering. Volume 20. Issue 1. Copyright 2017 by the Society of Petroleum Engineers (SPE). Reproduced with permission of SPE. Further reproduction prohibited without permission.

“Altering Wettability in Bakken Shale by Surfactant Additives and Potential of Improving Oil Recovery during Injection of Completion Fluids” by J.O. Alvarez and D.S. Schechter. SPE Paper 179688. Copyright 2016 by the Society of Petroleum Engineers (SPE). Reproduced with permission of SPE. Further reproduction prohibited without permission.

“Potential of Improving Oil Recovery with Surfactant Additives to Completion Fluids for the Bakken” by J.O. Alvarez, I. W. Rakananda Saputra and D.S. Schechter. Energy & Fuels. Volume 31. Issue 6. Copyright 2017 by American Chemical Society (ACS). Reproduced with permission of ACS. Further reproduction prohibited without permission.

reducing IFT and how these rock-fluid and fluid-fluid interactions impacted water penetration and oil recovery from ULR core from Wolfcamp, Eagle Ford, Bakken and Barnett.

The results showed that rock wettability shifted from oil and intermediate-wet to water-wet, and the use of surfactants moderately reduced IFT. These alterations in wettability and IFT changed the sign of capillary forces, favoring water imbibition and releasing trapped hydrocarbons in the rock pores. Hence, fluid imbibition enhanced oil recovery in these ULR samples. In contrast, aqueous solutions without surfactant were not able to alter wettability and IFT and showed limited imbibition and consequently low hydrocarbon recovery. At the end, wettability and IFT alteration played a major role in imbibition; however, in ULR, IFT should not be drastically reduced, as conceived in conventional EOR, because it may eliminate capillary forces as a driving mechanism.

In order to analyze further the impact of wettability and IFT alteration in capillary forces and imbibition (penetration magnitude), the surface response methodology was used to examine the relationship of these critical experimental variables (Box and Wilson 1951). To that end, the spontaneous imbibition experiment results showed Chapter VII were used. **Fig. 99** shows the impact of wettability and IFT in oil recovery for these ULR cores. As shown, IFT and contact angle values greater than 15 mN/m and 90 degrees respectively, show oil recoveries lower than 15 % of the OOIP. The reason behind this trend is that the ULR rock surface is oil-wet and IFT is elevated. These two variables directly affect capillary pressure giving it negative and large values limiting oil recovery by imbibition.

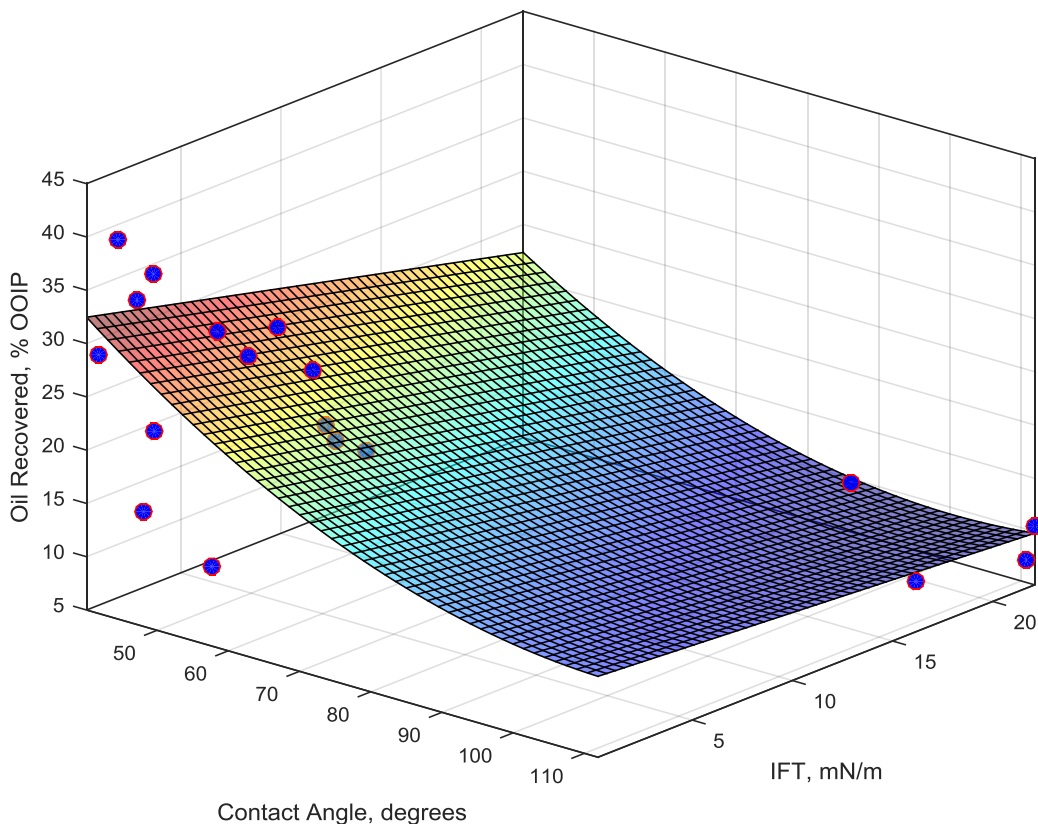


Figure 99. Effect of contact angle and IFT in oil recovered.

On the other hand, higher oil recoveries from the spontaneous imbibition experiments are observed when IFT and CA values are lower than 10 mN/m and 60 degrees, respectively. Low IFT between oil and brine phases reduces capillary pressures and favors fluid pentation into the rock. Also, low CA are a quantitative indication of water-wetness, which changes capillary pressure sign from negative to positive favoring fluid imbibition and consequently oil recovery.

The direct effect of capillary pressure and wettability in oil recovery is shown in **Fig. 100**. To recover oil by imbibition, capillary pressures must be positives in values. As

dictated by the Young-Laplace equation (Eq. 1), wettability must be water-wet (contact angle less than 90 degrees in an oil-water-rock system where water is the denser fluid) to have a positive capillary pressure. Fig. 100 shows a direct correlation between capillary pressure and oil recovery with higher recovery factors when capillary pressures are greater than zero. As explained in previous chapters, the oil recovered in spontaneous imbibition experiments when capillary pressures are negatives are due to gravity forces aided by oil and brine density differences.

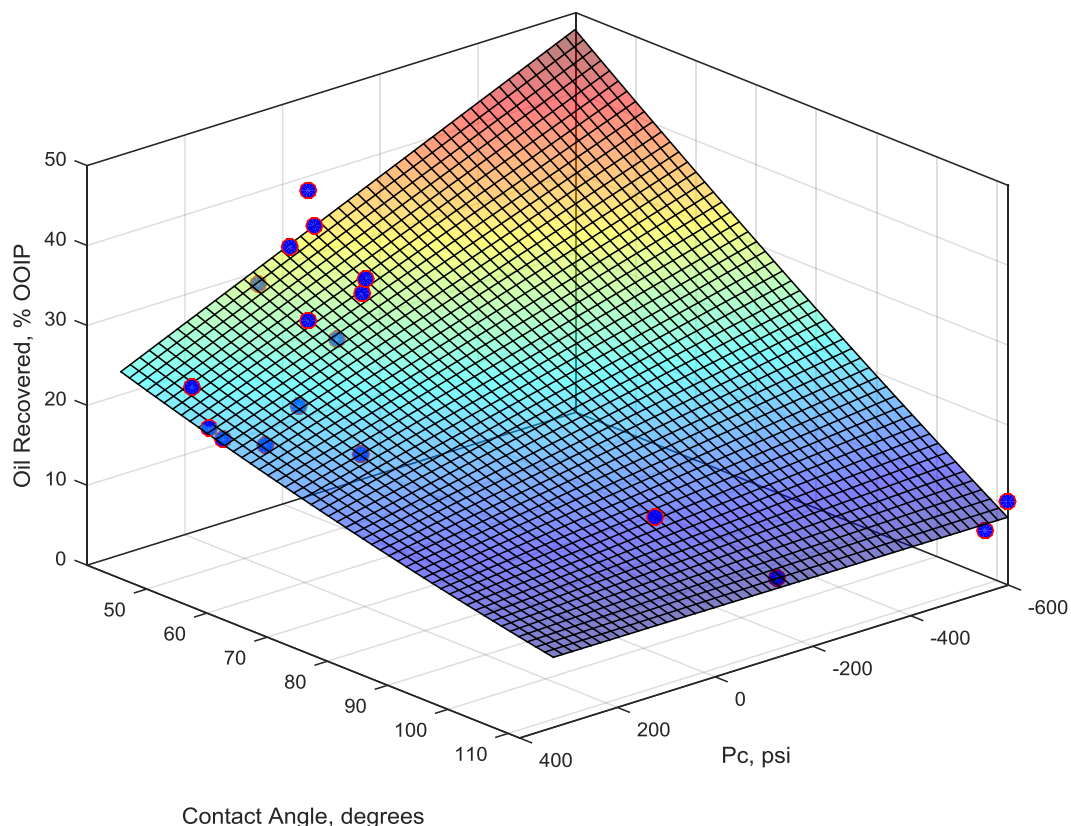


Figure 100. Effect of capillary pressure and contact angle in oil recovered.

Finally, during the experiments, CT scan technology was used to quantify fluid penetration (imbibition) into the core. Using response surface methodology, we examine the relationship among oil recovery, penetration magnitude (imbibition) and capillary pressure as shown in **Fig. 101**. As demonstrated in several laboratory studies presented in previous chapters, the effectiveness of fracture treatments in increasing recovery can be improved if proper surfactants are added to completion fluids, thereby altering wettability, reducing interfacial tension (IFT) and consequently improving water imbibition. Surfactants can diffuse into the cores and, by imbibition, displace liquid hydrocarbons from ULR providing higher oil recovery than aqueous solutions without chemical additives. The relation between oil recovery and imbibition (penetration magnitude) is clearly shown in Fig. 101. As penetration magnitude increases, as an indication of fluid imbibition into the rock, oil recovery is enhanced. Similarly, when capillary pressures are lower than zero, penetration magnitudes are the lowest suggesting limited imbibition. On the other hand, when capillary pressures are positive, due to surfactant capability of altering wettability, oil recoveries are significantly higher. This confirms that positive capillary pressure favors imbibition, which has a determinate effect on improving oil recovery from these ULR.

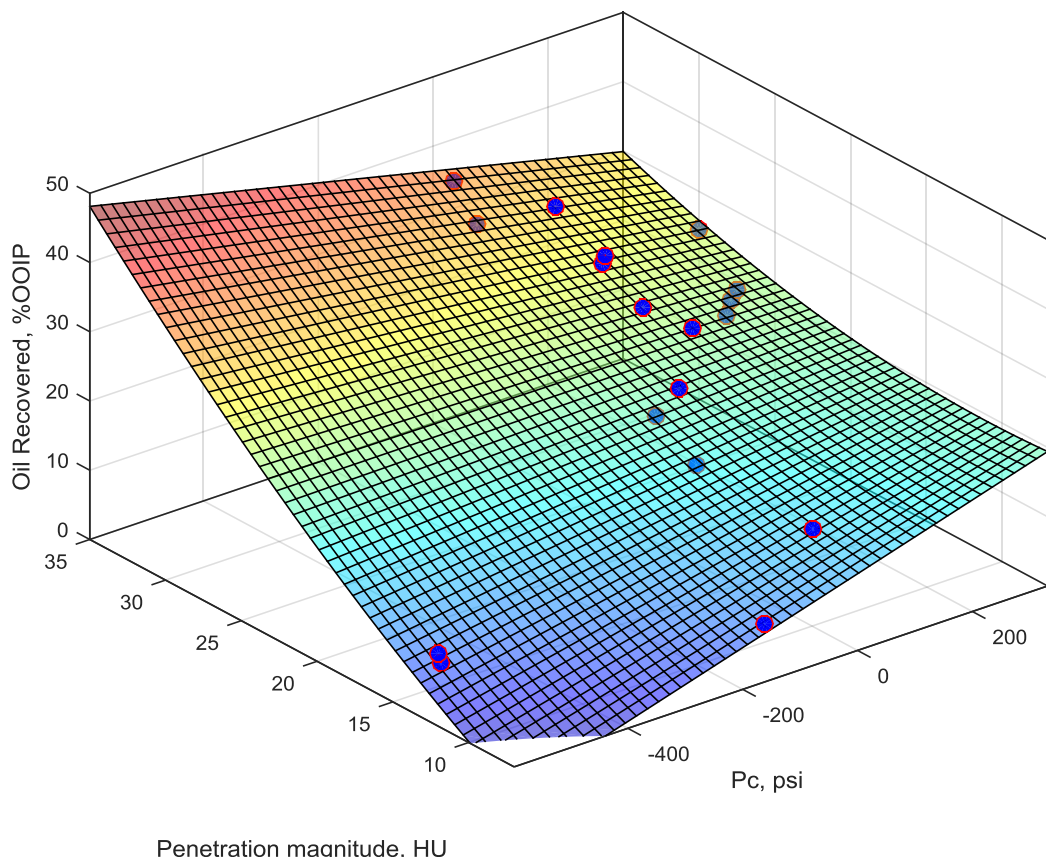


Figure 101. Effect of penetration magnitude and capillary pressure in oil recovered.

The results from this study give helpful awareness on designing a chemically compatible and better performing stimulating fluid at affordable costs, which can recover additional oil as compared to a conventional stimulation treatment with any surfactant additives. In addition, by scaling laboratory results, field production rates can be estimated under different fracture spacing scenarios corroborating that rock-fluid interactions and fracture density are key parameters for oil recovery in these ULR. The main conclusions and recommendations of this research work are as follows:

- Petrophysical analyses from ULR cores from Wolfcamp, Eagle Ford, Bakken and Barnett show siliceous and carbonate lithologies with clay contents up to 40 wt.% and TOC values up to 7 wt.%. In addition, petrophysical properties analyses show low porosity up to 11%, ultralow permeability up to 24 μ D and with small pore throat radius up to 0.034 μ m.
- Original wettability, determined by CA measurements, for Wolfcamp, Eagle Ford, Bakken and Barnett shows mostly intermediate towards oil-wet behavior with Wolfcamp exhibiting the greatest degree of oil-wetness.
- ULR wettability tends towards more oil-wet as the TOC content increases whereas lithology does not seem to have a direct impact on wetting affinity.
- Liquid hydrocarbons are capable of spontaneously imbibe into ULR core demonstrating affinity for oil as a qualitative indicator of intermediate to oil-wet behavior. ULR intermediate-wetness allows also water imbibition into cores from Wolfcamp, Eagle Ford, Bakken and Barnett, but in lower volumes than oil imbibition.
- All the surfactants tested altered the wettability of the shale samples from oil and intermediate-wet to water-wet. Initial ULR core wettability can be altered by using surfactant additives in completion fluids at concentrations of 1 and 2 gpt.
- Surfactant efficacy in altering wetting affinity strongly depends on rock mineral composition and surfactant type with negatively charged surfactants performing better in siliceous cores, and positively charged surfactants performing better in carbonate cores.

- Zeta potential values were higher in absolute value in solutions with surfactant additives implying stronger aqueous films as an indication of water wetness. This effect increased with increasing surfactant concentration.
- Zeta potential for surfactant-oil systems showed higher stability and stronger impact on the electric surface charge at the surfactant-oil interface when surfactants are added to completion fluids, which facilitates IFT reduction by oil solubilization in surfactant solution.
- Addition of surfactants reduces the IFT moderately with a more dramatic shift in wettability via contact angle measurements.
- Negatively charged surfactants are adsorbed more on siliceous rock compared to positively charged surfactants, while on carbonate-rich rock, they are adsorbed less than the positively charged surfactants confirming the role of rock mineralogy and surfactant charges on adsorption behavior.
- Spontaneous imbibition experiments showed that oil recovery was improved using surfactant as compared to frac water alone. Better performance by surfactants solutions was achieved by wettability and IFT alteration, which changed capillary forces favoring water imbibition and releasing trapped hydrocarbons in the rock pores.
- Wettability alteration and IFT reduction play a key role in determining the fluid penetration into the rock matrix and the resulting oil recovery, which is favored by a strong water-wet state and low to moderate IFT values.

- Oil recovery efficacy in spontaneous imbibition experiments relied on rock lithology and oil type with siliceous cores showing higher fluid penetration and oil recovery in anionic surfactants and carbonate cores showing better penetration and hydrocarbon recovery when submerged in nonionic-cationic surfactants. This demonstrated the importance of rock-fluid interactions.
- All surfactant formulations penetrated ULR core better than frac water. Penetration magnitude, a quantitative measure of the degree of imbibition, was also proportional to oil recovery among the samples tested.
- In spontaneous imbibition experiments, most the oil produced by imbibition was within 3-5 days from the start of experiments. The time scales are remarkably quick and recovery factors substantial considering the lack of conventional permeability. This suggest the possibility of designing/optimizing treatment duration and flowback schedules.
- Capillary pressure dominates imbibition in the studied ULR cores. When capillarity values change from negative to positive and IFT is reduced, oil recovery increases.
- Core-flooding results showed that soaking-flowback production schedule aided by surfactant additives had higher imbibition and recovered more oil from liquid-rich core compared to frac water alone.
- Upscaled laboratory results using dimensionless analysis showed that the presence of induced fractures close to main hydraulic fracture allows economic production

rates during primary depletion combined with the use of selected surfactant molecules can effectively improve EUR in fractured ULR.

- The results from this research provides important understanding in designing completion fluid treatments that better perform with specific rock lithologies and surfactant types to reduce costs and maximize oil recovery after stimulation.
- A set of correlated set of experiments was designed as a prescreening tool for possible field trials.
- Field-testing is recommended to scale up of laboratory experiments. The results obtained at lab scale may not necessarily correlate with field scale tests. For instance, lithology and heterogeneity of the reservoir plays a major role in determining the performance of these treatments; also, the proportions of rock-completion fluids vary from laboratory experiments to filed scale trial, which may affect water imbibition and oil recovery. Hence, comprehensive testing with rocks and fluid samples in different conditions and proportions can help pave way for a field trial.

REFERENCES

- A., Bhargaw, M., Kishore K. 2008. Oil Recovery From Fractured Carbonates by Surfactant-Aided Gravity Drainage: Laboratory Experiments and Mechanistic Simulations. *SPE Reservoir Evaluation & Engineering* 11 (1): 119-130.
- Alharthy, N., Teklu, T., Kazemi, H. et al. 2015. Enhanced Oil Recovery in Liquid-Rich Shale Reservoirs: Laboratory to Field. SPE Annual Technical Conference and Exhibition, 28-30 September, Houston, Texas, USA, Society of Petroleum Engineers. DOI: 10.2118/175034-MS.
- Alvarez, J. O., Neog, A., Jais, A. et al. 2014. Impact of Surfactants for Wettability Alteration in Stimulation Fluids and the Potential for Surfactant EOR in Unconventional Liquid Reservoirs. SPE Unconventional Resources Conference, 1-3 April, The Woodlands, Texas, USA, Society of Petroleum Engineers. DOI: 10.2118/169001-MS.
- Alvarez, J. O., Saputra, I. W. R., Schechter, D. S. 2017. Potential of Improving Oil Recovery with Surfactant Additives to Completion Fluids for the Bakken. *Energy & Fuels* 31 (6): 5982-5994.
- Alvarez, J. O., Schechter, D. S. 2016a. Altering Wettability in Bakken Shale by Surfactant Additives and Potential of Improving Oil Recovery During Injection of Completion Fluids. SPE Improved Oil Recovery Conference, 11-13 April, Tulsa, Oklahoma, USA, Society of Petroleum Engineers. DOI: 10.2118/179688-MS.
- Alvarez, J. O., Schechter, D. S. 2016b. Application of wettability alteration in the exploitation of unconventional liquid resources. *Petroleum Exploration and Development* 43 (5): 832-840.
- Alvarez, J. O., Schechter, D. S. 2016c. Wettability, Oil and Rock Characterization of the Most Important Unconventional Liquid Reservoirs in the United States and the Impact on Oil Recovery. Unconventional Resources Technology Conference, 1-3

August, San Antonio, Texas, USA, Unconventional Resources Technology Conference. DOI: 10.15530-URTEC-2016-2461651.

Alvarez, J. O., Schechter, D. S. 2017. Wettability Alteration and Spontaneous Imbibition in Unconventional Liquid Reservoirs by Surfactant Additives. *SPE Reservoir Evaluation & Engineering* 20 (01): 107-117.

Anderson, W. G. 1986a. Wettability Literature Survey- Part 1: Rock/Oil/Brine Interactions and the Effects of Core Handling on Wettability. *Journal of Petroleum Technology* 38 (10): 1125-1144.

Anderson, W. G. 1986b. Wettability Literature Survey- Part 2: Wettability Measurement. *Journal of Petroleum Technology* 38 (11): 1246-1262.

Anderson, W. G. 1987. Wettability Literature Survey- Part 4: Effects of Wettability on Capillary Pressure. *Journal of Petroleum Technology* 39 (10): 1283-1300.

Austad, T., Matre, B., Milter, J. et al. 1998. Chemical Flooding of Oil Reservoirs 8. Spontaneous Oil Expulsion from Oil- and Water-wet Low Permeable Chalk Material by Imbibition of Aqueous Surfactant Solutions. *Colloids and Surfaces A: Physicochemical and Engineering Aspects* 137 (1-3): 117-129.

Austad, T., Milter, J. 1997a. Spontaneous Imbibition of Water Into Low Permeable Chalk at Different Wettabilities Using Surfactants. International Symposium on Oilfield Chemistry, 18-21 February, Houston, Texas, USA, Society of Petroleum Engineers. DOI: 10.2118/37236-MS.

Austad, T., Milter, J. 1997b. Spontaneous Imbibition of Water Into Low Permeable Chalk at Different Wettabilities Using Surfactants, Society of Petroleum Engineers. DOI: 10.2118/37236-MS.

Babadagli, T., Al-Bemani, A., Boukadi, F. 1999. Analysis of Capillary Imbibition Recovery Considering the Simultaneous Effects of Gravity, Low IFT, and Boundary Conditions. SPE Asia Pacific Improved Oil Recovery Conference, 25-26 October, Kuala Lumpur, Malaysia, Society of Petroleum Engineers. DOI: 10.2118/57321-MS.

Basu, S., Sharma, M. M. 1997. Characterization of Mixed-Wettability States in Oil Reservoirs by Atomic Force Microscopy. *SPE Journal* 2 (04): 427-435.

Box, G. E. P., Wilson, K. B. 1951. On the Experimental Attainment of Optimum Conditions. *Journal of the Royal Statistical Society. Series B (Methodological)* 13 (1): 1-45.

Buckley, J. S., Liu, Y., Monsterleet, S. 1998. Mechanisms of Wetting Alteration by Crude Oils. *SPE Journal* 3 (01): 54-61.

Chen, H. L., Lucas, L. R., Nogaret, L. A. D. et al. 2001. Laboratory Monitoring of Surfactant Imbibition With Computerized Tomography. *SPE Reservoir Evaluation & Engineering* 4 (01): 16-25.

Chilingar, G. V., Yen, T. F. 1983. Some Notes on Wettability and Relative Permeabilities of Carbonate Reservoir Rocks, II. *Energy Sources* 7 (1): 67-75.

Craig, F, F. 1993. *The Reservoir Engineering Aspects Of Waterflooding*, Vol. 3. Richardson, TX, USA: Monograph Series, Society of Petroleum Engineers.

Cuiec, L. 1984. Rock/Crude-Oil Interactions and Wettability: An Attempt To Understand Their Interrelation. SPE Annual Technical Conference and Exhibition, 16-19 September, Houston, Texas, USA, Society of Petroleum Engineers. DOI: 10.2118/13211-MS.

Cuiec, L. E., Bourbiaux, B., Kalaydjian, F. 1994. Oil Recovery by Imbibition in Low-Permeability Chalk. *SPE Formation Evaluation* 9 (03): 200-208.

Doman, L. 2015. U.S. Remained World's Largest Producer of Petroleum and Natural Gas Hydrocarbons in 2014. *U.S Energy Information Administration*. <https://www.eia.gov/todayinenergy/detail.php?id=20692#>.

Downs, H. H., Hoover, P. D. 1989. Enhanced Oil Recovery by Wettability Alteration. Laboratory and Field Pilot Waterflood Studies. In *Oil-Field Chemistry*, Chap. 32,

577-595. Washington, DC, USA: ACS Symposium Series, American Chemical Society.

Du Prey, E. L. 1978. Gravity and Capillarity Effects on Imbibition in Porous Media. *Society of Petroleum Engineers Journal* 18 (03): 195-206.

Feng, L., Xu, L. 2015. Implications of Shale Oil Compositions on Surfactant Efficacy for Wettability Alteration. SPE Middle East Unconventional Resources Conference and Exhibition, 26-28 January, Muscat, Oman, Society of Petroleum Engineers. DOI: 10.2118/172974-MS.

Fischer, H., Wo, S., Morrow, N. R. 2008. Modeling the Effect of Viscosity Ratio on Spontaneous Imbibition. *SPE Reservoir Evaluation & Engineering* 11 (03): 577-589.

Guo, B., Schechter, D. S., Baker, R. O. 1998. An Integrated Study of Imbibition Waterflooding in the Naturally Fractured Spraberry. SPE Permian Basin Oil and Gas Recovery Conference, 23-26 March, Midland, Texas, USA, Society of Petroleum Engineers. DOI: 10.2118/39801-MS.

Gupta, A., Civan, F. 1994. An Improved Model for Laboratory Measurement of Matrix to Fracture Transfer Function Parameters in Immiscible Displacement. SPE Annual Technical Conference and Exhibition, 25-28 September, New Orleans, Louisiana, USA, Society of Petroleum Engineers. DOI: 10.2118/28929-MS.

Gupta, R., Mohanty, K. K. 2011. Wettability Alteration Mechanism for Oil Recovery from Fractured Carbonate Rocks. *Transport in Porous Media* 87 (2): 635-652.

Habibi, A., Binazadeh, M., Dehghanpour, H. et al. 2016. Advances in Understanding Wettability of Tight Oil Formations: A Montney Case Study. *SPE Reservoir Evaluation & Engineering* 19 (04): 583-603.

Handwerger, D. A., Keller, J., Vaughn, K. 2011. Improved Petrophysical Core Measurements on Tight Shale Reservoirs Using Retort and Crushed Samples. SPE Annual Technical Conference and Exhibition, 30 October-2 November, Denver, Colorado, USA, Society of Petroleum Engineers. DOI: 10.2118/147456-MS.

- Hansen, G., Hamouda, A. A., Denoyel, R. 2000. The Effect of Pressure on Contact Angles and Wettability in the Mica/water/n-decane System and the Calcite+stearic Acid/water/n-decane system. *Colloids and Surfaces A: Physicochemical and Engineering Aspects* 172 (1–3): 7-16.
- Hirasaki, G. 1991. Wettability: Fundamentals and Surface Forces. *SPE Formation Evaluation* 6 (02): 217-226.
- Hirasaki, G., Zhang, D. L. 2004. Surface Chemistry of Oil Recovery From Fractured, Oil-Wet, Carbonate Formations. *SPE Journal* 9 (02): 151-162.
- Ingle, J. D., Crouch, S. R. 1988. *Spectrochemical Analysis*. Old Tappan, NJ, USA, Prentice Hall College Book Division.
- Jarvie, D. M. 2012. Shale Resource Systems for Oil and Gas: Part 2—Shale-oil Resource Systems. *AAPG Memoir* 97: 89-119.
- Kao, R. L., Wasan, D. T., Nikolov, A. D. et al. 1988. Mechanisms of oil removal from a solid surface in the presence of anionic micellar solutions. *Colloids and Surfaces* 34 (4): 389-398.
- Kathel, P., Mohanty, K. K. 2013. EOR in Tight Oil Reservoirs through Wettability Alteration. SPE Annual Technical Conference and Exhibition, 30 September-2 October, New Orleans, Louisiana, USA, Society of Petroleum Engineers. DOI: 10.2118/166281-MS.
- Kolasinski, K. W. 2012. *Liquid Interfaces*. West Sussex, UK: Surface Science, John Wiley & Sons, Ltd.
- Kumar, K., Dao, E. K., Mohanty, K. K. 2008. Atomic Force Microscopy Study of Wettability Alteration by Surfactants. *SPE Journal* 13 (02): 137-145.
- Leverett, M. C. 1939. Flow of Oil-water Mixtures through Unconsolidated Sands. *Transactions of the AIME* 132 (01): 149-171.

Li, K., Horne, R. N. 2005. Extracting Capillary Pressure and Global Mobility from Spontaneous Imbibition Data in Oil-Water-Rock Systems. *SPE Journal* 10 (04): 458-465.

Li, K., Horne, R. N. 2006. Generalized Scaling Approach for Spontaneous Imbibition: An Analytical Model. *SPE Reservoir Evaluation & Engineering* 9 (03): 251-258.

Ma, S., Morrow, N. R., Zhang, X. 1995. Generalized Scaling Of Spontaneous Imbibition Data For Strongly Water-Wet Systems. Technical Meeting / Petroleum Conference of The South Saskatchewan Section, October 16 - 18, Regina, Petroleum Society of Canada. DOI: 10.2118/95-138.

Mattax, C. C., Kyte, J. R. 1962. Imbibition Oil Recovery from Fractured, Water-Drive Reservoir. *Society of Petroleum Engineers Journal* 2 (02): 177-184.

Mirchi, V., Saraji, S., Goual, L. et al. 2014a. Dynamic Interfacial Tensions and Contact Angles of Surfactant-in-Brine/Oil/Shale Systems: Implications to Enhanced Oil Recovery in Shale Oil Reservoirs. SPE Improved Oil Recovery Symposium, 12-16 April, Tulsa, Oklahoma, USA, Society of Petroleum Engineers. DOI: 10.2118/169171-MS.

Mirchi, V., Saraji, S., Goual, L. et al. 2014b. Experimental Investigation of Surfactant Flooding in Shale Oil Reservoirs: Dynamic Interfacial Tension, Adsorption, and Wettability. Unconventional Resources Technology Conference, 25-27 August, Denver, Colorado, USA, Unconventional Resources Technology Conference. DOI: 10.15530/URTEC-2014-1913287.

Mohammed, M., Babadagli, T. 2015. Wettability Alteration: A Comprehensive Review of Materials/methods and Testing the Selected Ones on Heavy-oil Containing Oil-wet Systems. *Advances in Colloid and Interface Science* 220: 54-77.

Morrow, N. R., Mason, G. 2001. Recovery of Oil by Spontaneous Imbibition. *Current Opinion in Colloid & Interface Science* 6 (4): 321-337.

Morsy, S., Sheng, J. J. 2014. Surfactant Preflood to Improve Waterflooding Performance in Shale Formations. SPE Western North American and Rocky Mountain Joint

Meeting, 17-18 April, Denver, Colorado, USA, Society of Petroleum Engineers.
DOI: 10.2118/169519-MS.

Nguyen, D., Wang, D., Oladapo, A. et al. 2014. Evaluation of Surfactants for Oil Recovery Potential in Shale Reservoirs. SPE Improved Oil Recovery Symposium, 12-16 April, Tulsa, Oklahoma, USA, Society of Petroleum Engineers. DOI: 10.2118/169085-MS.

Odusina, E. O., Sondergeld, C. H., Rai, C. S. 2011. NMR Study of Shale Wettability. Canadian Unconventional Resources Conference, 15-17 November, Calgary, Alberta, Canada, Society of Petroleum Engineers. DOI: 10.2118/147371-MS.

Rajayi, M., Kantzas, A. 2009. Effect of Temperature and Pressure on Contact Angle and Interfacial Tension of Quartz-Water-Bitumen Systems. Canadian International Petroleum Conference, 16-18 June, Calgary, Alberta, Canada, Petroleum Society of Canada. DOI: 10.2118/2009-195.

Salehi, M., Johnson, S. J., Liang, J. T. 2008. Mechanistic Study of Wettability Alteration Using Surfactants with Applications in Naturally Fractured Reservoirs. *Langmuir* 24 (24): 14099-14107.

Schechter, D. S., Zhou, D., Orr Jr, F. M. 1994. Low IFT Drainage and Imbibition. *Journal of Petroleum Science and Engineering* 11 (4): 283-300.

Schmid, K. S., Geiger, S. 2012. Universal Scaling of Spontaneous Imbibition for Water-wet Systems. *Water Resources Research* 48 (3): 1-13.

Shuler, P. J., Tang, H., Lu, Z. et al. 2011. Chemical Process for Improved Oil Recovery From Bakken Shale. Canadian Unconventional Resources Conference, 15-17 November, Calgary, Alberta, Canada, Society of Petroleum Engineers. DOI: 10.2118/147531-MS.

Somasundaran, P., Zhang, L. 2006. Adsorption of Surfactants on Minerals for Wettability Control in Improved Oil Recovery Processes. *Journal of Petroleum Science and Engineering* 52 (1-4): 198-212.

- Standnes, D. C. 2001. Enhanced Oil Recovery from Oil-Wet Carbonate Rock by Spntaneous Imbibition of Aqueous Surfactant Solutions. PhD Dissertation, Norwegian University of Science and Technology, Norway.
- Standnes, D. C., Austad, T. 2000a. Wettability Alteration in Chalk: 1. Preparation of Core Material and Oil Properties. *Journal of Petroleum Science and Engineering* 28 (3): 111-121.
- Standnes, D. C., Austad, T. 2000b. Wettability Alteration in Chalk: 2. Mechanism for Wettability Alteration from Oil-wet to Water-wet Using Surfactants. *Journal of Petroleum Science and Engineering* 28 (3): 123-143.
- Swanson, B. F. 1981. A Simple Correlation Between Permeabilities and Mercury Capillary Pressures. *Journal of Petroleum Technology* 33 (12): 2498-2504.
- Treibler, L. E., Owens, W. W. 1972. A Laboratory Evaluation of the Wettability of Fifty Oil-Producing Reservoirs. *Society of Petroleum Engineers Journal* 12 (06): 531-540.
- Wang, D., Butler, R., Zhang, J. et al. 2012. Wettability Survey in Bakken Shale With Surfactant-Formulation Imbibition. *SPE Reservoir Evaluation & Engineering* 15 (06): 695-705.
- Wang, D., Zhang, J., Butler, R. et al. 2016. Scaling Laboratory-Data Surfactant-Imbibition Rates to the Field in Fractured-Shale Formations. *SPE Reservoir Evaluation & Engineering* 19 (03): 440-449.
- Wang, W., Gupta, A. 1995. Investigation of the Effect of Temperature and Pressure on Wettability Using Modified Pendant Drop Method. SPE Annual Technical Conference and Exhibition, 22-25 October, Dallas, Texas, USA, Society of Petroleum Engineers. DOI: 10.2118/30544-MS.
- Wang, Y., Xu, H., Yu, W. et al. 2011. Surfactant Induced Reservoir Wettability Alteration: Recent Theoretical and Experimental Advances in Enhanced Oil Recovery. *Petroleum Science* 8 (4): 463-476.

Washburn, E. W. 1921. The Dynamics of Capillary Flow. *Physical Review* 17 (3): 273-283.

Xie, Q., Liu, Y., Wu, J. et al. 2014. Ions Tuning Water Flooding Experiments and Interpretation by Thermodynamics of Wettability. *Journal of Petroleum Science and Engineering* 124: 350-358.

Xu, L., Fu, Q. 2012. Ensuring Better Well Stimulation in Unconventional Oil and Gas Formations by Optimizing Surfactant Additives. SPE Western Regional Meeting, 21-23 March, Bakersfield, California, USA, Society of Petroleum Engineers. DOI: 10.2118/154242-MS.

Xu, L., He, K., Rane, J. P. et al. 2015. Spontaneously Imbibed Fluids for Increasing Contact Area Between Hydraulic Fracturing Fluids and Formation Matrix in Liquids-Rich Shale Plays. SPE Liquids-Rich Basins Conference—North America, 2-3 September, Midland, Texas, USA, Society of Petroleum Engineers. DOI: 10.2118/175536-MS.

Young, T. 1855. *Miscellaneous Works*, Vol. 1. London, UK, Murray Publications.

Zelenev, A. S., Champagne, L. M., Hamilton, M. 2011. Investigation of Interactions of Diluted Microemulsions with Shale Rock and Sand by Adsorption and Wettability Measurements. *Colloids and Surfaces A: Physicochemical and Engineering Aspects* 391 (1): 201-207.

Zhang, D. L., Shunhua, L., Puerto, M. et al. 2006. Wettability Alteration and Spontaneous Imbibition in Oil-wet Carbonate Formations. *Journal of Petroleum Science and Engineering* 52 (1-4): 213-226.

Zhang, J., Wang, D., Olatunji, K. 2016. Surfactant Adsorption Investigation in Ultra-Lower Permeable Rocks, SPE Low Perm Symposium, 5-6 May, Denver, Colorado, USA, Society of Petroleum Engineers. DOI: 10.2118/180214-MS.

Zhang, P., Austad, T. 2005. Waterflooding in Chalk - Relationship Between Oil Recovery, New Wettability Index, Brine Composition and Cationic Wettability Modifier.

SPE Europec/EAGE Annual Conference, 13-16 June, Madrid, Spain, Society of Petroleum Engineers. DOI: 10.2118/94209-MS.

Zhang, X., Morrow, N. R., Ma, S. 1996. Experimental Verification of a Modified Scaling Group for Spontaneous Imbibition. *SPE Reservoir Engineering* 11 (04): 280-285.

Zhou, D., Jia, L., Kamath, J. et al. 2002. Scaling of Counter-Current Imbibition Processes in Low-Permeability Porous Media. *Journal of Petroleum Science and Engineering* 33 (1-3): 61-74.